KINETIC MODELLING SIMULATION AND OPTIMAL OPERATION OF TRICKLE BED REACTOR FOR HYDROTREATING OF CRUDE OIL

Kinetic Parameters Estimation of Hydrotreating Reactions in Trickle Bed Reactor (TBR) via Pilot Plant Experiments; Optimal Design and Operation of an Industrial TBR with Heat Integration and Economic Evaluation

Aysar Talib Jarullah

BSc. Chem. Eng.

MSc. Chem. Eng.

Submitted for the Degree of

Doctor of Philosophy

School of Engineering, Design and Technology

University of Bradford

United Kingdom

2011

Abstract

Keywords: Hydrodesulfurization, hydrodenitrogenation, hydrodemetallization, hydrodeasphaltenization, oil upgrading, trickle-bed reactor, mathematical modelling, parameter estimation, quench process, heat integration

Catalytic hydrotreating (HDT) is a mature process technology practiced in the petroleum refining industries to treat oil fractions for the removal of impurities (such as sulfur, nitrogen, metals, asphaltene). Hydrotreating of whole crude oil is a new technology and is regarded as one of the more difficult tasks that have not been reported widely in the literature. In order to obtain useful models for the HDT process that can be confidently applied to reactor design, operation and control, the accurate estimation of kinetic parameters of the relevant reaction scheme are required. This thesis aims to develop a crude oil hydrotreating process (based on hydrotreating of whole crude oil followed by distillation) with high efficiency, selectivity and minimum energy consumption via pilot plant experiments, mathematical modelling and optimization.

To estimate the kinetic parameters and to validate the kinetic models under different operating conditions, a set of experiments were carried out in a continuous flow isothermal trickle bed reactor using crude oil as a feedstock and commercial cobalt-molybdenum on alumina (Co-Mo/γ-Al_2O_3) as a catalyst. The reactor temperature was varied from 335°C to 400°C, the hydrogen pressure from 4 to10 MPa and the liquid hourly space velocity (LHSV) from 0.5 to 1.5 hr^{-1}, keeping constant hydrogen to oil ratio (H_2/Oil) at 250 L/L. The main hydrotreating reactions were hydrodesulfurization (HDS), hydrodenitrogenation (HDN), hydrodeasphaltenization (HDAs) and hydrodemetallization (HDM) that includes hydrodevanadization (HDV) and hydrodenickelation (HDNi).

An optimization technique is used to evaluate the best kinetic models of a trickle-bed reactor (TBR) process utilized for HDS, HDAs, HDN, HDV and HDNi of crude oil based on pilot plant experiments. The minimization of the sum of the squared errors (*SSE*) between the experimental and estimated concentrations of sulfur (S), nitrogen (N), asphaltene (Asph), vanadium (V) and nickel (Ni) compounds in the products, is used as an objective function in the optimization problem using two approaches (linear (LN) and non-linear (NLN) regression).

The growing demand for high-quality middle distillates is increasing worldwide whereas the demand for low-value oil products, such as heavy oils and residues, is decreasing. Thus, maximizing the production of more liquid distillates of very high quality is of immediate interest to refiners. At the same time, environmental legislation has led to more strict specifications of petroleum derivatives. Crude oil hydrotreatment enhances the productivity of distillate fractions due to chemical reactions. The hydrotreated crude oil was distilled into the following fractions (using distillation pilot plant unit): light naphtha (L.N), heavy naphtha (H.N), heavy kerosene (H.K), light gas oil (L.G.O) and reduced crude residue (R.C.R) in order to compare the yield of these fractions produced by distillation after the HDT process with those produced by conventional methods (i.e. HDT of each fraction separately after the distillation). The yield of middle distillate showed greater yield compared to the middle distillate produced by conventional methods in addition to improve the properties of R.C.R. Kinetic models that enhance oil distillates productivity are also proposed based on the experimental data obtained in a pilot plant at different operation conditions using the discrete kinetic lumping approach. The kinetic models of crude oil hydrotreating are

assumed to include five lumps: gases (G), naphtha (N), heavy kerosene (H.K), light gas oil (L.G.O) and reduced crude residue (R.C.R). For all experiments, the sum of the squared errors (*SSE)* between the experimental product compositions and predicted values of compositions is minimized using optimization technique.

The kinetic models developed are then used to describe and analyse the behaviour of an industrial trickle bed reactor (TBR) used for crude oil hydrotreating with the optimal quench system based on experiments in order to evaluate the viability of large-scale processing of crude oil hydrotreating. The optimal distribution of the catalyst bed (in terms of optimal reactor length to diameter) with the best quench position and quench rate are investigated, based upon the total annual cost.

The energy consumption is very important for reducing environmental impact and maximizing the profitability of operation. Since high temperatures are employed in hydrotreating (HDT) processes, hot effluents can be used to heat other cold process streams. It is noticed that the energy consumption and recovery issues may be ignored for pilot plant experiments while these energies could not be ignored for large scale operations. Here, the heat integration of the HDT process during hydrotreating of crude oil in trickle bed reactor is addressed in order to recover most of the external energy. Experimental information obtained from a pilot scale, kinetics and reactor modelling tools, and commercial process data, are employed for the heat integration process model. The optimization problem is formulated to optimize some of the design and operating parameters of integrated process, and minimizing the overall annual cost is used as an objective function.

The economic analysis of the continuous whole industrial refining process that involves the developed hydrotreating (integrated hydrotreating process) unit with the other complementary units (until the units that used to produce middle distillate fractions) is also presented.

In all cases considered in this study, the gPROMS (**g**eneral **PRO**cess **M**odelling **S**ystem) package has been used for modelling, simulation and parameter estimation via optimization process.

Acknowledgements

I would like to express my sincere gratitude to Professor I.M. Mujtaba for his endless patience, invaluable guidance and advice, continuous co-operation, valuable comments, suggestions, unlimited help and support throughout this work.

I would also want to extend my sincere gratitude to Professor A.S. Wood for his wonderful guidance, receptiveness to my ideas and thoughts, encouragement and support from the beginning of my study.

Special thanks to my university (Tikrit University, Iraq) and my government for their encouragement and financial support throughout my study.

Thanks also go to all staff members of School of Engineering Design and Technology-Bradford University. In particular, I would like to thank John Purvis and Mick Cribb for their help and support.

I am thankful as well as to all staff of Baiji North Oil Company, particularly, Dr. Riyadh Hameed Hasan for their continuous help in providing information.

Last but not least, I want to express my great gratitude to my parents for their enormous love, brothers and sisters for their unconditional support and encouragement. My warmest thanks go to my wife, my son and my daughter for their love, understanding, and patience, during my study.

Above all, I am very much grateful to almighty Allah for giving me courage and good health for completing the venture.

Table of Contents

Abstract ii

Acknowledgements iv

Table of Contents v

List of Tables xi

List of Figures xiv

Nomenclature xx

Abbreviations xxviii

List of Papers Published from this Work xxxi

Chapter One - Introduction **1**

1.1 Background 1

1.2 Petroleum Refining and Current Industrial Practice 3

1.3 Impurities Problems in Crude Oil 8

1.4 Challenges 12

1.5 Scope of the Research 13

1.6 Aims and Objectives of This Work 17

1.7 Thesis Layout 19

Chapter Two - Literature Review **22**

2.1 Introduction 22

2.2 Hydrotreating Process (HDT) 22

2.2.1 Principle Reactions of HDT 25

2.2.2 Process Variables of HDT Process 27

2.2.2.1 Temperature 28

2.2.2.2 Pressure 28

2.2.2.3 Liquid Hourly Space Velocity (LHSV) 29

2.2.2.4 Gas Rates (H2/Oil ratio) 30
2.3 Trickle Bed Reactors 30
2.4 Process Modelling 34
2.4.1 Hydrotreating Kinetic Models 37
2.4.2 Hydrocracking Kinetic Models 48
2.5 Process Simulation 54
2.6 Process Optimization 55
2.7 Parameter Estimation Techniques 58
2.8 Conclusions 60

Chapter Three - Experimental Work: Results and Discussion 62
3.1 Introduction 62
3.2 Pilot Plants 63
3.2.1 Materials Used 63
3.2.1.1 Feed Oil 63
3.2.1.2 Catalyst 63
3.2.2 Equipment and Procedure 64
3.2.2.1 Hydrotreating Pilot Plant 64
3.2.2.1.1 Experimental Runs 66
3.2.2.1.1.1 Catalyst Presulfiding 68
3.2.2.1.1.2 Operating Conditions 69
3.2.2.1.1.3 Sample Analysis 70
3.2.2.1.1.3.1 Sulfur Analysis 71
3.2.2.1.1.3.2 Metal Analysis 71
3.2.2.1.1.3.3 Nitrogen Analysis 72
3.2.2.1.1.3.4 Asphaltene Analysis 72
3.2.2.1.1.3.5 Other Tests 72

3.2.2.2 Distillation Unit 73
3.3 Results and Discussion 77
3.3.1 Effect of Operating Conditions on Impurities Removal 77
3.3.1.1 Sulfur Removal 77
3.3.1.2 Nitrogen Removal 79
3.3.1.3 Metals Removal 81
3.3.1.4 Asphaltene Removal 84
3.3.2 Productivity of Middle Distillates 86
3.3.3 The Production of New Fuel Oils 93
3.4 Conclusions 94

Chapter Four - gPROMS: general Process Modelling System 96
4.1 Introduction 96
4.2 gPROMS Simulator 97
4.3 Model Development using gPROMS 99
4.4 Defining a Model 100
4.5 Defining a Process 101
4.5.1 UNIT Section 102
4.5.2 SET Section 103
4.5.3 ASSIGN Section 103
4.5.4 INITIAL Section 103
4.5.5 SOLUTION PARAMETERS Section 104
4.5.6 SCHEDULE Section 105
4.6 Optimization in gPROMS 105
4.7 Comparison of gPROMS with other Commercial Software 106
4.8 Conclusions 107

Chapter Five - Mathematical Modelling, Simulation and Optimization of Crude Oil HDT Reactions: Results and Discussion 109

5.1 Introduction 109

5.2 Mathematical Model of TBR for HDT Reactions 110

5.2.1 Model Equations 111

5.2.1.1 Mass Balance Equations in Gas Phase 113

5.2.1.2 Mass Balance Equations in Liquid Phase 114

5.2.1.3 Mass Balance Equations in Solid Phase 115

5.2.1.4 Chemical Reaction Rate 116

5.2.1.5 Gas–Liquid Mass Transfer Coefficients 118

5.2.1.6 Liquid–Solid Mass Transfer Coefficients 118

5.2.1.7 Molecular Diffusivity 119

5.2.1.8 Henry's Law Coefficient 120

5.2.1.9 Oil Density 120

5.2.1.10 Oil Viscosity 121

5.2.1.11 Characteristics of the Catalyst Bed 121

5.2.1.12 Effectiveness Factor (η) 122

5.2.1.13 Kinetic Parameters of the Models 124

5.2.2 Optimization Problem Formulation for Parameter Estimation 125

5.2.3 Results and Discussion 128

5.2.3.1 Estimation of Kinetic Parameters 129

5.2.3.2 Simulation of Simultaneous HDT Pilot Plant Reactor System 150

5.3 Mathematical Models for Increasing of Middle Distillates Yield 153

5.3.1 Model Equations 154

5.3.2 Optimization Problem Formulation 156

5.3.3 Results and Discussion 156

5.4 Conclusions 160

Chapter Six - Design of Industrial Trickle Bed Reactor: Optimal Operation of Commercial Hydrotreating Unit **163**

6.1 Introduction 163

6.2 Design of Industrial TBR 165

6.2.1 Optimal Ratio of L_R/D_R 167

6.2.1.1 Optimization Problem Formulation 169

6.2.1.2 Results and Discussion 170

6.2.2 Mathematical Model of Industrial TBR with Energy Balance 172

6.2.2.1 Quench Process 174

6.2.2.2 Model Equations for Quench Zone 181

6.2.2.3 Case Study 183

6.2.2.4 Results and Discussion 186

6.2.2.5 Simulation of an Industrial HDT Reactor 191

6.3 Heat Integration and Energy Consumption in HDT Process 198

6.3.1 Heat Exchangers 200

6.3.2 Energy Consumption and Recovery Issues 201

6.3.3 Model Equations 203

6.3.4 Optimization Problem Formulation 207

6.3.4.1 Cost Function 208

6.3.5 Results and Discussion 210

6.4 Economic Analysis of Industrial Refining Process 211

6.4.1 Process Description 212

6.4.2 Cost Model Equations 215

6.4.3 Results and Discussion 221

6.5 Conclusions 224

Chapter Seven - Conclusions and Future Work 226

7.1 Conclusions 226

7.2 Future work 230

References 232

Appendix 1: Derivation of Mass Balance Equations 259

A.1 Mass Balance in Gas Phase 259

A.2 Mass Balance in Liquid Phase 261

List of Tables

Table 1.1	Oil fractions destinations and ultimate products with their boiling ranges (Hsu and Robinson, 2006)	7
Table 2.1	Worldwide refining process units (Stell, 2003)	23
Table 2.2	Typical process conditions for various hydrotreatment processes	27
Table 2.3	Some applications of trickle – bed reactor processes	32
Table 2.4	Summary of hydrotreating process modelling works	47
Table 2.5	Summary of hydrocracking kinetic models	53
Table 3.1	Feedstock properties	63
Table 3.2	Catalyst commercial properties (Co-Mo/γ-Al_2O_3)	64
Table 3.3	Operating conditions used	70
Table 3.4	Other tests methods for calculating the feed and products properties	73
Table 3.5	Yield analysis results	89
Table 3.6	Properties of oil fractions produced by conventional methods	91
Table 3.7	Properties of oil fractions produced by separation of hydrotreated crude oil	92
Table 3.8	Comparison of properties of reduced crude residue (RCR) produced by hydrotreated crude oil and conventional methods	93
Table 5.1	Values of constant parameters used in the HDT models	128
Table 5.2	Comparison of kinetic parameter values estimated with two approaches for HDS, HDN, HDAs, HDV and HDNi models	131

Table 5.3	Simulation data of the pilot plant-TBR using two approaches (linear and non-linear regression) versus experimental data for HDS of crude oil	136
Table 5.4	Simulation data of the pilot plant-TBR using two approaches (linear and non-linear regression) versus experimental data for HDN of crude oil	137
Table 5.5	Simulation data of the pilot plant-TBR using two approaches (linear and non-linear regression) versus experimental data for HDAs of crude oil	138
Table 5.6	Simulation data of the pilot plant-TBR using two approaches (linear and non-linear regression) versus experimental data for HDV of crude oil	139
Table 5.7	Simulation data of the pilot plant-TBR using two approaches (linear and non-linear regression) versus experimental data for HDNi of crude oil	140
Table 5.8	Kinetic parameters of the proposed model	157
Table 5.9	Experimental and predicted product compositions for 5 lumps discrete model	159
Table 6.1	Differences in length and diameter between pilot plant and industrial TBR (Bhaskar et al., 2004)	166
Table 6.2	Simulation results between *A* and B with the cost	170
Table 6.3	Summary of optimization results between *A* and B with the cost	171
Table 6.4	Simulation results with addition 5 % on L_R/D_R ratio	171
Table 6.5	Quench positions and rate fractions for two beds with cost results	187

Table 6.6	Different simulation results for three beds with cost results	189
Table 6.7	Values of constant parameters, factors and coefficients used in this model	210
Table 6.8	Results of optimization problem for heat integration process	211
Table 6.9	Summary of fixed operating cost	217
Table 6.10	Values of constant parameters, factors and coefficients used in this model	222
Table 6.11	Economic and comparison results of the developed HDT process	223

List of Figures

Figure 1.1	Actual and projected energy consumption scenarios (Ancheyta and Speight, 2007)	2
Figure 1.2	Typical layout for an oil refinery (Hsu and Robinson, 2006)	4
Figure 1.3	Crude distillation (Ancheyta and Speight, 2007)	4
Figure 1.4	Distillation column with trays (Ali and Abdul-Karim, 1986)	6
Figure 1.5	Schematic of a Trickle bed reactor	11
Figure 2.1	Schematic illustration of a fixed bed	31
Figure 2.2	Trickle bed reactor with cocurrent downflow	33
Figure 3.1	General scheme of the hydrotreating pilot-plant unit	65
Figure 3.2	Reactor configuration	67
Figure 3.3	Presulfiding procedure and conditions	69
Figure 3.4	Laboratory distillation unit at atmospheric pressure	74
Figure 3.5	Laboratory distillation unit at vacuum pressure	75
Figure 3.6	Experimental data variation of sulfur content vs. LHSV at different temperature and pressure	78
Figure 3.7	Experimental data variation of sulfur conversion vs. LHSV at different temperature and pressure	79
Figure 3.8	Experimental data variation of nitrogen content vs. LHSV at different temperature and pressure	80
Figure 3.9	Experimental data variation of nitrogen conversion vs. LHSV at different temperature and pressure	80
Figure 3.10	Experimental data variation of vanadium content vs. LHSV at different temperature and pressure	82
Figure 3.11	Experimental data variation of vanadium conversion vs. LHSV at different temperature and pressure	82

Figure 3.12	Experimental data variation of nickel content vs. LHSV at different temperature and pressure	83
Figure 3.13	Experimental data variation of nickel conversion vs. LHSV at different temperature and pressure	83
Figure 3.14	Experimental data variation of asphaltene content vs. LHSV at different temperature and pressure	85
Figure 3.15	Experimental data variation of asphaltene conversion vs. LHSV at different temperature and pressure	85
Figure 3.16	The difference between the conventional method (A) and this study (B)	87
Figure 3.17	Comparison of productivity of oil fractions produced by distillation process after HDT process (present study) and produced by conventional methods (HDT process of each fraction separately after distillation process)	90
Figure 4.1	An overview of the gPROMS modelling environment	99
Figure 4.2	A part of kinetic model file of the hydrotreating of crude oil	102
Figure 4.3	Part of the processes file for the kinetic model of crude oil hydrotreating	105
Figure 4.4	Part of the optimization file for the kinetic model of crude oil hydrotreating	106
Figure 5.1	Assumptions for modeling and simulation of hydrotreating reactor	111
Figure 5.2	Concentration profiles in a trickle-bed reactor (Ancheyta and Speight, 2007)	112
Figure 5.3	Linear representation of Arrhenius equation for crude oil hydrotreating	130

Figure 5.4	Sensitivity analysis of estimated parameters for HDS reaction	132
Figure 5.5	Sensitivity analysis of estimated parameters for HDN reaction	133
Figure 5.6	Sensitivity analysis of estimated parameters for HDAs reaction	133
Figure 5.7	Sensitivity analysis of estimated parameters for HDV reaction	134
Figure 5.8	Sensitivity analysis of estimated parameters for HDNi reaction	134
Figure 5.9	Experimental data (points) and simulated (lines) variation of outlet sulfur content vs. liquid hourly space velocity at different reactor temperature and at pressure (a) 4 MPa, (b) 7 MPa, (c) 10 MPa	141
Figure 5.10	Experimental data (points) and simulated (lines) variation of outlet nitrogen content vs. liquid hourly space velocity at different reactor temperature and at pressure (a) 4 MPa, (b) 7 MPa, (c) 10 MPa	142
Figure 5.11	Experimental data (points) and simulated (lines) variation of outlet asphaltene content vs. liquid hourly space velocity at different reactor temperature and at pressure (a) 4 MPa, (b) 7 MPa, (c) 10 MPa	143
Figure 5.12	Experimental data (points) and simulated (lines) variation of outlet vanadium content vs. liquid hourly space velocity at different reactor temperature and at pressure (a) 4 MPa, (b) 7 MPa, (c) 10 MPa	144

Figure 5.13	Experimental data (points) and simulated (lines) variation of outlet nickel content vs. liquid hourly space velocity at different reactor temperature and at pressure (a) 4 MPa, (b) 7 MPa, (c) 10 MPa	145
Figure 5.14	Comparison between experimental and calculated concentrations of sulfur	147
Figure 5.15	Comparison between experimental and calculated concentrations of nitrogen	148
Figure 5.16	Comparison between experimental and calculated concentrations of asphaltene	148
Figure 5.17	Comparison between experimental and calculated concentrations of vanadium	149
Figure 5.18	Comparison between experimental and calculated concentrations of nickel	149
Figure 5.19	Concentration profiles of H_2 and H_2S in gas phase down through the reactor	150
Figure 5.20	Concentration profiles of H_2S in liquid and solid phase down through the reactor	152
Figure 5.21	Concentration profiles of H_2 in liquid and solid phase down through the reactor	152
Figure 5.22	Concentration profiles of S, N, Asph, V and Ni in liquid and solid phase down through the reactor	153
Figure 5.23	Proposed kinetic model for increasing of middle distillates yields	155
Figure 5.24	Arrhenius plot for the different kinetic parameters	158

Figure 5.25	Comparison between the experiment and predicted product compositions	160
Figure 6.1	Trickle bed reactor with multicatalytic bed and quench technologies	176
Figure 6.2	Hydrotreating reactor: quench zone	177
Figure 6.3	Model representation of quench zone	182
Figure 6.4	Reactor temperature profiles for base hydrotreater along bed length	186
Figure 6.5	Reactor configuration with catalyst beds and quench	188
Figure 6.6	Temperature profiles for case 6, 8 and 9 with two quenches-three beds	190
Figure 6.7	Conversion results for case 6 and 8	191
Figure 6.8	Hydrogen profiles with quenching along the industrial bed length	192
Figure 6.9	Hydrogen sulfide profiles with quenching along the industrial bed length	193
Figure 6.10	Predicted evaluation profiles of sulfur along the industrial bed length	193
Figure 6.11	Predicted evaluation profiles of nitrogen along the industrial bed length	194
Figure 6.12	Predicted evaluation profiles of asphaltene along the industrial bed length	194
Figure 6.13	Predicted evaluation profiles of vanadium along the industrial bed length	195
Figure 6.14	Predicted evaluation profiles of nickel along the industrial bed length	195

Figure 6.15	Industrial TBR configuration with feedstocks and products properties	197
Figure 6.16	Grid notation for heat exchangers	200
Figure 6.17	Process of heat integrated reaction system	202
Figure 6.18	Heat exchanger H.E1	203
Figure 6.19	Heat exchanger H.E2	204
Figure 6.20	Heat exchanger CO1	205
Figure 6.21	Layout of a developed HDT unit with middle distillates production units	212
Figure 6.22	Schematic of conventional middle distillates production unit with HDT units	214
Figure A.1	Schematic representation of a typical TBR	259

Nomenclature

a	Dimensionless number
a_L	Gas–liquid interfacial area, cm^{-1}
a_S	Liquid–solid interfacial area, cm^{-1}
ACC	Annualized capital cost, \$/yr
A_{C1}	Heat transfer area of C1, m^2
A_{CO1}	Heat transfer area of CO1, m^2
A_{HE1}	Heat transfer area of H.E1, m^2
A_{HE2}	Heat transfer area of H.E2, m^2
A_{HE3}	Heat transfer area of H.E3, m^2
A_t	Total heat transfer area, m^2
A_C	Surface area, cm^2
A^0_j	Pre-exponential factor for reaction j, $(mol/cm^3)^{1-n}(cm^3/g.sec)(mol/cm^3)^{-m}$
bhp	Brake horsepower
CC	Capital cost, \$
C_{Cmpr}	Compression cost, \$/yr
C_{Col}	Cooling cost, \$/yr
C_{col}	Column cost, \$
C_{comp}	Compressor cost, \$
C_{Dis}	Distillation column cost, \$
$C_{F,2}$	Furnace cost, \$
C_H	Heating cost, \$/yr
C_{HE}	Heat exchanger cost, \$
C_{Swe}	Sweeting column cost, \$
C_{tray}	Tray cost, \$
C^L_i	Concentration of i compound in the liquid phase, mol/cm^3

C_i^S	Concentration of *i* compound in the solid phase, mol/cm^3
$C_{P,2}$	Pump cost, $
cp	Specific heat capacity, J/g.K
C_{PU}	Pumping cost, $/yr
C_R	Capital cost of the reactor, $
C_t	Overall annual process cost, $/yr
cp_w	Heat capacity of water, J/g.K
cv	Specific heat capacity at constant volume, J/g.K
De_i	Effective diffusivity of *i* compound in the catalyst pores, cm^2/sec
d_c	Diameter of cylindrical catalyst particle, cm
D_i^L	Molecular diffusivity of *i* compound in the liquid, cm^2/sec
$D_{K\,i}$	Knudsen diffusivity of *i* compound, cm^2/sec
D_R	Reactor diameter, cm
D_r^L	Radial mass dispersion coefficient, cm^2/sec
d_s	Diameter of spherical catalyst particle, cm
EA_j	Activation energy for *j* process, J/mol
FOC	Fixed operating cost, $/yr
F_C, F_m, F_p, F_d, F_T	Dimensionless factors
G_L	Liquid mass velocity, g/cm^2.sec
g	Gravitational constant, cm/sec^2
g_i	Gas mass flow rate of the *i* stream , g/sec
h_{H_2}	Henry‘s coefficient for hydrogen, MPa.cm^3/mol
h_{H_2S}	Henry‘s coefficient for hydrogen sulfide, MPa.cm^3/mol
hp	Compressor horsepower
k_i	kinetic constants, (wt%)$^{1-n}$ hr^{-1} (eqs. 5.98-5.102)

K_j	Reaction rate constant for *j* reaction, $(mol/cm^3)^{1-n}(cm^3/g.sec)(mol/cm^3)^{-m}$
K_{H_2S}	Adsorption equilibrium constant of H_2S, cm^3/mol
K_i^L	Gas–liquid mass transfer coefficient for *i* compound, cm/sec
K_i^S	liquid–solid mass transfer coefficient for *i* compound, cm/sec
L	Length of particle, cm
L_c	Length of cylindrical catalyst particle, cm
l_i	Liquid mass flow rate of the *i* stream , g/sec
L_R	Length of reactor bed, cm
m_j	Order of reaction of hydrogen in reaction *j*
$m_{w,2}$	Mass flow rate of cooling water, g/sec
n_j	Order of reaction of *i* compound in reaction *j*
Mw	Molecular weight
OAC	Overall annualized cost, $/yr
p	Reactor total pressure, psia (eq.5.63)
P	Reactor total pressure, bar (eq.6.27), MPa (eq.6.28)
$P_{H_2}^G$	Partial pressure of hydrogen, MPa
$P_{H_2S}^G$	Partial pressure of hydrogen sulfide, MPa
P_e	Peclet number
P_{in}	Inlet pressure, lb/ft^3
P_{out}	Outlet pressure, lb/ft^3
q	Quench mass flow rate, g/sec
Q	Quench
Q_i	Heat duties of $H.E_{1,2,3}$, CO1, C1 and $F_{1,2}$, J/sec
Q_{in}	Volumetric flow rate at compressor section, ft^3/min
$Q_{p,2}$	Power pump, kW

r	Particle radius, cm
r_g	Pore radius, cm
r_j	Chemical reaction rate of j reaction, wt% hr^{-1} (eqs. 5.98-5.102)
r_j	Chemical reaction rate of j reaction per unit mass of catalyst, $mol/g.sec^{-1}$
R	Universal gas constant, J/mol.K
Re_L	Reynold number
TAC	Total annual cost, $/yr
$TACC$	Total annual capital cost, $/yr
$TAOC$	Total annual operating cost, $/yr
TCC	Total capital cost, $
TCI	Total capital cost of installed equipment, $
S_g	Specific surface area of particle, cm^2/g
S_p	Total geometric external area of particle, cm^2
$Sp.gr_{15.6}$	Specific gravity of oil at 15.6°C
T_{meABP}	Mean average boiling point, °R
T_{C0}	Inlet temperature of the cold fluid to H.E1, K
T_{C1}	Outlet temperature of the cold fluid from H.E1, K
T_{Cr1}	Inlet temperature of the cold fluid to H.E3, K
T_{Cr2}	Outlet temperature of the cold fluid from H.E3, K
T_{Fout}	Outlet temperature from F2, K
T_{FP}	Outlet product temperature from CO1, K
T_{H0}	Inlet temperature of the cold fluid to H.E2, K
T_{H1}	Outlet temperature of the cold fluid from H.E2, K
T_{N1}	Inlet temperature of the hot naphtha to C1, K
T_{N2}	Outlet temperature of the hot naphtha from C1, K
T_P	Outlet temperature of the hot products mixture from H.E2, K

T_{P1}	Inlet temperature of the hot products mixture to H.E1, K
T_{P2}	Outlet temperature of the hot products mixture from H.E1, K
T_R	Inlet reactor temperature, K
T_{RCR1}	Inlet temperature of the hot R.C.R to H.E3, K
T_{RCR2}	Outlet temperature of the hot R.C.R from H.E3, K
Tw_1	Inlet water temperature to CO1, K
Tw_2	Outlet water temperature from CO1, K
T_{WC1}	Inlet water temperature to C1, K
T_{WC2}	Outlet water temperature from C1, K
U_{C1}	Overall heat transfer coefficient for C1, $W/m^2 K$
U_{CO1}	Overall heat transfer coefficient for CO1, $W/m^2 K$
U_{HE1}	Overall heat transfer coefficient for H.E1, $W/m^2 K$
U_{HE2}	Overall heat transfer coefficient for H.E2, $W/m^2 K$
U_{HE3}	Overall heat transfer coefficient for H.E3, $W/m^2 K$
u_g	Velocity of the gas, cm/sec
u_L	Velocity of the liquid, cm/sec
x_i	Mass fraction of *i* compound
v	Volume, cm^3
$y_{1,2}$	Mass fraction of quench fluid
V_g	Pore volume per unit mass of catalyst, cm^3/g
V_G	Volumetric flow rate of gas, cm^3/sec
V_{H_2}	Molar gas volume of H_2 at standard conditions, Nl/mol
V_{H_2S}	Molar gas volume of H_2S at standard conditions, Nl/mol
V_L	Volumetric flow rate of crude oil, cm^3/sec
V_N	Volumetric flow rate of naphtha, cm^3/sec
VOC	Variable operating cost, $/yr

V_p	Total geometric volume of catalyst, cm^3
V_{RCR}	Volumetric flow rate of RCR, cm^3/sec
z	Axial position along the catalyst bed, cm
z_0	Bottom of the reactor, cm
z_f	Top of the reactor, cm

Greek letters

ΔH_R	Overall heat of reaction, J/mol
ρ_B	Bulk density of the catalyst particles, g/cm^3
ρ_{cat}	Density of the catalyst particles, g/cm^3
ρ_L	Liquid density at process conditions, lb/ft^3 (eq.5.62)
$\rho_{15.6}$	Specific gravity of oil at 15.6°C
ρ_G	Gas density, g/cm^3
ρ_{20}	Density of the oil at 20°C, g/cm^3
ρ_0	Density of oil at 15.6°C and 101.3 kPa, lb/ft^3
ρ_p	Particle density, g/cm^3
η_j	Catalyst effectiveness factor for *j* reaction
η_{ise}	Isentropic efficiency
ε	Void fraction of the catalyst bed
ε_g	Gas phase fraction
ε_l	Liquid phase fraction
μ_L	Liquid viscosity at process conditions, mPa.sec (eq.5.65)
υ_C^L	Critical specific volume of liquid feedstock, ft^3/mol
$\upsilon_C^{H_2}$	Critical specific volume of H_2, cm^3/mol

$\upsilon_C^{H_2S}$	Critical specific volume of H_2S, cm^3/mol
υ_L	Molar volume of liquid feedstock, cm^3/mol
υ_i	Molar volume of *i* compound, cm^3/mol
λ_{H_2}	Solubility coefficient of H_2, $Nl.kg^{-1}. MPa^{-1}$
λ_{H_2S}	Solubility coefficient of H_2S, $Nl.kg^{-1}. MPa^{-1}$
$\Delta\rho_P$	Pressure dependence of liquid density, lb/ft^3
$\Delta\rho_T$	Temperature correction of liquid density, lb/ft^3
ϕ_i	Thiele Modulus of *i* compound in reaction *j*
θ	Particle porosity
τ	Tortuosity factor, Residence time (hr)
γ	Specific heat ratio
ΔT_{lm}	log mean temperature difference

Superscripts

exp	Experimental
cal	Calculated
G	Gas phase
H_2	Hydrogen
H_2S	Hydrogen sulfide
L	Liquid phase or gas-liquid interface
Q	Quench
S	Solid phase or liquid-solid interface

Subscripts

Asph	Asphaltene
B	Bulk
c	Cylindrical, Catalyst
CH_4	Methane
F	Feed
g	Gas
G	Gases
H_2	Hydrogen
H_2S	Hydrogen sulphide
HK	Heavy Kerosene
L, l	Liquid
LGO	Light Gas Oil
N	Nitrogen, Naphtha
NH_3	Ammonia
Ni	Nickel
p	Particle, Product
r	Radial
R	Reactor, R.C.R
s	Spherical
sul	Sulfur
V	Vanadium

Abbreviations

API	American Petroleum Institute
AR	Atmospheric Residue
ASTM	American Society for Testing and Materials
Asph	Asphaltenes
C	Carbon
C1	Condenser
CAD	Computer–Aided Design
CM	Conventional Method
CO1	Cooler
Co–Mo	Cobalt–Molybdenum
DAEs	Differential and algebraic equations
DAO	Deasphaltened Oil
DMDS	Dimethyl disulfide
$F_{1,2}$	$Furnace_{1,2}$
FCC	Fluidized Catalytic Cracking
G	Gases
GA	Genetic Algorithm
gPROMS	general Process Modelling System
$H.E_{1,2}$	$Heat\ Exchanger_{1,2}$
H.P.S	High pressure separator
HDA	Hydrodearomatization
HDAs	Hydrpdeasphaltenezation
HDC	Hydrocracking
HDM	Hydrodemetalization
HDN	Hydrodenitrogenation

HDNi	Hydrodenickelation
HDO	Hydrodeoxygenation
HDS	Hydrodesulfurization
HDT	Hydrotreating
HDV	Hydrodevanadization
H.N	Heavy Naphtha
H.K	Heavy Kerosene
HGO	Heavy Gas Oil
HTA	Tri–aromatics
HTO	Olefins saturation
IBP	Initial Boiling Point
IP	Institute of Petroleum
L.G.O	Light Gas Oil
L.P.S	Low pressure separator
LHSV	Liquid Hourly Space Velocity
L.N	Light Naphtha
LO	Light Oils
LP	Linear Programming
M&S	Marshall and Swift index for cost escalation
N	Nitrogen, Naphtha
NB	Basic nitrogen compounds
Ni	Nickel
NLP	Non Linear Programming
N_{NB}	Nonbasic nitrogen compounds
ODEs	Ordinary Differential Equations
P	Pressure

P_1	$Pumps_1$
PSE	Process System Enterprise
R.C.R	Reduced Crude Residue
S	Sulfur
Sp.gr	Specific gravity
SSE	Sum of the Squared Errors
SOP	Successive Quadratic Programming
T	Temperature
TBRs	Trickle Bed Reactors
TEL	Tetra Ethyl Lead
V	Vanadium
V.G.O	Vacuum Gas Oil
V.R	Vacuum Residue

List of Papers Published from this Work

1. Aysar T. Jarullah, Iqbal M. Mujtaba, Alastair S. Wood. Operating Conditions Optimization of Crude Oil Hydrodeasphaltenization in Trickle Bed Reactor. *IChemE Computer Aided Process Engineering Subject Group*. PhD Poster Day 2010, University of Leeds, UK, 12 May 2010.

2. Aysar T. Jarullah, Iqbal M. Mujtaba, Alastair S. Wood. Kinetic Parameter Estimation and Simulation of Trickle Bed Reactor for Hydrodesulfurization of Crude Oil. *Chemical Engineering Science*, Volume **66**, Issue 5, Pages 859-871, 2011.

3. Aysar T. Jarullah, Iqbal M. Mujtaba, Alastair S. Wood. Improvement of the Middle Distillate Yields during Crude Oil Hydrotreatment in a Trickle Bed Reactor. *Energy & Fuels*, Volume **25**, Issue 2, Pages 773-781, 2011.

4. Aysar T. Jarullah, Iqbal M. Mujtaba, Alastair S. Wood. Kinetic model development and simulation of simultaneous hydrodenitrogenation and hydrodemetallization of crude oil in trickle bed reactor. *Fuel*, Volume **90**, Issue 6, Pages 2165-2181, 2011.

5. Aysar T. Jarullah, Iqbal M. Mujtaba, Alastair S. Wood. Enhancement of Productivity of Distillate Fractions by Crude Oil Hydrotreatment: Development of Kinetic Model for the Hydrotreating Process. *Computer Aided Chemical Engineering,* Volume **29**, Part A, Pages 261-265, 2011.

6. Aysar T. Jarullah, Iqbal M. Mujtaba, Alastair S. Wood. Modelling and Optimization of Crude Oil Hydrotreating Process in Trickle Bed Reactor: Energy Consumption and Recovery Issues. *Chemical Product and Process Modeling*, Volume **6**, Issue 2, Art 3, Pages 1-19, 2011.

7. Aysar T. Jarullah, Iqbal M. Mujtaba, Alastair S. Wood. Whole Crude Oil Hydrotreating from Small Scale Laboratory Pilot Plant to Large Scale Trickle-Bed Reactor for: Analysis of Operational Issues through Modelling. *Accepted in Energy & Fuels*.

8. Aysar T. Jarullah, Iqbal M. Mujtaba, Alastair S. Wood. Improving Fuel Quality by Whole Crude Oil Hydrotreating: A Kinetic Model for Hydrodeasphaltenization in a Trickle Bed Reactor. *Submitted to Applied Energy*.

Chapter One

Introduction

1.1 Background

Petroleum has remained a significant part of our lives and will do so for the next decades. The fuels that are produced from petroleum supply more than half of the world's total supply of energy. Gasoline, kerosene, and diesel oil provide fuel for automobiles, tractors, trucks, aircraft, and ships. Fuel oil, heavy oil and natural gas are employed for heating homes and commercial buildings in addition to generating electricity. Petroleum products represent the main materials utilized for synthetic fibers manufacturing (for clothing), plastics, paints, fertilizers, insecticides, soaps, and synthetic rubber. Today, the uses of petroleum as a source of raw material in manufacturing are central to the functioning of modern industry (Hsu and Robinson, 2006).

Petroleum refining is now in an important transition period as the industry has moved into the 21st century and the market demand for petroleum products has shown a significant growth in recent years. This means that the demand of transportation fuels will, without doubt, show an increase in demand during the next decade, which can be fulfilled by the processing of heavier feedstocks (Ancheyta and Speight, 2007).

Petroleum is by far the most commonly used source of energy, especially as a source of liquid fuels (Figure 1.1). World energy usage has increased by an average of 1.7% annually from 1997-2007 (Stacy et al., 2008). In fact, according to the vast use of petroleum, the last 100 years could very easily be dubbed as the oil century (Ryan, 1998).

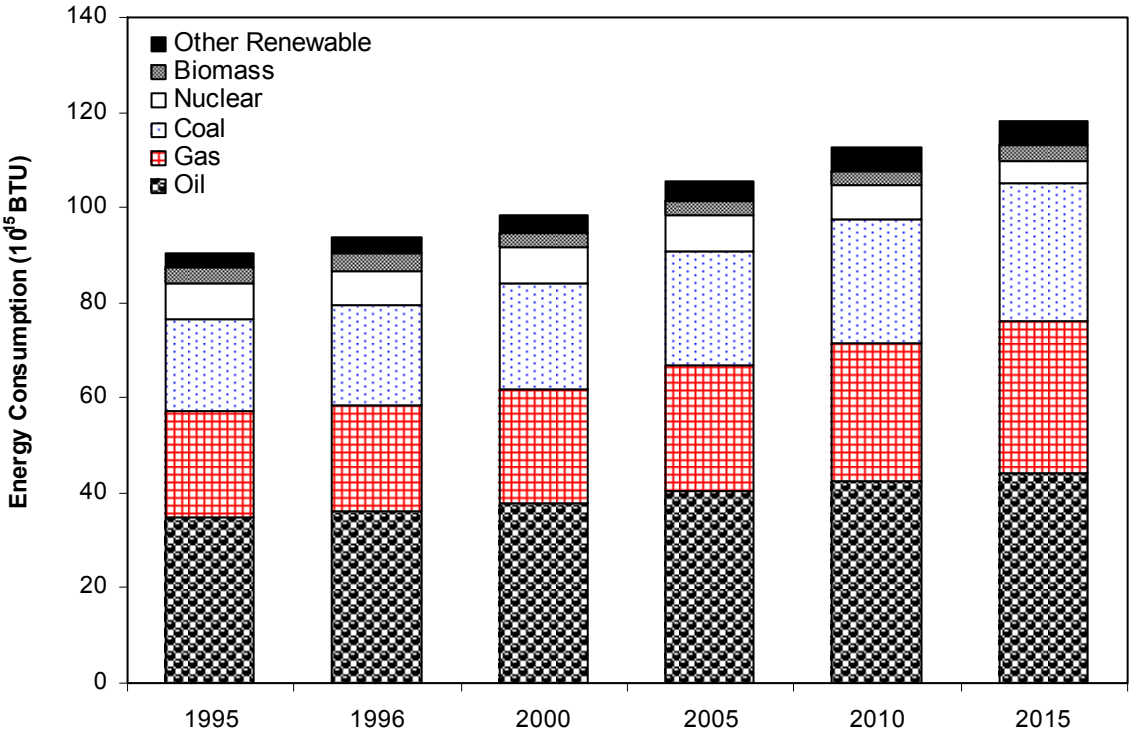

Figure 1.1: Actual and projected energy consumption scenarios (Ancheyta and Speight, 2007)

As a result, petroleum is projected to be the major source of energy over the coming decades. In this respect, fossil fuels and their associates (heavy oils and residua) are extremely significant in any energy scenario, particularly those scenarios that relate to the production of liquid fuels (Ancheyta and Speight, 2007; Khalfallah, 2009).

It is a fact that in recent years, the average quality of petroleum has declined, which has caused the nature of crude oil refining to change considerably (Swain, 1998). This, of course, has led to the need for managing crude quality more effectively through evaluation and product sepcifications (Waguespack and Healey, 1998; Speight, 2006). The declining reserves of light oils in the world have resulted in an increasing need for developing choices to remove the impurities (such as sulfur, nitrogen, metals, asphaltene) and upgrade the heavy feedstocks, specifically heavy oil and bitumen. This has resulted in a diversity of operation choices that specialize in contaminants removal during refining (Armstrong et al., 1997).

The increasing supply of heavy oils as refinery feedstocks is a serious matter and it is necessary that refineries are able to accommodate these heavy feedstocks. For satisfying the changing pattern of product demand, important investments in refining conversion operations will be essential to profitably use these heavy feedstocks. The most efficient and economical solution to this problem will depend widely on individual country and company situations. However, the most promising technologies will likely include the conversion of heavy crude oil, vacuum bottom residua, asphalt from deasphalting processes, and bitumen from tar sand deposits (Hsu and Robinson, 2006).

With all of the scenarios in place, there is no doubt that *petroleum* and its relatives (residua, heavy oils as well as tar sand bitumen) will be required for producing a considerable proportion of liquid fuels into the foreseeable future.

1.2 Petroleum Refining and Current Industrial Practice

A typical petroleum refinery is a complex chemical processing and manufacturing unit, with crude oil feedstock going in and refined fractions (products) coming out. Refining occurs by fractionation (distillation) of crude oil into a series of product streams based on boiling ranges for each fraction. Figure 1.2 shows a typical layout for an oil refinery.

Crude oil distillation (Figure 1.3) is more complex than product distillation, in part due to the fact that crude oil contains water, salts, and suspended solids. These materials are removed from crude oil before the distillation process in order to reduce corrosion, plugging, and fouling in crude heaters and towers, and in order to prevent the poisoning of catalysts in downstream units by a process, which is called desalting. There are two typical methods that are commonly used for crude oil desalting: chemical and electrostatic separation, utilize hot water for dissolving the salts and collect suspended solids.

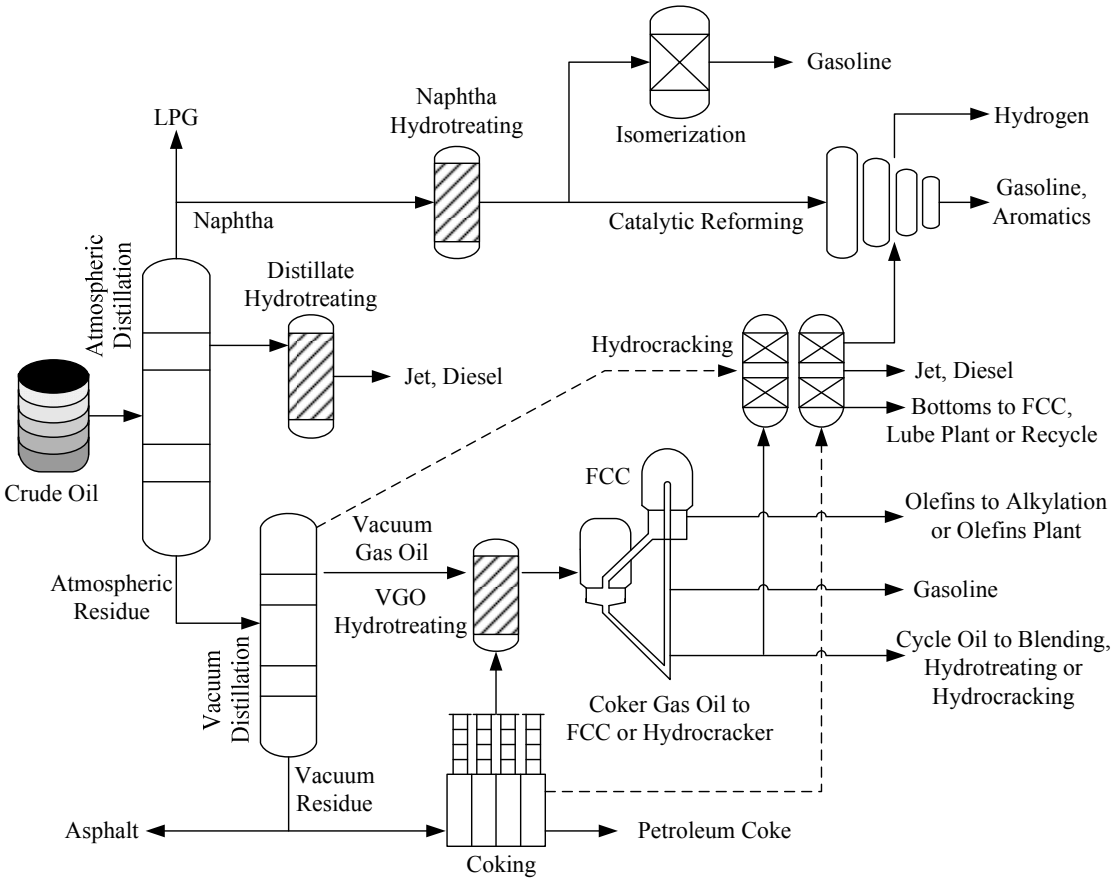

Figure 1.2: Typical layout for an oil refinery (Hsu and Robinson, 2006)

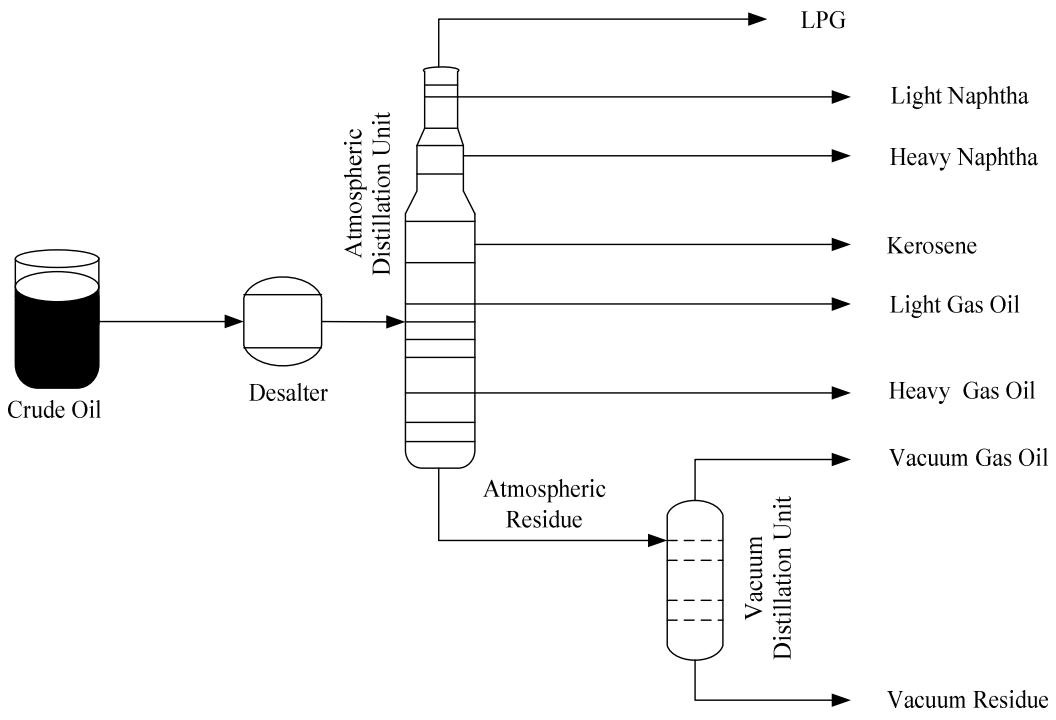

Figure 1.3: Crude distillation (Ancheyta and Speight, 2007)

In a chemical desalting process, water and surfactants are added to the crude oil, which is heated in order to dissolve salts and other contaminants, and then is sent to a settling tank where the water and oil separate. In a second method (electrostatic desalting), chemicals are replaced with a strong electrostatic charge, which drives the separation of water from oil (Ali and Abdul-Karim, 1986).

Modern operation of crude oil distillation columns can process 200,000 barrels of oil per day (Hsu and Robinson, 2006). These towers can be up to 50 meters high and contain 20 to 40 fractionation trays spaced at regular intervals. Before entering the distillation column, desalted crude oil passes through a network of pre-heat exchangers in order to heat it initially with hot material drawn from the bottom of the distillation tower to raise its temperature up to 232.2°C and then to a heating furnace, which brings the temperature up to about 343.3°C. This is to do with heat recovery and energy saving (Ashaibani and Mujtaba, 2007). This part of the process is essential because the carbon will be deposited inside the pipes and equipment through which it flows when the oil gets much hotter. The hot crude oil enters the distillation column and most of it vaporizes. Unvaporized heavy oil cuts and residue will drop to the bottom of the column, where it is drawn off. Inside the tower distillation column, there are the so-called trays (Figure 1.4), which help in the separation of crude oil to the required light derivatives. These trays permit the vapors from below to pass through and contact with the condensed liquid on top of the tray, thus providing excellent contact between vapor and liquid. Condensed liquid flows down through a pipe to the hotter tray below, where the higher temperature causes re-evaporation. A given molecule evaporates and condenses many times before finally leaving the tower.

Products are collected from the top, bottom and side of the column. Side draw products are taken from trays at which the temperature corresponds to the cut point for a desired product. In modern towers, a portion of each side draw stream is returned to the tower

to control tray temperatures and further enhance separation. Part of the top product is also returned; this “reflux” plays a major role in controlling temperature at the top of the tower.

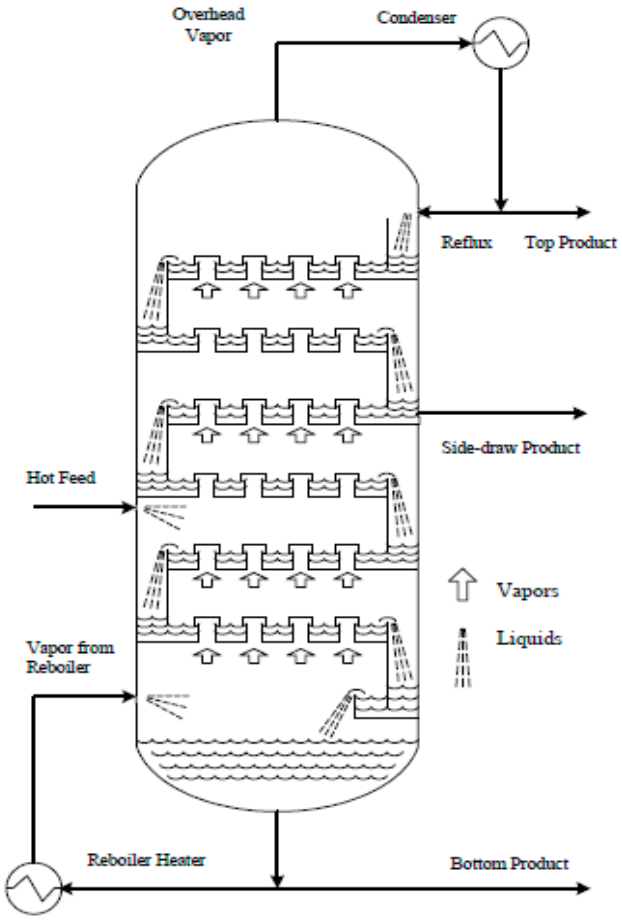

Figure 1.4: Distillation column with trays (Ali and Abdul-Karim, 1986)

The reduced crude residue-R.C.R (the part remaining at the bottom of the atmospheric distillation - above 350 ^{0}C) will be sent to a vacuum distillation tower, which recovers additional liquid at 4.8 to 10.3 kPa. The vacuum, which is created by a vacuum pump, is pulled from the top of the tower. The overhead stream – light vacuum gas oil, can be utilized as a lube base stock, heavy fuel oil, or as feed to a conversion unit. Heavy vacuum gas oil is pulled from a side draw. The remaining part at the bottom of the vacuum distillation column is called Vacuum Residue (V.R). This part is taken to the Deasphaltened (DAO) and De–wax Units in order to remove the asphaltenes and wax

respectively. The oil product is called Bright-stock. The vacuum residue (V.R) can be sent to a coking or visbreaking unit for further processing. After leaving the tower, products stream go to the downstream process units, where each compound (such as light naphtha (L.N), heavy naphtha (H.N), heavy kerosene (H.K), diesel oil, light gas oil, (L.G.O), vacuum gas oil (V.G.O) or bright-stock) will be sent to the hydrotreating units in order to remove the impurities (mainly sulfur, nitrogen, metals and asphaltene). Table 1.1 shows some of oil fractions destinations and ultimate products with their boiling ranges.

Table 1.1: Oil fractions destinations and ultimate products with their boiling ranges (Hsu and Robinson, 2006)

Oil Fractions	**Approx. Boiling Ranges (^{0}C)**	**Next Destination**	**Ultimate Products**
LPG	-40 to 0	Sweetener	Propane fuel
Light Naphtha	IBP - 85	Hydrotreating	Gasoline
Heavy Naphtha	85 – 200	Cat. Reformer	Gasoline, aromatics
Kerosene	170 – 270	Hydrotreating	Jet fuel, diesel No.1
Gas Oil	180 – 240	Hydrotreating	Heating oil, diesel No.2
Vacuum Gas Oil	340 - 566	FCC	Gasoline, LGO, gases
		Hydrotreating	Fuel oil, FCC, feed
		Lube Plant	Lube basestock
		Hydrocracking	Gasoline, jet fuel, diesel, FCC feed, basestock
Vacuum Residue	> 540	Coker	Coke, coker gas oil,
		Visbreaking	Visbreaker gas oil, resid
		Asphalt Unit	Deasphalted oil, asphalt
		Hydrotreating	FCC feed

The most valuable products from crude oil are gasoline, kerosene (jet fuel) and diesel oil. In order to enhance the amount of these fractions, heavier streams are cracked down into smaller molecules by a Fluid Catalytic Cracking (FCC) unit. The profitability of the FCC operation depends mainly on the type of catalyst used in the FCC unit and upon the kind of feedstock being processed. FCC generally uses a solid acid zeolite catalyst.

The larger molecules are broken into smaller molecules in order to create additional material in the naphtha range for producing more valuable product, gasoline (Harding et al., 2001).

Two additional operations, Catalytic reforming and Alkylation processes, are employed for improving the fuel quality, especially gasoline. The reforming process takes straight chain hydrocarbons from naphtha cuts and rearranges them into compounds containing benzene rings. In the unit, hydrogen is produced as a by product of the reaction. Catalytic reforming utilizes Platinum (Pt) based catalyst to isomerize linear paraffins to branched paraffins having high octane number like 2,3-dimethylbutane (Fowler and Book, 2002).

The second process employed for improving the gasoline quality is alkylation, that includes the combination of small hydrocarbon molecules into larger molecules. In this reactions, *n*-butene reacts with isobutane to generate 2,2,4-trimethylpentane (isooctane), and other branched paraffins. Alkylation also utilizes an acid catalyst, but owing to excessive coking, just liquid acid catalysts are currently employed (Ackerman et al., 2002).

1.3 Impurities Problems in Crude Oil

Crude oil is a very complex material consisting of different hydrocarbon compounds in addition to sulfur, nitrogen, oxygen and some metallic compounds, containing nickel, vanadium, iron and copper (Ali and Abdul-Karim, 1986). Market demands for different crude oil derivatives are high. The average consumption of different fuels such as Gasoline, Kerosene, Jet fuels, etc is equivalent to 40-50% of crude oil consumption and the worldwide consumption will increase in the next years (Ray et al., 1995). Therefore, it is necessary to increase distillate production at high quality.

The presence of sulfur, nitrogen, oxygen and metallic compounds in crude oil has a significant impact upon the quality of oil products in addition to the harm they can cause. Sulfur compounds lead to environmental pollution through atmospheric contamination by oxidization resulting from combustion forming sulfur dioxides, which will be oxidized later with ultraviolet rays to SO_3. These compounds react with atmospheric water to form sulfuric acid that causes many lung diseases, like asthma and shortness of breath. It also leads to soil pollution with acid materials, decreases the life of machinery, corrodes pipes, machines and equipment, affecting the additives used for the purpose of increasing the octane number, reducing the activity of Tetra Ethyl Lead (TEL) added to gasoline. As a result, the engine metal will erode, leading to the destruction of metallic parts. The same is true with gas oil and diesel fuel as well as lubricating oils. Also, their emissions are very dangerous to human safety and environment. In addition, these impurities cause catalyst poisoning and reduce the catalyst activity. Therefore, environmental regulations have enforced substantial decrease of sulfur compounds in fuels (Gajardo, 1982; Ali and Abdul-Karim, 1986; Kim and Choi, 1987; Mahmood et al., 1990; Andari, 1996; Speight, 2000).

The presence of nitrogen compounds in crude oil or oil fractions has also a detrimental effect for refining industries. Nitrogen compounds are responsible for catalyst poisoning and reducing catalyst activity, where these impurities lead to dye formation that causes catalyst poisoning leading to reduced activity of the catalyst (Gajardo, 1982; Al-Humaidan, 2004). Furthermore, nitrogen compounds have toxic effects on the storage stability of oil products and affect the colour of oil products (Speight, 2000). Andari et al. (1996) have demonstrated the impact of nitrogen and sulfur compounds through their studies of Naphtha, Kerosene and Diesel oils derived from Al-Kuwait crude oil and they proved that these compounds showed unwanted influence on the stability of fuel in addition to the environmental pollution. Kaernbach et al. (1990) confirmed that the

nitrogen compounds significantly affect the catalyst activity through their works on the vacuum residue.

Metallic compounds in crude oil have also been of great interest to researchers due to the problems caused by these compounds. The existence of metallic compounds in crude oil and its fractions has harmful effects. These compounds have a very bad influence on the hydrotreating (HDT) efficiency, plug the pores of catalysts used, cause rapid deactivation for the hydroprocessing catalyst, where they tend to deposit on the catalyst, and seem to act to reduce HDT activity by decreasing catalyst surface area (Abbas, 1999; Pereira et al., 1990; Bartholdy and Cooper, 1993). Also, the presence of vanadium and nickel in addition to iron and copper affects the activity of cracking catalysts and increase the level of coal deposited. The presence of these compounds, especially vanadium in the fuel used in the high power machines as gaseous turbines, leads to the formation of some sediment on the turbine, which can lead to a change in the balance of the rotating parts of tubine (Ali and Abdul-Karim, 1986; Gary and Handwerk, 1994). Furthermore, the ash resulting from the combustion of fuels containing sodium and particularly vanadium reacts with refractory furnace linings to lower their fusion points and hence cause their destruction (Speight, 2000).

Asphaltenes, which are well known to be coke precursors, as they are the most complex molecules present in petroleum, complex mixture of high-boiling, high-molecular weight compounds and consist of condensed polynuclear aromatics carrying alkyl, cycloalkyl, and have highly undesirable compounds such as sulfur, nitrogen, nickel and vanadium, and their content varies greatly in crude oils (Benito et al., 1997; Callejas and Martı´nez, 2000; Areff, 2001). Asphaltenes are mainly responsible for catalyst deactivation during catalytic hydrotreating or hydrocracking of heavy oils and residues owing to their tendency to form coke. In the particular case of hydrotreating (HDT) of heavy oils, asphaltenes affect the overall rate of HDT reactions, they precipitate on the

catalyst surface and close the pore mouth, acting as a coke precursor that leads to the deactivation of the catalyst and cause a many troubles throughout the petroleum refinery (Wauquier, 1995; Abbas, 1999; Trejo and Ancheyta, 2005; Calemma et al., 1998). The presence of polar chemical functions of asphaltenes in oil formations probably limits the hydrocarbons production. The asphaltenes compounds are rather responsible for high density and viscosity of crude oils and heavy oils, which leads to transport problems (Wauquier, 1995; Ting et al., 2003).

Many scientists have studied the probability of getting rid of such compounds by many approaches. One of the prominent methods was removing them with hydrogen, which is called the hydrotreating process (HDT) (Shimura, 1986). In the petroleum refining industry, HDT reactions that include Hydrodesulfurization (HDS), Hydrodenitrogenation (HDN), Hydrodeasphaltenization (HDAs), Hydrodemetalliztion (HDM), Hydrodeoxygenation (HDO), and Hydrocracking (HDC) are carried out in Trickle Bed Reactors (TBRs) (Figure 1.5). These reactors in which three phases, liquid (oil), gas (mostly hydrogen) and solid catalyst particle are frequently preferred due to ease of control and used for different feedstocks (Areff, 2001; Macı´as and Ancheyta, 2004). More details about HDT and TBR process will be discussed in chapter 2.

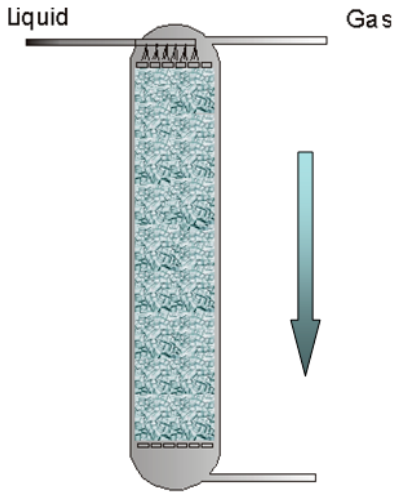

Figure 1.5: Schematic of a Trickle bed reactor

1.4 Challenges

The hydrotreating process is one of the most important processes in refineries for reducing the content of the sulfur, nitrogen, oxygen, metallic and other contaminants from oil fractions at high operating conditions. The process of crude oil hydrotreating is a new challenge and new technology that has not been considered previously. Conventionally, all hydrotreating processes are carried out on each oil cut separately, and not on the full crude oil (i.e. after the separation of crude oil to its derivatives, such as gasoline, kerosene, light and heavy gas oil). This means that a large amount of the impurities, namely, sulfur, nitrogen, metals, aromatics and asphaltenes will be deposited at the bottom of the atmospheric and vacuum distillation column. In addition, hydrotreating each oil cut separately is fairly easy due to the ability to control the reaction, the knowledge of physical and chemical properties, the kind of reaction and its condition. Hydrotreating of crude oil is regarded as a difficult challenge since the crude oil involves a lot of compounds and multiple phases, in addition to difficult structures. Additionally, hydrotreating of crude oil in the existence of asphaltenes that contain a large amount of these impurities, especially metals that close the active sites on the catalyst is one of the more difficult and significant problems. The expected benefits of directly hydrotreating crude oil are improvements of middle distillates productivity due to conversion of heavy compounds and long molecules that is concentrated in heavy fractions to light compounds. This is in contrast to conventional processes that are carried out for each cut separately, which means that the heavy compounds and long molecules will be deposited at the bottom of the atmospheric and vacuum distillation column, making them difficult to hydrotreat using normal operations and conditions.

Furthermore, the mathematical modelling of the hydrotreating of crude oil is a hard task in view of the intricate physiochemical changes that are undergone in the feed together with transport phenomena and mechanisms of catalyst deactivation in the reaction

system. The major challenge is the accurate evaluation of the kinetic models, which can confidently predict the product compounds at different process conditions. For HDS, HDN, HDAs, HDV and HDNi reactions, the development of such kinetic models is a hard task due to the great variety of structures.

1.5 Scope of the Research

This research is focused on the optimal design of a trickle bed reactor (TBR) for crude oil hydrotreating in order to achieve the goal of reducing the impurities (mainly, sulfur (S), nitrogen (N), asphaltene (Asph), vanadium (V), nickel (Ni)), while at the same time increasing the productivity of oil fractions. Also sought is the improvement of the properties of reduced crude residue-R.C.R (used as a main feedstock to vacuum distillation units in order to produce base oil and vacuum gas oil (V.G.O) in addition to lubricating oils) and the possibility of producting of new fuel oils and a comparison in the productivity and cost between oil fractions produced by distillation process after HDT and those produced by conventional methods (HDT process of each fraction separately after distillation).

The worldwide request for transportation fuel or middle distillates (such as car fuel, Jet fuel, diesel fuel) with fuel quality, which satisfies environmental legislations, is growing (Ho, 2010). This demand dictates the necessity for conversion capacity, which will be able to selectively produce oil fractions, especially middle distillates. Therefore, the petroleum refining industry has made efforts to find solutions for processing greater quantity of heavy oils for increasing the production of transportation fuels (Alvarez and Ancheyta, 2009). In order to meet the challenges, a number of technologies have been developed to refine and improve heavy oils into more valuable transportation fuels beside content of the impurities such as, sulfur (S), nitrogen (N), metals (V and Ni) and

asphaltene (Asph). Among these technologies, catalytic hydrotreating process (HDT), has the potential for increasing the productivity of distillate cuts and also simultaneously reducing the concentration of contaminates, mainly S, N, V, Ni and Asph (Valavarasu et al., 2003; Hossain et al., 2004) and at the same time increasing the quality and quantity of distillate fractions.

The HDT route includes contact of the oil feedstocks with hydrogen at high reaction temperature and pressure. The compounds that have high molecular weight in the oil feedstock will be cracked and saturated with H_2 to yield distillate fractions with increasing H/C ratio and decreasing content of the impurities. This process is carried out by using high activity hydrotreating catalysts, which have the following main features: (a) enhancing the elimination of undesirable impurities (S, N, V, Ni, Asph) by promoting HDS, HDN, HDV, HDNi and HDAs reactions, respectively, (b) precipitating the conversion of the high molecular weight compounds into light compounds, (c) reinforcing hydrogenation of the cracked compounds that lead to increased H/C ratio of the products, and (d) reducing the coke formation (Marafi et al., 2006).

The HDT process involves a number of reactions mentioned in the previous section. Therefore, it is important to find the chemical reactions for such a process. Through the removal of the contaminates during HDT reactions, some conversion in the boiling range of the feedstock also takes place due to the impurities containing molecules which are cracked into lighter products. In addition, mild hydrocracking of the oil feedstock could occure through HDT process depending on the severity of the operation. All these reactions will bring some conversion for the heavy cuts into valuable derivative (lighter) cuts (Bej et al., 2001).

For the purpose of achieving the target of removing the percentage of impurities as much as possible with the current HDT process, utilizing high temperature and pressure,

high hydrogen consumption, large volume and more catalyst is indispensable but costly. Thus, it is necessary to find a method that can operate under moderate operating conditions and has high efficiency to reduce all types of contaminant compounds and to produce clean fuel.

Many investigations on hydrotreating process (includes different reactions, such as HDS, HDN, HDAs, HDV, HDNi) have been reported widely. These studies have been carried out using several oily feedstocks (*but not the full crude oil*), such as vacuum gas oil, kerosene, naphtha, diesel and different fractions (more details can be found in Chapter 2).

With this background, the present research is focused on the following:

- Reducing the content of impurities (S, N, Asph, V and Ni) during hydrotreating of crude oil as low as possible under moderate operating conditions from crude oil, which leads to a reduction of these impurities from oil distillates fractions.
- Increasing the oil distillates productivity (especially gasoline, kerosene and gas oil) via HDT of crude oil directly before distillation. As a result, the profitability will increase.
- Improving the properties of reduced crude residue (R.C.R) during hydrotreating of crude oil before the distillation processes and produce new fuel oil.
- Minimizing the sum of the squared errors (*SSE*) between the experimental and estimated concentrations to find the best kinetic models, which can be used confidently to reactor design, operation and control. In this work, five kinetic models (HDS, HDN, HDAs, HDV and HDNi) in addition to kinetic models for increasing of oil distillates productivity (include 5 lumps: gases(G), naphtha (N), heavy kerosene (H.K), light gas oil (L.G.O) and reduced crude residue (R.C.R)) are used to evaluate the optimal design of TBR used for crude oil HDT. The

optimization technique to obtain the best kinetic models in TBR processes for the reactions considered in this study based on the pilot plant experimental work. A series of experimental works is conducted in a continuous flow isothermal trickle bed reactor, using crude oil as a feedstock and the commercial cobalt-molybdenum on alumina (Co-Mo/γ-Al_2O_3) as a catalyst. For oil distillates productivity, a laboratory distillation unit at atmospheric and vacuum pressure are employed for feedstock and hydrotreated product composition.

- Optimizing the quench position and rate for controlling the temperature of industrial trickle bed reactor used for crude oil HDT by using quench model. A rigorous and nonisothermal model that includes all the reactions studied in this work are developed and utilized in the optimization framework.
- Minimizing the energy consumption via a heat integration process and optimizing the design and operation of the industrial TBR (with large-scale operation). This includes a total cost comparison between oil distillates produced by the conventional method (HDT process of each cut separately after distillation process) and produced by the current process. The kinetic models generated depending on the experiments with nonisothermal and rigorous models at various operating conditions are used in the optimization framework to find the optimal design of industrial TBR.

In all case studies, the gPROMS software (general PROcess Modelling System, 2005) has been employed for modelling, simulation and optimization for all the operations considered in this work. The optimization problem is posed as a Non-Linear Programming (NLP) problem and is solved using a Successive Quadratic Programming (SQP) method within the gPROMS package.

1.6 Aims and Objectives of This Work

This thesis aims to develop kinetic models that represent a three-phase heterogeneous trickle bed reactor to describe the behaviour of crude oil hydrotreating process with high efficiency, productivity, minimum cost depending on the experimental work under moderate operating conditions. The model based on the gas-liquid and liquid-solid mass transfer phenomena (two–film theory), incorporates reactions such as HDS, HDN, HDAs, HDM, which includes HDV and HDNi in addition to kinetic models for increasing the oil distillates productivity using the mathematical models from the literature.

The objectives of the work can be highlighted as follows:

- To carry out a literature survey on the modelling, simulation and optimization of trickle bed reactor (TBR) processes. Reaction kinetic models for different operations (such as HDS, HDN, HDAs, HDM, HDC) and several oily feedstocks.
- Experimental work to describe the performance of crude oil hydroprocessing in a pilot–plant trickle bed reactor (TBR) system in order to determine the best kinetic parameters and to validate the model at different operating conditions for obtaining helpful models for HDT reactions, which can be confidently used for reactor design, operation and control. It includes:
    - ✓ Hydrodesulfurization (HDS) process.
    - ✓ Hydrodenitrogenation (HDN) process.
    - ✓ Hydrodemetallization (HDM) that involves HDV and HDNi processes.
    - ✓ Hydrodeasphaltenization (HDAs) process.
    - ✓ Distillation process at atmospheric and vacuum pressure for hydrotreated product fractionation to get light naphtha (L.N), heavy naphtha (H.N),

heavy kerosene (H.K), light gas oil (L.G.O) and reduced crude residue (RCR).

Different operating conditions are employed for hydrotreating conditions, which are:

- ✓ Reaction temperature (T).
- ✓ Hydrogen pressure (P).
- ✓ Liquid hourly space velocity (LHSV).
- ✓ Hydrogen to oil ratio (H_2/Oil).

- To develop the best kinetic models for HDS, HDN, HDAs, HDV and HDNi reactions in addition to kinetic models for increasing the oil distillates productivity, which can be accurately applied to design of reactor, operation and control. The optimization technique to get the best kinetic models in TBR processes for the reactions studied in this work in order to estimate the optimal design of industrial TBR used for crude oil HDT is based on the sum of the squared errors (*SSE*) between the experimental and calculated concentrations of S, N, Asph, V, Ni, G, L.N, H.N, H.K, L.G.O and R.C.R.
- To increase the productivity of oil distillates (mainly L.N, H.N, H.K, L.G.O) during HDT of crude oil directly before distillation leading to an increase in process profitability.
- To enhance the specifications of R.C.R produced by crude oil hydrotreating directly and consider the possibility of producing new fuel oils.
- To compare the yield of oil fractions produced by the distillation process after HDT process (this study) with those produced by conventional methods.
- To control the temperature of an industrial trickle bed reactor used for crude oil HDT via a quench model.
- To reduce the energy consumption on scaling up a heat integrated of hydrotreating process and the optimize design and operation of the industrial

trickle bed reactor employed for crude oil hydroprocessing directly then separation process to its fractions.

- To compare the results between oil fractions produced by hydrotreating of crude oil directly then distillation operation (this study) and produced by hydrotreating process of each fraction separately after distillation process (the conventional method).

1.7 Thesis Layout

This thesis focuses upon the optimal operations and kinetics of trickle bed reactor for hydrotreating of crude oil. The structure of the thesis is presented below:

Chapter 1: Introduction

This thesis begins with a general introduction, in which the importance of petroleum and the energy consumption scenarios are hightlighted. A typical petroleum refinery and the main problems of the impurities are presented in addition to the challenges and targets of crude oil hydrotreating. The scope of this research, aims and objectives of this research and thesis layout haves are set out.

Chapter 2: Literature review

Chapter Two takes a look at the past work in the field of hydrotreating operation and reviews issues related to the modelling, simulation and optimization processes in addition to the principle reactions and operating variables of hydrotreating processes. The application of a trickle bed reactor and the major advantages for these reactors are also investigated. A brief description of parameter estimation techniques is also provided.

Chapter 3: Experimental Work, Results and Discussions

Chapter Three describes the experimental procedures for hydrotreating of crude oil in pilot plant trickle bed reactor, and distillation process. The results obtained via the HDT reaction and oil distillates yields via distillation process of hydrotreated crude oil are presented. A comparison of oil distillates yield between the conventional methods and the present study, in addition to the properties of reduced crude residua, are also discussed.

Chapter 4: gPROMS Software : genal Process Modelling System

Chapter Four presents an overview, application and features of the gPROMS software package that has been employed for modelling, simulation and optimization of the trickle bed reactor system for crude oil hydrotreating. Its advantages and the reasons why it was adopted for use in this study are also highlighted in this chapter.

Chapter 5: Mathematical Modelling, Simulation and Optimization of Crude Oil HDT: Results and Discussions

Chapter Five shows the mathematical models that used to describe the performance of trickle bed reactor for crude oil hydrotreating. HDT kinetic models include HDS, HDN, HDAs, HDV and HDNi in addition to kinetic of oil distillate yields. Optimization techniques will be used to obtain the best values of kinetic parameters used for HDT of crude oil based on pilot plant experiments. The model simulation results and the effect of operating conditions upon impurities removal are presented. The kinetic models obtained will be used to predict the concentration profiles of H_2, H_2S, S, N, Asph, V and Ni along the catalyst bed length in different phases, which provides further insight of the process. Kinetic models for increasing oil distillate yields are also presented.

Chapter 6: Optimization of Industrial Trickle Bed Reactor: Optimal Operation of Commercial Hydrotreating Unit

Chapter Six provides a large scale trickle bed reactor with the optimal operation of industrial HDT unit with the heat balance equations and the optimal distribution of the catalyst bed. The control of the reaction temperature is studied due to the exothermic behaviour of such a reactor by using a quench process. The quench position and quench rate with several beds is investigated based on the minimum annual cost. The heat integration process and energy consumption in addition to the economic analysis of the continuous whole process of industrial refining units is also discussed.

Chapter 7: Conclusions and Future Work

Chapter Seven presents the conclusions, highlighting what has been achieved in this work and making suggestions for future work.

Chapter Two

Literature Review

2.1 Introduction

In this chapter a review of past work on the hydrotreating processes (which involves HDS, HDN, HDA, HDM, HDAs and HDC) is presented. The principle reactions of the hydrotreating process and the main operating conditions used in HDT process are considered briefly. Trickle bed reactors with their applications, in addition to the main features of these reactors, are reviewed.

Also, this chapter will present some literature for hydrotreating process modelling, the aspects of modelling, simulation and optimization processes, kinetic models of middle distillate yields and kinetic parameter estimation techniques.

2.2 Hydrotreating Process (HDT)

The first use of HDT was in America in the 1950s, and then this process started in Japan, Europe and other countries (Ray et al., 1995). It is a conversion process driven by the catalytic reaction of hydrogen with the feedstock to produce higher-value hydrocarbon products and to reduce the content of impurities, such as sulfur, nitrogen, asphaltene and metallic compounds from crude oil or oil fractions at high temperatures and hydrogen pressures through converting sulfur in sulfuric compounds and nitrogen in nitrogenic compounds to hydrogen sulfide gas and ammonia, respectively (Abbas, 1999; Areff, 2001). Also occurring is the conversion of unsaturated hydrocarbonic compounds such as olefins to saturated hydrocarbonic compounds in addition to decreasing the aromatic content and converting it to paraffins and cyclic paraffins (Gary

and Handwerk, 1994). Hydrotreating is also used prior to catalytic cracking to reduce the contaminants and to improve product yield, as well as to upgrade middle-distillate petroleum fractions into finished kerosene, diesel fuel and gas oil (Mahmood, 1990). Hydrotreating can cause the asphaltenes to become less soluble by hydrogenating the oil. The result is that it becomes a poor solvent for asphaltenes (Bartholdy and Andersen, 2000). Actually, hydrotreating capacity has been increasing continuously (about 6% per year since 1976) and reached nearly 50% of the total refining capacity (McCulloch, 1983).

Hydrotreating is the most common process units in the modern petroleum refining industry. There are more than 1300 hydrotreating units and the world's hydrotreating capacity is nearly half as large as the world's crude distillation capacity as shown in Table 2.1.

Table 2.1: Worldwide refining process units (Stell, 2003)

	Crude Distillation	**Cocking + Visbreaking**	**FCC**	**Catalytic Reforming**	**HDT**	**HDC**
Number of Units	>710	>330	360	550	1316	168
Total world capacity[a]	82.0	8.0	14.3	11.3	40.3	4.6
Average capacity[b]	114000	45700	39700	20500	30600	27400

[a] Million barrels per day; [b] Barrels per day

Hydrotreating process is carried out under certain conditions of pressure, temperature and liquid hourly space velocity (LHSV) (Ali and Abdul-Karim, 1986; Mahmood et al., 1990; Bhaskar et al., 2002; Al-Humaidan, 2004; Latz et al., 2009; Wua et al., 2009).

The expressions hydrotreatment, hydroprocessing, hydrofining, hydrocracking and hydrodesulfurization (HDS) are used in the industry depending on what is important. If the goal of the process is to remove sulfur, the process is called hydrodesulfurization (HDS) and if it aims to remove nitrogen, the process will be termed hydrodenitrogenation (HDN). Additionaly, the process is called hydrodemetallization (HDM), hydrodeasphaltenization (HDAs) and hydrogenation when the process is used to reduce metals, asphaltenes and olefin saturation, respectively (Ali and Abdul-Karim, 1986; Mahmood et al., 1990; Magee and Dolbear, 1998; Marafi and Stanislaus, 2008).

Hydrotreating reactions are usually referred to as mild processes whose main purpose is to reduce the impurities or to saturate olefins without any change in the boiling range of the feed. The hydrocracking reactions refer to the processes that aims to reduce the boiling range and in which most of the feed is converted to products that have boiling ranges less than that of the feed (Gary and Handwerk, 1994).

Hydrotreating processes can be classified as destructive and non-destructive. The first part, which also is called hydrocracking, can be defined as a process that is characterized by cleavage of C-C linkages and is accompanied by hydrogen saturation of the fragments to produce lower boiling products. This type of reaction requires high temperatures. Non-destructive hydrotreating (also named HDT or hydrofining) is more usually used for the purpose of upgrading product quality without any change in the boiling ranges (Batholomew, 1983; Gary and Handwerk, 1994; Speight, 2000).

It is well known that the hydrotreating process depends on the compound type, where the HDT of higher boiling cuts is more difficult than the lower boiling cuts. The difficulty of impurities removal increases when the process transfers from paraffines to naphthenes then to aromatics (Meyers, 1997; Speight, 2000).

Paraffins < Naphthenes < Aromatics

Hydrotreating processes have been studied by many investigators for the purpose of obtaining a large economic benefit by reducing the undesirable compounds in petroleum fractions.

Mohammed et al. (1987) focused their studies on removing sulfur compounds from Al-Qayaral deasphaltened vacuum residue. Myszka et al. (1989) studied the hydrodesulfurization of heavy vacuum oil derived from Romashkino crude. Ma et al. (1995) and Isoda et al. (1998) worked to remove sulfur compounds from vacuum gas oil. Hydrodesulfurization (HDS), hydrodemetallization (HDM), hydrodenitrogenation (HDN) and hydrodeasphaltenization (HDAs) have been studied using seven different catalysts by Maity et al. (2003) during Maya heavy crude hydrotreating. Marafi et al. (2003) investigated these reactions by using three types of catalyst during the hydrotreating of Al-Kuwait atmospheric residue. Mapiour et al. (2009) investigated the influence of hydrogen purity on hydrodesulfurization, hydrodenitrogenation and also aromatics hydration during hydroprocessing of heavy gas oil derived from oil sands bitumen. Bahzad and Kam (2009) applied the HDS process to upgrade atmospheric residues of Al-Kuwait heavy oils into valuable products. Further HDT processes will be presented with process modelling in this Chapter.

2.2.1 Principle Reactions of HDT

Crude oil (petroleum stocks) are extremely complex mixtures of hydrocarbonic and nonhydrocarbonic compounds that have in addition to carbon and hydrogen, significant amounts of sulfur, nitrogen and various metals. These compounds are different in type, molecular weight, molecular structure as well as the physical and chemical properties (Areff, 2001).

The basic chemical concept of hydrodesulfurization (HDS) and hydrodenitrogenation (HDN) processes is to convert sulfur and nitrogen compounds in the feedstock to desulfurized and denitrogenated hydrocarbon products, and hydrogen sulfide (H_2S) and ammonia (NH_3), respectively (Speight, 2000; Areff, 2001). Hydrodemetallization reactions (HDM) occur at the same time with HDS reactions. The HDM reaction is thermo catalytic and it produces metallic sulfides such as NiS and V_3S_4. The reactions lead to the deposition of sulfides on the active sites of the catalyst (Leprince, 2001). The reactions of the hydrodeasphaltenization (HDAs) process during hydrotreating are complex due to the presence of different physical and chemical processes. Most studies in hydrodeasphaltenization have been focused on thermal decomposition that includes many simultaneous reactions. Investigations on asphaltene converting of several oil feedstocks have indicated that the large molecules during hydrotreating process will be converted into smaller molecules and the hydrogenation of condensed polyaromatic rings that found in asphaltene compounds are almost entirely suppressed (Abbas, 1999; Trejo and Ancheyta, 2005). These reactions (HDS, HDN, HDM, HDAs) are commonly performed in a three-phase reactor (gas-liquid-solid), which is called a trickle bed reactor (TBR) (Rodriguez and Ancheyta, 2004). The general hydrotreating reactions can be expressed as follows (Areff, 2001; Leprince, 2001; Leyva et al., 2007):

HDS: $R - S + H_2 \rightarrow R + H_2S$

HDN: $R - NH_2 + H_2 \rightarrow RH + NH_3$

HDM: $R - M + H_2 \rightarrow RH + M$

HDAs: $R - Asph + H_2 \rightarrow RH + Asph - R(\text{smaller hydrocarbons})$

R represents the hydrocarbon molecule.

Other reactions can happen in the HDT of heavy oils such as hydrocracking and hydrogenation of aromatics rings. At high temperatures in the hydrotreating process,

hydrocracking reactions that include the breaking of the C-C bonds are most likely to happen (also a reduction of molecular weight is noticed), e.g.

$$RCH_2CH_2R + H_2 \longrightarrow RCH_3 + RCH_3$$

or

$$C_{10}H_{22} + H_2 \longrightarrow C_4H_{10} + C_6H_{14}$$

Hydrogenation of unsaturated hydrocarbonic compound is also a significant class of reactions happening through the HDT operation, e.g. Gully and Ballard (1963) and Girgis and Gates (1991).

$$C_5H_{10} + H_2 \longrightarrow C_5H_{12}$$

2.2.2 Process Variables of HDT Process

The range of operating conditions that are used in hydrotreating is very wide. The choice of operating conditions is determined by the feedstock type, the required product level, and the purity and availability of hydrogen in addition to economic considerations (Turaga, 2000). In conventional processes, the range of operating conditions for HDT of different petroleum fractions is summarized in Table 2.2 (Topsoe et al., 1996).

Table 2.2: Typical process conditions for various hydrotreatment processes

Feedstock	**Temperature (K)**	**Pressure (atm)**	**LHSV (hr^{-1})**
Naphtha	593	15-30	3-8
Kerosene	603	30-45	2-5
Atmospheric gas oil	613	38-60	1.5-4
Vacuum gas oil	633	75-135	1-2
Atmospheric residue	643-683	120-195	0.2-0.5
Vacuum residue	673-713	150-225	0.2-0.5

There are four process variables frequently reported in the literature as the most important in hydrotreating operations: reaction temperature, liquid hourly space velocity

(LHSV), hydrogen partial pressure and hydrogen to oil ratio (H_2/Oil) ratio. In general, for a specific feedstock and catalyst, the degree of impurities removal and conversion increases with increasing severity of the reaction, that is, increasing pressure, temperature, or H_2/Oil ratio, and decreasing space velocity. The effect of these parameters on the HDT process is briefly discussed below.

2.2.2.1 Temperature

Temperature plays a significant role in the HDT process. An increase in reaction temperature can substantially enhance the rate of catalytic reaction and hence increase the sulfur, nitrogen, asphaltene and metal removal. In addition to catalytic improvement, temperature increase may significantly enhance the thermal cracking. The rate of heavy hydrocarbons will be decreased when the reaction temperature increases. On the other hand, the rate of diffusion inside the active site of the catalyst will increase and as a result the rate of reaction will be increased (Hobson, 1984; Scherzer and Gruia, 1996).

The best range of temperature used in the refineries lies between 553K and 683K (except heavy vacuum residue), where under 553K the reaction rates tend to be slow and above 683K there is undesirable side reaction. At temperatures above 683K, the activity of the catalyst used will decrease due to coke formation that deposits on the catalyst (Hobson, 1984; Speight, 2000).

2.2.2.2 Pressure

Hydrogen partial pressure is another parameter that mainly affects the rate of reaction by promoting the reaction between hydrogen and feedstock compounds. The performance of any hydroprocessing reactor and process is limited by the hydrogen partial pressure at the inlet to the reactor. Generally, when the boiling range of

feedstock increases from naphtha through to vacuum residue, the impurities compounds such as sulfur, nitrogen and other heteroatoms become more complex and require higher partial pressure to cause them to react with these compounds. Furthermore, to prevent rapid catalyst deactivation by deposition of coke (Hobson, 1984; Ancheyta and Speight, 2007).

More specifically, the partial pressure of hydrogen has a direct influence on the rate of reaction of HDS, HDN, HDAs and HDM of the feedstock. In addition, the system pressure impacts both the degree of hydrogenation of unsaturated compounds in the feedstock as well as the reaction rate of hydrocarbon cracking. Refinery experience indicates that the HDT processes conducted at higher partial pressure of hydrogen will produce products with lower sulfur, nitrogen and aromatics contents (Al-Humaidan, 2004).

The choice of operating partial pressure of hydrogen must therefore be made with care in order to ensure that the process operates under HDT conditions and to prevent high deactivation of catalyst used (Chung, 1982; Gary and Handwerk, 1994).

2.2.2.3 Liquid Hourly Space Velocity (LHSV)

Liquid hourly space velocity is another operational parameter that impacts on the hydroprocessing efficiency and also upon the life of the catalyst. LHSV can be defined as the ratio of the feed volumetric flow rate to the catalyst volume. The reciprocal of liquid hourly space velocity gives the residence time of feedstock along the catalyst bed. Although the volume of catalyst for the HDT process will be constant, the liquid hourly space velocity will vary directly with the rate of feedstock (Speight, 2000).

A decrease in LHSV will cause an increase in feed contact time (residence time) in catalyst. On the other hand, a decrease in the LHSV will generally bring an increase in

the extent of the HDS, HDN, HDM, HDAs and HDC processes and as a result, increase the reaction severity and the efficiency of the hydrotreating processes (Chung, 1982). It could be necessary to increase the reaction temperature when the feed rate is increased in order to maintain a fixed rate of HDS, HDN, HDM, HDAs and HDC (Chung, 1982).

The residual sulfur, metals, nitrogen and other impurities from any catalytic hydrotreating process is proportional to the LHSV utilized. Thus, the heavier residue cuts require longer residence time for the reaction to go to completion compared with the lighter residue cuts (Hobson, 1984).

2.2.2.4 Gas Rates (H_2/Oil ratio)

The choice of gas flow rate is governed by economic considerations. Recycle is utilized to maintain the H_2 partial pressure and the physical contact of the hydrogen with the catalyst and hydrocarbon for ensuring adequate conversion and impurities removal. To make the process economically feasible, the unused hydrogen is recycled back to the reactor. Thus, for diesel oil, atmosphere residue and other heavy feedstock, it is normal to have a gas compressor to recycle gas back through the reactor (Hobson, 1984; Speight, 2000; Al-Humaidan, 2004).

2.3 Trickle Bed Reactors (TBRs)

A trickle–bed expression is generally used to a reactor in which a gas phase (hydrogen frequently) and a liquid phase (feedstock oil) flow cocurrently downward through a solid fixed particles (catalyst–bed), where the reaction take place. The older term used was "trickling filter", that has long been utilized for organic removal from wastewater streams by the action of aerobic bacteria (Satterfield, 1975). The trickle bed reactor consists of a cylindrical column in which a fixed bed of catalyst particles (Figure 2.1) is randomly dumped. The catalyst particle that has 1-3 mm (diameter) may be cylindrical,

spherical or have more advanced forms like multilobes. Very high impurities conversion can be obtained owing to the plug flow characteristics of fixed–bed reactors (Boelhouwer, 2001).

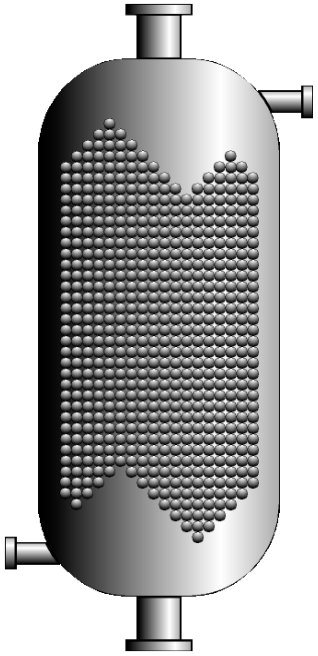

Figure 2.1: Schematic illustration of a fixed bed

Trickle–bed reactors have been largely employed to a moderate operation in chemical processing. Most published data about their commercial implementation concerns the operation with hydrogen of different oil cuts, especially the hydrodesulfurization and hydrocracking of heavy oil feedstocks. Their industrial improvement during the 1950s by Shell and by British Petroleum has been described by LeNobel and Choufoer (1959), Lister (1964) and Van Deemter (1964). The improvement of HDS and HDC operations by Esso, Gulf, Union Oil and others has been explained in the proceedings of the different World Petroleum Congresses (Satterfield, 1975). There are many applications of trickle–bed reactors in chemical processing. Table 2.3 lists some of the hydrotreating operations carried out in trickle–bed reactors.

Table 2.3: Some applications of trickle – bed reactor processes

Trickle-bed process	**Reference**
HDN of various compounds	(Flinn et al., 1963)
HDN of a lube oil distillate	(Gilbert and Kartzmark, 1965)
HDA of naphthenic lub oil distillate	(Henry and Gilbert, 1973)
HDS of petroleum residue	(Papayannakos and Marangozis, 1984)
HDS, HDM and HDAs of RCR	(Abdul-Halim et al., 1987)
HDM of residues	(Trambouze, 1993)
HDS of oil fractions	(Froment et al., 1994)
HDT of heavy residue oils	(Li et al., 1995)
HDS of VGO	(Korsten and Hoffmann, 1996)
HDS of Basrah reduced crude oil	(Abbas, 1999)
HDS of VGO	(Van Hasselt et al., 1999)
HDS and HDN of middle distillates	(Cotta et al., 2000)
HDA and HDS of VGO	(Areff, 2001)
HDS of diesel oils	(Kumar et al., 2001)
HDS, HDN and HDA of gas oil	(Ancheyta et al., 2002a)
HDT of heavy oil	(Ancheyta et al., 2002b)
HDS and HDM of diesel	(Chowdhury et al., 2002)
HDS of atmospheric gas oil	(Bhaskar et al., 2002)
HDM, HDS, HDN and HDC of Kuwait AR	(Marafi et al., 2003)
HDT of light diesel feedstock	(Avraam and Vasalos, 2003)
HDS of middle distillates	(Pedernera et al., 2003)
HDS and HDA of diesel	(Cheng et al., 2004)
HDS of gas oil	(Macı´as and Ancheyta, 2004)
HDS, HDN, HDA and HDC of diesel fractions	(Bhaskar et al., 2004)
HDS, HDN and HDA of VGO	(Rodriguez and Ancheyta, 2004)
HDC of heavy oil fractions	(Ancheyta et al., 2005)
HDM and HDS of Maya oil	(Rana et al., 2005)
HDC of heavy oils	(Sanchez et al., 2005)
HDS, HDN and HDA of VGO	(Jimenez et al., 2005)
HDS of dibenzothiophene	(Iliuta et al., 2006)
HDA of Benzene	(Metaxas and Papayannakos,2006)
HDS, HDN and HDA of VGO	(Mederos et al., 2006)
HDT of VGO	(Mederos and Ancheyta, 2007)
HDT of VGO	(Jimenes et al., 2007b)
HDC of Maya crude oil	(Sanchez and Ancheyta, 2007)
HDS of gas oil	(Shokri et al., 2007)
HDS, HDN and HDA of VGO	(Jimenez et al., 2007a)
HDS of gas oil	(Kallinikos et al., 2008)
HDS of thiophene	(Ge et al., 2008)
HDS, HDN, HDM, HDC and HDAs of AR	(Alvarez and Ancheyta, 2008a)
HDS, HDN and HAD of VGO	(Alvarez and Ancheyta, 2008b)
HDT of petroleum diesel mixtures	(Sebos et al., 2009)
HDT of HGO	(Mapiour et al., 2009)
HDS of thiophene	(Suo et al., 2009)
HDS, HDN and HAD of HGO	(Mapiour et al., 2010)
HDT of HGO	(El Kady et al., 2010)
HDT of LGO	(Boahene et al., 2011)
HDS and HDA of LGO	(Chen et al., 2011)

Trickle–bed reactors with cocurrent downflow (Figure 2.2) are widely used in hydrotreating operations. This type of TBR has many features, where the liquid flow approaches plug flow behaviour with very low catalyst loss (i.e. the catalyst is effectively wetted). This feature is very significant when costly catalyst is utilized. These factors allow high conversion to be achieved in a single reactor. Also, the volume ratio of liquid to solid (liquid hold-up) in this type of reactor is low; thuse minimizing the homogeneous reaction (less occurrences of homogeneous side–reactions) and this could be significant in the HDT reaction.

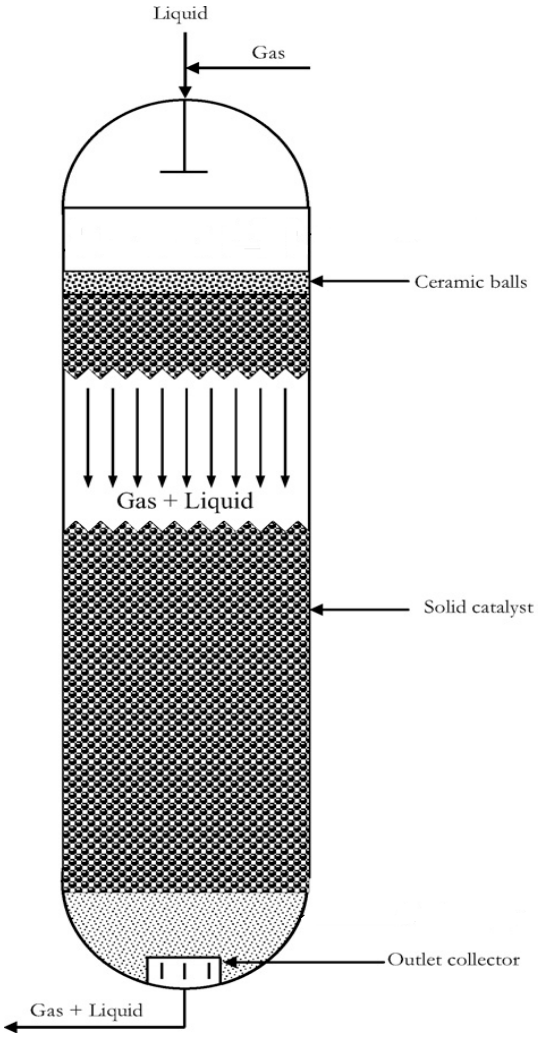

Figure 2.2: Trickle bed reactor with cocurrent downflow

Generally, in a gas–liquid–solid process, both the gas–liquid and liquid–solid interfacial mass or heat transfer resistances are significant. Owing to the thinness of the liquid film

in this reactor, these two resistances can be combined and the overall resistance of the liquid film will be lower than those obtained in other kinds of gas–solid–liquid process.

The TBR process is also generally operated under cocurrent downflow conditions, thus flooding is not a problem in such a reactor and the trickle flow process gives a lower pressure drop than cocurrent upflow or countercurrent flow, which reduces pumping cost. Low pressure drop will allow an essentially uniform partial pressure of the gaseous reactant across the length of the reactor (hydrogen in HDT processes). This will be significant for ensuring H_2-rich conditions at the surface of the catalyst. TBR cocurrent downflow can be carried out at high pressure and temperature and when the temperature rise is important (hydrocracking reactions), it may be conveniently controlled by the addition of "quench fluid " from the side of the reactor.

In addition to the above, the gas–liquid–solid cocurrent downflow generally allows simple construction (easy design) with no moving parts with lower the operating and investment costs (Bondi, 1971; Satterfield, 1975; Hofmann, 1977; Goto and Smith, 1978; Gates et al., 1979; Ramachandran and Chaudhari, 1980; Doraiswamy and Sharma, 1984; Zhukova et al., 1990; Gianetto and Specchia, 1992; Al-Dahhan et al., 1997; Sutikno, 1999; Lopez and Dassori, 2001).

2.4 Process Modelling

Process models are very profitable. They have been employed for operator training, safety systems design, design of operation and also for operation control systems design. The improvement of faster computer and advanced numerical methods has enabled modelling and solution of complete processes. System mathematical modelling deals with quantitative rather than a qualitative treating of the process. Nevertheless, the

term itself has a very wide scope of application and many advantages, some of these are (Khalfalla, 2009):

- It is less time consuming.
- Utilizing a mathematical model is cheaper than using the real system. It enables a wide range of information to be learnt about a system without having turn to lengthy and expensive runs on the plant.
- More secure. The result is much less fatal when something goes wrong during the study.

A mathematical model is a set of variables and a set of equations that build relationships among the variables for describing some aspects of the behaviour of the system under investigation. The variables describe some properties of the process, for instance, measured process outputs frequently in the shape of signals, timing data and counters. The real model is the collection of functions which describe the relations among the various variables (Khalfalla, 2009). Eykhoff, (1974) has defined a mathematical model as "a representation of the essential aspects of an existing system (or a system to be constructed) which presents knowledge of that system in usable form". However, for the complex systems encountered in several engineering contexts, the models are frequently sets of relations that exhibit highly non–linear equations. For several chemical engineering models, the non–linear behaviour is further complicated by the exponential reliance of the reaction rates on the temperature (Arrhenius type equations) also by the severity of the rate expressions utilized within the mass and energy balance models. These complex models can mostly be solved by the use of sophisticated numerical methods.

Real life is full of models and cause–and–effect relations, whether between natural events (rainfall, earthquakes, sunrise), living things (humans or animals) or other natural

operations (growth, death). There are generally well documented causes for any of these phenomena to happen. The documentation of these relations generally results in a model of operation (Ekpo, 2006).

The enormous rise in computing power during the past two decades, also the ongoing search for better and more advanced numerical ways and Computer–Aided Design (CAD) materials in the past half century has been excellent for operation modelling undertaken in academia and industry (Kiparissides, 1996). The numerical solution accomplished for the full process can thus be utilized with higher confidence than a lot of separate solutions.

Generally, there are three types of model, according to Bonvin (1998):-

1- Data driven black box models.

2- Knowledge driven white box models.

3- Hybrid grey box models.

The derivation of black–box models is based on empirical observations of the process behaviour. Black–box models are generally improved during an observation of the relation between various inputs and their corresponding outputs in a particular system. From this input–output data, a black box relation can be accomplished. Despite this, this type of mode is easy to obtain, however, problems generally arise when it is employed to extrapolate as its exactness in such cases can be severely restricted. Another drawback is that data can only exist for measurable variables; hence no relation can be formed for variables that can not be measured, such as heat of reaction. The problem with using a wide group of functions for describing a process is that calculating the variables becomes increasingly difficult when the number of variables increases (Giannakopoulos, 2002; Khalfalla, 2009).

Knowledge driven white–box models on the other hand are referred to as mathematical modelling, and are termed "mechanistic first principles models". For a process, the model can be developed from stoichiometric and kinetic knowledge of the mass and energy balances of the process. In such a model the impact of temperature, concentration and any other control variables upon the rate of each reaction is reported by the kinetic model, and the reactor model relates the state variables of the process to other variables such as the composition of inlet streams and other system constraints. White–box models are not as simple to obtain as their black–box counterparts, and owing to the extreme non-linear behaviour of several engineering processes, can be very difficult. In order to reduce some of complexity, assumptions are generally made and an easy to understand model which does not appropriately describe the process is sometime still preferred over a very detailed on that needs lot of computing time (Giannakopoulos, 2002; Ekpo, 2006; Khalfalla, 2009). In a white–box model, equations are generally derived based on the following considerations (Ekpo, 2006).

- Mass and energy balances.
- System constraints.
- Thermo–physical properties of the process.

The grey – box model is a hybrid of the previous two cases mentioned above.

In this study, a white–box model is used for the hydrotreating modelling and simulation of TBR pilot–plant.

2.4.1 Hydrotreating Kinetic Models

The primary objective of this work is to develop a kinetic model that can accurately predict the hydrotreating performance of crude oil under different operating conditions. In order to develop a reliable catalytic hydrotreating model, it is important to fully understand the operation and all accompanied phenomena related to modelling aspects.

This part of the project presents some literature for the hydrotreating process modelling (includes HDS, HDN, HDM, HDAs, HDA and HDC).

Froment et al. (1994) used rate equations to develop a one–dimensional heterogeneous nonisothermal model in hydrotreating diesel oil fractions. A feedstock mixture consists of benzothiophene, di-benzothiophene and 4,6-dimethyldibenzothiophene as sulfur compounds and quinoline as nitrogen compounds. The model accounts for concentration gradient inside the catalyst particles. Integration in the axial direction was performed using a fourth order Runge-Kutta method and the intraparticle integration was carried out using the Orthogonal Collocation method.

Korsten and Hoffmann (1996) developed a three–phase reactor model for describing the hydrotreating reaction of vacuum gas oil in a trickle–bed reactor operated under high–pressure pilot plant and isothermal conditions. The model is based on two–film theory and involves correlations for estimating mass–transfer coefficients, gas solubilities and the gases and oils properties at operating conditions. The chemical reaction rate was described by Langmuir–Hinshelwood kinetics. The model equations were solved numerically by a Runge-Kutta method and the model presented (simulation process) shows good agreement with the experimental data that was carried out over a wide range of pressure, hydrogen to oil ratio, temperature and liquid hourly space velocity.

Tsamatsoulis and Papayannakos (1998) investigated a kinetic model for hydrodesulfurization of vacuum gas oil in a trickle–bed reactor using several catalysts. The kinetic model has been estimated by utilizing a plug–flow model for the liquid phase as well as by using non-ideal liquid flow. Differences in the chemical reaction rates and the mechanism parameters were discussed. The kinetic parameters of the model were determined using the fourth order Runge-Kutta method and the Marquardt-

Levenberg nonlinear regression algorithm to fit simultaneously the values of sulfur and hydrogen concentration predicted by the models to the experimental data.

Van Hasselt et al. (1999) used a computer model to compare a conventional nonisothermal cocurrent trickle–bed reactor with two different configurations suggested for the process of the reactor: counter current and semi–counter current, taking the hydrodesulfurization of vacuum gas oil as a case study. They found that the counter current flow application results in a significant increase of impurities conversion.

A one–dimensional homogeneous model for HDS and HDN of middle distillates was investigated under wide operating conditions by Cotta et al. (2000). They applied a power law model for each reaction (HDS, HDN) to simulate the HDT of diesel in an adiabatic trickle–bed reactor. Mass and energy balances were presented along the catalyst bed length. The data generated were compared with conventional hydrotreating commercial reactors and they found that a larger reactor length is required for the nitrogen conversion. The parameters of kinetic equations were calculated using the 4^{th} order Runge-Kutta-Gill algorithm to solve the ordinary differential equations and using the Marquardt method for searching a set of kinetic parameters.

Matos and Guirardello (2000b) developed a mathematical model to simulate heavy oil hydrodesulfurization and hydrodemetallization catalytic processes. The system was modelled as an isothermal reactor with cocurrent upflow. The model equations were solved numerically using the Orthogonal Collocation method.

Kumar et al. (2001) developed a kinetic model for hydrodesulfurization of diesel oils in a cocurrent downflow trickle bed reactor using two types of catalysts. A power law model was employed to estimate the kinetic parameters for both the catalysts. The kinetic parameters were determined using exponential regression analysis.

Bhaskar et al. (2002) reported on the effects of hydrodynamic parameters and reaction rates on reactor performance. They applied the three phase heterogeneous model for describing the performance of a pilot plant trickle–bed reactor used for atmospheric gas oil hydrodesulfurization. The developed model was compared with experimental observations. The algebraic equations were solved using Newton-Raphson algorithm for the given bulk phase concentration of receptive compounds. The differential equations were then solved simultaneously using Runge-Kutta method. The results obtained from pilot plant operated under wide range of operating conditions during HDS of atmospheric gas oil showed good agreement with the predicted results.

Chowdhury et al. (2002) developed a kinetic mathematical model for a two phase flow reactor, including both mass transfer and chemical reaction in the reactor. Diesel oil hydrodesulfurization and hydrogenation of mono-, di- and polyaromatics were investigated in a TBR operated under isothermal conditions. Model equations were solved with a 4^{th} order Runge-Kutta method. Data obtained are compared satisfactorily with the experimental results.

Avramm and Vasalos (2003) presented a steady–state model for three phase trickle flow fixed bed reactors applied to hydrotreating of light oil feedstocks containing volatile compounds. Mass balances, energy balances and overall two phase flow momentum balance were considered in detail. All physical and chemical properties were estimated as a function of process conditions. Four general chemical reactions were described: hydrodesulfurization (HDS), hydrodenitrogenation (HDN), olefins saturation (HTO) and hydrogenation of di-, mono– and tri–aromatics (HTA). Chemical reaction rate was described by a Langmuir–Hinshelwood mechanisms, aromatic hydrogenation equilibrium and inhibition by H_2S, NH_3 and aromatics were taken into account. A collocation method for solving extended system of nonlinear equations was used

successfully. The experimental data obtained from a pilot plant unit showed excellent agreement with the mathematical model employed.

Perdernera et al. (2003) studied the effect of the oil fractions compositions on the conversion of sulfur compounds. Their model is an extension of that reported by Chowdhury et al. (2002). The model is fully integrated in Aspen Plus in a User model Block, and shows good agreement with experimental result obtained through hydrotreating of straight run gas oil at lab scale.

Bhaskar et al. (2004) developed a gas–liquid–solid model to simulate the performance of pilot plant and commercial trickle bed reactors applied to the hydrotreating of diesel cuts. A three phase heterogeneous model was used and based on two–film theory, where mass transfer phenomena at gas–liquid and liquid–solid interfaces was incorporated. The main hydroprocessing reactions are modelled: hydrodesulfurization, hydrodearomatization, hydrodenitrogenation, olefins saturation and hydrocracking. Their model was solved to calculate kinetic parameters for different HDT reactions using the results obtained in lab scale experiments. A Runge-Kutta fourth order numerical technique was used to integrate the differential equations along the catalyst bed length. The Newton-Raphson method was used to solve the nonlinear equations concerning the surface concentrations of various compounds. The model simulations showed good agreement with the experimental results. They also applied a three-phase non–isothermal heterogeneous model to simulate the performance of a commercial reactor at different operating conditions using the kinetic parameter calculated from pilot–plant experiments. The model was also employed to investigate the effect of operating conditions on product quality.

Redriguez and Ancheyta (2004) extended the model suggested by Korsten and Hoffman (1996) to involve mathematical correlations for the rate of hydrodesulfurization,

hydrodenitrogenation and aromatics hydrogenation reactions. Langmuir–Hinshelwood kinetics were employed to describe the hydrodesulfurization reaction whereas a consecutive reaction scheme was used in the HDN reactions, where nonbasic nitrogen compounds (N_{NB}) were converted to basic nitrogen compounds (N_B) by a hydrogenation process. The kinetics of hydrogenation of aromatics was reported by a first–order reversible reaction. The model was validated with experimental data generated at a pilot plant through hydrotreatment of vacuum gas oil under isothermal conditions. The values of the kinetic parameters were estimated using the Least-squares criterion with a nonlinear regression procedure based on Marquardt algorithm. Results showed good agreement between the theoretical and experimental data. The model used for the pilot plant was also applied to simulate the behaviour of an industrial HDT plant operated under non–isothermal conditions.

Yamade and Goto (2004) employed the model suggested by Korsten and Hoffman (1996) to simulate the vacuum gas oil hydrodesulfurization in a gas–liquid–solid reactor for both cases of countercurrent and cocurrent flow.

A steady–state one–dimensional heterogeneous model was developed by Jimenez et al. (2005) in order to simulate the performance of a pilot plant reactor applied to the hydrotreating of VGO, where the hydrodesulfurization, hydrodenitrogenation and hydrogenation of aromatics reactions were involved. The model was also used to study the effects of naphthalene and phenantrene (aromatics molecules), and also nitrogen compounds such as carbazol and acridine, on the sulfur removal during HDT. In addition, all physical and chemical properties were estimated as functions of operating conditions. Integration along the catalyst bed length was solved using a fourth order Runge-Kutta-Gill method and orthogonal collocation was used successfully for the intraparticle integration. A comparison between experimental and predicted results showed an average absolute error for all calculations lower than 5%.

A simple kinetic model have been employed by Sertic–Bionde et al. (2005) in order to investigate the impact of some reaction factors on hydrotreating of atmospheric gas oil and light cyclic oil obtained from fluid catalytic cracking unit using a trickle bed reactor. The model also simulated the conversion of hydrodesulfurization. Estimation of kinetic parameters was theoretically estimated using nonlinear least-squares analysis.

Trejo and Ancheyta (2005) studied the mechanisms of asphaltene conversion during hydrotreatment of Maya heavy oil. Experimental work was carried out in a pilot plant under different pressures, temperatures and LHSVs. The results generated from asphaltene hydrocracking were used to calculate reaction orders and activation energy using a power law model. Estimation of kinetic parameters and calculated concentrations of asphaltenes were solved using Marquardt's algorithm. The kinetic model was tested with experimental results and the average error was found to be lower than 5%.

A dynamic heterogeneous one-dimensional model of TBR reactors was described by Mederos et al. (2006) for catalytic oil fractions hydrotreating. The main hydrotreating reactions were HDS, HDN and HDA. Their model was based on the three phase reactor model and two–film theory reported in the literature. The model also included all necessary correlations for calculating heat and mass transfer coefficients, gases solubilities, and oil and gases properties. The model was employed to simulate isothermal and non-isothermal patterns of process. The model equations were solved using the fourth order Runge-Kutta method. Experimental results generated from hydrotreating of VGO were used for model validation and showed good agreement.

Jimenez et al. (2007a) generated one–dimensional heterogeneous model for simulating an industrial trickle bed reactor for hydrotreating VGO and heavy oil fractions. The model of an industrial reactor based on the experimental results was obtained under

standard industrial conditions at lab scale. The main chemical reactions taken into account were HDS, HDN and aromatics hydrogenation. Differential equations systems in the axial direction were solved along the reactor bed length using the fourth order Runge-Kutta-Gill algorithm. The intraparticle integration was solved using orthogonal oollocation method. A good agreement between experimental and theoretical results was obtained.

Jimenez et al. (2007b) investigated the kinetic reaction effect on the modelling of trickle bed reactor for hydrotreating of VGO. Their model was based on the mathematical model developed in previous work and many kinetic models found in literature. The integration in the axial direction in the reactor was performed with the 4^{th} order Runge-Kutta method, and intraparticle integration was carried out using an orthogonal collocation method. The model showed good agreement with different data sets, pilot plant and industrial information.

A model to predict the behaviour of trickle bed reactors for oil fractions catalytic hydrotreatment with cocurrent and countercurrent operation modes was described by Mederos and Ancheyta (2007). The trickle bed reactor model was one–dimensional heterogeneous plug flow and involved the major reactions present in the hydrotreating operation: HDS, HDN and HDA. The experimental results generated from the pilot plant operated under isothermal conditions with cocurrent process, were used to compare both patterns of operation. The performance of pilot plant and commercial trickle bed reactors was simulated, and the results were discussed in terms of variations with time and reactor length of temperature, partial pressure and concentrations. The model equations were solved using the fourth order Runge-Kutta method.

Shokri et al. (2007) used a trickle bed reactor for describing the HDS reaction of gas oil. The model employed was based on the two–film theory and the reaction rate equations

were described by the kinetics suggested by Vanrysseiberghe and Formet (1996). The simulation data were used to calculate the optimum operating conditions for the HDS pilot plant. The integration along the catalyst bed and in the radial direction was carried out using a fourth order Runge-Kutta routine and orthogonal collocation, respectively.

Alvarez and Ancheyta (2008a) presented a three phase heterogeneous plug flow reactor model for describing the behaviour of residue hydrotreating in a multi–fixed bed reactor system. The main hydrotreating reactions were HDS, HDN, HDM, HDAs and HDC, and mass transfer phenomena between gas–liquid and liquid–solid were taken into account. HDS reaction has been modelled by Langmuir–Hinshelwood kinetics, whereas the HDN, HDM, HDAs and HDC were described by power law mechanisms. In order to calculate kinetic parameters, a set of experiments were conducted in a multi reactor pilot plant at several operating conditions. The optimal set of kinetic parameters was calculated using the Levenberg-Marquardt algorithm. The predicted model was found to be satisfactory with experimental results obtained from the lab–scale. The model was also applied to an industrial HDT unit of residue with a multi bed adiabatic reactor.

A heterogeneous one–dimensional trickle bed reactor model for describing and simulating an industrial vacuum gas oil hydrotreater was developed by Alvares and Ancheyta (2008b). The most relevant vacuum gas oil HDT reactions were HDS, HDN and aromatics hydrogenation. The model was based on TBR models suggested by Korsten and Hoffmann (1996); and Rodriguez and Ancheyta (2004). Properties of hydrocarbons, gas solubilities and mass–transfer coefficients were described in detail. They observed a large impact of the resulting reaction temperature upon impurity conversion by affecting reaction constant and gas-liquid equilibrium.

Bahzad and Kam (2009) developed a mathematical model to simulate the performance of a pilot plant reactor during atmospheric residue hydrodesulfurization derived from

Al–Kuwait heavy crude. They found some discrepancies between predictions and pilot plant data that may be attributed to the type of catalyst used.

Mapiour et al. (2010) studied the effect of operating conditions upon hydrotreating of heavy gas oil (HGO) derived from Athabasca bitumen. The main hydrotreating reactions are hydrodesulfurization, hydrodenitrogentaion and hydrodearomatization (HDA). The experimental results have been employed to develop the kinetic models used to describe the performance of these reactions.

A one-dimensional, plug-flow trickle bed reactor model was developed by Chen et al. (2011) for modelling and simulation of a steady state, adiabatic commercial HDT reactor used for light gas oil hydrotreatment reactions. Hydrodesulfurization and hydrodearomatization processes were considered as the main HDT reactions. The effect of operating conditions on impurities removals has also been investigated. It was noticed that an increased pressure increases the reactor temperature and HDS and HDA conversions.

Farahani and Shahhosseini (2011) discussed the process of hydrodesulfurization of heavy gas oil. A nonisothermal heterogeneous reactor model was developed and then simulated with a three stage trickle bed reactor and kinetic models based on the Langmuir-Hingshelwood approach. The presence of stagnant liquid between catalyst particles and the heat production owing to highly exothermic HDS reactions was taken into account. The simulation results showed good agreement between the simulation results and the experimental data.

A summary of work carried out for the hydrotreating process modelling is given in Table 2.4. The present study considers the pilot plant and industrial TBR used for crude oil hydrotreating in cocurrent downflow with hydrotreating reactions, mainly, HDS, HDN HDAs, HDV and HDNi.

Table 2.4: Summary of hydrotreating process modelling works

Authors (Year)	Feedstock	Chemical Reaction	Mode of Operation
Froment et al. (1994)	Diesel oil fractions	HDS, HDN	Non-isothermal, cocurrent downflow
Korsten and Hoffmann (1996)	VGO	HDS	Isothermal, cocurrent downflow
Tsamatsoulis and Papayannakos (1998)	VGO	HDS	Isothermal,
Van Hasselt et al. (1999)	VGO	HDS	Non-isothermal, cocurrent, semi-cocurrent, countercurrent
Cotta et al. (2000)	Middle distillate	HDS, HDN, HTO	Non-isothermal, cocurrent downflow
Matos and Guirardello (2000b)	Heavy oil fractions	HDS, HDM	Isothermal, cocurrent upward
Kumar et al. (2001)	Diesel oil	HDS	Isothermal, cocurrent downflow
Bhaskar et al. (2002)	Atmospheric gas oil	HDS	Isothermal, cocurrent downflow
Chowdhury et al. (2002)	Diesel oil	HDS, HDA	Isothermal, cocurrent downflow
Avramm and Vasalos (2003)	Light oil	HDS, HDN, HTO, HDA	Non-isothermal
Perdernera et al. (2003)	Middle distillate	HDS, HDN, HDA	Non-isothermal, cocurrent downflow
Bhaskar et al. (2004)	Diesel fractions	HDS, HDA, HDN, HDC, HTO	Non-isothermal, isothermal, cocurrent downflow
Redriguez and Ancheyta (2004)	VGO	HDS, HAD, HDN	Non-isothermal, isothermal, cocurrent downflow
Jimenez et al. (2005)	VGO	HDS, HDN, HDA	Isothermal, cocurrent downflow
Sertic–Bionde et al. (2005)	Atmospheric gas oil, light Oil	HDS	Isothermal
Trejo and Ancheyta (2005)	Maya heavy oil	HDAs	Isothermal
Mederos et al. (2006)	Oil fractions	HDS, HDN, HDA	Non-isothermal, isothermal, cocurrent downflow
Jimenez et al. (2007a)	VGO	HDS, HDN, HDA	Isothermal, cocurrent upflow
Jimenez et al. (2007b)	VGO	HDS	Isothermal, cocurrent downflow
Mederos and Ancheyta (2007)	Oil fractions	HDS, HDN, HDA	Isothermal, non-isothermal, cocurrent, countercurrent

Table 2.4 cont'd

Shokri et al. (2007)	Gas Oil	HDS	Non-isothermal
Alvarez and Ancheyta (2008a)	Atmospheric residue	HDS, HDN, HDM, HDC, HDAs	Non-isothermal, isothermal, cocurrent downflow
Bahzad and Kam (2009)	Atmospheric residue	HDS	Non-isothermal
Mapiour et al. (2010)	HGO	HDS, HDN, HDA	Isothermal
Chen et al. (2011)	LGO	HDS, HDA	Non-isothermal, cocurrent downflow
Farahani and hahhosseini (2011)	HGO	HDS	Non-isothermal, cocurrent downflow
This study (2011)	**Crude oil**	**HDS, HDN, HDAs, HDV, HDNi**	**Non-isothermal, isothermal, cocurrent downflow**

2.4.2 Hydrocracking Kinetic Models

The growing demand for middle distillates and the increasing production of heavy crude oils have placed hydrocracking as one of the most important secondary petroleum refinery operations. Selected literature of hydrocracking kinetic models is reviewed in this section.

Several reviews on hydrocracking technology have been reported in the literature. Probably the first complete review was done by Choudhary and Saraf (1975). Many aspects of hydrocracking were mentioned, such as types of hydrocracking, feed impacts, catalysis, catalyst acidity, pore diffusion, and catalyst poisons on hydrocracking reactions. Some of the general points of distinction among the main hydrocracking processes have also been discussed. In their study, nothing is reported about the kinetic modelling of hydrocracking.

The kinetic model of gas oil hydrocracking was investigated by Qader and Hill (1969) in a continuous fixed-bed reactor. The liquid product was distilled into gasoline, middle distillate and diesel. This review seems to be the first experimental study in which kinetics of hydrocracking of real feed is studied.

Mosby et al. (1986) studied a kinetic model for describing the performance of a residue hydrocracking using lumped first-order kinetics. For developing the kinetic model, stoichiometry concepts of a complex reacting mixture were applied. The liquid product has been distilled into four fractions: naphtha, middle distillates, gas oil and residue. Residue cut was then distilled under vacuum system in order to obtain the gas oil and residue fractions. All the experimental results were then used to estimate the optimal parameter values.

A detailed kinetic model of hydrocracking of vacuum gas oils with seven lumps (in which different fraction temperatures are considered) was reported by Krishna and Saxena (1989). These lumps are sulfur compounds, heavy and light aromatics, naphthenes, and paraffins. Sulfur compounds are regarded to be a heavy lump. Experimental data reported by Bennett and Bourne (1972) was used to validate the kinetic model.

Yui and Sanford (1989) suggested a kinetic model for hydrocracking of heavy gas oil in a pilot–plant with a trickle bed reactor at various operating conditions. The feeds and total liquid products were distilled into naphtha, LGO, and HGO. The kinetic reaction was modelled as a first order reaction and considered the impact of operating condition on the total liquid product yield.

Mohanty et al. (1990) investigated the technology, chemistry, catalysts, kinetics, and reactor modelling of hydrocracking. Also, a few studies have reported on the kinetics and reactor modelling of petroleum fractions.

Modelling of hydrocracking reactor was developed by Mohanty et al. (1991) in for a two-stage industrial scale for hydrocracking of vacuum gas oil (VGO). The feed and products have been lumped into 23 pseudocomponents (each characterized by its boiling range and specific gravity) for the HDC reactions. The model assumes that each pseudocomponent can only form lighter products by a pseudohomogeneous first order reaction. The kinetic parameters were evaluated using information from literature and plant data. The model estimations indicate that the reactor temperature has a great imact upon the product yields. The developed model was validated against plant data and showed good agreement.

Chaudhuri et al. (1995) studied the state-of-the-art of mild hydrocracking operations, involving data characterization, reaction networks, and kinetics. Comparisons between hydrocracking and mild hydrocracking were also discussed. A few kinetic models for hydrocracking were investigated. The authors observed that the complexity of the commercial feedstocks suggests that the use of pseudocomponents would continue in the study of reaction kinetics.

Callejas and Martínez (1999) investigated the kinetics of Maya residue hydrocracking. First-order kinetic models have been used that include three-lump species: atmospheric residuum (AR), light oils (LO), and gases.

Aoyagi et al. (2003) discussed the kinetic models of hydrotreating and hydrocracking of conventional gas oils, coker gas oils, and gas oils derived from Athabasca bitumen. The review was interested in studying the effect of feed specifications on product yield and composition. A kinetic model was developed and the kinetic parameters were adjusted based on experimental data from a system with two reactors in series, each one with a different catalyst. The model considers that the main reaction in the first reactor is

hydrotreating while hydrocracking reaction is the most significant reaction in the second reactor.

Valavarasu et al. (2003) focused their contribution on important points of mild hydrocracking, such as processes, catalysts, reactions, and kinetics. The advantages of mild hydrocracking process in terms of improving product qualities and increased distillates were summarized. These investigators also emphasized that the available literature on the kinetics models of hydrocracking is scarce and that structural modelling based on complete hydrocarbon structures needs to be investigated in detail.

Sa´nchez et al. (2005) developed a five-lump kinetic model for moderate hydrocracking of heavy oils: unconverted residue, vacuum gas oil, distillates, naphtha and gases. The model involves 10 kinetic parameters, which were calculated depending on the experimental results obtained in a fixed-bed down-flow reactor, with Maya heavy oil. The kinetic model was developed for basic reactor modelling studies of a process for hydrotreating of heavy petroleum oils that operates at moderate reaction conditions and improves the quality of the feed while keeping the conversion level low.

Kinetics of moderate hydrocracking of heavy oil has investigated by Sanchez and Ancheyta (2007). The kinetic mechanism model was developed with five lumps: gases naphtha, middle distillates, vacuum gas oil and residue. The experimental data was gathered under different operating conditions in the TBR at a pilot plant scale. The results obtained from the hydrocracking of residue were adjusted to second order reaction mechanisms. Estimated product compositions showed a good agreement, with average errors percentage less than 5%.

Elizalde et al. (2009) applied a continuous kinetic lumping model for hydrocracking of heavy oil at moderate reaction conditions. The model parameters were determined from experimental data generated in an isothermal fixed bed reactor at different operating

conditions. The optimized values of model parameters have been used for predicting results obtained at various reaction conditions from which they were derived. Comparisons between experimental data and predictions using the continuous lumping kinetic model showed good agreement with average absolute error lower than 5%.

Sadighi et al. (2010) studied hydrocracking of VGO in a pilot scale unit under different operating conditions. In order to describe the yield of hydrocracking products, a five-lump discrete lumping approach (VGO or residue, diesel, kerosene, naphtha and gas to match main products of pilot plant reactor) with ten reactions was investigated.

A kinetic model for predicting the product quality of vacuum gas oil (VGO) hydrocracking process was developed by Haitham et al. (2011). Experimental data were obtained using a pilot plant hydrocracking catalytic reactor loaded with the same catalyst type used in the actual refinery. Model parameters were calculated and related to the specific gravity of the cracked product. Model validation results showed that the developed model is capable of predicting the distillation curves of the hydrocracked products accurately, especially at high operating severity. Simplicity and accuracy of the proposed model makes it suitable for online analysis, to evaluate the conversion as well as the product distribution of hydrocracking units in refineries.

The hydrocracking kinetic models reviewed are summarized in Table 2.5. The present study also considers the kinetic model for increasing the oil distillates productivity based on the experimental data obtained in a pilot plant TBR at different operation conditions using the discrete kinetic lumping approach.

Table 2.5: Summary of hydrocracking kinetic models

Authors (Year)	Feedstock	Main Features
Qader and Hill (1969)	Gas Oil	Three lumps, first experimental study in which kinetics of hydrocracking of real feed is discussed.
Mosby et al. (1986)	Residue	Four lumps, stoichiometry concepts of a complex reacting mixture were applied to develop the model.
Krishna and Saxena (1989)	VGO	Seven lumps, experimental data reported by Bennett and Bourne (1972) have been used to validate the kinetic model.
Yui and Sanford (1989)	HGO	Three lumps, first order kinetic model.
Mohanty et al. (1990)	Petroleum Fractions	Technology, chemistry, catalysts, kinetics, and reactor modelling of hydrocracking were discussed.
Mohanty et al. (1991)	VGO	Implemented Stangeland's kinetic model in a computer model for a two-stage industrial scale, first order reaction with 23 pseudo components.
Chaudhuri et al. (1995)	Petroleum Fractions	State-of-the-art of mild hydrocracking operations, the comparisons between hydrocracking and mild hydrocracking, pseudo components would continue in the study of reaction kinetics.
Callejas and Martı´nez (1999)	Maya Residue	Three lumps, first-order kinetic models
Aoyagi et al. (2003)	Gas Oil	Kinetics models of hydrotreating and hydrocracking of different gas oil were developed based on experimental data from a system with two reactors in series.
Valavarasu et al. (2003)	VGO	Improving product qualities and increased distillates were summarized. Kinetics models of hydrocracking are scarce and structural modelling needs to be studied in detail.
Sa´nchez et al. (2005)	Heavy Oils	Five-lumps, moderate HDC, the kinetic model were developed for basic reactor modelling of HDT process.
Sanchez and Ancheyta (2007)	Heavy Oils	Five-lumps, second order reaction kinetic.
Elizalde et al. (2009)	Heavy Oils	Continuous lumping model, moderate conditions, the comparisons between experimental data and predictions.
Sadighi et al. (2010)	VGO	Five-lumps, describe the yield of HDC products.
Haitham et al (2011)	VGO	Predict the product quality, model parameters were calculated and related to the specific gravity of the cracked product.
This study (2011)	**Crude oil**	Five lumps, predict the product quality, kinetic parameters are estimated based on experiments at different operating conditions.

2.5 Process Simulation

Simulation can be defined as a science that deals with the study of a process or its parts by changing its mathematical or physical models. Information on the existence of solutions in different domains of the process parameters can be often gained for a moderate computational cost on modern computer platforms. This is only actual possibility in a majority of cases. Solution of the model equations utilizing computers is known as computer simulation (Khalfalla, 2009).

Simulators of chemical operations simplify the process of estimating the various design alternatives without the need for making a lot of system assumptions and considering the total system structure (Teresa et al., 2003). A system simulator has the ability to input and modify the configuration of the system flowsheet and to perform design estimations regarding the full system flowsheet, before they are tried on the real unit. In this way it is possible to model and predict the manner of the operation flowsheet as well as studying various process scenarios, such as various feedstocks, high flow rates and modified operating conditions, in combination with estimations of the system economics and effects of potential environmental effect.

System simulation is an engineering instrument utilized for the design and optimization of dynamic and steady–state chemical operation. System simulation has several advantages; it is much easier to incorporate real operation and economics data into a simulation model in place of constructing a pilot–plant (Khalfalla, 2009).

In this study, the gPROMS software package is used for modelling, simulation and optimization during crude oil hydrotreating in a trickle bed reactor. More details about gPROMS is presented in Chapter 4.

2.6 Process Optimization

Optimization is the employment of specific approaches to estimate the efficient solution to a problem or design for an operation. This approach is one of the main quantitative tools in industrial decision making. Very large problems in the design, process, construction, chemical plants analysis and other industrial operations, can be solved by optimization methodologies.

A well–known approach to the basis of optimization was first written centuries ago on the walls of an old Roman bathhouse in connection with the selection between two aspirants for the Emperor of Rome. It read "Do doubus mails, minus est simper aligendum" of two evils, all the time select the lesser (Edgar et al., 2001).

Optimization addresses issues in engineering, business, physical, chemical, architecture, economics and management, etc. The range of techniques available is nearly as wide. The purpose of optimization is to find the values of the system (design) variables that give the best value of the performance criterion. Typical problems in chemical engineering operation design or plant process have several, and possibly an infinite number of solutions. Optimization is concerned with choosing the best among the full collection of possible solutions by efficient quantitative ways. Computers and accompanying applications packages make the necessary computations feasible and cost effective (Edgar et al., 2001; Aziz, 1998).

Engineers work to develop the initial design of equipment and then strive for improvements of the process involving that equipment once it is installed to achieve the biggest production, largest profit, the minimum cost, the least energy usage and so on.

In plant processes, benefits arise from developing plant performance, such as improved yields of precious products or reduced yields of impurities, reduced energy consumption

and higher processing rates. Optimization can also lead to a decrease in upkeep costs and to better staff utilization. Also, intangible benefits arise from the interactions among plant workers, engineers and management (Edgar et al., 2001).

Optimization can be applied in many ways to chemical operations and plants. Typical projects in which optimization has been utilized involve (Edgar et al., 2001; Ekpo, 2006):

- Operation equipment such as reactors, heat exchanger, columns, etc.
- Determination of plant data to build a model of an operation.
- Estimation of better sites for plant location.
- Sizing of pipeline and layout.
- Complete plant design and equipment.
- Routing of tankers for distribution of crude and petroleum products.
- Planning and scheduling of building.
- Minimization of inventory charges.
- Allocation of resources or services among numerous operations.

Every optimization problem needs to find a set of independent variables (parameters) that optimize a given quantity, possibly subject to limitations on the allowed parameter values. Generally, an optimization problem consists of the following (Khalfalla, 2009):

a) An objective function that is to be optimized, such as maximum conversion, maximum profit, minimum cost and minimum time.
b) Controllable inputs that are the collection of decision variables that affect the value of the objective function. Decision variables are necessary. If there are no variables, we can not define the objective function and the problem constraints can not be satisfied.

c) Uncontrollable inputs, called parameters. These parameters could be fixed values accompanied with a particular problem. The values of these parameters will change in each problem variation.

d) Constraints that are relations between the controllable and uncontrollable inputs (or between the decision variables and the parameters).

The scope of unconstrained optimization is a wide and significant one for which many algorithms and software are available.

A general optimization problem can be stated mathematically as follows:

$$\text{Minimize or maximize} \quad Z = f(x), \qquad x = x_1 , x_2 , \ldots\ldots, x_n$$

$$\text{Subject to} \quad C_i(x) = 0, \qquad i = 1 , 2 , \ldots\ldots\ldots, m$$

$$C_i(x) \geq 0, \qquad i = m + 1 , 2 , \ldots\ldots, R$$

$f(x)$ is the objective function, x is the vector of n independent variables and $C_i(x)$ is the set of constraint functions. Constraint equations of the type $C_i(x) = 0$ are called equality constraints (e.g. model equations), while $C_i(x) \geq 0$ are called inequality constraints (e.g. lower and upper bounds of operating variables). There is no single method or algorithm of optimization that can be used efficiently for all problems. The method selected for any certain problem will depend primarily on (Edgar et al., 2001):

- The character of the objective function(s), whether or not it is clearly known.
- The number of dependent and independent variables.
- The nature of the constraints.

The general aim of optimization is to select a collection of values of the design variables subject to the different constraints, which will produce the desired optimum response for the selected objective function.

2.7 Parameter Estimation Techniques

In the behavioural sciences, the estimation of parameters in one's model plays an important role in validating the model. Parameter estimation is the process of using observations from a system in order to develop a mathematical model that adequately represents the system characteristics. The assumed model consists of a finite set of parameters, the values of which are evaluated utilizing estimation techniques. The idea behind modelling an engineering system or process is to improve its performance or to design a control system. Mathematical modelling via parameter estimation is one of the approaches that leads to deeper understanding of a system's characteristics. These parameters often describe the stability and control behaviour of the system. Estimation of these parameters from the data of the process is thus a significant step in the analysis of the model system (Raol et al., 2004).

For chemical engineers, the benefits of developing kinetic models with accurate parameter evaluations are increasing due to the development of control strategies and operation optimization based upon fundamental process models. Unknown kinetic parameters can be determined successfully depending on the experimental information. The predicted values from the model employed should match with the measurement information (experimental data) as closely as possible so that errors between experimental and theoretical data are minimized (Poyton et al., 2006). The domain of parameter estimation techniques is wide; some of the parameter estimation techniques can be summarized as follows:

- State estimation (Stephanopoulos and San, 1984; Kosanovich et al., 1995; Soroush, 1997).
- Calorimetric (Carloff et al., 1994; Barandiaran et al., 1995; Regnier et al., 1996).

- Model inversion for parameter estimation (Tatiraju and Soroush, 1998).
- Optimization (Muske and Rawlings, 1995; Robertson et al., 1996).

Optimization as an approach is very popular and has been widely employed in the chemical process industry to estimate different kinetic parameters. Many optimization techniques have been developed recently, among them:

- Regularization methods, augmented Lagrangian methods, and level set approaches (Ahn et al., 2010).
- Linear and non-linear approaches (Kuzmic, 1996; Mendes and Kell, 1998).

Non-linear optimization is used widely and is commonly utilized to evaluate the best values of kinetic parameters despite the popularity of the linear programming (LP) method due to its ability to handle a lot of parameters. The LP method cannot be applied to any system due to the need for a linear objective function in terms of the adjustable parameters (Mendes and Kell, 1998). Several techniques of non-linear optimization are used to estimate kinetic parameters, such as:

- Stochastic methods (Rinnooy Kan and Timmer, 1989).
- Maximum likelihood estimation (Tjoa and Biegler, 1991).
- Newton's method (Fletcher, 1987).
- Levenberg-Marquardt method (Levenberg, 1944; Marquardt, 1963).
- Genetic algorithms (GAs) (Holland, 1975; Alonge et al., 1998; Bollas et al., 2004; Orlowska et al., 2006; Abbasi and Fatemi, 2009).
- Evolutionary algorithms (Nangsue et al., 1999).
- Adaptive GAs (Abdelhadi et al., 2004).
- Bayesian parameter estimation (Liebermeister and Klipp, 2006; Huang and McBean, 2007; Ma and Weng, 2009).

- Successive Quadratic Programming (Tjoa and Biegler, 1992).
- Differential evolution (Ursem and Vadstrup, 2003).

The Levenberg-Marquardt method and Successive Quadratic Programming (SQP) methods have largely been used for hydrotreating reactions (Tsamatsoulis and Papayannakas, 1998; Marroquin et al**.,** 2005; Sa´nchez et al., 2005; Trejo and Ancheyta, 2005; Resendiz et al., 2007; Sanchez and Ancheyta, 2007; Alvarez and Ancheyta, 2008a; Elizalde et al., 2009).

2.8 Conclusions

This chapter was concerned with a review of past research into hydrotreating processes. It has been observed that the hydrotreating process is one of the most important processes that are carried out in refineries to improve product yield and to remove impurities, such as sulfur, nitrogen, vanadium, nickel and asphaltene in addition to saturating the unsaturate hydrocarbonic compounds. It has been noted that the main process variables of hydrotreating reactions, which are reaction temperature, hydrogen partial pressure, liquid hourly space velocity and H_2/oil ration, influence the degree of impurities removal.

Trickle bed reactors can be used for large operations in chemical process and have many features. Modelling, simulation and optimization processes with kinetic models of hydrotreating reactions in addition to the application of optimization to the design and operation of chemical process and plants are presented.

Developing a kinetic model that can accurately predict the hydrotreating performance of crude oil under different operating conditions is important in order to develop a reliable

catalytic hydrotreating model, which can significantly applied to process design and operation and fully understand the operation with all accompanied phenomena related to modelling aspect are required.

The kinetic parameter estimation techniques are also discussed briefly in this chapter. It can be concluded that the evaluation of the kinetic parameters in trickle bed reactors applied to HDT reactions are necessary for ensuring accurate model calculations and good model based decision, so that the model can be effectively used for simulation, optimization and control.

Chapter Three

Experimental Work: Results and Discussion

3.1 Introduction

Experimental data are required to estimate the best kinetic parameters, to validate the model under different operating conditions, to design and predict the expected behaviour of crude oil hydrotreating processes with increasing the productivity of oil distillates at commercial or industrial scale, and to facilitate adequate reactor modelling. Although the models reported in the literature were used successfully to describe the behaviour of pilot plant reactors, little effort has been made towards scaling up to an industrial reactor. Furthermore, several of the models presented (on different oil fractions and not on full crude oil) have not considered all of the significant reactions taking place in a hydrotreating unit. In the present investigation, efforts are made for developing adequate mathematical models that can account for all of the main reactions, and can simulate the behaviour of both pilot plant and commercial scale TBRs.

In this chapter we review detailed pilot plant experiments (such as feedstock, catalyst type, pilot plant equipments, catalyst presulfiding, experimental runs, sample analysis, etc.), which include hydrotreating reactions (that comprises, HDS, HDN, HDAs, HDV and HDNi reactions) at different operating conditions, and distillation process (that involves, light naphtha (L.N), heavy naphtha (H.N), heavy kerosene (H.K), light gas oil (L.G.O) and reduced crude residue (R.C.R)). Also, in this chapter, we present and discuss results obtained via experimental work during hydrotreating of crude oil using trickle bed reactor.

3.2 Pilot Plants

3.2.1 Materials Used

3.2.1.1 Feed Oil

Iraqi crude oil was used as a real feed in all experiments for hydrotreating processes. The main properties of the feedstock used in this work are shown in Table 3.1.

Table 3.1: Feedstock properties

Chemical specification	Units	Value
Specific Gravity at 15.6 ^{0}C	-	0.8558
API	-	33.84237
Viscosity at 37.8 ^{0}C	cSt	5.7
Pour point	°C	-36
Molecular Weight	kg/kg mole	227.5
Mean Average Boiling Point	°C	291
Sulfur content	wt %	2.0
CCR	wt %	5.1
Vanadium content	ppm	26.5
Nickel content	ppm	17
Nitrogen content	wt %	0.1
Asphaltenes content	wt %	1.2
Ash content	wt %	0.008

3.2.1.2 Catalyst

The catalyst used for the hydrotreating (HDT) processes in the work was commercial cobalt–molybdenum on alumina (Co-Mo/γ-Al_2O_3), similar to the type used in the industrial reactor in the Baiji Refinery (North Oil Company- Iraq). The catalyst used was an extrudate with a cylindrical shape and an equivalent diameter of 1.8 mm. The surface area and pore volume of the catalyst are 180 m^2/g and 0.5 cm^3/g, respectively. The properties of the catalyst are listed in Table 3.2.

Table 3.2: Catalyst commercial properties (Co-Mo/γ-Al_2O_3)

Chemical specifications	**Units**	**Value**
MoO_3	wt %	15
NiO	wt %	3
SiO_2	wt %	1.1
Na_2O	wt %	0.07
Fe	wt %	0.04
SO_2	wt %	2
Al_2O_3		Balance
Physical specifications	**Units**	**Value**
Form	-	Extrude
Surface area	m^2/g	180
Pore volume	cm^3/g	0.5
Bulk density	g/cm^3	0.67
Mean particle diameter	mm	1.8

3.2.2 Equipment and Procedure

3.2.2.1 Hydrotreating Pilot Plant

Pilot plants play an important role in petroleum refining industries. They are particularly utilized in the assessment of the performance of the catalytic process, providing valuable information that can be used as a predictive tool for industrial performance. The process flow diagram of the hydrotreating pilot plant is illustrated in Figure 3.1. Basically, the pilot plant consists of four sections: the feed section, the reactor section, the products sections, and the gases section.

The feed section has two modules, a gas supply module and a feed supply module. The gas supply module provides the unit with high-pressure hydrogen required for hydrotreating reactions. The hydrogen is fed to the reactor through a heated high-pressure line.

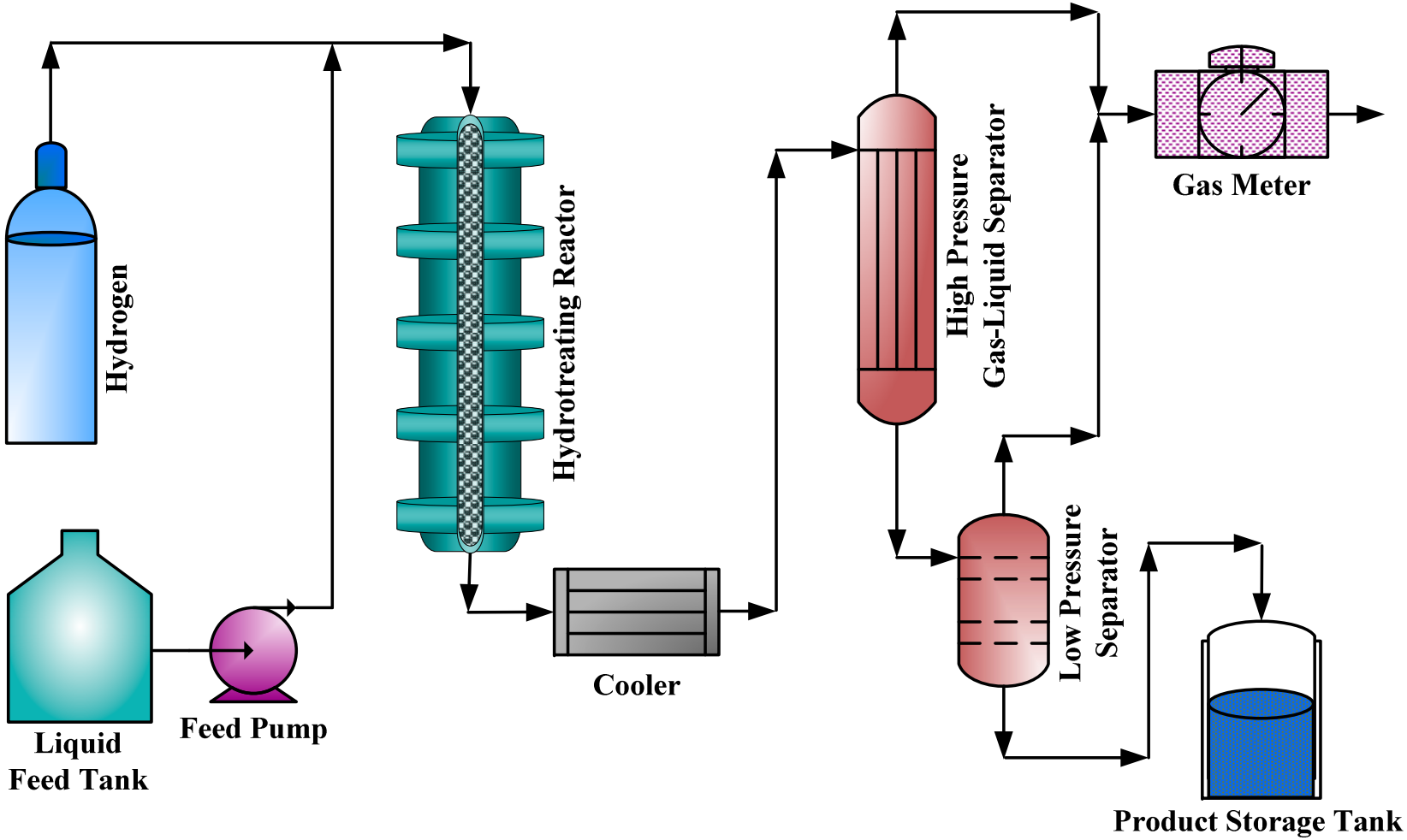

Figure 3.1: General scheme of the hydrotreating pilot-plant unit

The unit was supplied with an electrical gas inlet flow sensor and hydrogen flow rate. The feed supply module primarily consists of a liquid feed tank and a feed pump. The feed tank is a cylindrical tank with a capacity of 2 litres. The unit was supplied with a high-pressure dosing pump to introduce the feed oil into the reactor. A calibrated micrometer was fitted in the pump to monitor the feedstock flow rate. The reactor section is most the critical zone in the unit. The feedstock and hydrogen pass through the reactor in a down concurrent flow mode. The reactor tube was made of stainless steel with an inside diameter of 2cm and a length of 65cm. The length of the reactor is divided into three parts (reactor configuration is shown in Figure 3.2). The first part, of 20cm, was packed with inert particles (glass beads of 4mm diameter). This entrance section was employed to heat up the mixture to the required temperature, to ensure homogeneous flow distribution of gas and liquid and to avoid end effects. The following section of length 27.8cm contained a packing of 60.3g catalyst. The bottom section (17.2cm) was packed with inert particles in order to ensure as serve as disengaging section. The reactor was operated in isothermal mode by independent temperature control of five zone electric furnaces, which provided an isothermal temperature along the active reactor section.

The product section consists of low and high gas-liquid separators and a products storage tank. The reactor outlet feeds the high pressure and temperature separator where the liquid and gas are separated. Finally, in the gases section, the exiting gas is passed through a gas flow meter before being released.

3.2.2.1.1 Experimental Runs

The main HDT reactions considered in this work are hydrodesulfurization (HDS), hydrodenitrogenation (HDN), hydrodemetallization (includes hydrodevanadization (HDV) and hydrodenickelation (HDNi)) and hydrodeasphaltenization (HDAs).

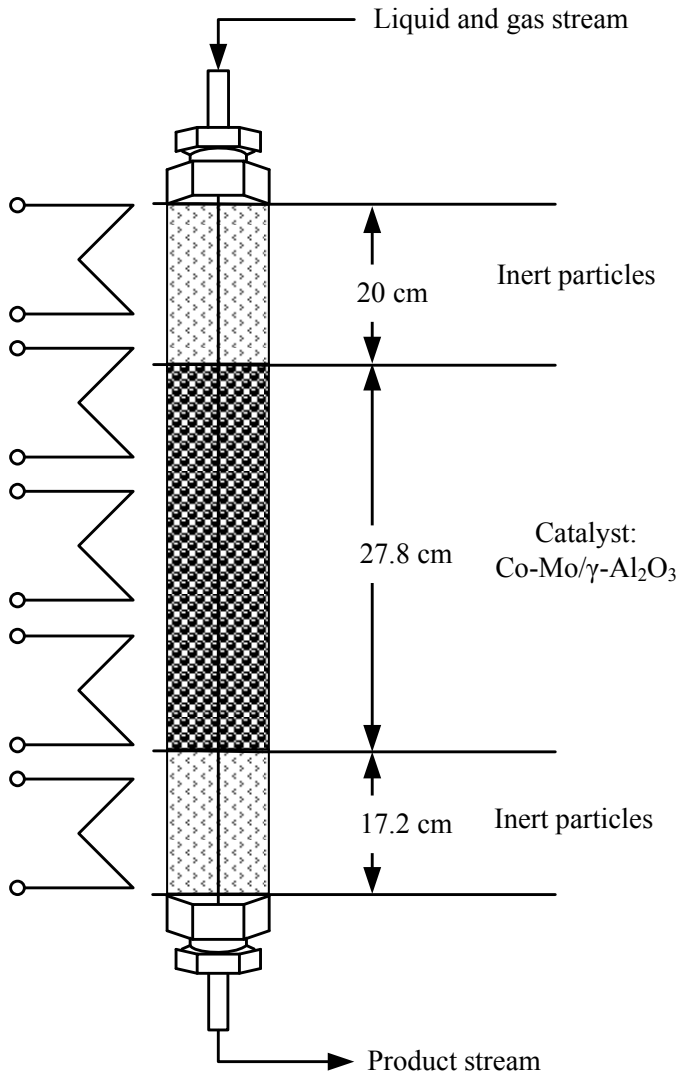

Figure 3.2: Reactor configuration

These reactions were carried out in a continuous flow trickle bed reactor (TBR) using crude oil as a feedstock and cobalt–molybdenum as a catalyst. The data obtained from these experiments are used to development the kinetic models that can represent the HDS, HDN, HDV, HDNi, HDAs and oil productivity reactions to determine kinetic parameters and to validate the model under various operating conditions.

In this section, a number of experimental procedures will be covered such as catalyst presulfiding, operating conditions and sample analysis. Before starting any run, a leak test must be carried out. This test is performed with nitrogen (N_2) at 130 bar for 12 hours. Once the leak test is passed, the run will start with catalyst presulfiding.

3.2.2.1.1.1 Catalyst Presulfiding

Catalyst presulfiding has been widely practiced in the petroleum refining industry. Its positive effect has been significantly observed in the HDT processes, where it creates the essential surface required for optimum activity by transforming the form of active sites from metal oxide to metal sulfide. The sulfiding prereatment optimizes the catalyst performance in two different aspects. Firstly, it improves the catalyst activity by permitting deeper diffusion of feed into the catalyst pellets. Better access of large molecules into the internal pores enhances the conversion rate and the distribution of metal deposits. The second effect of presulfiding is the reduction of the extent of early deactivation caused by coke deposition (Absi-Halabi et al., 1989). It has been observed that presulfiding practice reduces the coke formation tendency by passivating the high active acidic oxide site. The coke deposition mechanism of presulfided catalyst allowed it to have a substantially higher surface area than the unsulfided catalyst (Absi-Halabi et al., 1996; Absi-Halabi and Stanislaus, 1996).

The catalyst presulfiding process is carried out using either a dry or a wet method. In the dry method, hydrogen sulfide (H_2S) is injected with the hydrogen stream to sulfide the catalyst. On the contrary, the wet method is achieved by pumping gas oil that is spiked with carbon disulfide (CS_2) or dimethyl disulfide (DMDS). In this work, the wet presulfiding method was used. $90cm^3$ of the fresh catalyst was charged to the hydrotreating reactor after drying at 120^0C for 2 hours, where the presulfiding process starts by increasing the reactor temperature up to 120^0C. At this temperature, pumping of the presulfiding feed to the reactor starts. Catalyst presulfiding is accomplished by a solution of 0.6 vol% of CS_2 in commercial gas oil. After two hours, the reactor temperature gradually increases to 210^0C and remains there for 4 hours at 100 bar with $2.0hr^{-1}$ liquid hourly space velocity and without hydrogen flow. Then, the reactor temperature is ramped to 300^0C. The next step in the catalyst activation takes 16 hours

with the following conditions: pressure 100 bar, LHSV 1 h^{-1} and hydrogen flow rate 30 litre/hr. Finally, the feed is switched to crude oil. Two hours later, the reactor temperature gradually increased to the reaction temperature, which is 335°C. Figure 3.3 shows the presulfiding procedure and conditions.

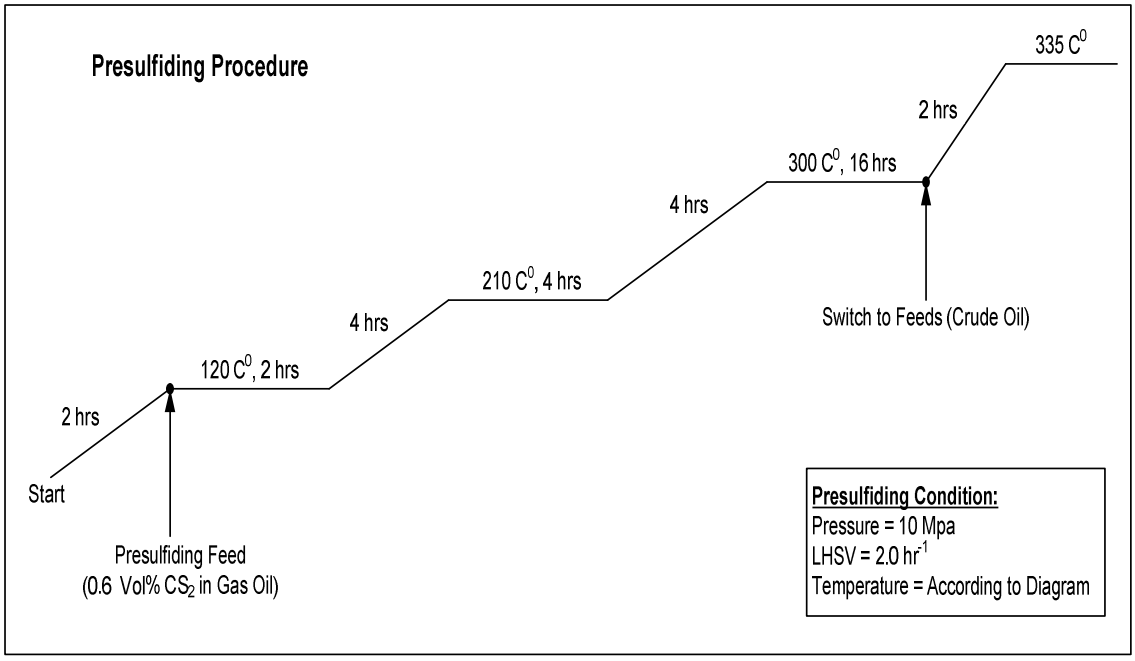

Figure 3.3: Presulfiding procedure and conditions

3.2.2.1.1.2 Operating Conditions

The major effect of operational variables employed in HDT units and their influence on the reactor performance can be summarized as follows. To improve the sulfur conversion and other conversions, three procedures can be chosen: increase of temperature, decrease of liquid hourly space velocity and increase of pressure. However, there are many limitations that should be taken into account during the HDT process. An increase in reactor temperature, particularly above 410^0C, will lead to severe hydrocracking reactions and will give undesirable compounds in addition to reduced catalyst life. A decrease in liquid hourly space velocity will decrease the plant capacity, and hence new hydrotreating reactors will have to be added in order to keep

the existing production capacity. Also, an increase in hydrogen pressure above 100 atm (10.13Mpa) is not favourable, the partial pressure does not increase owing to existing physical constraints of maximum pressure (Fogler, 1999; Jimenez et al., 2005; Jimenez et al., 2007b). The ranges of operating conditions used in this study for crude oil hydrotreating reactions are indicated in Table 3.3.

Table 3.3: Operating conditions used

Run	LHSV (hr^{-1})	P (Mpa)	T (^0C)
1	0.5	4	335
2	1.0	4	335
3	1.5	4	335
4	0.5	4	370
5	1.0	4	370
6	1.5	4	370
7	0.5	4	400
8	1.0	4	400
9	1.5	4	400
10	0.5	7	335
11	1.0	7	335
12	1.5	7	335
13	0.5	7	370
14	1.0	7	370
15	1.5	7	370
16	0.5	7	400
17	1.0	7	400
18	1.5	7	400
19	0.5	10	335
20	1.0	10	335
21	1.5	10	335
22	0.5	10	370
23	1.0	10	370
24	1.5	10	370
25	0.5	10	400
26	1.0	10	400
27	1.5	10	400

3.2.2.1.1.3 Sample Analysis

All analytical techniques that have been used for the characterization of the feedstock and its derived products were accurate and repeatable. Average results have been taken

into accounts for each run with maximum deviation of 2% among all runs. A bomb method (ASTM: D-129) was used to calculate the sulfur content in the feedstock and the products samples. Metal content (V and Ni) were analyzed by IP-285. ASTM: D-4629 method was utilized to calculate the total nitrogen content in the feed and product samples. The standard method (IP-143) was used to estimate the asphaltene content in the feedstock and products.

3.2.2.1.1.3.1 Sulfur Analysis

The sulfur content in the feedstock and products were determined according to the bomb method (ASTM: D-129). This method consists mainly of bomb, sample cup, firing wire and cotton wick. The sample is oxidized by combustion in the bomb containing oxygen under pressure at 3 MPa. The oxidation products as sulfite in the bomb and with hydrogen peroxide will be converted into sulfuric acid, then dissolved in ethanol after dilution to 250 ml (vol%), and mixed with barium chloride in a burette using thorin as a reagent.

3.2.2.1.1.3.2 Metal Analysis

The vanadium and nickel content of the feedstock and hydrotreated samples were calculated using IP-285 method. The main set up of this method consists of a ceramic pot, a thermal furnace, and sulfuric acid. The method depends on the sample burning inside the furnace at a high temperature (550^0C). The residual ash generated is dissolved in HNO_3, H_3PO_4 and sodium tungustate ($Na_2Wo_4.2H_2O$) for vanadium, and in ammonium citrate ($C(OH)(COOH)(CH_2COOH)_2$) and ammonium di-methyl glyoxime ($CH_3C(:NOH)C(:NOH)CH_3$) for nickel. After that, the concentrations of vanadium and nickel are determined at wavelengths 405 nm and 440 nm in a Spectro-Photo-Meter for vanadium and nickel, respectively.

3.2.2.1.1.3.3 Nitrogen Analysis

The nitrogen content in the feedstock and products were estimated by using ASTM: D-4629 method. This method includes a furnace, a combustion tube, drier tube, a chemiluminescent detector, magnesium perchlorate (Mg(ClO4)2), oxygen (high purity grade-99.8%), an inert gas (helium high purity grade), carbazole, solvent (Isooctane), flow controllers, and a micro-liter syringe. The sample of crude oil is introduced by syringe into a stream of inert gas (helium) then is vaporized and carried to a high temperature zone where oxygen is introduced and organically bound nitrogen is converted to nitric oxide (NO). The NO contacts ozone, and will be converted to nitrogen oxide (NO_2). A photomultiplier tube detects the light emitted as the excited NO_2 decays and the resulting signal is a measure of the nitrogen contained in the sample.

3.2.2.1.1.3.4 Asphaltene Analysis

The asphaltene content of the feedstock and hydrotreated samples are calculated using the IP-143 method. This method consists mainly of 3 flasks, filter paper, a water bath, n-heptane, toluene, a desiccator, a vacuum pump, an oven, and a sensitive balance. The method was carried out by taking a sample of the substance to be examined (20g) and dissolving it in n-heptane. It is then put it in a water bath for 30 min. After that, the solution generated is filtrated and washed by n-heptane again. The filter paper is dried in an oven at 80-100°C for 30 min and then the sample is weighted by a sensitive balance. After this, 200 ml of toluene is used for washing the sample, which is then filtered, dried and weighed. The amount of asphaltene is calculated by different weights.

3.2.2.1.1.3.5 Other Tests

Other tests to measure the feed and products properties are summarized in Table 3.4.

Table 3.4: Other tests methods for calculating the feed and products properties

Test Type	Test Method
Specific Gravity	IP-120
Viscosity	ASTM: D-445
Pour Point	ASTM: D-97
CCR	ASTM: D-524
Ash Content	ASTM: D-482

3.2.2.2 Distillation Unit

Figures 3.3 and 3.4 show the laboratory distillation unit at atmospheric and vacuum pressure used for hydrotreated product fractionation. This unit consists mainly of the following parts:-

- Bottom flask in which the feedstock shipped (capacity of 5 litres).
- Electric heating mantle.
- Thermocouple (to measure the temperature of the raw material during the distillation process.
- Oldershew (15 trays).
- Divider (designed to put a pair of a mercury thermometer to measure the temperature of the steam rising and liquid condensed).
- Condenser.
- Reflux regulator (a magnetic rod placed inside the condenser).
- Receiver cooler.
- Receiver.
- Vacuum pump.
- Trap.
- Vacuum controller.

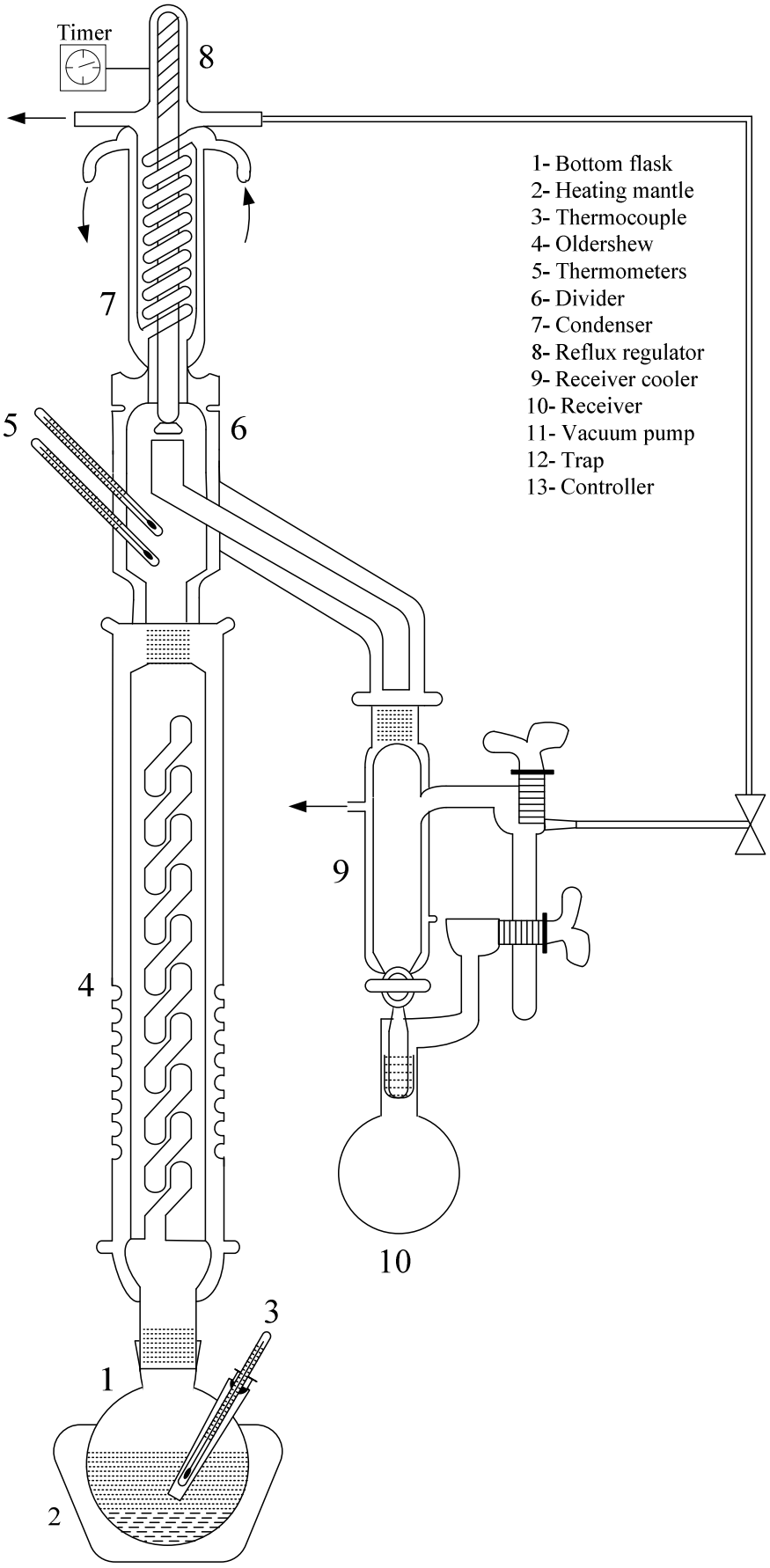

Figure 3.4: Laboratory distillation unit at atmospheric pressure

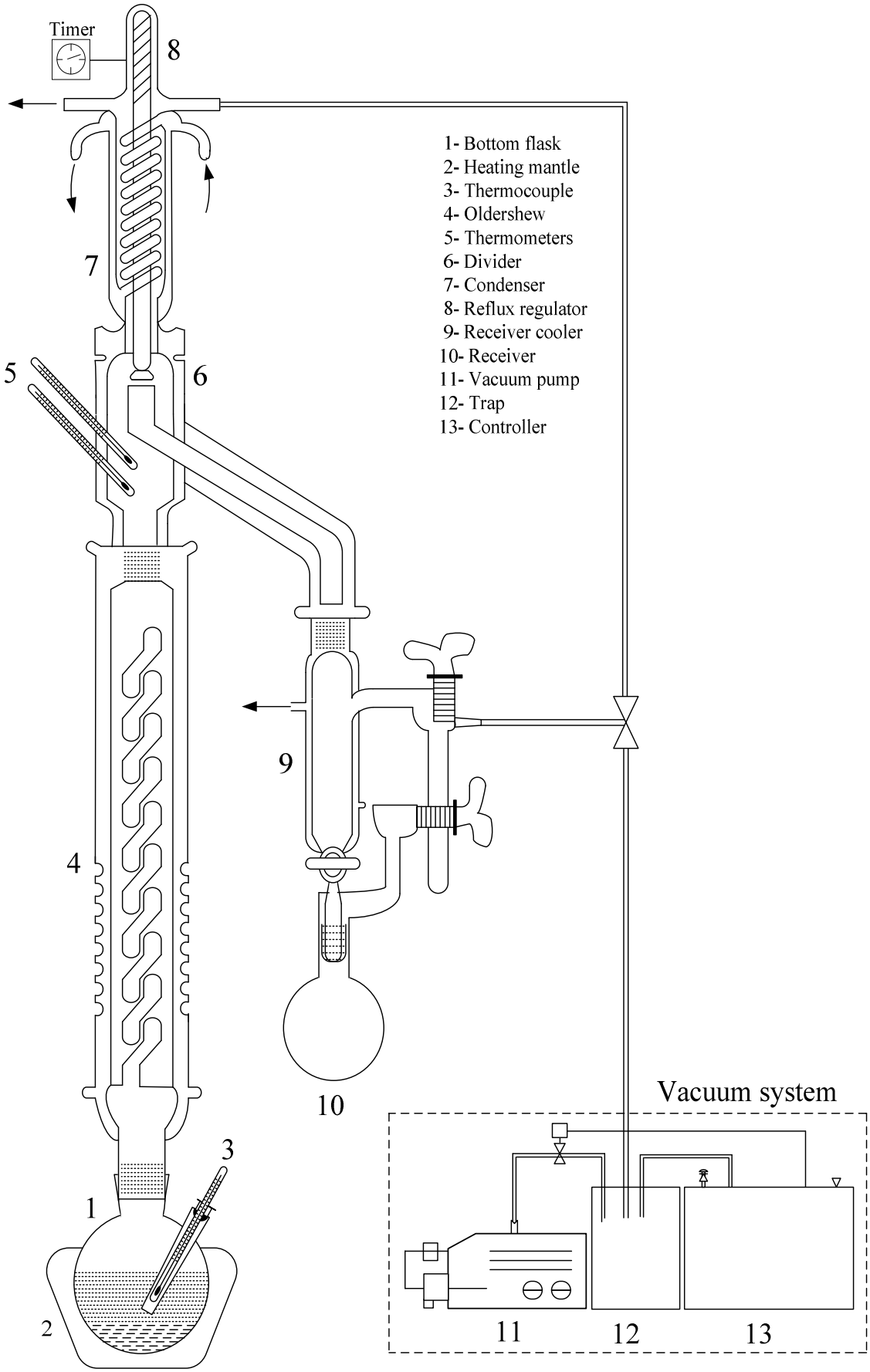

Figure 3.5: Laboratory distillation unit at vacuum pressure

The hydrotreated feedstock is charged in a 5 litre round bottom flask, with an electric heating mantle of 1.2kW. The heating mantle is connected with a step down transformer to provide heat input adjustment. The temperature of the liquid crude oil in the flask was recorded by using a thermocouple through a glass jacket inside the distillation flask. A mercury thermometer located at the top of the distillation column recorded the boiling point of the distilled fraction. The 15 tray-distillation column is 50mm in diameter and 750 mm in length. The still head includes a high efficiency reflux condenser. The cooling medium was alcohol at temperature as low as -29°C in order to provide the necessary cooling in the early stage of distillation to reduce the loss of light hydrocarbons. The cooling medium was turned to ordinary tap water after the distillation temperature exceeded 20^0C. No distillates were collected before equilibrium was attained in the trays. A magnetic rod connected to the reflux timer was used to obtain the desired reflux ratio, where the reflux ratio was 3:5.

The distillation unit was operated at atmospheric pressure until the distillation temperature reached 200 ^{0}C, then the distillation unit system was connected to a vacuum system. The vacuum system consisted of a high efficiency vacuum pump with highly tightened tube connections in order to provide a vacuum pressure as low as possible. The vacuum distillation unit was connected to the vacuum pump through a vapour trap and the distillation continued using pressure 1-0.1 mm Hg.

3.3 Results and Discussion

3.3.1 Effect of Operating Conditions on Impurities Removal

A primary role of hydrotreating processes is to improve the quality of the oil feedstock by removing impurities. Crude oils are characterized by having many impurities that can exert substantial effect upon the properties of the finished products and the efficiencies of refining operations. The efficiencies of desulfurization, denitrogenation, demetallization and deasphaltenization are measured by the degree of sulfur, nitrogen, metals and asphaltene removals, respectively. The effectiveness of these HDT reactions is influenced by process parameters. Therefore, the impact of reaction parameters, which are process temperature, liquid hourly space velocity (LHSV) and reactor pressure on the quality of hydrotreated product, will be discussed.

A series of experimental work for HDS, HDN, HDV, HDNi and HDAs of crude oil were carried out under a wide range of operating conditions: 335^0C-400^0C reaction temperature, 0.5-1.5 hr^{-1} liquid hourly space velocity (LHSV) and 4-10 Mpa pressure at a constant H_2 / Oil ratio of 250 L/L.

3.3.1.1 Sulfur Removal

Figures 3.6 and 3.7 show the effect of operating conditions (reaction temperature, hydrogen pressure and liquid hourly space velocity) on the sulfur content and removal in all products. It has been observed that the sulfur content in all products decreased with increasing temperature and pressure and decreasing liquid hourly space velocity. Similar behaviour has also been reported by many studies for the hydrodesulfurization process using several oily feedstocks (but not on the full crude oil) (Areff, 2001; Bhaskar et al., 2002; Alvarez and Ancheyta, 2008a).

The high removal of sulfur at high temperatures are due to several reasons, such as the high effectiveness of thiophenic sulfur compounds found in the heavy cuts of crude oil (Ali and Abdul-Karim, 1986). Also, the increase in temperature raises the activation energy, leading to an increase in the number of particles of sulfur compounds interacted. This leads to cleavage of the long-sulfur compounds and spread within the catalyst. Furthermore, high temperatures increase the rate of proliferation and osmosis in the pores of the catalyst on the active sites where HDS reactions occur because of the low viscosity (Isoda et al., 1998). Increased sulfur removals by decreasing in LHSV are attributable to increased contact time (residence time) between the molecules of reactants and catalyst, and provide sufficient time for the reaction process (Kim and Choi, 1987; Al-Humaidan, 2004).

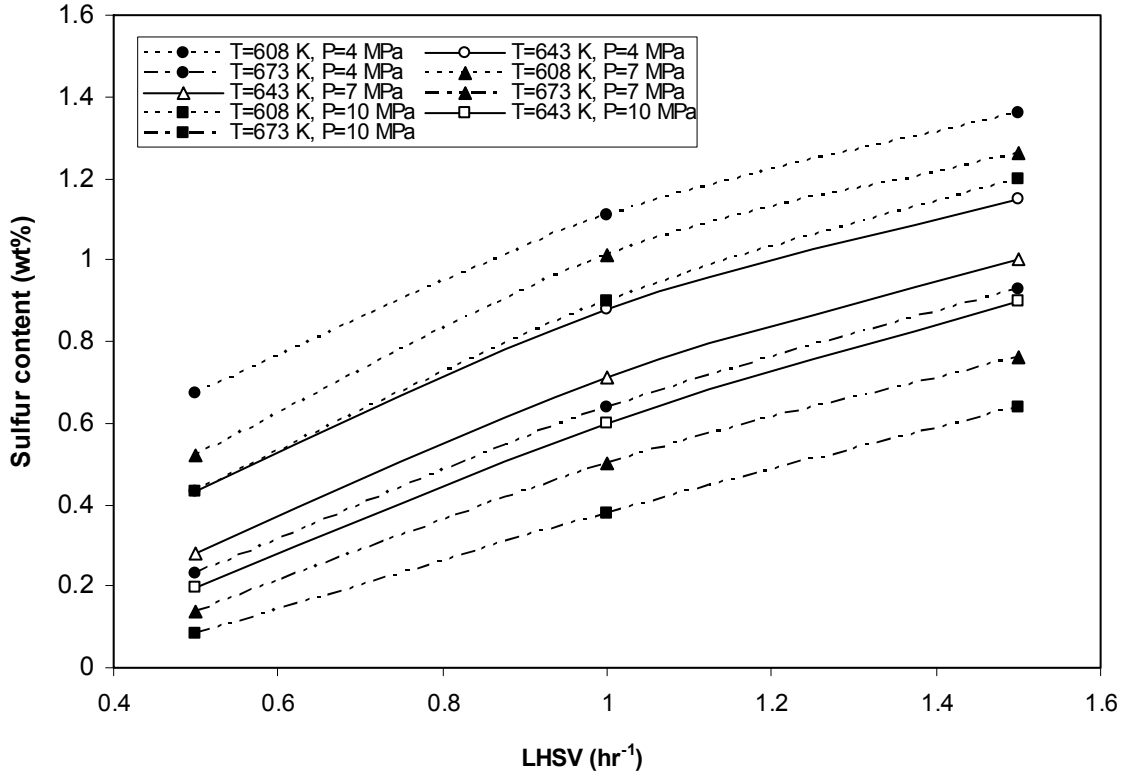

Figure 3.6: Experimental data variation of sulfur content vs. LHSV at different temperature and pressure

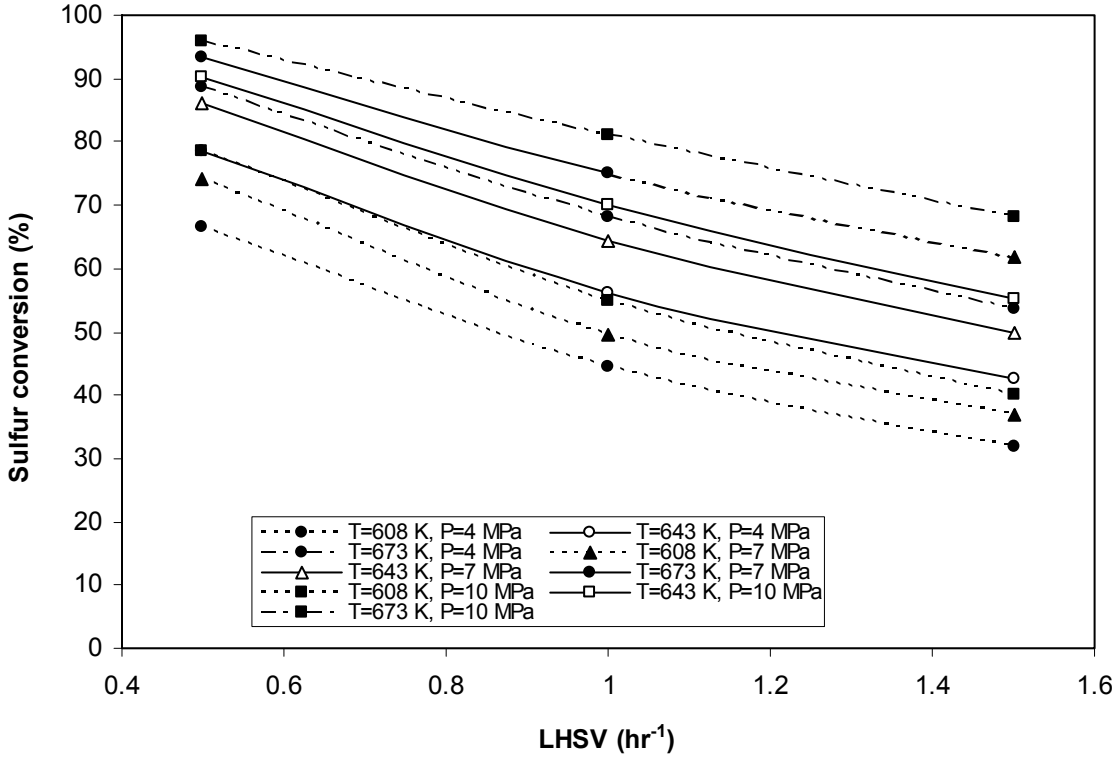

Figure 3.7: Experimental data variation of sulfur conversion vs. LHSV at different temperature and pressure

3.3.1.2 Nitrogen Removal

The hydrodenitrogenation (HDN) reaction is considered to be one of the hardest HDT reactions owing to the complexity of nitrogen compounds. The rate at which the denitrogenation reaction happens depends upon the saturation rate of aromatic rings. The hydrodenitrogenation reaction increases the hydrogen consumption and the amount of heat generated (Meyers, 1997). The experimental results for HDN reactions showed that the results of an increase in reaction temperature and pressure and decrease in LHSV is improved product quality by reducing the content of nitrogen, in all products and increasing in the removal of these impurities as shown in Figures 3.8 and 3.9. Similar outcomes have also been found by several investigations for the HDN process using different oil fractions (but not on the full crude oil) (Maria and Martinez, 1999; Ancheyta et al., 2001; Rodriguez and Ancheyta, 2004).

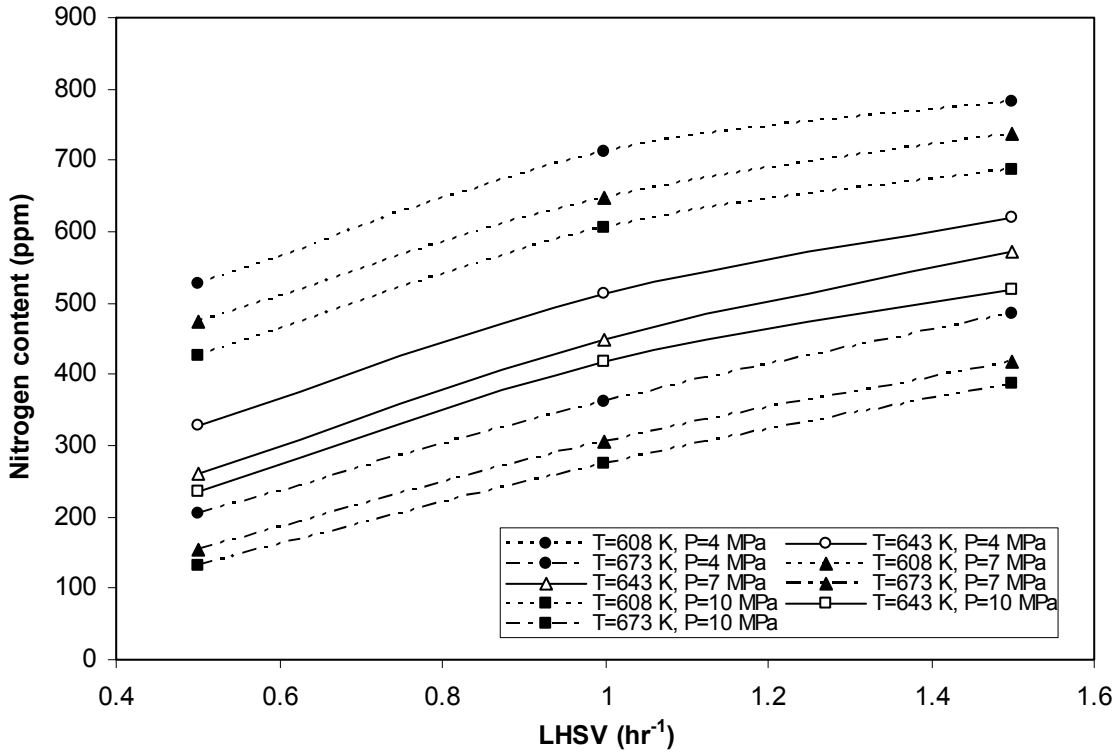

Figure 3.8: Experimental data variation of nitrogen content vs. LHSV at different temperature and pressure

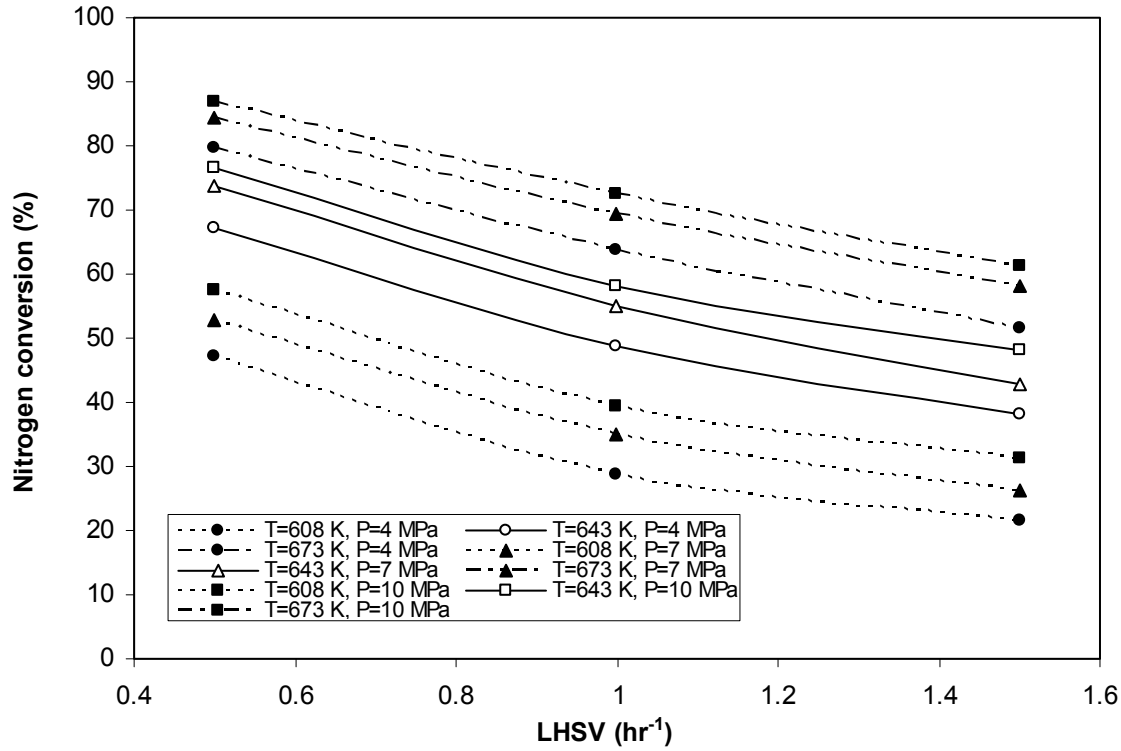

Figure 3.9: Experimental data variation of nitrogen conversion vs. LHSV at different temperature and pressure

The increase in nitrogen removal at high temperature can be attributed to the unreactive nitrogen compounds (or the compounds containing these impurities) becoming activated enough to react with hydrogen. Also, the large molecules are converted into smaller molecules at high temperature, which can more easily diffuse inside the catalyst pores and reach the inner active sites where the HDN reactions occur as a result of rising activation energy leading to an increase in the number of particles of nitrogen compounds reacted (Isoda et al., 1998). Oil diffusivity increases through the catalyst pores due to a decrease in the oil viscosity. As the liquid hourly space velocity decreases, denitrogenation increases because the residence time increases between the molecules of reactants and catalyst, providing adequate time for the reaction process (Al-Humaidan, 2004).

3.3.1.3 Metals Removal

As mentioned previously, the presence of metals in crude oil or oil fractions adversely affects the hydrotreating efficiency. Experimental results for hydrodemetallization (HDM) reaction are plotted in Figures 3.10 and 3.11 for the HDV reaction, and in Figures 3.12 and 3.13 for the HDNi reaction. By studying these figures, it is clearly seen that the vanadium and nickel content in all products decrease at high temperature and pressure, and low LHSV. This is explained by highlighting that a high reaction temperature leads to an increase in the reactions between metal compounds (or the compounds containing these impurities) and hydrogen. The highest removal of vanadium and nickel is observed at maximum temperature and pressure, and minimum LHSV due to an increase in the destruction of large molecules, especially heavy molecules that contain a large amount of metals, which can more easily spread inside the catalyst pores and increase the compounds reacted in addition to increase the activation energy of these compounds according to increase in the reaction temperature (Isoda et al., 1998; Abbas, 1999; Speight, 2000).

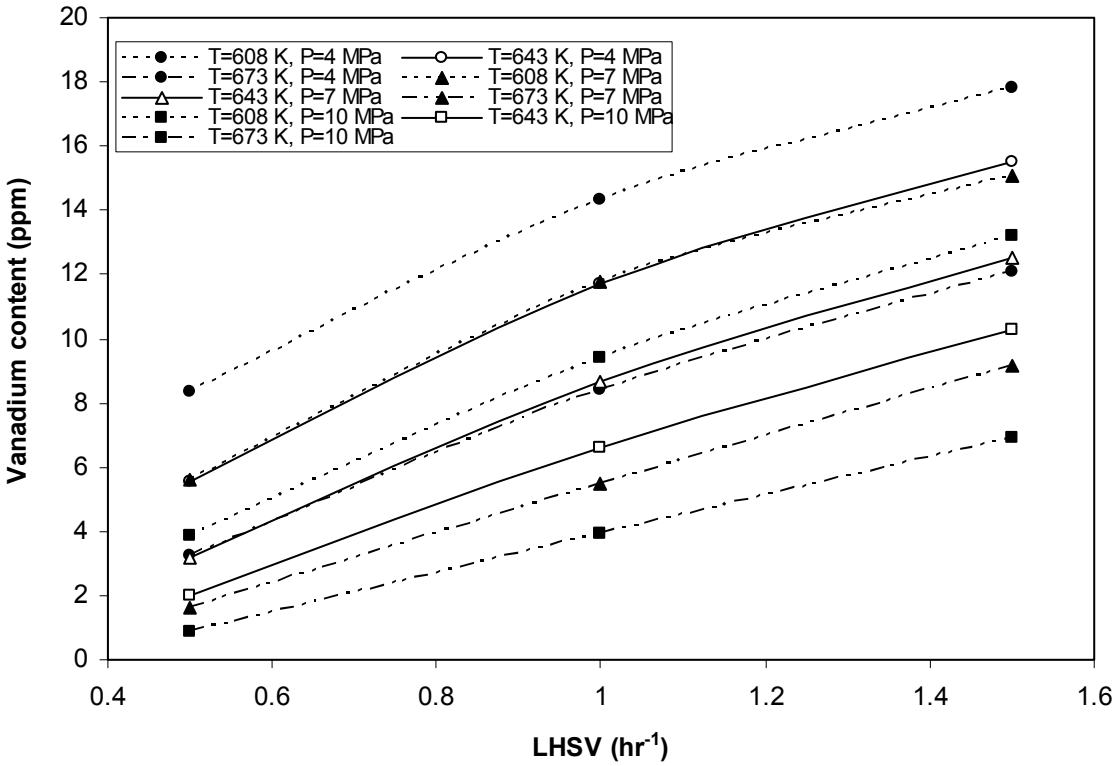

Figure 3.10: Experimental data variation of vanadium content vs. LHSV at different temperature and pressure

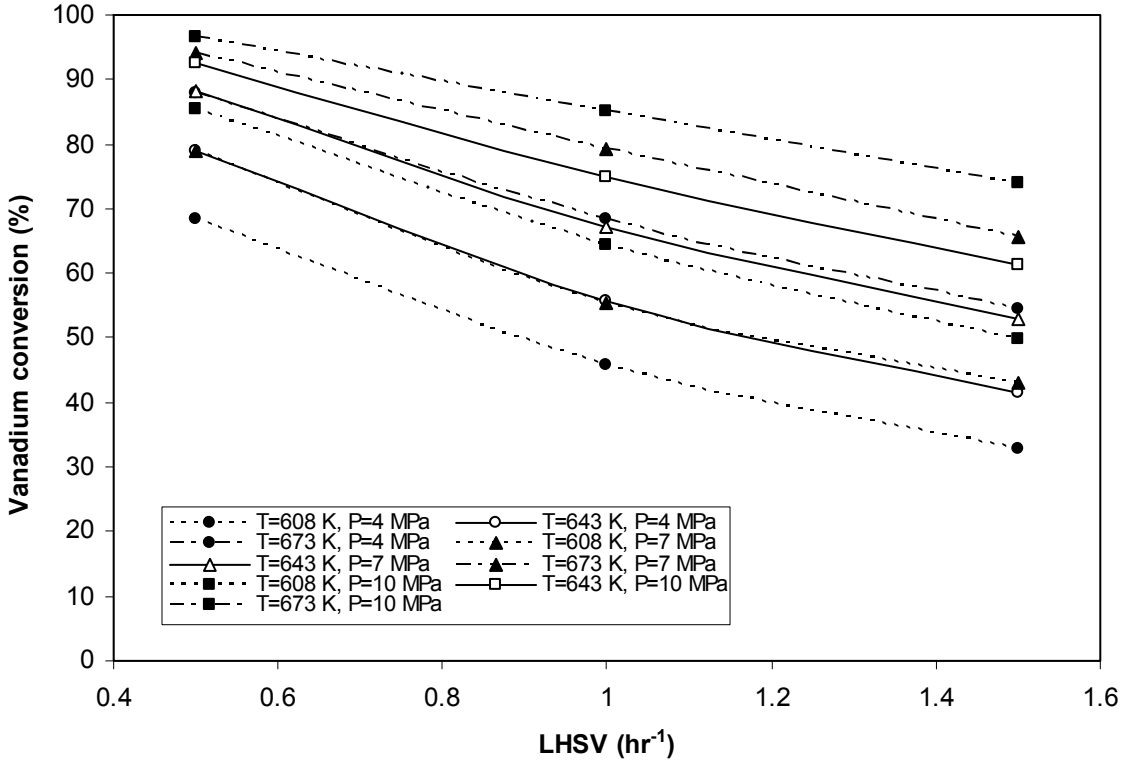

Figure 3.11: Experimental data variation of vanadium conversion vs. LHSV at different temperature and pressure

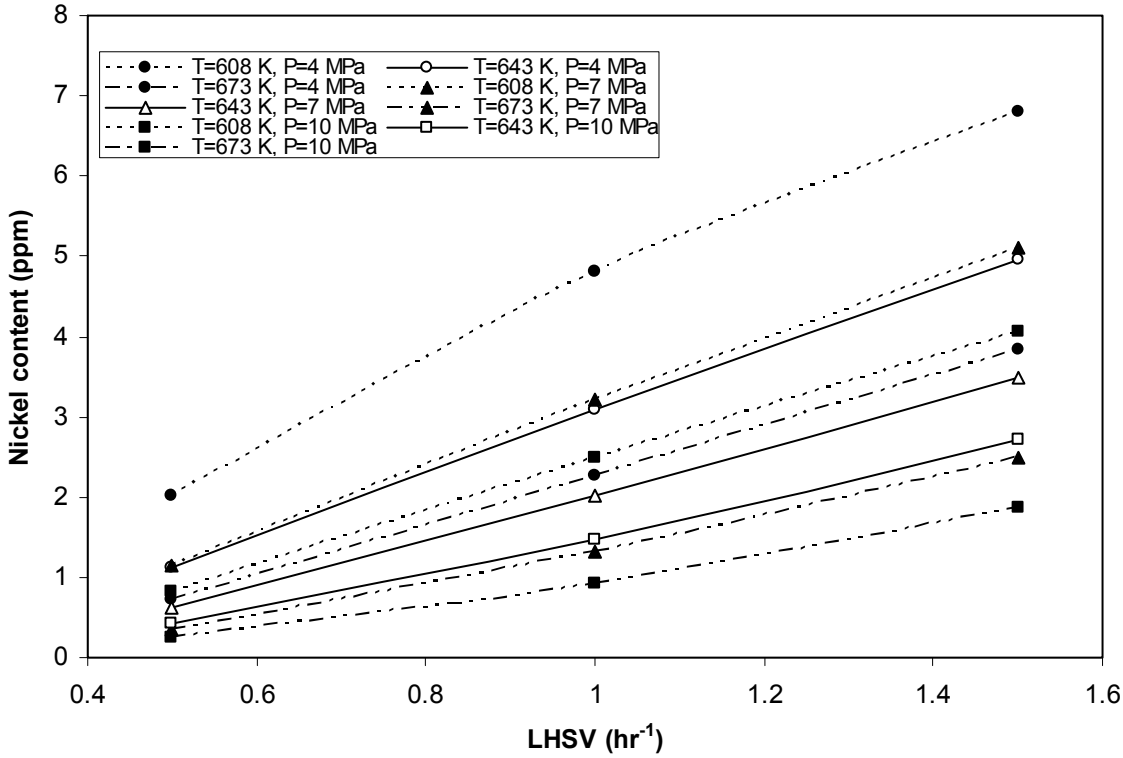

Figure 3.12: Experimental data variation of nickel content vs. LHSV at different temperature and pressure

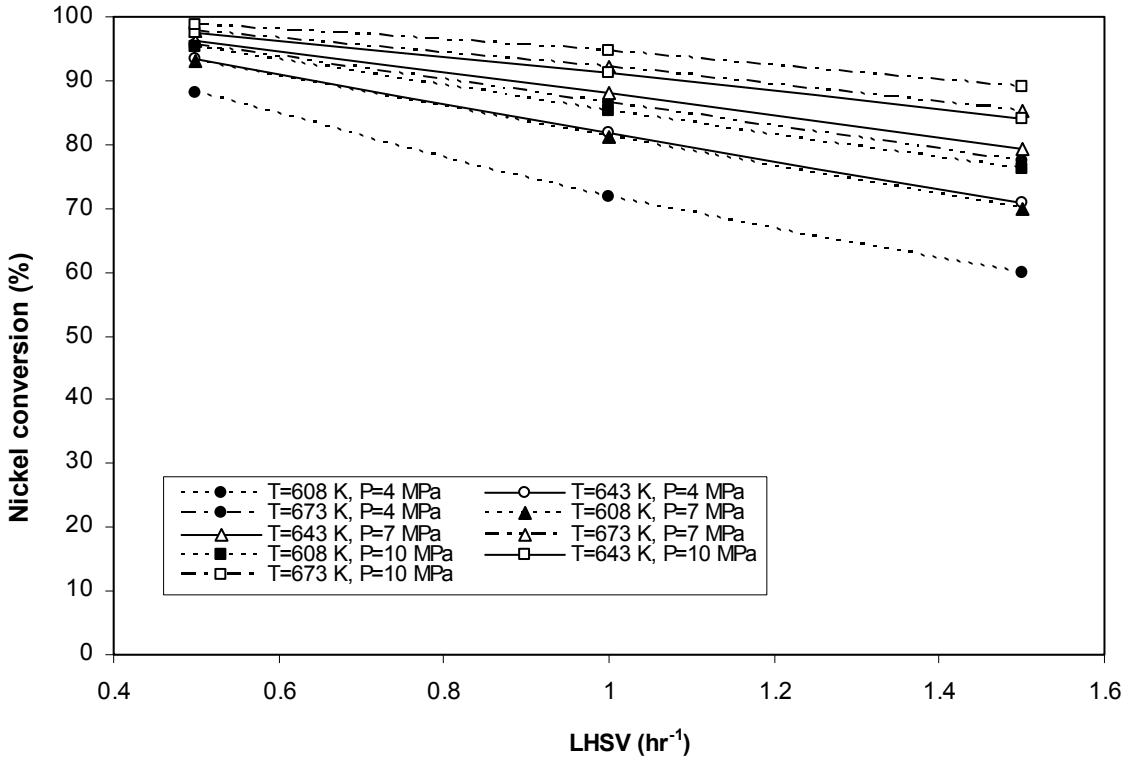

Figure 3.13: Experimental data variation of nickel conversion vs. LHSV at different temperature and pressure

LHSV is inversely related to devanadization and denickelation rates as shown in the Figures above (devanadization and denickelation decrease as LHSV increases). This result is logical since the rate of devanadization and denickelation is expected to intensify as the reaction time between feed and catalyst increases. Removal increases in vanadium and nickel have also been reported by other researchers utilizing various oily cuts (but not on the full crude oil) (Abbas, 1999; Maria and Martinez, 1999; Al-Humaidan, 2004; Alvarez and Ancheyta, 2008).

3.3.1.4 Asphaltene Removal

The effect of operating conditions (reaction temperature, pressure and liquid hourly space velocity) on asphaltene concentrations and removal in products are presented in Figures 3.14 and 3.15. The experimental observations showed that the most severe reaction conditions yield the lower asphaltene content in crude oil hydrotreated. The expected behaviour is observed: the higher temperature and pressure, and the lower LHSV produce lower asphaltene concentrations. The same phenomena was noted by several investigators employing various feedstocks, but not upon the full crude oil (Ancheyta et al., 2001; Alvarez and Ancheyta, 2008a).

A significant decline in the asphaltene content at high temperatures indicates that asphaltene hydrocracking is higher at an elevated temperature and the hydrocracking of asphaltene molecules is prominent. The large molecules are decomposed into smaller molecules that diffuse more easily within the catalyst where the HDAs reactions happen. Also, at high temperature, the oil viscosity will decrease leading to high diffusion through the catalyst pores. The asphaltene compound molecules reaction increases by increasing the reaction temperature due to an increase in the activation energy of these compounds (Isoda et al., 1998; Abbas, 1999).

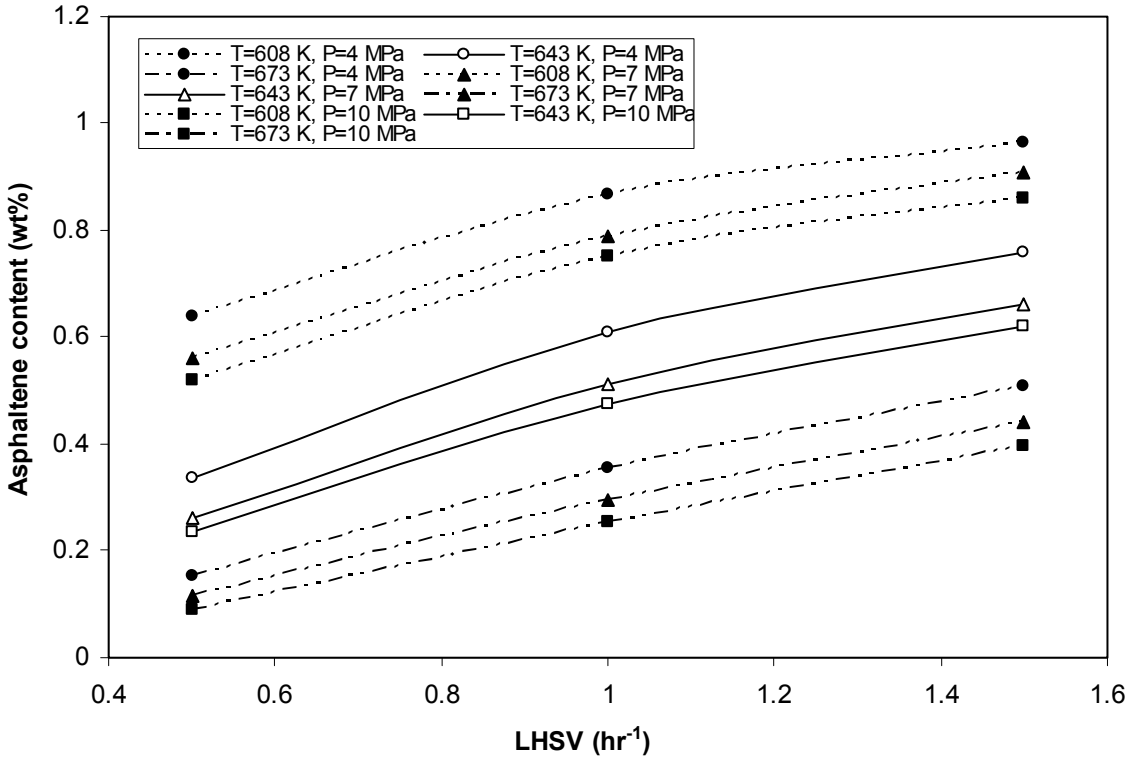

Figure 3.14: Experimental data variation of asphaltene content vs. LHSV at different temperature and pressure

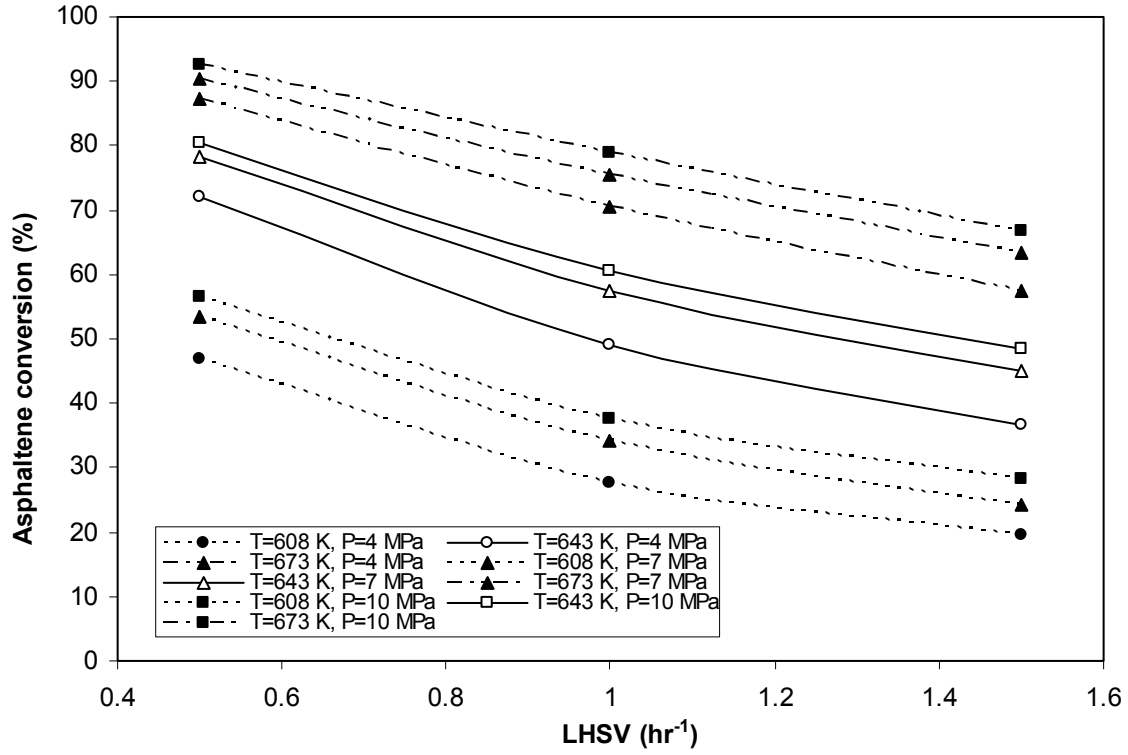

Figure 3.15: Experimental data variation of asphaltene conversion vs. LHSV at different temperature and pressure

It has also been noticed from experimental results that all HDAs reactions are significantly influenced by LHSV. The decrease in LHSV results an in improved quality of hydrotreated crude oil by reducing the content of asphaltene in all products and increasing the removal of these impurities as a result of increasing the contact time (Ancheyta et al., 2001; Trejo and Ancheyta, 2005).

With all the reactions (HDS, HDN, HDV, HDNi and HDAs) the most significant reduction in S, N, V, Ni and Asph content is observed when the reactor pressure is increased. The reason for increasing sulfur, nitrogen, vanadium, nickel and asphaltene removal by increasing hydrogen pressure is that the higher the pressure the better is the contact between the hydrogen, hydrocarbons and the catalyst (Ancheyta *et al.,* 2001). However, at very high reactor pressure, the activity of the catalyst used is reduced due to the adhesion of carbon upon the surface of the catalyst (Tamburrano, 1994).

3.3.2 Productivity of Middle Distillates

As mentioned earlier, the market demand for middle distillates is increasing in comparison to that for heavy oils. Thus, it is important to increase the productivity of middle distillates. Directly crude oil hydrotreating is a new technology and plays an important role in coping with these challenges.

The advantages envisaged via direct crude oil HDT are increasing valuable fractions yield in addition to reducing impurities. Figure 3.16 illustrates the difference between the conventional method (after the separation of crude oil into its derivatives, such as naphtha, kerosene, gas oil with hydrotreating processes used for each fraction separately (Figure 3.16 A)) and the present study (HDT of full crude oil then distillation (Figure 3.16 B)).

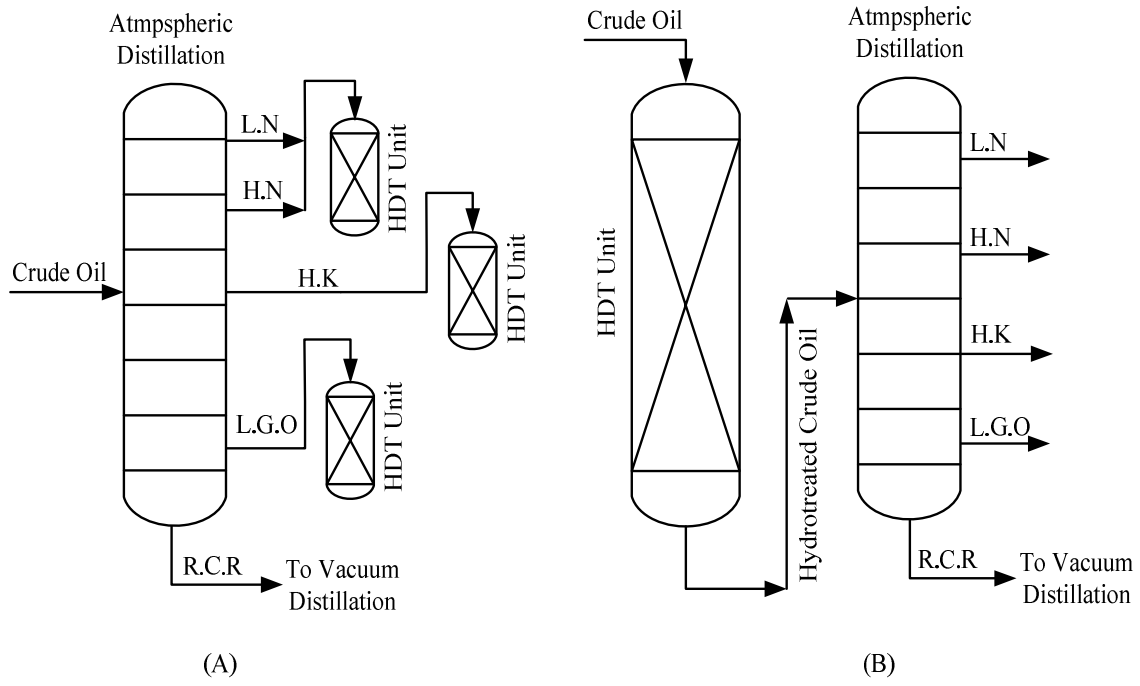

Figure 3.16: The difference between the conventional method (A) and this study (B)

The middle distillates fractions (naphtha, kerosene and light gas oil) are the most important products of refining processes and represent the main source of transportation fuels. Naphtha is a significant cut because it is mainly used as a feedstock for producing high-octane gasoline (used for car fuels). It is also utilized in the petrochemical industry to produce olefins in steam crackers and in the chemical industry for solvent (cleaning) applications. Kerosene is regarded as the major feed to power jet-engined aircraft (jet fuel) and some rockets, in addition to its use as a heating fuel and other industrial uses such as producing detergents. Light gas oil is employed as a main fuel for some cars, trucks, tractors, ships and railroad. Also, it is utilized in heating homes and diesel power plants for electrical generators (Mahmood et al., 1990).

The experimental work related to oil distillates productivity is carried out with process variable that have the most important influence upon yield. These are the reaction temperature and liquid hourly space velocity (Al-Humaidan, 2004). Therefore, the

distillation process has been conducted upon the crude oil, hydrotreated under the following operating conditions:

- Reaction temperature: 335-400^{0}C.
- Liquid hourly space velocity: 0.5-1.5hr^{-1}.
- Hydrogen pressure: 10 Mpa.
- Hydrogen to oil ratio (H_2/Oil): 250 L/L.

The hydrotreated crude oil at these conditions was distilled into the following fractions:

- Light naphtha (IBP-90^{0}C).
- Heavy naphtha (90-150^{0}C).
- Heavy kerosene (150-230^{0}C).
- Light gas oil (230-350 ^{0}C).
- Reduced crude residue (350^{0}C+).
- Gases (100 – (naphtha + heavy kerosene + light gas oil + reduced crude residue)).

Table 3.5 shows the experimental results for product compositions. It is clearly observed that the conversion of high boiling point molecules (such as those contained in the residue fraction) into lighter molecules increases when the reaction temperature is increased and LHSV is decreased. This behaviour can be attributed to the severity of the reaction at high operating conditions. At a low temperature of 335^{0}C (with different LHSV) there is no conversion of product compositions and they are almost unchanged, which means that the conversion of large molecules can be achieved at high operating conditions.

Table 3.5: Yield analysis results

Temperature	Lumps	LHSV (1/hr)			
		0	**1.5**	**1.0**	**0.5**
		Feed (wt%)	**Products (wt%)**		
335 ^{0}C	Gases	3.47	3.48	3.48	3.6
	L.N	5.9	5.91	5.91	5.93
	H.N	8.9	8.91	8.92	8.97
	H.K	12.8	12.81	12.82	12.9
	L.G.O	19.0	19.01	19.02	19.2
	R.C.R	49.93	49.88	49.85	49.4
370 ^{0}C	Gases	3.47	3.7	3.8	4.0
	L.N	5.9	6.0	6.4	6.8
	H.N	8.9	9.2	9.5	9.9
	H.K	12.8	13.3	13.5	13.8
	L.G.O	19.0	19.2	19.5	20.0
	R.C.R	49.93	48.6	47.3	45.5
400 ^{0}C	Gases	3.47	3.8	4.0	4.3
	L.N	5.9	6.2	6.7	7.1
	H.N	8.9	9.4	9.8	10.4
	H.K	12.8	13.6	14.0	14.8
	L.G.O	19.0	19.9	20.5	21.1
	R.C.R	49.93	47.1	45.0	42.3

The highest conversion from R.C.R to oil distillates is seen at a high reaction temperature and low LHSV. Figure 3.17 illustrates the comparison between the

productivity of middle fractions distilled from hydrotreated crude oil at maximum conditions (400^0C reaction temperature and $0.5hr^{-1}$ LHSV) and middle distillates produced by a conventional method (after the separation of crude oil into its derivatives). As can be seen from Figure 3.17, the productivity of L.N, H.N, H.K, and L.G.O increases when hydrotreating full crude oil before distillation, with a decrease in R.C.R percent. This increase in the percent of the yield fractions is due to conversion of heavy compounds and long molecules that are concentrated in heavy fractions (like R.C.R) to light compounds is as a result of hydrotreating of crude oil before the distillation process. In contrast, the conventional processes carried out for each separate fraction result in heavy compounds and long molecules being deposited at the bottom of the atmospheric and vacuum distillation columns. Hydrotreating them using normal operations and conditions is difficult.

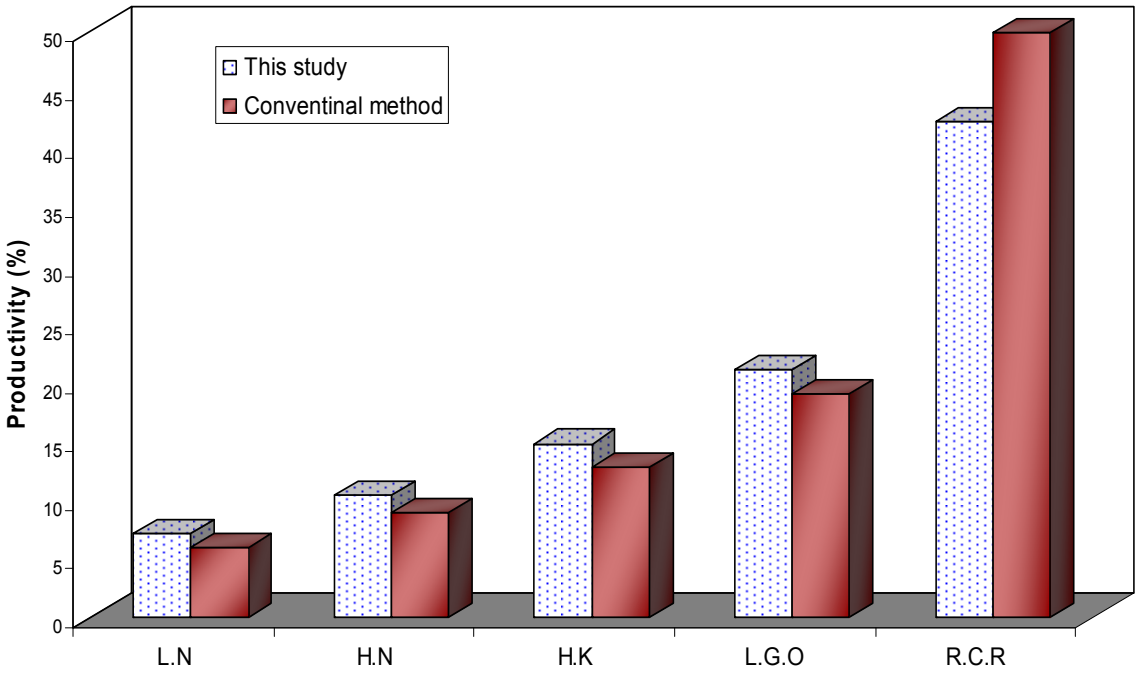

Figure 3.17: Comparison of productivity of oil fractions produced by distillation process after HDT process (present study) and produced by conventional methods (HDT process of each fraction separately after distillation process)

Tables 3.6 and 3.7 show the properties of oil fractions produced by conventional methods and produced by the separation of hydrotreated crude oil, respectively. This process is done in order to compare the main properties of oil fractions produced by both methods.

Table 3.6: Properties of oil fractions produced by conventional methods

Property	**Oil Fractions**			
	Light Naphtha (L.N)	**Heavy Naphtha (H.N)**	**Heavy Kerosene (H.K)**	**Light Gas Oil (L.G.O)**
Sp.gr @ 15.6 ^{0}C	0.6625	0.7385	0.7918	0.8389
Sulfur content (ppm)	1.0	4.0	9.0	41.0
Distilled (vol.)	^{0}C	^{0}C	^{0}C	^{0}C
I.B.P	40	100	171	220
5 %	45	105	176	230
10 %	48	107	181	240
20 %	50	110	188	252
30 %	52	113	193	264
40 %	54	116	196	272
50 %	58	119	199	280
60 %	60	123	204	289
70 %	65	127	209	295
80 %	70	132	216	305
90 %	78	139	225	317
95 %	87	146	232	326
Ep %	89	149	245	338
T.D %	98.0	99.0	99.0	97.0
Loss %	2.0	0.5	0.0	0.0
Rest %	0.0	0.5	1.0	3.0

Table 3.7: Properties of oil fractions produced by separation of hydrotreated crude oil

Property	Oil Fractions			
	Light Naphtha (L.N)	**Heavy Naphtha (H.N)**	**Heavy Kerosene (H.K)**	**Light Gas Oil (L.G.O)**
Sp.gr @15.6 ^{0}C	0.6513	0.7311	0.7723	0.8324
Sulfur content (ppm)	5.1	11.0	18.0	49.0
Distilled (vol.)	^{0}C	^{0}C	^{0}C	^{0}C
I.B.P	30	91	159	218
5 %	36	95	166	227
10 %	40	101	171	236
20 %	43	107	179	243
30 %	45	111	184	255
40 %	49	114	188	262
50 %	54	116	191	271
60 %	59	120	199	279
70 %	64	125	206	288
80 %	70	131	215	297
90 %	75	137	223	314
95 %	83	141	234	322
Ep %	85	144	237	335
T.D %	98.0	99.0	99.5	98.5
Loss %	2.0	1	0.0	0.0
Rest %	0.0	0.0	0.5	1.5

As can be seen from the results, the main properties of oil fractions produced by the separation of hydrotreated crude oil are almost the same as those produced by conventional method. In other words, the specific gravity (sp.gr) of oil cuts produced by present study is less than the sp.gr of the same fractions produced by conventional methods, which gives a clear indication of incremental productivity improvement of these fractions.

3.3.3 The Production of New Fuel Oils

After separation of hydrotreated crude oil into its fractions, the remaining part at the bottom of the distillation column is called reduced crude residue (R.C.R) and has a boiling range above 350^0C. R.C.R is mainly used as a feedstock to vacuum distillation units to produce base oils in addition to producing vacuum gas oil and lubricating oils under certain conditions. Also, it is utilized as a component of fuel oil used in power plants, as fuel for furnaces and as a component of diesel oil (Mahmood et al., 1990). During hydrotreating of full crude oil directly with hydrogen, it can be observed that the properties of R.C.R produced via hydrotreating of crude oil directly are better than the properties of R.C.R produced by conventional processes as shown in Table 3.8 (the hydrotreating conditions were: 400^0C reaction temperature, $0.5hr^{-1}$ LHSV, and 10MPa hydrogen pressure). The sulfur content, nitrogen content, metals content and asphaltene content are much lower compared with these contents of R.C.R produced by conventional methods, thus producing a good fuel oil as shown in Table 3.8.

Table 3.8: Comparison of properties of reduced crude residue (RCR) produced by hydrotreated crude oil and conventional methods

Specifications	**Units**	**By conventional method**	**By crude oil hydrotreating**
Specific Gravity @ 15.6 ^{0}C	-	0.9540	0.9392
API	-	16.82	19.16
Viscosity @ 50 ^{0}C	cSt	236.8	191.4
Pour point	°C	+14	+2
Sulfur content	wt %	4.0	0.811
Vanadium content	ppm	59.88	16.42
Nickel content	ppm	37.47	10.16
Nitrogen content	wt %	0.1763	0.04122
Asphaltenes content	wt %	5.9	0.91

It is also noted that the viscosity and density of R.C.R are less than those found in R.C.R produced by conventional methods, which makes flow easy at low temperatures and gives an indication of increasing the light cuts. Therefore, residual fuel oil produced by a conventional method is less useful because it is so viscous that it has to be heated with a special heating system before use it, in addition to containing high amounts of contaminants in comparison with this study. With residual fuel oil produced by hydrotreated crude oil, power plants and large ships are able to use it dirctly. This decrease in the viscosity and density due to the saturation of olefins and aromatics during the hydrotreating process and sufficient time for the saturation process leading to conversion of a large part of them into saturated compounds, such as paraffins and cycloparaffins that have low viscosity and density. In addition, a part of these compounds is converted to light compounds due to the cracking of the bonds for heavy compounds, which have a long chain and high density and viscosity (Ali and Abdul-Karim, 1986; Abbas, 1999; Mahmood et al., 1990; Areff, 2001).

Furthermore, hydrotreating of R.C.R directly requires additional processes and hard operating conditions since they contain heavy and complex compounds as well as large quantities of impurities. Thus, the catalyst used will be rapidly deactivated because of plugging the active sites of the catalyst due to coke deposition leading to reduced efficiency of the HDT process (Ancheyta et al., 2001).

3.4 Conclusions

This chapter reviewed details of pilot plant experiments that involve hydrotreating reactions at different operating conditions (HDS, HDN, HDAs, HDV and HDNi reactions), and the distillation process (light naphtha (L.N), heavy naphtha (H.N), heavy

kerosene (H.K), light gas oil (L.G.O) and reduced crude residue (R.C.R)). Also, this chapter presented and discussed results obtained via experimental work.

HDT has the ability of increasing the productivity of distillate fractions and simultaneously reducing the impurities contents (sulfur, nitrogen, vanadium, nickel and asphaltene). The effect of different hydrotreating operation variables such as reaction temperature, hydrogen pressure and liquid hourly space velocity (LHSV) upon the quality of crude oil during HDT of crude oil was investigated. The crude oil becomes more purified by removing the impurities (S, N, V, Ni and Asph) with increasing reaction temperature and pressure, and decreasing LHSV.

To compare the productivity of oil fractions produced by a distillation process after the HDT process with those produced by conventional methods, the hydrotreated crude oil has been distilled into light naphtha (L.N), heavy naphtha (H.N), heavy kerosene (H.K), light gas oil (L.G.O) and reduced crude residue (R.C.R). The productivity of middle distillate showed greater yield compared with the middle distillate produced by conventional methods, and consequently the R.C.R yield decreases.

It can also be noticed that the specifications of R.C.R produced by crude oil directly hydrotreating are better than the specifications of R.C.R produced by conventional processes. The contents of sulfur, nitrogen, metals and asphaltene are much lower in comparison with these contents of R.C.R produced by conventional methods, which allows the production of good fuel oils.

Chapter Four

gPROMS: general Process Modelling System

4.1 Introduction

This chapter briefly discusses the main advantages of the software employed for modelling, simulation and optimization of the crude oil hydrotreating process carried out in this work.

A general simulator has a large scope for application in industry. These packages frequently have advanced languages and formalisms for model improvement, which allow the description of difficult differential and algebraic models.

A process simulator has the ability to input and modify the configuration of the process flowsheet and to perform design evaluations by considering the complete process flowsheet, before they are tried on the real plant. In this way it is possible to model and predict the behaviour of the process flowsheet and to study different operation scenarios (such as various feedstocks, high flowrates, modified operating conditions, etc.). Examples of commercially available operation simulators, which can be employed for modelling chemical operations, are: ASPEN PLUS (Aspen Technology), CHEMCAD (ChemStations), HYSYS (hyprotech ltd), gPROMS (Process Systems Enterprise ltd), etc. With ever-increasing capacities in computer power to describe operation parts, an operation simulator makes it possible to do complex analyses and to explore various design alternatives. In addition to the conventional experimental ways, such as pilot–plant, bench scale, market improvement plant, etc., the use of modelling and simulation has become increasingly powerful and popular.

There are several specific modelling packages that can be employed for simulating some operations. Generally, simulators can be divided into two types: specific and general packages. Specific packages need and give detailed data, whereas the general one can be utilized for any operation (Khalfalla, 2009).

4.2 gPROMS Simulator

The gPROMS (**g**eneral **PRO**cess **M**odelling **S**ystem) package is an equation oriented general goal modelling, simulation and optimization instrument for combined continuous and discrete operation that makes it particularly suitable for the modelling and simulation of any steady–state or dynamic plant process. gPROMS has a large scope of application in chemical processes and it can be employed for both steady–state and dynamic modelling. In addition, gPROMS can be used for performing process parameter and the evaluation of calculations for difficult operations under several process conditions. It is extremely useful for continuous operations that frequently exhibit transient behaviour owing to abnormal conditions.

gPROMS was developed by Process System Enterprise (PSE), based at Imperial College, and has largely been employed for industrial applications (Winkel et al., 1995). According to its developers, gPROMS counts the following amongst its several features (PSE, 2004):

- Clear and simple language; equations of physical systems can be written as clearly as they appear in technical papers or books without any reformulation. This has the advantage of allowing the user to focus on the modelling task at hand, rather than get caught up in the complication of the syntax.
- gPROMS simulators handle symmetric-asymmetric, reversible-irreversible, continuous-discontinuous and direct systems. These activities of gPROMS for

process solution make it more robust and faster. This has important consequences for solution robustness and speed, and allows the simple of situation, which often present a considerable hindrance to solution in other simulators.

- The solvers within the gPROMS environment are designed particularly for broad scale systems. A large number of differential and algebraic equations (more than 100,000) can be handled within gPROMS in addition to handling partial differential equations (PDEs). This modelling power is of great advantage to its employers and the generality of the package means that it can be applied to any process that can be described by a mathematical model.
- gPROMS allows simultaneous optimization of equipment sizes and operating procedures that saves capital and operating cost in the long run.
- Single or multi-dimensional arrays of both variables and equations can be described either implicitly or explicitly. All variables, other than those that are functions of time only, are featured as distributions over one or more continuous and/or discrete domains.
- gPROMS allows using a single process can be applied for many optimization task and single equipment model (described by many equations) for multiple operation procedures (process). It provides greater flexibility and model evaluation time is reduced.

Due to the above advantages of gPROMS, and several others not mentioned here, gPROMS (version 2.3.4) has been chosen as the software of choice for modelling, simulation and optimization of hydrotreating of crude oil using a trickle bed reactor as carried out in the present work. The details for utilizing gPROMS for model

improvement, simulation and optimization (as described in this work) are presented in the rest of the chapter.

4.3 Model Development using gPROMS

An overview of the gPROMS model builder at start up is shown in Figure 4.1.

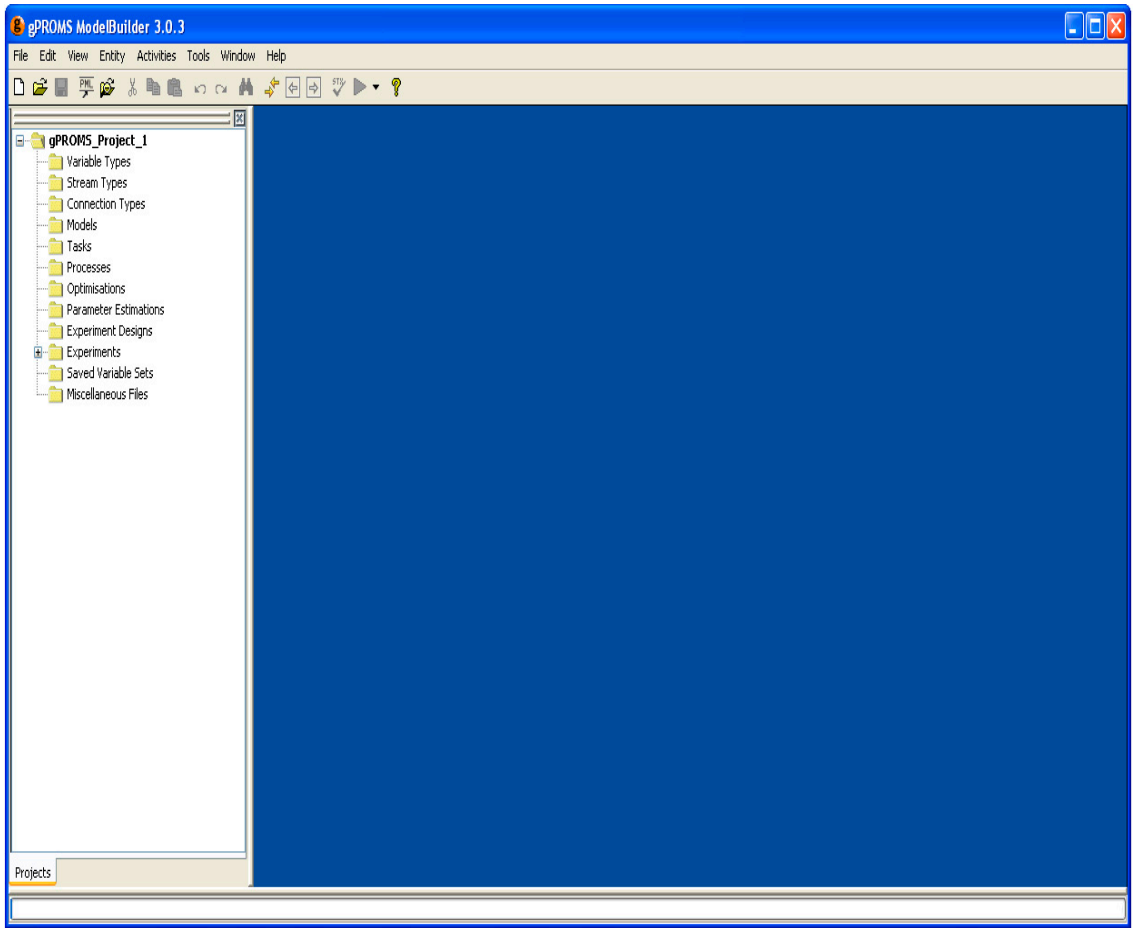

Figure 4.1: An overview of the gPROMS modelling environment

On the left hand pane are a number of entries corresponding to a set of gPROMS sections. Some of these sections are Variable Types, Stream Types, Models, Tasks, Processes, Optimizations, etc. In this work in carrying out most of the tasks only four of these sections are employed. These are: VARIABLE TYPES (the type and range of the variables used in the model are specified); MODELS (the actual hydrotreating model is written that is described by a set of differential and algebraic equations); PROCESSES

(contains specifications for simulating the hydrotreating process); OPTIMIZATIONS (optimization of the hydrotreating process is written). These sections are further discussed in the parts that follow.

4.4 Defining a Model

As previously mentioned, the MODEL section is where a process model (a set differential and algebraic equation) is written. A model file in gPROMS can be divided into three main sections: PARAMETERS, VARIABLES and EQUATIONS. The PARAMETER section is where the parameters of the model are declared. Parameters are fixed values, which cannot be estimated by the simulation. Their values should be fixed before simulation starts, and remain unchanged throughout. An example of a parameter from the hydrotreating model is the catalyst particle diameter, dp, which is declared in the model file as

```
dp      AS  REAL  # Catalyst Particle Diameter
```

REAL refers to the type of parameter (i.e. a real value), and # is the comment sign in gPROMS after which a description of the parameter can be written in long hand. The universal gas constant is also an example of a parameter declared for the hydrotreating process described in this work.

The VARIABLE section is where all the variables of the model declared. Values of the variables may be assigned or calculated by simulation. The Variables type also has to be declared and defined for each variable in the VARIABLE section. An example of a variable from the hydrotreating model is pressure, which is declared in the model as

```
PRESS   AS  Pressure    # Process Pressure (MPa)
```

Press is the name given to the process pressure in the above example. The variable type is defined in the VARIABLE folder as

```
Pressure    1      :      0.5      :      15
```

Pressure is the variable type and the numbers after it are lower bound, default value and upper bound, respectively.

The EQUATION section is where the model equations are written. An example is the equation for the adsorption equilibrium constant of hydrogen sulfide (K_{H_2S}) in the kinetic model of crude oil hydrotreating:

$$K_{H_2S} = 41769 \cdot 8411 \cdot \exp\left(\frac{2761}{R \cdot T(K)}\right)$$

The above equation is stated in the model file as

```
KH2S = 41769.8411 * EXP(2761 / (Rg * TK)) ;
```

The simplicity of the gPROMS code can be seen in the example treated so far. A part of the gPROMS model file for the HDT of crude oil model is shown in Figure 4.2.

4.5 Defining a Process

In the Processes entity, the specifications for running simulations with the hydrotreating processes are defined. A Process is separated into sections that contain information necessary to define a simulation activity. The major Process sections utilized for carrying out simulation studies in this work consist of the following parts:

- UNIT
- SET
- ASSIGN

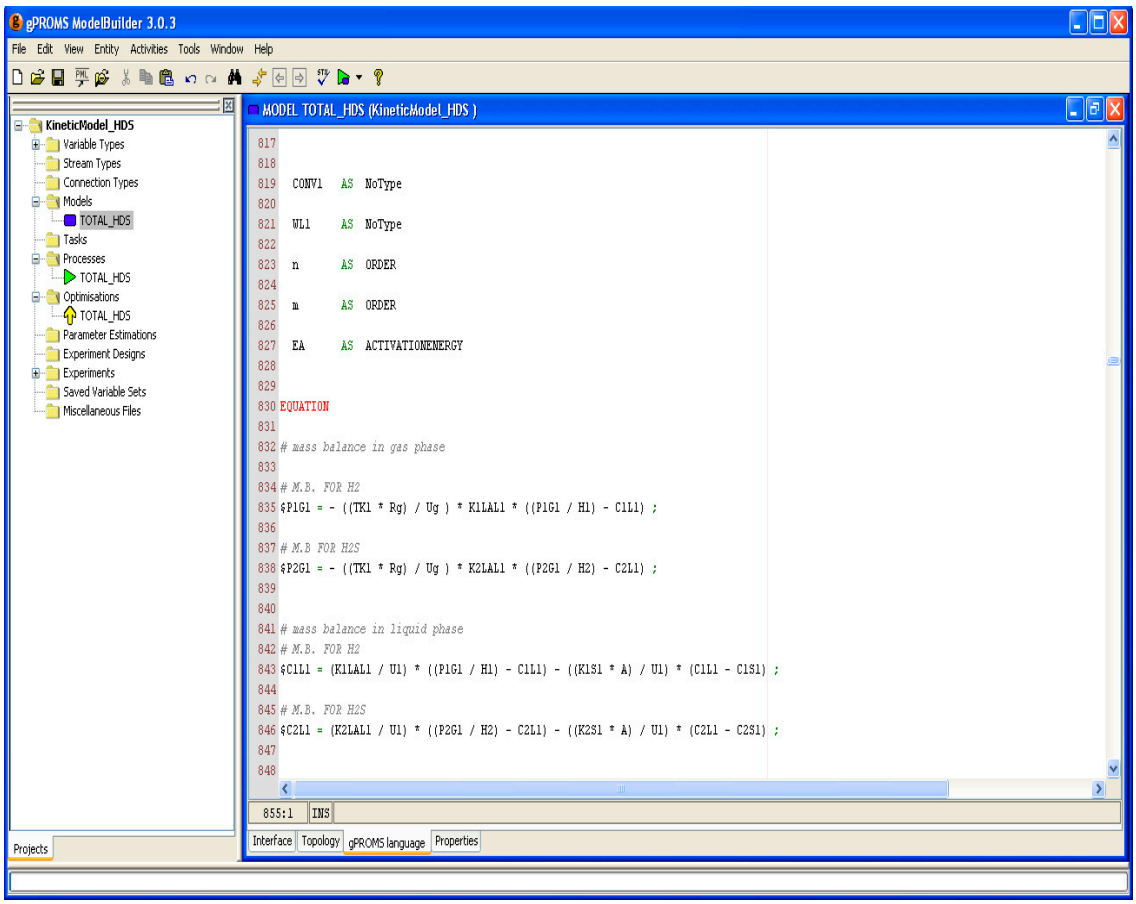

Figure 4.2: A part of kinetic model file of the hydrotreating of crude oil

- INITIAL
- SOLUTION PARAMETERS
- SCHEDULE

The roles of these parts are discussed in the following subsections.

4.5.1 UNIT Section

As earlier stated, gPROMS can be used to model a complete process. In such a case, the various equipment units in the process are modelled and simulated separately. These different units can be linked to one another to give a complete picture of the overall process. In the unit part, the specific item of equipment to which the process files refers to is indicated. Equipment items are declared as instances of MODELs.

4.5.2 SET Section

In this part, the values of the parameters declared under the PARAMETERS section in the model file are assigned. For instance, the value of the catalyst particle diameter, dp, is assigned under the SET section as

```
dp          := 0.18 ;   # cm
```

4.5.3 ASSIGN Section

In the ASSIGN section, the input parameters to the model are specified. In a typical model, the number of variables is generally more than the number of equations. In order to make the number of equations equal to the number of variables to avoid over or under specifying the system, some the extra variables are assigned in this part. For example, in the kinetic model for crude oil hydrodesulfurization, the variables assigned in the ASSIGN section are the order of the sulfur concentration, order of hydrogen concentration, pre exponential factor and activation energy.

Note that through the optimization process, the value assigned in the ASSIGN section are overridden as the software searches for the best control values to satisfy a given set of process constraints.

4.5.4 INITIAL Section

The INITIAL section is used for specifying the initial conditions of a simulation activity. In the models of hydrotreating of crude oil used in this work, the initial conditions are the values of the differential variables at length $z = 0$. In gPROMS, initial conditions are treated as general equations in gPROMS and as such, it is possible to estimate the value of an initial state by an equation rather than by assigning it a fixed value.

4.5.5 SOLUTION PARAMETERS Section

gPROMS provides a range of mathematical solvers for simulation, optimization and parameter calculation. gPROMS supports an open software architecture regarding mathematical solvers for simulation, optimization and parameter calculation (Gosling, 2005).

The SOLUTION PARAMETERS section of the PROCESS allows the specification of parameters of the results and the mathematical solvers for each type of activity (simulation, optimization and parameter estimation). As the number of solvers and subsolvers available in gPROMS for the solution of simulation, optimization and parameter calculation activities for both steady state and dynamic models are enormous. The model developer defines mathematical solvers and output specifications for the process output. Output specifications are utilized for display results in EXCEL and gRMS using the keywords gExcelOutput and gRMS, respectively. The gExcelOutput opens a Microsoft Excel file that displays the results of the simulation, whereas in gRMS, the results are sent to the internal gPROMS results management system.

There are three standard mathematical solvers for the solution of sets of nonlinear algebraic equation in gPROMS: BDNLSOL, NLSOL and SPARSE: BNDLSOL (Block Decomposition Non Linear solver). NLSOL is nonlinear solver, with and without block decomposition. SPARSE is sophisticated implementation of a Newton-type block decomposion. Two mathematical solvers (DASOLV and SRADAU) solve mixed sets of differential and algebraic equations in gPROMS. A SRQPD, which employs a Sequential Quadratic Programming (SQP) method for the solution of the Non Linear Programming (NLP) problem, has been used in this work for the hydrotreating of crude oil model.

4.5.6 SCHEDULE Section

In the SCHEDULE section, the operating schedule of the process is specified. One goal of modelling is to study a model's behaviour under various operating conditions (i.e. external manipulations). The information on these manipulations is specified in this section. A part of the gPROMS Processes file for the kinetic model of crude oil hydrotreating is shown in Figure 4.3.

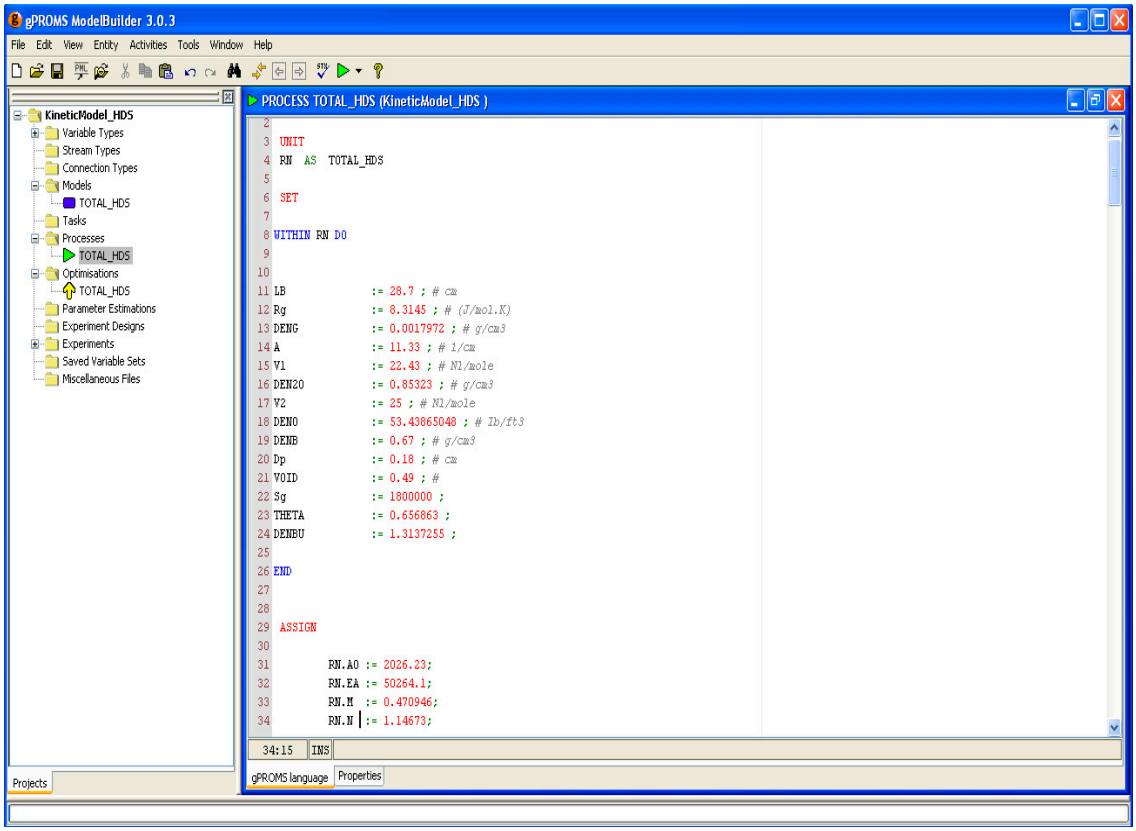

Figure 4.3: Part of the processes file for the kinetic model of crude oil hydrotreating

4.6 Optimization in gPROMS

In the optimization entity, the parameters for steady state or dynamic optimization problems are specified. In several cases, the values are expressed in the form: [guessed value, lower bound, upper bound]. Some of the specifications for the optimization

process involve the length horizon or time horizon for the process, the number of intervals, the numerical values of the intervals, the values of the control variables within the intervals and the end point constraints. The objective function to be maximized or minimized is also specified within the optimization file.

A part of the gPROMS Optimization file for the kinetic model of crude oil hydrotreating is shown in Figure 4.4.

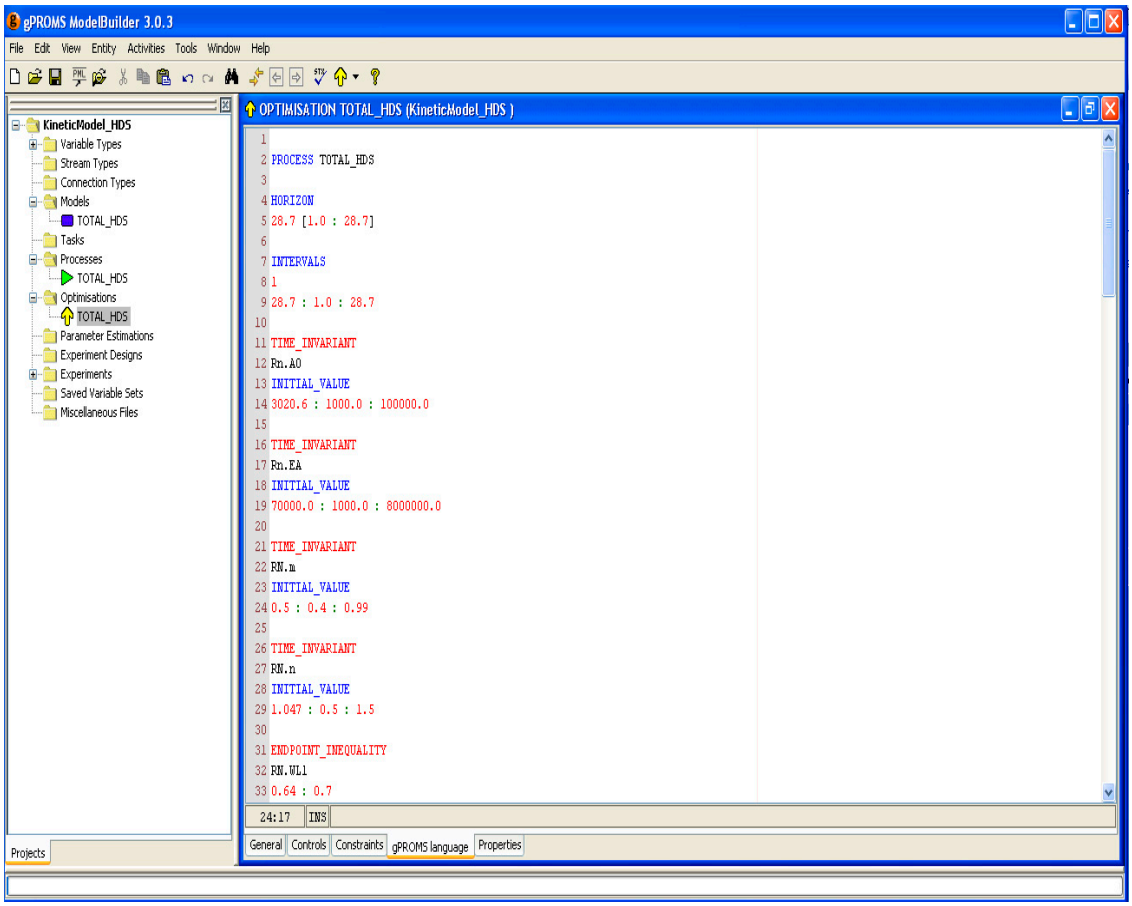

Figure 4.4: Part of the optimization file for the kinetic model of crude oil hydrotreating

4.7 Comparison of gPROMS with other Commercial Software

Many commercial software packages (such as Hysys, CEMCAD, Matlab, PROII, ASCEND, SpeedUp, OMOLA) for simulation, optimization, optimal control and design

are widely available these days as a consequence of powerful improvement in computer facilities and efficiency. Each of these commercial packages is developed with different characteristics. Some of them have high-quality application flexibility. Therefore, looking for appropriate software for a specific purpose is quite important in order to achieve the required target and to provide modelling languages that allow us to describe many operations.

Tjil (2005) compared the performance of Aspen Custom Modeller (ACM) with the performance of gPROMS to optimize the Sec-Butyl Alcohol (SBA) stripper. The SBA model was built in both softwares to perform parameter estimation and assesses their capabilities. CAPE-OPEN was employed to use the some physical and thermodynamic properties of the components in both softwares (ASC and gPROMS). Different aspects of parameter estimation were assessed for both softwares such as: experimental data input, output interpretation, combination of objective functions and optimization solvers and their ability. Tjil (2005) concluded that the parameter estimation capabilities of gPROMS were better than ACM.

4.8 Conclusions

The gPROMS software package used for modelling, simulation and optimization of the crude oil hydrotreating processes in this work has been discussed in this chapter. gPROMS has several features that make it an attractive and suitable tool for the modelling and simulation of any plant process (steady state and dynamic). Some of its numerous features involve; clear and concise language, an equation oriented general purpose modelling, simulation and optimization tool for combined discrete and continuous processes, robustness and flexibility of this software as mentioned, modelling power and the ability to model process discontinuities and operating

conditions among several others. Due to these benefits and many others, gPROMS has been chosen to employ for modelling, simulation and optimization processes in this work.

This chapter only discusses the gPROMS advantages, which were used for carrying out the work contained in this thesis using a kinetic model as an illustration. Further information about gPROMS and its more sophisticated features can be found in the developer's website (www.psenterprise.com), Oh and Pantelides (1996), Georgiadis et al. (2005) and in the gPROMS user guide (gPROMS, 2004).

Chapter Five

Mathematical Modelling, Simulation and Optimization of Crude Oil HDT Reactions: Results and Discussion

5.1 Introduction

Building models is one of the major occupations of engineering and science. Interpreting these models and studying their properties is another significant task that depends on the purpose for which the model is to be used. The use of models in chemical engineering is well established, this is reflected in the improvement of powerful computers and sophisticated numerical methods that has enabled the mathematical modelling and solution of real systems. Models are used because it is too expensive or time consuming or risky to use a real system to carry out studies. Models are typically employed in engineering design and optimization because they offer the cheapest and fastest way of studying the impact of changes in design variables on system performance (Ingham et al., 1994).

The objective of this chapter is to present mathematical models to simulate crude oil hydrotreating processes (include HDS, HDN, HDAs, HDV, HDNi and kinetics of increasing the oil distillates yields) and to describe the behaviour of the trickle bed reactor used for these reactions. In order to obtain useful models for HDT reactions that can be confidently applied to reactor design, operation and control, the accurate estimation of kinetic parameters of the relevant reaction scheme are required. Optimization techniques are used to obtain the best values of kinetic parameters in the trickle bed reactor process used for HDT of crude oil based on pilot plant experiments. The results obtained by modelling of hydrotreating of crude oil reactions, optimization

processes for parameter estimation, sensitivity analysis of the calculated kinetic parameters are also discussed.

5.2 Mathematical Model of TBR for HDT Reactions

An essential stage in the improvement of any model is the formulation of the appropriate mass and energy balance equations. To these should be added suitable kinetic equations of chemical reaction rates, rates of mass and heat transfer and equations representing process property changes. The basic mathematical model can be provided by combination of these relationships (Ingham et al., 1994).

A three–phase heterogeneous model has been developed for describing the behaviour of pilot-plant trickle-bed reactors applied to the HDT of crude oil. The model is based upon two-film theory and includes correlations for calculating mass–transfer coefficients, oil density, Henry's coefficients, solubility of hydrogen, oil viscosity, diffusivity, molar volume, specific surface area, etc. under the operating conditions, using information presented in the literature. Mathematical modelling of the HDT process is a difficult task due to the complex physical and chemical changes that the feed undergoes, along with the mass transfer phenomena in the reaction system. Kinetic aspects are a major factor of reactor modelling, but in this case, the conversion of a large amount of sulfur, nitrogen, asphaltene, vanadium and nickel compounds make it a huge problem. The following assumptions were used to create the mathematical models for HDT processes (McCulloch, 1983; Korsten and Hoffmann, 1996; Isoda et al., 1998; Cotta et al., 2000; Matos and Guirardello, 2000a; Kumar et al., 2001; Bhaskar et al., 2002; Chowdhury et al., 2002; Macı´as and Ancheyta, 2004; Rodriguez and Ancheyta, 2004; Yamada and Goto, 2004; Jimenez et al., 2005; Shokri and Zarrinpashne, 2006; Mederos et al., 2006; Jimenez et al., 2007a; Jimenez et al., 2007b; Alvarez and Ancheyta, 2008a; Alvarez and Ancheyta, 2008b; Alvarez et al., 2009):

- No radial concentrations gradients;
- Steady–state operation of the reactor;
- One-dimensional heterogeneous model;
- Isothermal and constant pressure operation of the reactor;
- The effect of catalyst deactivation on kinetic parameters is negligible.

The required data and available tools with the assumptions underlying modelling and simulation processes for crude oil hydrotreating are shown in Figure 5.1.

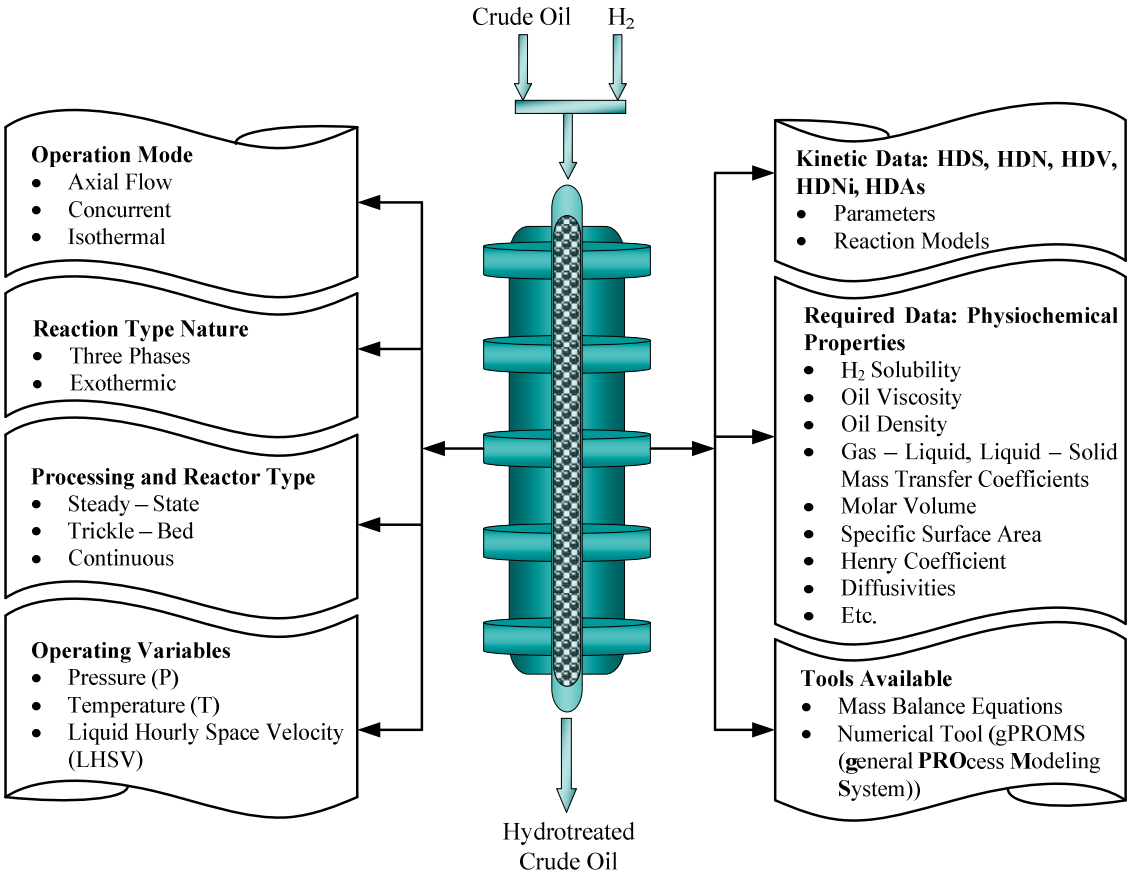

Figure 5.1: Assumptions for modeling and simulation of hydrotreating reactor

5.2.1 Model Equations

The reactor model considers the main crude oil hydrotreating reactions (HDS, HDN, HDAs, HDV and HDNi) that take place on the catalyst surface. The concentration

profile of reactants and products in a trickle bed reactor model is shown schematically in Figure 5.2.

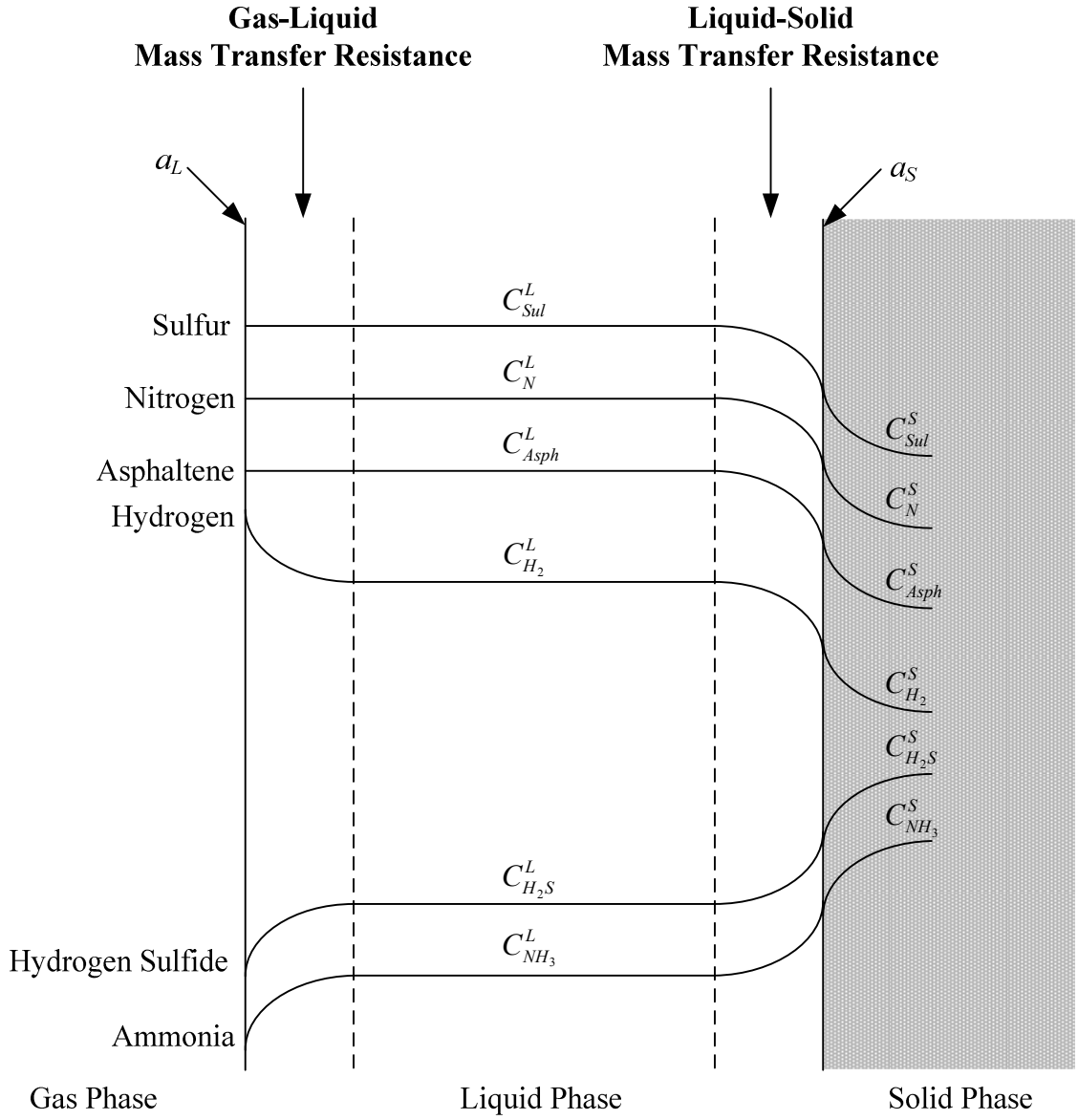

Figure 5.2: Concentration profiles in a trickle-bed reactor (Ancheyta and Speight, 2007)

For the reactions to happen, hydrogen (being the major constituent of the gas–phase) has to be transferred to the liquid phase and then to the catalyst surface in order to react with other reactants, such as sulfur, nitrogen, etc. The reaction products such as hydrogen sulfide and ammonia generated by chemical reaction on the catalyst surface will be transported to the gas phase. The hydrogen sulfide (H_2S) formed on the solid

surface of the catalyst owing to hydrodesulfurization reaction gets transferred to the liquid phase and then subsequently to the gas phase. The H_2S present in the liquid phase will be adsorbed on the catalyst sites and hence inhibits HDS reactions (Nickos and Marangozis, 1984; Korsten and Hoffmann, 1996; Bhaskar et al., 2002). Therefore, the distribution and mass transfer rate of H_2S in the various phases are very significant in modelling hydrotreating reactions. These influences are neglected in a homogeneous model.

The mass transfer of reactants and products in the heterogeneous model are taken into account in all the phases. The mathematical model equations are based on the transfer coefficients of the process at gas–liquid, liquid–solid interfaces and also involve the mass transfer rates in addition to distribution of reactants and products in various phases. The mass balance for each compound in each phase can be described as follows (Korsten and Hoffmann, 1996; Baskar et al. 2002; Alvarez and Ancheyta, 2008b):

5.2.1.1 Mass Balance Equations in Gas Phase

Hydrogen: $$\frac{dP_{H_2}^G}{dz} = -\frac{RT}{u_g} k_{H_2}^L a_L \left(\frac{P_{H_2}^G}{h_{H_2}} - C_{H_2}^L \right) \tag{5.1}$$

H_2S: $$\frac{dP_{H_2S}^G}{dz} = -\frac{RT}{u_g} k_{H_2S}^L a_L \left(\frac{P_{H_2S}^G}{h_{H_2S}} - C_{H_2S}^L \right) \tag{5.2}$$

Equations 5.1 and 5.2 include a system of ordinary differential equations (ODEs) that relate the partial pressures of H_2 and H_2S to the mass transfer of the compounds across the gas–liquid interface. These equations can be solved to give partial pressure profiles of hydrogen and hydrogen sulfide along the catalyst bed length when the concentrations of these compounds in the liquid phase are known.

5.2.1.2 Mass Balance Equations in Liquid Phase

The differential equations of mass balance for the concentrations of hydrogen and hydrogen sulfide in the liquid phase can be written by equating the concentrations gradient to the mass transfer of H_2 and H_2S across the gas–liquid and liquid–solid as follows (Baskar et al. 2004; (Rodriguez and Ancheyta, 2004; Mederos and Ancheyta, 2007):

Hydrogen: $$\frac{dC_{H_2}^L}{dz} = \frac{1}{u_l}\left[k_{H_2}^L a_L\left(\frac{P_{H_2}^G}{h_{H_2}} - C_{H_2}^L\right) - k_{H_2}^S a_S\left(C_{H_2}^L - C_{H_2}^S\right)\right] \tag{5.3}$$

H_2S: $$\frac{dC_{H_2S}^L}{dz} = \frac{1}{u_l}\left[k_{H_2S}^L a_L\left(\frac{P_{H_2S}^G}{h_{H_2S}} - C_{H_2S}^L\right) - k_{H_2S}^S a_S\left(C_{H_2S}^L - C_{H_2S}^S\right)\right] \tag{5.4}$$

Equations (5.3) and (5.4) represent the mass balance equations for the gaseous compounds (H_2 and H_2S), while the mass balance equation for the liquid compounds (sulfur, nitrogen, asphaltene, vanadium and nickel) can be written by equating their liquid–phase concentration gradients to their mass transfer between the liquid–phase and the solid phase. Thus, the mass balance equations in liquid phase can be written as (Korsten and Hoffmann, 1996; Mederos et al., 2006; Alvarez and Ancheyta, 2008a):

Sulfur: $$\frac{dC_{sul}^L}{dz} = -\frac{1}{u_l}k_{sul}^S a_S\left(C_{sul}^L - C_{sul}^S\right) \tag{5.5}$$

Nitrogen: $$\frac{dC_N^L}{dz} = -\frac{1}{u_l}k_N^S a_S\left(C_N^L - C_N^S\right) \tag{5.6}$$

Asphaltene: $$\frac{dC_{Asph}^L}{dz} = -\frac{1}{u_l}k_{Asph}^S a_S\left(C_{Asph}^L - C_{Asph}^S\right) \tag{5.7}$$

Vanadium: $$\frac{dC_V^L}{dz} = -\frac{1}{u_l}k_V^S a_S\left(C_V^L - C_V^S\right) \tag{5.8}$$

Nickel: $$\frac{dC_{Ni}^L}{dz} = -\frac{1}{u_l}k_{Ni}^S a_S\left(C_{Ni}^L - C_{Ni}^S\right) \tag{5.9}$$

The concentrations of these compounds on the catalyst surface change as the reactions proceed along the catalyst bed length. The derivation of these equations is presented in Appendix A.

5.2.1.3 Mass Balance Equations in Solid Phase

The solution of the above equations requires surface concentrations of H_2, H_2S, S, N, Asph, V and Ni. At steady–state, the compounds transported between the liquid phase and the solid phase (on the surface of the catalyst) are consumed or produced through the chemical reaction. By equating the liquid–solid interfacial mass transfer of H_2, H_2S, S, N, Asph, V and Ni components with their reaction rates, we obtain the following equations (Chowdhury et al., 2002; Baskar et al. 2004; Rodriguez and Ancheyta, 2004; Alvarez and Ancheyta, 2008a):

Hydrogen: $$k_{H_2}^S a_S \left(C_{H_2}^L - C_{H_2}^S\right) = \rho_B \sum \eta_j r_j \tag{5.10}$$

H_2S: $$k_{H_2S}^S a_S \left(C_{H_2S}^L - C_{H_2S}^S\right) = -\rho_B \eta_{HDS} r_{HDS} \tag{5.11}$$

Sulfur: $$k_{sul}^S a_S \left(C_{sul}^L - C_{sul}^S\right) = \rho_B \eta_{HDS} r_{HDS} \tag{5.12}$$

Nitrogen: $$k_N^S a_S \left(C_N^L - C_N^S\right) = \rho_B \eta_{HDN} r_{HDN} \tag{5.13}$$

Asphaltene: $$k_{Asph}^S a_S \left(C_{Asph}^L - C_{Asph}^S\right) = \rho_B \eta_{HDAs} r_{HDAs} \tag{5.14}$$

Vanadium: $$k_V^S a_S \left(C_V^L - C_V^S\right) = \rho_B \eta_{HDV} r_{HDV} \tag{5.15}$$

Nickel: $$k_{Ni}^S a_S \left(C_{Ni}^L - C_{Ni}^S\right) = \rho_B \eta_{HDNi} r_{HDNi} \tag{5.16}$$

j = HDS, HDN, HDAs, HDV and HDNi. Equations (5.10) to (5.16) are the algebraic equations relating the extent of chemical reactions at the solid surface.

To solve the equations (5.1) to (5.9), boundary conditions are required for $P_{H_2}^G$, $P_{H_2S}^G$, $C_{H_2}^L$, $C_{H_2S}^L$, C_{sul}^L, C_N^L, C_{Asph}^L, C_V^L, and C_{Ni}^L at $z = 0$ as follows:

$$P_{H_2}^{G}\ (z = 0) = P_{H_2}^{G}\ (\text{initial}) \tag{5.17}$$

$$P_{H_2S}^{G}\ (z = 0) = 0 \tag{5.18}$$

$$C_{H_2}^{L}\ (z = 0) = C_{H_2}^{L}\ (\text{initial}) \tag{5.19}$$

$$C_{H_2S}^{L}(z = 0) = 0 \tag{5.20}$$

$$C_{sul}^{L}\ (z = 0) = C_{sul}^{L}\ (\text{initial}) \tag{5.21}$$

$$C_{N}^{L}(z = 0) = C_{N}^{L}\ (\text{initial}) \tag{5.22}$$

$$C_{Asph}^{l}(z = 0) = C_{Asph}^{l}\ (\text{initial}) \tag{5.23}$$

$$C_{V}^{L}(z = 0) = C_{V}^{L}\ (\text{initial}) \tag{5.24}$$

$$C_{Ni}^{L}(z = 0) = C_{Ni}^{L}\ (\text{initial}) \tag{5.25}$$

5.2.1.4 Chemical Reaction Rate

Developing kinetic models for crude oil hydrotreating reactions is not a simple task because of the complexities of crude oil composition and its analysis. Impurities are found in more than one form in crude oil; for example, sulfur compounds can be found as mercaptane, sulfide, thiophene, dibenzothiophene and their alkyl derivatives shapes, and nitrogen compounds as pyridine, quinoline, pyrrole, indole and carbazole, whereas metals occur as porphyrine, vanadyl and non-vanadyl (Wauquier, 1995; Marafi et al., 2003). Each form is described by its own reactivity and complex reaction ways, which are specific to each feed. For such a complex feed, the rate of chemical reaction is usually lumped into a single power law reaction (Lababidi et al., 1998). For most of the reactions that include the effect of inhibiting species like H_2S, Langmuir-Hinshelwood models are used.

According to Vrinat (1983) and Girgis and Gates (1991), the hydrodesulfurization reactions are irreversible under general process conditions. Also, the concentrations of

H_2 and sulfur have a positive impact on the rate of reaction, while the H_2S adsorbed on the active catalyst sites inhibits the reaction rate. The hydrodesulfurization reaction is described by the following kinetic equation of the Langmuir–Hinshelwood model that accounts for hydrogen sulfide inhibiting influence (Bhaskar et al., 2004; Alvarez and Ancheyta, 2008a).

$$r_{HDS} = K_{HDS} \frac{\left(C_{sul}^{S}\right)^{n_{HDS}} \left(C_{H_2}^{S}\right)^{m_{HDS}}}{\left(1 + K_{H_2S} C_{H_2S}^{S}\right)^2} \tag{5.26}$$

The adsorption equilibrium constant of hydrogen sulfide ($K_{H_2S}^{S}$) can be described by the Van‘t Hoff equation (Mederos et al., 2006).

$$K_{H_2S} = 41769 \cdot 8411 \exp\left(\frac{2761}{RT}\right) \tag{5.27}$$

The HDN, HDAs, HDV and HDNi reactions are also irreversible under usual operational conditions. Modelling of such reactions is a hard task due to the large numbers of components of crude oil. For such a complex feed, the reaction rate equation is generally lumped into a single power low reaction (Alvarez and Ancheyta, 2008a). HDN, HDAs, HDV and HDNi reactions are modelled by the power law models with respect to the concentration of nitrogen, asphaltene, vanadium and nickel and with hydrogen as follows:

$$r_{HDN} = K_{HDN} \left(C_{N}^{S}\right)^{n_{HDN}} \left(C_{H_2}^{S}\right)^{m_{HDN}} \tag{5.28}$$

$$r_{HDAs} = K_{HDAs} \left(C_{Asph}^{S}\right)^{n_{HDAs}} \left(C_{H_2}^{S}\right)^{m_{HDAs}} \tag{5.29}$$

$$r_{HDV} = K_{HDV} \left(C_{V}^{S}\right)^{n_{HDV}} \left(C_{H_2}^{S}\right)^{m_{HDV}} \tag{5.30}$$

$$r_{HDNi} = K_{HDNi} \left(C_{Ni}^{S}\right)^{n_{HDNi}} \left(C_{H_2}^{S}\right)^{m_{HDNi}} \tag{5.31}$$

Reaction rate constant for HDS, HDN, HDAs, HDV and HDNi reactions can be determined for each reaction using the Arrhenius equation as follows:

$$K_{HDS} = A^0_{HDS} \exp\left(-\frac{EA_{HDS}}{RT}\right) \tag{5.32}$$

$$K_{HDN} = A^0_{HDN} \exp\left(-\frac{EA_{HDN}}{RT}\right) \tag{5.33}$$

$$K_{HDAs} = A^0_{HDAs} \exp\left(-\frac{EA_{HDAs}}{RT}\right) \tag{5.34}$$

$$K_{HDV} = A^0_{HDV} \exp\left(-\frac{EA_{HDV}}{RT}\right) \tag{5.35}$$

$$K_{HDNi} = A^0_{HDN} \exp\left(-\frac{EA_{HDN}}{RT}\right) \tag{5.36}$$

j = HDS, HDN, HDAs, HDV and HDNi.

5.2.1.5 Gas–Liquid Mass Transfer Coefficients

The correlations used for estimating the gas–liquid mass transfer coefficients are (Rodriguez and Ancheyta, 2004; Mederos et al., 2006):

Hydrogen: $$\frac{K^L_{H_2} a_L}{D^L_{H_2}} = 7\left(\frac{G_L}{\mu_L}\right)^{0.4}\left(\frac{\mu_L}{\rho_L D^L_{H_2}}\right)^{0.5} \tag{5.37}$$

H_2S: $$\frac{K^L_{H_2S} a_L}{D^L_{H_2S}} = 7\left(\frac{G_L}{\mu_L}\right)^{0.4}\left(\frac{\mu_L}{\rho_L D^L_{H_2S}}\right)^{0.5} \tag{5.38}$$

5.2.1.6 Liquid–Solid Mass Transfer Coefficients

The liquid–solid mass transfer coefficients can be calculated from the Van Krevelen–Krekels equation as published by Froment and Bischoff (1990), Bhaskar et al., (2002) and Mederos and Ancheyta, (2007), as follows:

Hydrogen: $$\frac{K^S_{H_2}}{D^L_{H_2} a_S} = 1.8\left(\frac{G_L}{a_S \mu_L}\right)^{0.5}\left(\frac{\mu_L}{\rho_L D^L_{H_2}}\right)^{1/3} \tag{5.39}$$

H_2S: $$\frac{K^S_{H_2S}}{D^L_{H_2S} a_S} = 1.8\left(\frac{G_L}{a_S \mu_L}\right)^{0.5}\left(\frac{\mu_L}{\rho_L D^L_{H_2S}}\right)^{1/3} \tag{5.40}$$

Sulfur: $$\frac{K_{sul}^{S}}{D_{sul}^{L}a_S}=1.8\left(\frac{G_L}{a_S\mu_L}\right)^{0.5}\left(\frac{\mu_L}{\rho_L D_{sul}^{L}}\right)^{1/3} \quad (5.41)$$

Nitrogen: $$\frac{K_{N}^{S}}{D_{N}^{L}a_S}=1.8\left(\frac{G_L}{a_S\mu_L}\right)^{0.5}\left(\frac{\mu_L}{\rho_L D_{N}^{L}}\right)^{1/3} \quad (5.42)$$

Asphaltene: $$\frac{K_{Asph}^{S}}{D_{Asph}^{L}a_S}=1.8\left(\frac{G_L}{a_S\mu_L}\right)^{0.5}\left(\frac{\mu_L}{\rho_L D_{Asph}^{L}}\right)^{1/3} \quad (5.43)$$

Vanadium: $$\frac{K_{V}^{S}}{D_{V}^{L}a_S}=1.8\left(\frac{G_L}{a_S\mu_L}\right)^{0.5}\left(\frac{\mu_L}{\rho_L D_{V}^{L}}\right)^{1/3} \quad (5.44)$$

Nickel: $$\frac{K_{Ni}^{S}}{D_{Ni}^{L}a_S}=1.8\left(\frac{G_L}{a_S\mu_L}\right)^{0.5}\left(\frac{\mu_L}{\rho_L D_{Ni}^{L}}\right)^{1/3} \quad (5.45)$$

5.2.1.7 Molecular Diffusivity

To determine the liquid–solid and gas–liquid mass transfer coefficients, it is necessary to know the molecular diffusivity of H_2, H_2S, S, N, Asph, V and Ni in the liquid, which can be calculated by a Tyn-calus correlation (Reid et al., 1987; Dudukovic et al., 2002):

Hydrogen: $$D_{H_2}^{L}=8.93\times10^{-8}\frac{\upsilon_L^{0.267}}{\upsilon_{H_2}^{0.433}}\frac{T}{\mu_L} \quad (5.46)$$

H_2S: $$D_{H_2S}^{L}=8.93\times10^{-8}\frac{\upsilon_L^{0.267}}{\upsilon_{H_2S}^{0.433}}\frac{T}{\mu_L} \quad (5.47)$$

Sulfur: $$D_{sul}^{L}=8.93\times10^{-8}\frac{\upsilon_L^{0.267}}{\upsilon_{sul}^{0.433}}\frac{T}{\mu_L} \quad (5.48)$$

Nitrogen: $$D_{N}^{L}=8.93\times10^{-8}\frac{\upsilon_L^{0.267}}{\upsilon_{N}^{0.433}}\frac{T}{\mu_L} \quad (5.49)$$

Asphaltene: $$D_{Asph}^{L}=8.93\times10^{-8}\frac{\upsilon_L^{0.267}}{\upsilon_{Asph}^{0.433}}\frac{T}{\mu_L} \quad (5.50)$$

Vanadium: $$D_{V}^{L}=8.93\times10^{-8}\frac{\upsilon_L^{0.267}}{\upsilon_{V}^{0.433}}\frac{T}{\mu_L} \quad (5.51)$$

Nickel: $$D_{Ni}^{L}=8.93\times10^{-8}\frac{\upsilon_L^{0.267}}{\upsilon_{Ni}^{0.433}}\frac{T}{\mu_L} \quad (5.52)$$

The molar volume of crude oil, H_2 and H_2S can be estimated from the following equations (Dudukovic et al., 2002; Macı´as and Ancheyta, 2004):

Crude oil: $\upsilon_L = 0.285\left(\upsilon_C^L\right)^{1.048}$ (5.53)

Hydrogen: $\upsilon_{H_2} = 0.285\left(\upsilon_C^{H_2}\right)^{1.048}$ (5.54)

H_2S: $\upsilon_{H_2S} = 0.285\left(\upsilon_C^{H_2S}\right)^{1.048}$ (5.55)

The critical specific volume of liquid (crude oil) can be obtained from a Riazi–Daubert correlation (Ahmed, 1989; Macı´as and Ancheyta, 2004):

$$\upsilon_C^L = \left(7.5214\times10^{-3}\left(T_{meABP}\right)^{0.2896}\left(\rho_{15.6}\right)^{-0.7666}\right)\cdot Mw \tag{5.56}$$

5.2.1.8 Henry's Law Coefficient

Henry's coefficients for H_2 and H_2S can be calculated from solubility coefficients (Mederos and Ancheyta, 2007; Alvarez and Ancheyta, 2008a):

Hydrogen: $h_{H_2} = \dfrac{V_{H_2}}{\lambda_{H_2}\rho_L}$ (5.57)

H_2S: $h_{H_2S} = \dfrac{V_{H_2S}}{\lambda_{H_2S}\rho_L}$ (5.58)

Korsten and Hoffmann (1996) presented the following equations for the solubility of hydrogen and hydrogen sulfide in hydrocarbon mixtures:

Hydrogen: $$\lambda_{H_2} = -0.559729 - 0.42947\times10^{-3}T + 3.07539\times10^{-3}\left(\frac{T}{\rho_{20}}\right) + 1.94593\times10^{-6}\left(T\right)^2 + \left(\frac{0.835783}{\left(\rho_{20}\right)^2}\right)$$ (5.59)

H_2S: $\lambda_{H_2S} = \exp\left(3.367 - 0.00847T\right)$ (5.60)

5.2.1.9 Oil Density

The oil density (ρ_L) as a function of temperature and pressure can be estimated by the Standing–Katz equation, as published in Ahmed, (1989) and Macı´as and Ancheyta, (2004):

$$\rho_L = \rho_\circ + \Delta\rho_P - \Delta\rho_T \tag{5.61}$$

$$\Delta\rho_P = \left[0.167 + 16.181\times10^{-0.0425\rho_\circ}\right]\cdot\left[\frac{P}{1000}\right] - 0.01\times \left[0.299 + 263\times10^{-0.0603\rho_\circ}\right]\cdot\left[\frac{P}{1000}\right]^2 \tag{5.62}$$

$$\Delta\rho_T = \left[0.0133 + 152.4\left(\rho_\circ + \Delta\rho_P\right)^{-2.45}\right]\cdot\left(T-520\right) - \left[8.1\times10^{-6} - 0.0622\times10^{-0.764\left(\rho_\circ+\Delta\rho_P\right)}\right]\cdot\left(T-520\right)^2 \tag{5.63}$$

5.2.1.10 Oil Viscosity

Glaso's equation, as presented in Ahmed (1980), Korsten and Hoffmann (1996) and Shokri and Zarrinpashne (2006) is used a generalized mathematical equation for oil viscosity. The equation has the following form:

$$\mu_L = 3.141\times10^{10}\left(T-460\right)^{-3.444}\left[\log_{10}\left(API\right)\right]^a \tag{5.64}$$

$$a = 10.313\left[\log_{10}\left(T-460\right)\right] - 36\cdot447 \tag{5.65}$$

$$API = \frac{141.5}{sp.gr_{15.6}} - 131.5 \tag{5.66}$$

5.2.1.11 Characteristics of the Catalyst Bed

The surface area of the particles per unit volume of the bed can be estimated as (Shah, 1979; Froment and Bischoff, 1990):

$$as = \frac{A_C\left(1-\varepsilon\right)}{v} \tag{5.67}$$

For cylindrical particle: $$as = \frac{2\pi\, rL}{\pi\, r^2 L}\left(1-\varepsilon\right) = \frac{2}{r}\left(1-\varepsilon\right) = \frac{4\left(1-\varepsilon\right)}{d_c} \tag{5.68}$$

The bed void fraction of the catalyst (ε) is calculated by the following equation. This equation has been developed for a packed bed of spheres (Froment and Bischoff, 1990; Macı´as and Ancheyta, 2004):

$$\varepsilon = 0.38 + 0.073\left[1 + \frac{\left(\left(\frac{D_R}{d_s}\right) - 2\right)^2}{\left(\frac{D_R}{d_s}\right)^2}\right] \tag{5.69}$$

For cylindrical particles, the equivalent spherical diameter is given by the equation (Mears, 1971; Shah, 1979):

$$d_s = \left[d_c L_c + \left(\frac{d_c^2}{2}\right)\right]^{1/2} \tag{5.70}$$

5.2.1.12 Effectiveness Factor (η)

Internal diffusion limitations are usually expressed in terms of the catalyst effectiveness factor (η) (Satterfield, 1975). It has been noted that the chemical reaction rate decreases with increasing particle size. In the literature, the effectiveness factor has been reported to be in the range of 0.0057 to 1 (Scamangas and Marangozis, 1982; Li et al., 1995). Because the particle size of the catalyst is small, the effectiveness factor (η) can be estimated as function of Thiele Modulus (ϕ) (Marroquin et al., 2005). The generalized Thiele Modulus for n^{th}-*order* irreversible reaction is (Froment and Bischoff, 1990):

$$\phi = \frac{V_P}{S_P}\left[\left(\frac{n+1}{2}\right)\left(\frac{KC_{As}^{n-1}\rho_P}{D_e}\right)\right]^{0.5} \tag{5.71}$$

$$\rho_P = \frac{\rho_B}{1-\varepsilon} \tag{5.72}$$

For HDS, HDN, HDAs, HDV and HDNi reactions, the Thiele Modulus can be stated as:

$$\phi_{HDS} = \frac{V_P}{S_P}\left[\left(\frac{n_{HDS}+1}{2}\right)\left(\frac{K_{HDS}C_{sul}^{s(n_{HDS}-1)}\rho_P}{De_{sul}}\right)\right]^{0.5} \tag{5.73}$$

$$De_{sul} = \frac{\theta}{\tau}\left(\frac{1}{(1/D_{sul}^{L}) + (1/D_{K_{sul}})}\right) \tag{5.74}$$

$$\phi_{HDN} = \frac{V_P}{S_P}\left[\left(\frac{n_{HDN}+1}{2}\right)\left(\frac{K_{HDN}C_N^{s(n_{HDN}-1)}\rho_P}{De_N}\right)\right]^{0.5} \tag{5.75}$$

$$De_N = \frac{\theta}{\tau}\left(\frac{1}{(1/D_N^L)+(1/D_{K_N})}\right) \tag{5.76}$$

$$\phi_{HDAs} = \frac{V_P}{S_P}\left[\left(\frac{n_{HDAs}+1}{2}\right)\left(\frac{K_{HDAs}C_{Asph}^{s(n_{HDAs}-1)}\rho_P}{De_{Asph}}\right)\right]^{0.5} \tag{5.77}$$

$$De_{Asphl} = \frac{\theta}{\tau}\left(\frac{1}{(1/D_{Asphl}^L)+(1/D_{K_{Asph}})}\right) \tag{5.78}$$

$$\phi_{HDV} = \frac{V_P}{S_P}\left[\left(\frac{n_{HDV}+1}{2}\right)\left(\frac{K_{HDV}C_V^{s(n_{HDV}-1)}\rho_P}{De_V}\right)\right]^{0.5} \tag{5.79}$$

$$De_V = \frac{\theta}{\tau}\left(\frac{1}{(1/D_V^L)+(1/D_{K_V})}\right) \tag{5.80}$$

$$\phi_{HDNi} = \frac{V_P}{S_P}\left[\left(\frac{n_{HDNi}+1}{2}\right)\left(\frac{K_{HDNi}C_{Ni}^{s(n_{HDNi}-1)}\rho_P}{De_{Ni}}\right)\right]^{0.5} \tag{5.81}$$

$$De_{Ni} = \frac{\theta}{\tau}\left(\frac{1}{(1/D_{Ni}^L)+(1/D_{K_{Ni}})}\right) \tag{5.82}$$

The tortuosity factor (τ) generally has a value of 2 to 7 (Satterfield, 1975). Usually, tortuosity factor is assumed to be 4 according to literature reports (Satterfield, 1975; Macı´as and Ancheyta, 2004; Marroquin et al., 2005). Knudsen diffusivity factor (D_{K_j}) for each reaction is evaluated as follows (Carberry, 1976; Froment and Bischoff, 1990):

$$D_{K_{sul}} = 9700\, r_g\left(\frac{T}{M_{sul}}\right)^{0.5} \tag{5.83}$$

$$D_{K_N} = 9700\, r_g\left(\frac{T}{M_N}\right)^{0.5} \tag{5.84}$$

$$D_{K_{Asph}} = 9700\, r_g\left(\frac{T}{M_{Asph}}\right)^{0.5} \tag{5.85}$$

$$D_{K_V} = 9700\, r_g\left(\frac{T}{M_V}\right)^{0.5} \tag{5.86}$$

$$D_{K_{Ni}} = 9700\, r_g\left(\frac{T}{M_{Ni}}\right)^{0.5} \tag{5.87}$$

$$r_g = \frac{2\theta}{S_g \rho_P} \tag{5.88}$$

$$\theta = \rho_P V_g \tag{5.89}$$

The following equation is employed for determining the values of η (Aris, 1975; Li et al., 1995; Chang et al., 1998):

$$\eta_{HDS} = \frac{\tanh \phi_{HDS}}{\phi_{HDS}} \tag{5.90}$$

$$\eta_{HDN} = \frac{\tanh \phi_{HDN}}{\phi_{HDN}} \tag{5.91}$$

$$\eta_{HDAs} = \frac{\tanh \phi_{HDAs}}{\phi_{HDAs}} \tag{5.92}$$

$$\eta_{HDV} = \frac{\tanh \phi_{HDV}}{\phi_{HDV}} \tag{5.93}$$

$$\eta_{HDNi} = \frac{\tanh \phi_{HDNi}}{\phi_{HDNi}} \tag{5.94}$$

5.2.1.13 Kinetic Parameters of the Models

The evaluation of kinetic parameters with high accurcy of the relevant reactions scheme are necessary for obtaining a rigorous model that can be confidently applied to reactor design and process optimization. In the model presented above, the reaction orders of sulfur, nitrogen, asphaltene, vanadium and nickel compounds (n_j), hydrogen compound order (m_j), reaction rate constants (K_j), activation energies (EA_j) and pre-exponential factors (A^0_j) for each reaction, parameters of equations (5.26) and (5.28-5.36) are such significant parameters for the HDS, HDN, HDAs, HDV and HDNi processes. The major focus is to accurately calculate these parameters.

In order to evaluate the best values of kinetic parameters in this study, two approaches have been employed depending upon the S, N, Asph, V and Ni content in hydrotreated products under varies operating conditions. They are as follows:

A. Non-linear regression to simultaneously obtain the reaction orders of sulfur, nitrogen, asphaltene, vanadium and nickel compound (n_j), hydrogen compound order (m_j) and reaction rate constants (K_j) for each reaction separately, then linear regression with the Arrhenius equation to estimate the activation energy (EA_j) and pre-exponential factor ($A^0{}_j$) for each reaction separately.

B. Non-linear regression to determine n_j, m_j, EA_j and $A^0{}_j$ simultaneously for each reaction separately.

Both approaches are applied for each process separately using the following objective function based upon the minimization of the sum of squared errors (*SSE*) between the experimental concentrations of S, N, Asph, V and Ni compound ($C_{i,y}^{\exp}$) and calculated ($C_{i,y}^{cal}$), in the products:

$$SSE = \sum_{y=1}^{N_{Data}} \left[C_{i,y}^{\exp} - C_{i,y}^{cal} \right]^2 \tag{5.95}$$

i = S, N, Asph, V and Ni

5.2.2 Optimization Problem Formulation for Parameter Estimation

The optimization problem formulation for each reaction separately (HDS, HDN, HDAs, HDV and HDNi) can be described as follows:

Given the reactor configuration, the feedstock, the catalyst, reaction temperature, hydrogen pressure and liquid hourly space velocity.

Optimize for the first approach: the reaction order of S, N, Asph, V and Ni compounds (n_j), hydrogen compound order (m_j) and reaction rate constants ($K^1{}_j$, $K^2{}_j$, $K^3{}_j$) for each reaction separately at different temperatures (335°C, 370°C, 400°C, respectively).

for the second approach: the reaction order of S, N, Asph, V and Ni compounds (n_j), hydrogen compound order (m_j), the activation energy (EA_j) and pre-exponential factor (A^0_j) simultaneously (for each reaction separately).

So as to minimize the sum of squared errors (*SSE*).

Subject to process constraints and linear bounds on all optimization variables in the process.

Mathematically, using the first approach, the problem can be presented as:

Min *SSE*

n_j, mj, K^i_j *(i=1,2,3, j= HDS, HDN, HDAs, HDV, HDNi)*

s.t $f(z, x(z), \dot{x}(z), u(z), \underline{v}) = 0$, $[z_0, z_f]$ (model, equality constraints)

$n_j^L \le n_j \le n_j^U$ (inequality constraints)

$m_j^L \le m_j \le m_j^U$ (inequality constraints)

$K^i_j{}^L \le K^i_j \le K^i_j{}^U$, $i=1,2,3$ (inequality constraints)

Using the second approach, the problem can be expressed as:

Min *SSE*

n_j, m_j, EA_j, A^0_j *(j= HDS, HDN, HDAs, HDV, HDNi)*

s.t $f(z, x(z), \dot{x}(z), u(z), \underline{v}) = 0$, $[z_0, z_f]$ (model, equality constraints)

$n_j^L \le n_j \le n_j^U$ (inequality constraints)

$m_j^L \le m_j \le m_j^U$ (inequality constraints)

$EA_j{}^L \le EA_j \le EA_j{}^U$ (inequality constraints)

$A^0_j{}^L \le A^0_j \le A^0_j{}^U$ (inequality constraints)

$f(z, x(z), \dot{x}(z), u(z), \underline{v}) = 0$ represents the process models presented in section 5.2.1, where z is the independent variable (length of the reactor bed), $u(z)$ is the decision variables (n_j, m_j, K_j, EA_j, A^0_j), $x(z)$ gives the set of all differential and algebraic variables (such as $P^G_{H_2}, C^L_{H_2S}, C^S_{sul}, r_{HDS}, \ldots$), $\dot{x}(z)$ denotes the derivative of differential variables with respect to length of the bed reactor (such as $dP^G_{H_2}/dz, dC^L_{H_2}/dz, \ldots$), and $\underline{v}$ represents the design variables or the length independent constant parameters (such as $R, \rho_{15.6}, T_{meABP}, V_{H_2}$, ..). The length interval of interest is $[z_0, z_f]$ and the function f is assumed to be continuously differentiable with respect to all its arguments (Morrison, 1984; Ekpo and Mujtaba, 2007).

The optimization solution method employed by gPROMS is a two-step method known as the feasible path approach. The first step performs a simulation to converge all the equality constraints (described by f) and to satisfy the inequality constraints. The second step performs the optimization (updates the values of the decision variables such as the kinetic parameters) (Mujtaba, 2004). The optimization problem is posed as a Non-Linear Programming (NLP) problem and is solved using a Successive Quadratic Programming (SQP) method within gPROMS software.

5.2.3 Results and Discussion

The values of constant parameters used in these models are given in Table 5.1

Table 5.1: Values of constant parameters used in the HDT models

Parameter	**Unit**	**Value**
R	J/mol.K	8.314
ρ_B	g/cm^3	0.67
$\upsilon_C^{H_2}$	cm^3/mol	65.1[a]
$\upsilon_C^{H_2S}$	cm^3/mol	98.6[a]
υ_{sul}	cm^3/mol	15.53[b]
υ_N	cm^3/mol	17.3[c]
υ_{Asph}	cm^3/mol	352.986
υ_V	cm^3/mol	8.55[d]
υ_{Ni}	cm^3/mol	6.59[e]
$\rho_{15.6}$	g/cm^3	0.8558
Mw	kg/kg.mol	227.5
T_{meABP}	°C	291
V_{H_2}	Nl/mole	22.43[f]
V_{H_2S}	Nl/mole	25[g]
ρ_{20}	g/cm^3	0.85323
D_R	cm	2.0
L_c	cm	0.4
d_c	cm	0.18
V_P	cm^3	0.0101736
S_p	cm^2	0.22608
S_g	cm^2/g	1800000
V_g	cm^3 /g	0.5
τ	-	4

[a] Reid et al., 1987;

[b] EnvironmentalChemistry.com,1995a;

[c] EnvironmentalChemistry.com, 1995b;

[d] EnvironmentalChemistry.com., 1995c;

[e] EnvironmentalChemistry.com, 1995d;

[e] AirLiquid.GasEncyclopaedia, 2008a;

[f] AirLiquid.GasEncyclopaedia, 2008b.

5.2.3.1 Estimation of Kinetic Parameters

The kinetic parameters for crude oil hydrodesulfurization, hydrodenitrogenation, hydrodeasphaltenization, hydrodevanadization and hydrodenickelation presented in the present work have been estimated depending on the experimental data using the TBR model.

In the first approach, the reaction order of S, N, Asph, V and Ni (n_j, $_{j=HDS, HDN, HDAs, HDV, HDNi}$), the hydrogen order ($m_j$) and reaction rate constants (K^i_j, $_{i=1,2,3}$) for each reaction separately were determined simultaneously. Linearization was then used for estimating the activation energy (EA_j) and the pre-exponential factor (A^0_j) for each reaction separately. To estimate activation energies and pre-exponential factors for each reaction, the Arrhenius equation described previously (equations (5.32) to (5.36) is used for this purpose. The Arrhenius-based dependence of the kinetic model is demonstrated in Figure 5.3 for all processes. A plot of $\ln K_j$ versus 1/T gives a straight line with a slope equal to $-EA_j/R$ and intercept equal to $\ln A^0_j$. In the second approach, the activation energies (EA_j), pre-exponential factors (A^0_j), reaction order of S, N, Asph, V and Ni (n_j) and hydrogen order (m_j) were determined simultaneously for each reaction separately. The generated kinetic parameters for HDS, HDN, HDAs, HDV and HDNi processes are presented in Table 5.2 for both approaches, respectively.

It is observed from Table 5.2 that the second approach gives a smaller sum of squared errors (*SSE*) than the first approach, for all reactions. It can be concluded depending on the objective function (*SSE)* that parameter estimation with the second approach is more accurate. In other words, determining the activation energy and pre-exponential factor by linearization process of Arrhenius equation gives a higher error in comparison to those obtained by simultaneous estimation of kinetic parameters via non-linear regression.

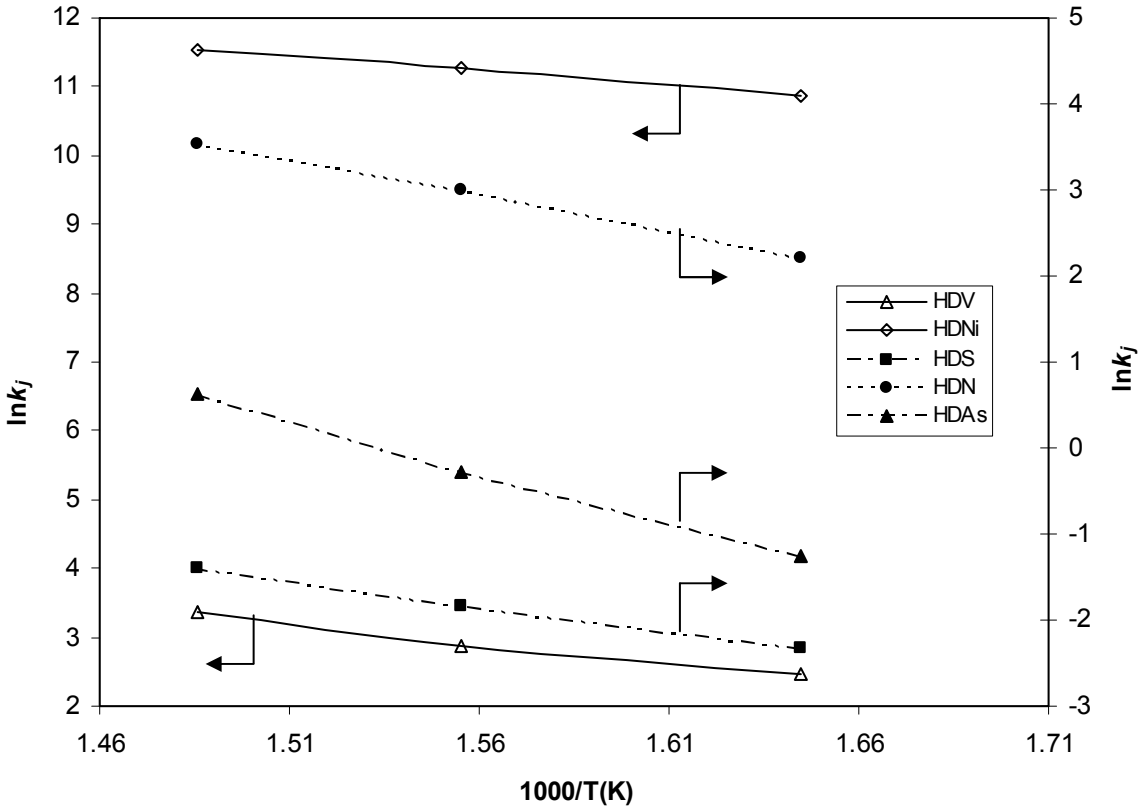

Figure 5.3: Linear representation of Arrhenius equation for crude oil hydrotreating

The best reaction orders of sulfur, nitrogen, asphaltene, vanadium and nickel were 1.147, 1.6723, 1.452, 1.2514 and 1.6884, respectively, while, the best orders of H_2 for HDS, HDN, HDAs, HDV and HDNi were 0.4709, 0.3555, 0.3068, 0.6337 and 0.5667, respectively, which is typical for lumped kinetics.

Many authors have extensively studied the reaction kinetics of hydrotreating processes for different distillate fractions (not of crude oil which is the focus of this work) and reported that HDT reactions follow half to second order kinetics for sulfur (Korsten and Hoffmann, 1996; Maria and Martinez, 1999; Kumar et al., 2001; Bhaskar et al., 2002; Rodriguez and Ancheyta, 2004; Mederos and Ancheyta, 2007; Alvarez and Accheyta, 2008a), and zero to one order kinetics for hydrogen (Korsten and Hoffmann, 1996; Kumar et al., 2001; Bhaskar et al., 2004; Cheng et al., 2004).

Table 5.2: Comparison of kinetic parameter values estimated with two approaches for HDS, HDN, HDAs, HDV and HDNi models

First approach (Linear)					
	HDS	**HDN**	**HDV**	**HDAs**	**HDNi**
$K^i_{j,\ i=1}$	0.09797	9.06245	11.6142	0.283440	51827.2
$K^i_{j,\ i=2}$	0.15934	20.0872	17.5322	0.754769	77768.1
$K^i_{j,\ i=3}$	0.24584	34.3759	28.8485	1.857120	103539
m	0.4656	0.3325	0.6267	0.3039	0.5633
n	1.149	1.6302	1.2482	1.449	1.6819
EA_j	48010.02	69973.95	47172.80	98030.374	36288.95
A^0_j	1293.75	9435596.91	127388.9139	73221525.5	0.683×10^{8}
SSE	0.000895	3.5442×10^{-6}	0.24521638	6.5×10^{-4}	0.01000841
Second approach (Nonlinear)					
	HDS	**HDN**	**HDV**	**HDAs**	**HDNi**
m	0.4709	0.3555	0.6337	0.3068	0.5667
n	1.147	1.6723	1.2514	1.452	1.6884
EA_j	50264.10	71775.5	46181.6	104481	37678.3
A^0_j	2026.23	2.85×10^{7}	126566	2.56134×10^{8}	1.045×10^{8}
SSE	0.000819	2.8957×10^{-6}	0.2225156	6.3×10^{-4}	0.007773

For the purpose of assessing the kinetic parameters and providing sufficient evidence to ensure that values of kinetic parameters estimated do correspond to the global minimum of the objective function so that the developed process models is accurate, sensitivity analyses for n_j, m_j, EA_j and A^0_j values were performed. The information obtained from parametric sensitivity analysis is very useful for optimization and parameter calculation. It gives a clear indication which parameter has the largest influence on the accuracy of the kinetic model. Sensitivity analysis is used for each of the calculated parameters by means of perturbations of the parameter value and is preferably in the range of ±10%, keeping the other parameters at their nominal values (Resendiz et al., 2007; Alcazar and

Ancheyta, 2007; Rao, et al., 2009). For each perturbation in the parameter values, the objective function is re-determined and then for each parameter the perturbation percentage is plotted against the corresponding value of the objective function as shown in Figures 5.4 to 5.8 for each reaction separately (for each parameter). When all the perturbations in all the kinetic parameters give the same minimum of the objective function with their original values (0% perturbation), that means the global minimum has been achieved. On the other hand, if at least one parameter does not give the same minimum than the others at 0% perturbation, means poor nonlinear parameter evaluation. From Figures 5.4 to 5.8, it is clearly seen that the estimated kinetic parameters are the optimum since at 0% perturbation the perturbations of *n, m,* EA_{HDT} and A^0_{HDT} give the same minimum of the objective function (SSE) with their original values. Therefore, it is demonstrated that the global minimum has been achieved. It is also observed from these Figures that *n* has the greatest effect on HDT kinetic model compared to EA_{HDT}, *m*, and A^0_{HDT}, respectively.

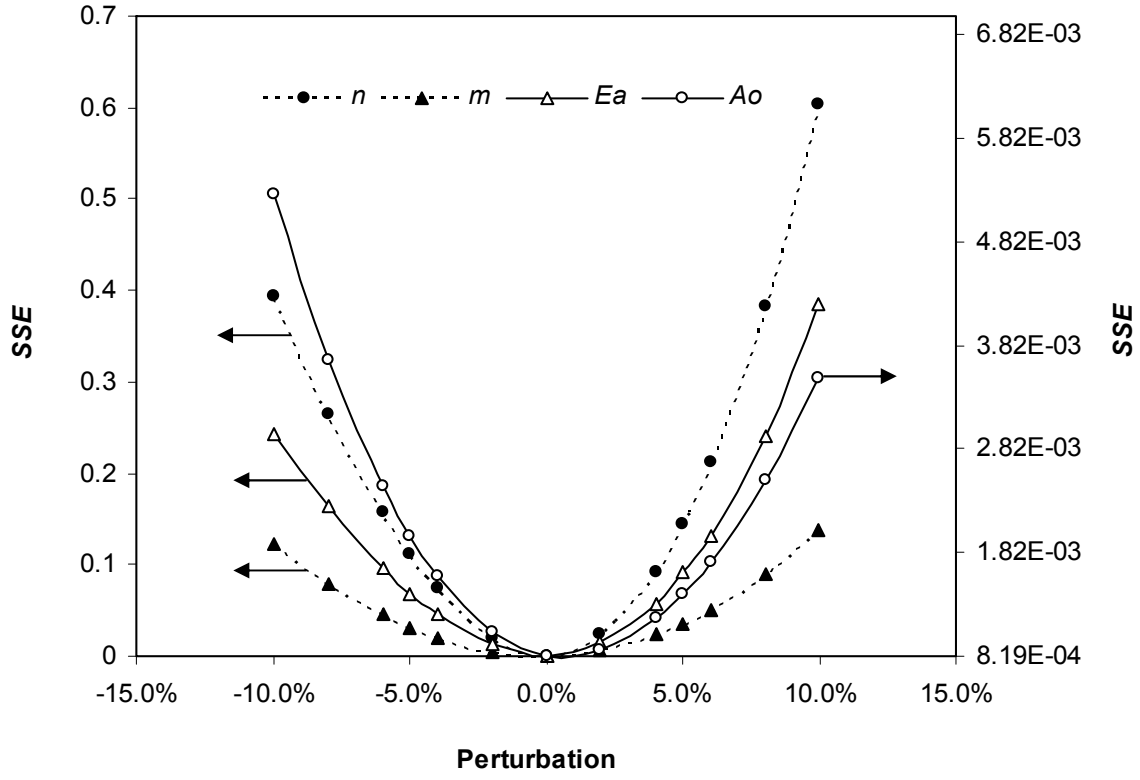

Figure 5.4: Sensitivity analysis of estimated parameters for HDS reaction

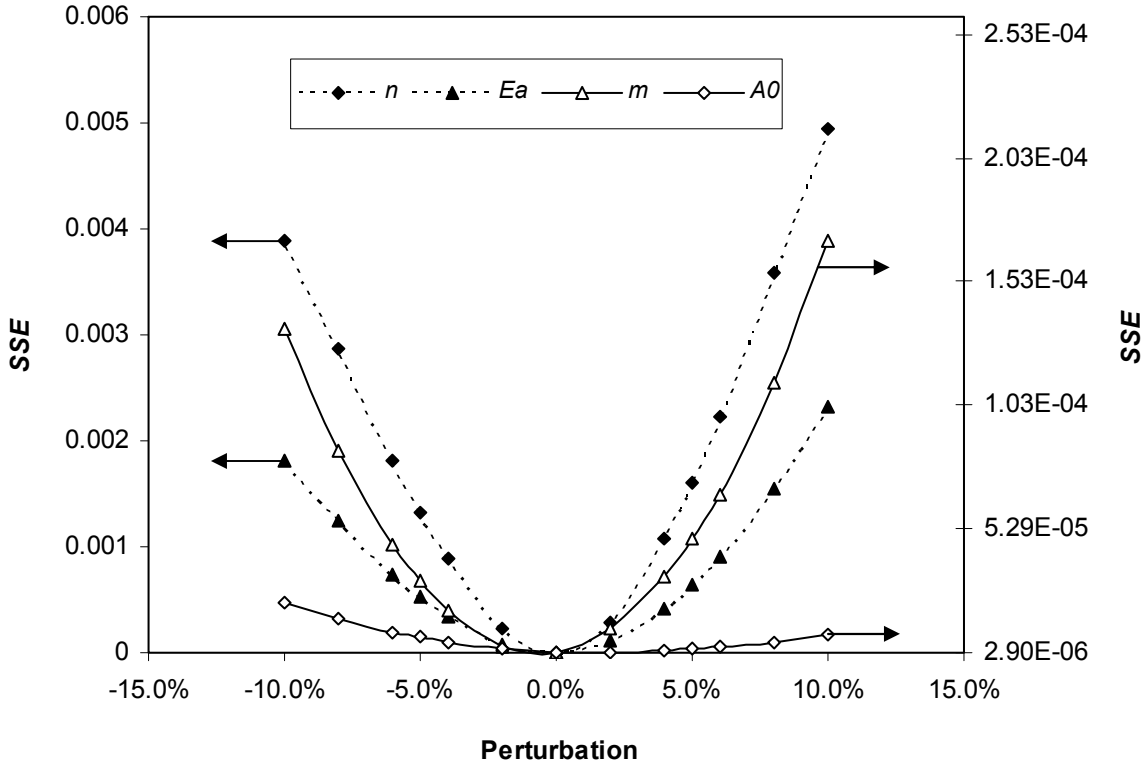

Figure 5.5: Sensitivity analysis of estimated parameters for HDN reaction

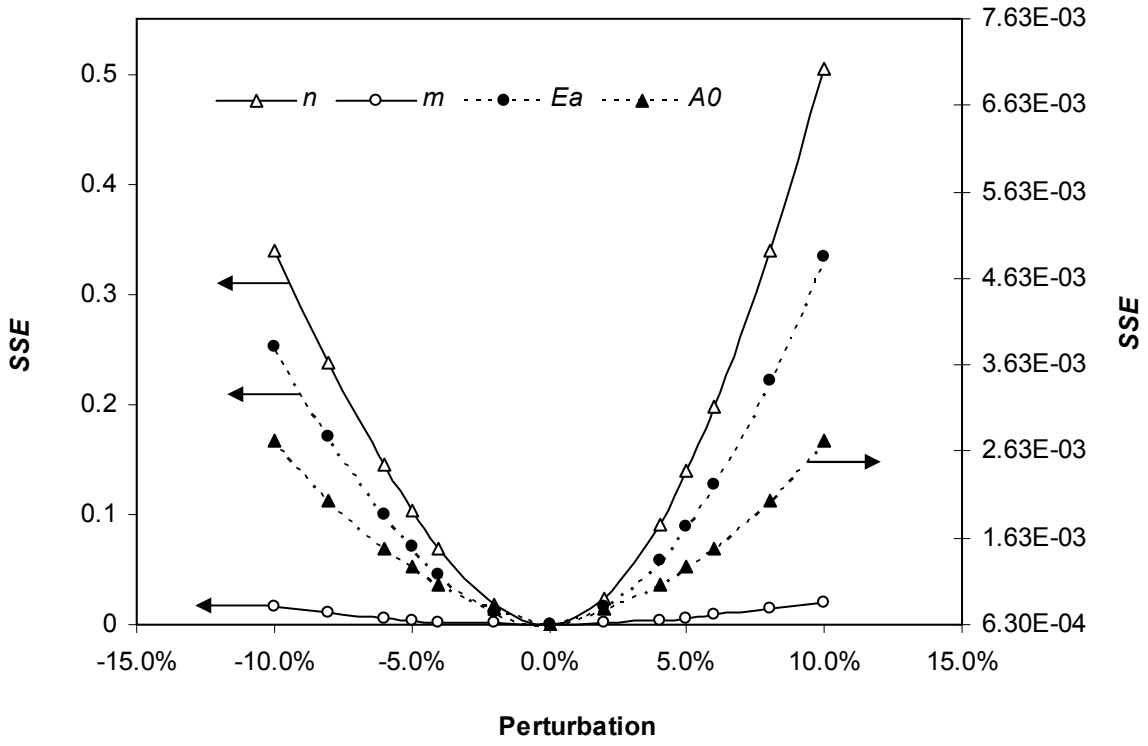

Figure 5.6: Sensitivity analysis of estimated parameters for HDAs reaction

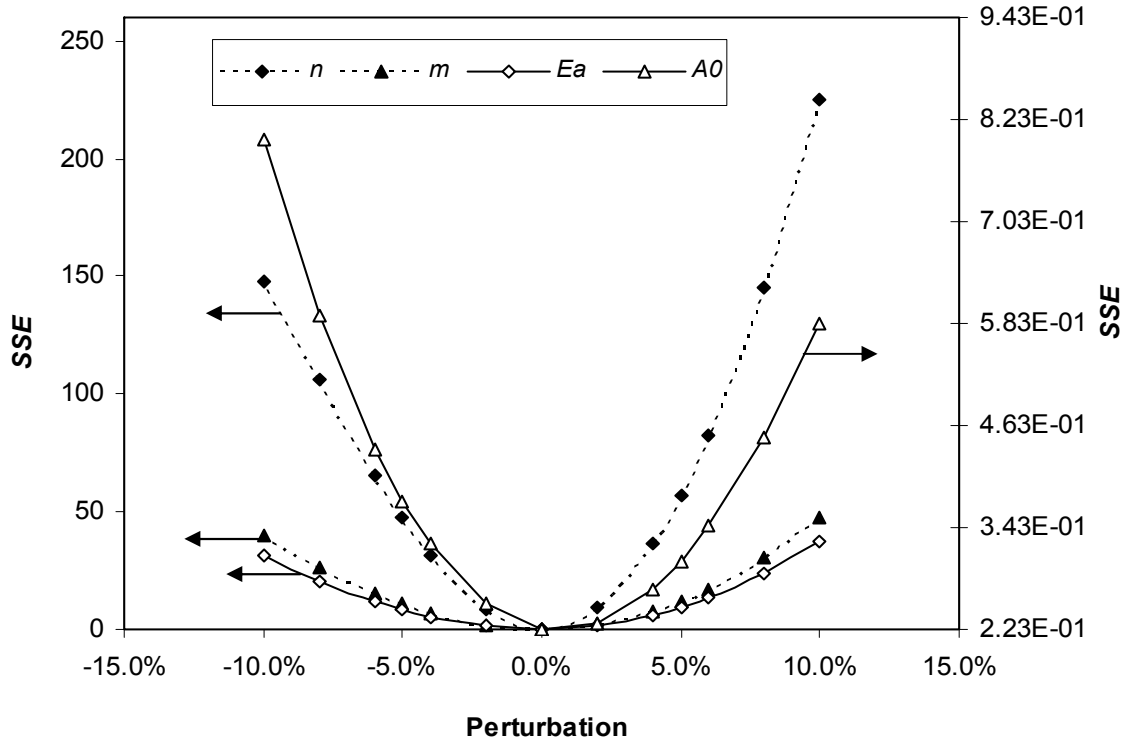

Figure 5.7: Sensitivity analysis of estimated parameters for HDV reaction

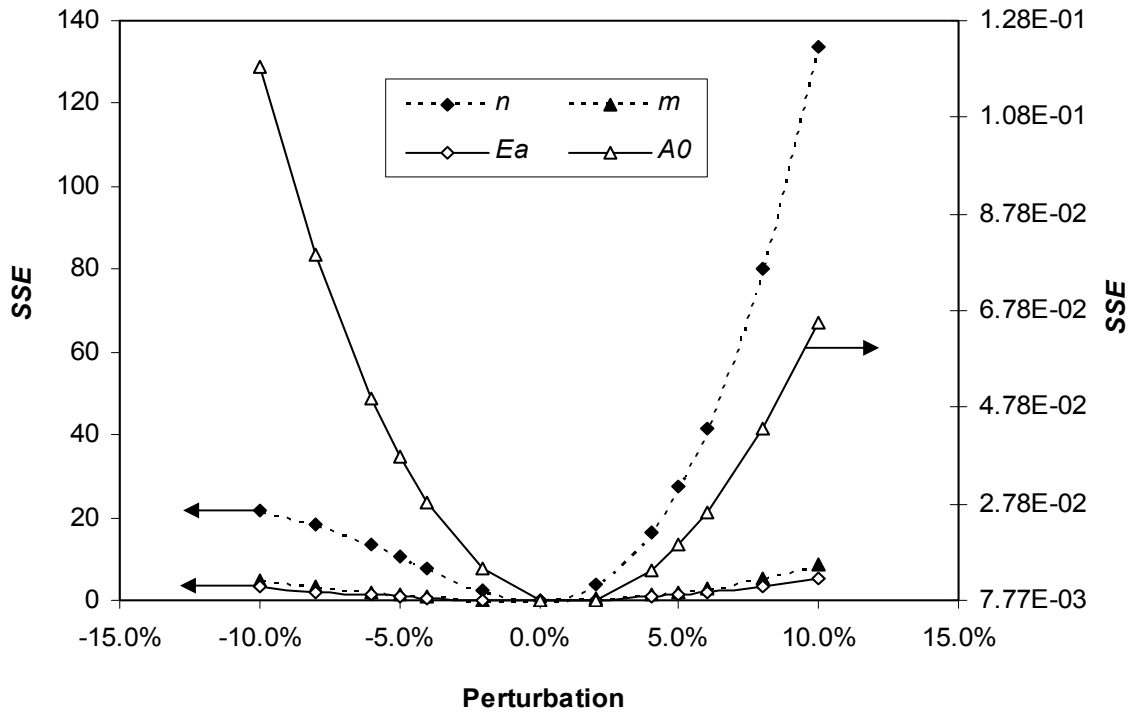

Figure 5.8: Sensitivity analysis of estimated parameters for HDNi reaction

A comparison between experimental results and model prediction results for HDS, HDN, HDAs, HDV and HDNi of crude oil is shown in Tables 5.3 to 5.7, and plotted in Figures 5.9 to 5.13 (using the second approach where the experimental data are represented in the form of points; while the simulation results are represented in the form of curves, each curve representing 3 simulated points). As can be observed from the results, the model was found to simulate the performance of the pilot plant TBR with very good agreement in the range of operating conditions studied between both concentrations with average absolute error less than 5% by using second approach. It is also noted from these figures that the removal of sulfur, nitrogen, asphaltene, vanadium and nickel increases with increasing temperature and pressure and decreases with liquid hourly space velocity. These increases happen due to the kinetic parameters used to describe HDS, HDN, HDAs, HDV and HDNi processes in this model are affected by the operating conditions.

Table 5.3: Simulation data of the pilot plant-TBR using two approaches (linear and non-linear regression) versus experimental data for HDS of crude oil

Operating conditions			Experimental results		Simulated results					
LHSV (hr^{-1})	P (Mpa)	T (^0C)	Sulfur (wt%)	Conversion (%)	Sulfur(wt%)-Non-linear regression	Conversion (%)	Absolute error %	Sulfur (wt%)-Linear regression	Conversion (%)	Absolute error %
0.5	4	335	0.670	66.50	0.6980	65.10	4.18	0.6816	65.92	1.73
1.0	4	335	1.110	44.50	1.1607	41.96	4.57	1.1460	42.70	3.24
1.5	4	335	1.360	32.00	1.3820	30.90	1.62	1.3699	31.50	0.73
0.5	4	370	0.430	78.50	0.4106	79.47	4.51	0.4043	79.78	5.98
1.0	4	370	0.880	56.00	0.8829	55.85	0.33	0.8753	56.23	0.53
1.5	4	370	1.150	42.50	1.1477	42.61	0.20	1.1407	42.96	0.81
0.5	4	400	0.229	88.50	0.2306	88.47	0.69	0.2303	88.48	0.57
1.0	4	400	0.640	68.00	0.6558	67.21	2.47	0.6544	67.28	2.25
1.5	4	400	0.930	53.50	0.9384	53.08	0.90	0.9368	53.16	0.73
0.5	7	335	0.520	74.00	0.5283	73.58	1.59	0.5148	74.26	1.00
1.0	7	335	1.010	49.50	1.0043	49.78	0.56	0.9904	50.48	1.94
1.5	7	335	1.260	37.00	1.2518	37.41	0.65	1.2398	38.01	1.60
0.5	7	370	0.280	86.00	0.2703	86.48	3.46	0.2668	86.66	4.71
1.0	7	370	0.710	64.50	0.7112	64.44	0.17	0.7056	64.72	0.62
1.5	7	370	1.001	49.95	0.9907	50.46	1.03	0.9851	50.74	1.59
0.5	7	400	0.135	93.25	0.1309	93.45	3.04	0.1319	93.40	2.29
1.0	7	400	0.500	75.00	0.4882	75.59	2.36	0.4889	75.55	2.22
1.5	7	400	0.761	61.95	0.7686	61.57	0.99	0.7689	61.55	1.04
0.5	10	335	0.430	78.50	0.4268	78.66	0.74	0.4154	79.23	3.39
1.0	10	335	0.900	55.00	0.8991	55.04	0.10	0.8861	55.69	1.54
1.5	10	335	1.200	40.00	1.1607	41.96	3.27	1.1491	42.54	4.24
0.5	10	370	0.196	90.20	0.1964	90.18	0.20	0.1944	90.28	0.82
1.0	10	370	0.597	70.15	0.6026	69.87	0.94	0.5984	70.08	0.71
1.5	10	370	0.898	55.10	0.8854	55.73	1.40	0.8809	55.95	1.90
0.5	10	400	0.082	95.90	0.0852	95.74	3.90	0.0865	95.67	5.49
1.0	10	400	0.376	81.20	0.3893	80.53	3.54	0.3912	80.44	4.04
1.5	10	400	0.640	68.00	0.6596	67.02	3.06	0.6614	66.93	3.34

Model Prediction

			Sulfur content-wt% (using 2nd approach)	Conversion %
0.75	10	400	0.2317	88.41
1.25	4	370	1.0328	48.36
0.5	7	385	0.1915	90.42
1.5	5.5	335	1.3099	34.50

Table 5.4: Simulation data of the pilot plant-TBR using two approaches (linear and non-linear regression) versus experimental data for HDN of crude oil

Operating conditions			Experimental results		Simulated results					
LHSV (hr^{-1})	P (Mpa)	T (^0C)	Nitrogen (wt%) $*10^4$	Conversion (%)	Nitrogen(wt%) -Non-linear regression $*10^4$	Conversion (%)	Absolute error %	Nitrogen (wt%)-Linear regression$*10^4$	Conversion (%)	Absolute error %
0.5	4	335	526.9	47.31	520.127	47.99	1.28	515.685	48.43	2.13
1.0	4	335	713.2	28.68	698.521	30.15	2.06	695.861	30.41	2.43
1.5	4	335	783.5	21.65	780.680	21.93	0.36	778.809	22.12	0.59
0.5	4	370	327.9	67.21	322.559	67.74	1.63	317.915	68.21	3.04
1.0	4	370	512.7	48.73	519.305	48.07	1.29	515.863	48.41	0.62
1.5	4	370	618.9	38.11	629.749	37.02	1.75	627.083	37.29	1.32
0.5	4	400	203.7	79.63	195.061	80.49	4.24	190.502	80.95	6.48
1.0	4	400	362.8	63.72	370.197	63.98	2.04	365.697	63.43	0.79
1.5	4	400	485.3	51.47	488.288	51.17	0.61	484.208	51.58	0.22
0.5	7	335	472.5	52.75	462.947	53.70	2.02	461.683	53.83	2.29
1.0	7	335	649.0	35.10	650.889	34.91	0.29	650.981	34.91	0.30
1.5	7	335	738.1	26.19	742.125	25.79	0.54	742.535	25.75	0.60
0.5	7	370	261.0	73.90	270.503	72.95	3.64	268.869	73.11	3.01
1.0	7	370	449.1	55.09	461.380	53.86	2.73	461.318	53.87	2.72
1.5	7	370	571.9	42.81	576.263	42.37	0.76	576.777	42.32	0.85
0.5	7	400	155.3	84.47	155.966	84.40	0.43	153.883	84.61	0.91
1.0	7	400	305.5	69.45	314.128	68.59	2.82	313.029	68.69	2.46
1.5	7	400	418.6	58.14	429.321	57.10	2.56	428.802	57.12	2.44
0.5	10	335	424.9	57.51	426.147	57.38	0.29	426.907	57.31	0.47
1.0	10	335	605.3	39.47	618.237	38.18	2.14	620.312	37.97	2.48
1.5	10	335	687.9	31.21	714.953	28.50	3.93	717.100	28.29	4.24
0.5	10	370	234.2	76.58	239.509	76.05	2.27	239.521	76.05	2.27
1.0	10	370	418.5	58.15	424.078	57.59	1.36	426.166	57.38	1.83
1.5	10	370	518.3	48.17	540.414	45.96	4.27	543.119	45.69	4.79
0.5	10	400	130.5	86.95	134.069	86.60	2.73	133.209	86.68	2.07
1.0	10	400	274.4	72.56	280.075	72.99	2.14	280.913	71.91	2.45
1.5	10	400	387.1	61.29	391.755	60.82	1.20	393.466	60.65	1.64

Model Prediction

			Nitrogen content-wt%$*10^4$ (using 2nd approach)	Conversion %
0.75	10	400	211.237	78.88
1.25	4	370	581.522	41.58
0.5	7	385	207.057	79.29
1.5	5.5	335	759.339	24.07

Table 5.5: Simulation data of the pilot plant-TBR using two approaches (linear and non-linear regression) versus experimental data for HDAs of crude oil

Operating conditions			Experimental results		Simulated results					
LHSV (hr^{-1})	P (Mpa)	T (^0C)	Asphaltene (wt%)	Conversion (%)	Asphaltene (wt%)-Non-linear regression	Conversion (%)	Absolute error %	Asphaltene (wt%)-Linear regression	Conversion (%)	Absolute error %
0.5	4	335	0.639	46.75	0.6414	46.55	0.37	0.6177	48.52	3.33
1.0	4	335	0.868	27.67	0.8614	28.22	0.76	0.8439	29.67	2.78
1.5	4	335	0.966	19.50	0.9577	20.19	0.86	0.9443	21.31	2.25
0.5	4	370	0.335	72.08	0.3248	72.93	3.04	0.3196	73.37	4.59
1.0	4	370	0.610	49.17	0.5848	51.27	4.13	0.5793	51.72	5.03
1.5	4	370	0.760	36.67	0.7304	39.13	3.89	0.7255	39.54	4.54
0.5	4	400	0.153	87.25	0.1473	87.72	3.72	0.1507	87.44	1.50
1.0	4	400	0.355	70.42	0.3622	69.82	2.03	0.3673	69.39	3.46
1.5	4	400	0.510	57.50	0.5179	56.84	1.55	0.5231	56.41	2.57
0.5	7	335	0.560	53.33	0.5779	51.84	3.19	0.5544	53.80	1.00
1.0	7	335	0.790	34.17	0.8126	32.30	2.86	0.7939	33.84	0.49
1.5	7	335	0.910	24.17	0.9196	23.37	1.05	0.9049	24.59	0.56
0.5	7	370	0.262	78.16	0.2672	77.73	1.98	0.2629	78.09	0.34
1.0	7	370	0.512	57.33	0.5192	56.73	1.41	0.5142	57.15	0.43
1.5	7	370	0.660	45.00	0.6705	44.12	1.59	0.6659	44.51	0.89
0.5	7	400	0.116	90.33	0.1109	90.76	4.39	0.1140	90.50	1.72
1.0	7	400	0.295	75.42	0.3007	74.94	1.93	0.3060	74.50	3.73
1.5	7	400	0.440	63.33	0.4511	62.41	2.52	0.4569	61.92	3.84
0.5	10	335	0.520	56.67	0.5369	55.26	3.25	0.5133	57.22	1.29
1.0	10	335	0.750	37.50	0.7790	35.08	3.87	0.7597	39.70	1.29
1.5	10	335	0.860	28.33	0.8929	25.59	3.82	0.8774	26.90	2.02
0.5	10	370	0.236	80.33	0.2332	80.57	1.19	0.2296	80.87	2.71
1.0	10	370	0.475	60.42	0.4769	60.26	0.40	0.4724	60.63	0.55
1.5	10	370	0.620	48.33	0.6305	47.46	1.69	0.6262	47.82	1.00
0.5	10	400	0.089	92.58	0.0913	92.40	2.58	0.0943	92.14	5.95
1.0	10	400	0.255	78.75	0.2638	78.02	3.45	0.2692	77.57	5.57
1.5	10	400	0.398	66.83	0.4089	65.92	2.74	0.4151	65.41	4.29

Model Prediction

			Asphaltene content-wt% (using 2nd approach)	Conversion %
0.75	10	400	0.1784	85.13
1.25	4	370	0.6670	44.42
0.5	7	385	0.1761	85.32
1.5	5.5	335	0.9366	21.95

Table 5.6: Simulation data of the pilot plant-TBR using two approaches (linear and non-linear regression) versus experimental data for HDV of crude oil

Operating conditions			Experimental results		Simulated results					
LHSV (hr^{-1})	P (Mpa)	T (^0C)	Vanadium (ppm)	Conversion (%)	Vanadium (ppm) -Non-linear regression	Conversion (%)	Absolute error %	Vanadium (ppm)-Linear regression	Conversion (%)	Absolute error %
0.5	4	335	8.33	68.57	8.7285	67.06	4.78	8.8067	66.77	5.72
1.0	4	335	14.34	45.89	14.8970	43.78	3.88	14.9717	43.50	4.40
1.5	4	335	17.79	32.87	17.9588	32.23	0.95	18.0212	31.99	1.30
0.5	4	370	5.54	79.09	5.4501	79.43	1.62	5.4742	79.34	1.19
1.0	4	370	11.70	55.85	11.5338	56.48	1.42	11.5673	56.35	1.13
1.5	4	370	15.50	41.51	15.0635	43.16	2.82	15.0956	43.03	2.61
0.5	4	400	3.21	87.89	3.3443	87.38	4.18	3.3369	87.41	3.95
1.0	4	400	8.40	68.30	8.7822	66.86	4.55	8.7786	66.87	4.51
1.5	4	400	12.10	54.34	12.4675	52.95	3.04	12.4665	52.96	3.03
0.5	7	335	5.60	78.87	5.6783	78.57	1.39	5.7757	78.20	3.14
1.0	7	335	11.80	55.47	11.7911	55.50	0.07	11.9066	55.07	0.90
1.5	7	335	15.10	43.02	15.2933	42.29	1.28	15.3980	41.89	1.97
0.5	7	370	3.15	88.11	3.0253	88.58	3.96	3.0627	88.44	2.77
1.0	7	370	8.66	67.32	8.2894	68.72	4.28	8.3549	68.47	3.52
1.5	7	370	12.50	52.83	11.9719	54.82	4.22	12.0408	54.56	3.67
0.5	7	400	1.59	94.00	1.5953	93.98	0.33	1.6031	93.95	0.82
1.0	7	400	5.46	79.40	5.7222	78.41	4.80	5.7473	78.31	5.26
1.5	7	400	9.13	65.55	9.2212	65.20	0.99	9.2535	65.08	1.35
0.5	10	335	3.84	85.51	4.0098	84.87	4.42	4.1076	84.50	6.97
1.0	10	335	9.42	64.45	9.7152	63.34	3.13	9.8530	62.82	4.59
1.5	10	335	13.23	50.00	13.3718	49.54	1.07	13.5055	49.03	2.08
0.5	10	370	1.98	92.53	1.8949	92.85	4.29	1.9317	92.71	2.44
1.0	10	370	6.63	74.98	6.3250	76.13	4.60	6.4044	75.83	3.40
1.5	10	370	10.27	61.24	9.8966	62.65	3.63	9.9876	62.31	2.75
0.5	10	400	0.891	96.64	0.8945	96.62	0.39	0.9046	96.59	1.53
1.0	10	400	3.95	85.10	4.0452	84.73	2.41	4.0814	84.59	3.33
1.5	10	400	6.89	74.00	7.1969	72.84	4.45	7.2474	72.65	5.19

Model Prediction

			Vanadium content-ppm (using 2nd approach)	Conversion %
0.75	10	400	2.3663	91.11
1.25	4	370	13.5225	48.97
0.5	7	385	2.2216	91.62
1.5	5.5	335	16.4992	37.74

Table 5.7: Simulation data of the pilot plant-TBR using two approaches (linear and non-linear regression) versus experimental data for HDNi of crude oil

Operating conditions			Experimental results		Simulated results					
LHSV (hr^{-1})	P (Mpa)	T (^0C)	Nickel (ppm)	Conversion (%)	Nickel (ppm)-Non-linear regression	Conversion (%)	Absolute error %	Nickel (ppm)-Linear regression	Conversion (%)	Absolute error %
0.5	4	335	2.01	88.18	1.9415	88.58	3.41	1.9085	88.77	5.05
1.0	4	335	4.80	71.76	4.6963	72.37	2.16	4.6497	72.65	3.13
1.5	4	335	6.80	60.00	6.7802	60.12	0.29	6.7326	60.39	0.99
0.5	4	370	1.11	93.47	1.1284	93.36	1.66	1.1189	93.42	0.80
1.0	4	370	3.10	81.76	3.2142	81.09	3.68	3.2029	81.16	3.32
1.5	4	370	4.95	70.88	5.0643	70.21	2.31	5.0546	70.27	2.11
0.5	4	400	0.73	95.70	0.6992	95.89	4.22	0.6993	95.89	4.20
1.0	4	400	2.28	86.59	2.2616	86.69	0.81	2.2694	86.65	0.46
1.5	4	400	3.85	77.35	3.8354	77.44	0.38	3.8505	77.35	0.01
0.5	7	335	1.15	93.23	1.1560	93.20	0.52	1.1352	93.32	1.29
1.0	7	335	3.22	81.06	3.2666	80.78	1.45	3.2322	81.99	0.38
1.5	7	335	5.10	70.00	5.1268	69.84	0.52	5.0888	70.06	0.22
0.5	7	370	0.62	96.35	0.6256	96.32	0.90	0.6207	96.35	0.11
1.0	7	370	2.02	88.12	2.0754	87.79	2.74	2.0699	87.82	2.47
1.5	7	370	3.50	79.41	3.5784	78.95	2.24	3.5755	78.97	2.16
0.5	7	400	0.36	97.88	0.3685	97.83	2.36	0.3692	97.83	2.55
1.0	7	400	1.33	92.18	1.3756	91.91	3.43	1.3832	91.86	4.00
1.5	7	400	2.48	85.41	2.5588	84.95	3.18	2.5747	84.85	3.82
0.5	10	335	0.81	95.23	0.8016	95.28	1.04	0.7868	95.37	2.86
1.0	10	335	2.50	85.29	2.4969	85.31	0.12	2.4700	85.47	1.20
1.5	10	335	4.07	76.06	4.1474	75.60	1.90	4.1162	75.79	1.13
0.5	10	370	0.42	97.53	0.4162	97.55	0.90	0.4131	97.57	1.64
1.0	10	370	1.48	91.29	1.5114	91.11	2.12	1.5085	91.13	1.92
1.5	10	370	2.71	84.06	2.7638	83.74	1.98	2.7636	83.74	1.98
0.5	10	400	0.24	98.59	0.2386	98.60	0.58	0.2394	98.59	0.25
1.0	10	400	0.93	94.53	0.9653	94.32	3.79	0.9719	94.28	4.50
1.5	10	400	1.87	89.00	1.9028	88.81	1.75	1.9177	88.72	2.55

Model Prediction

			Nickel content-ppm (using 2nd approach)	Conversion %
0.75	10	400	0.5579	96.72
1.25	4	370	4.1857	75.38
0.5	7	385	0.4799	97.18
1.5	5.5	335	5.8272	65.72

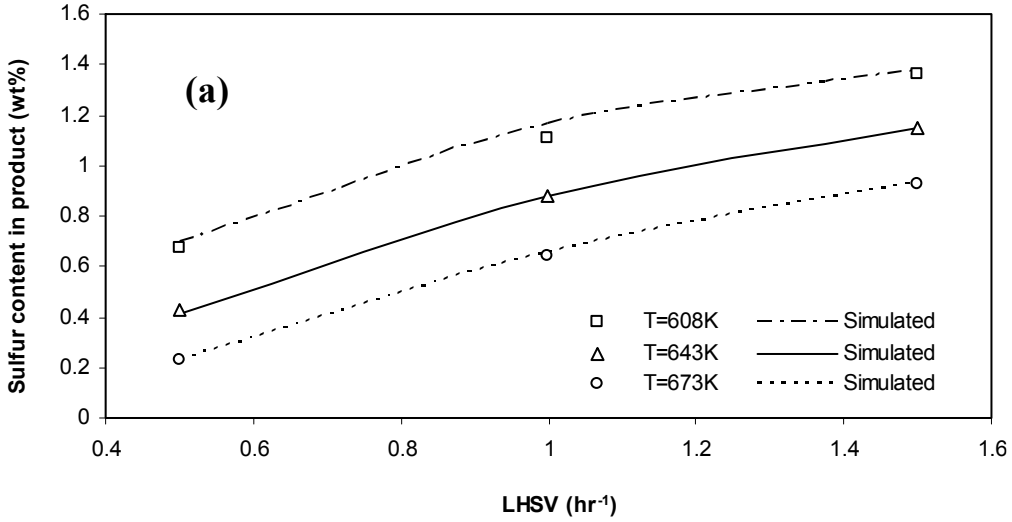

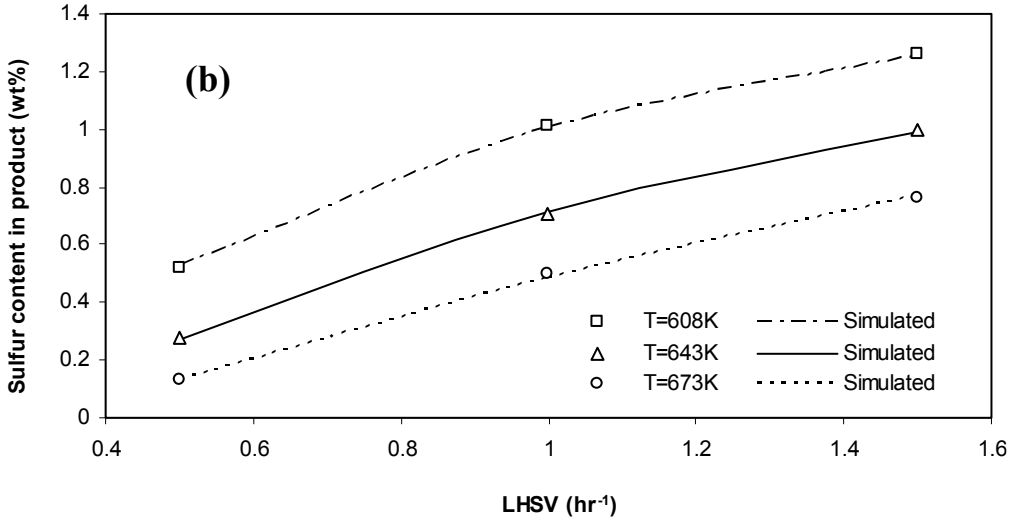

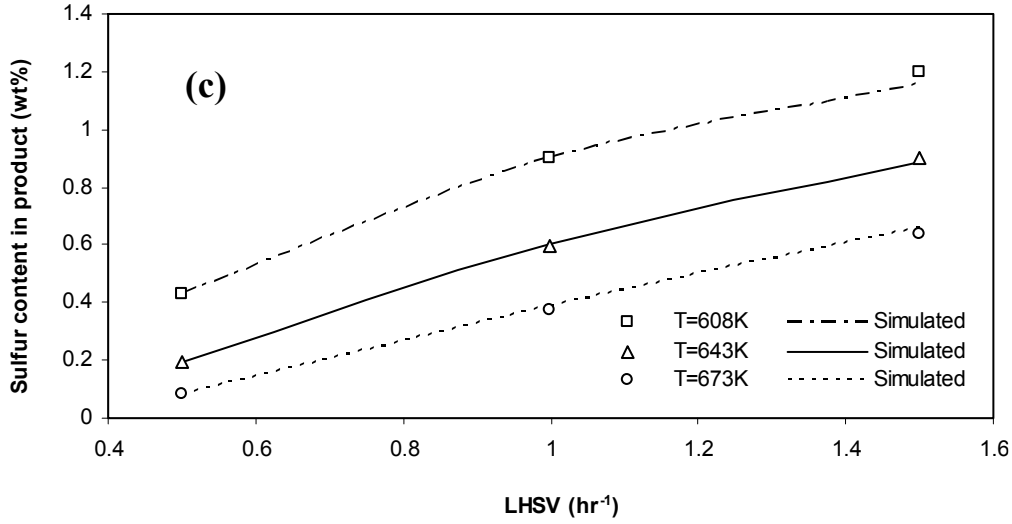

Figure 5.9: Experimental data (points) and simulated (lines) variation of outlet sulfur content vs. liquid hourly space velocity at different reactor temperature and at pressure (a) 4 MPa, (b) 7 MPa, (c) 10 MPa

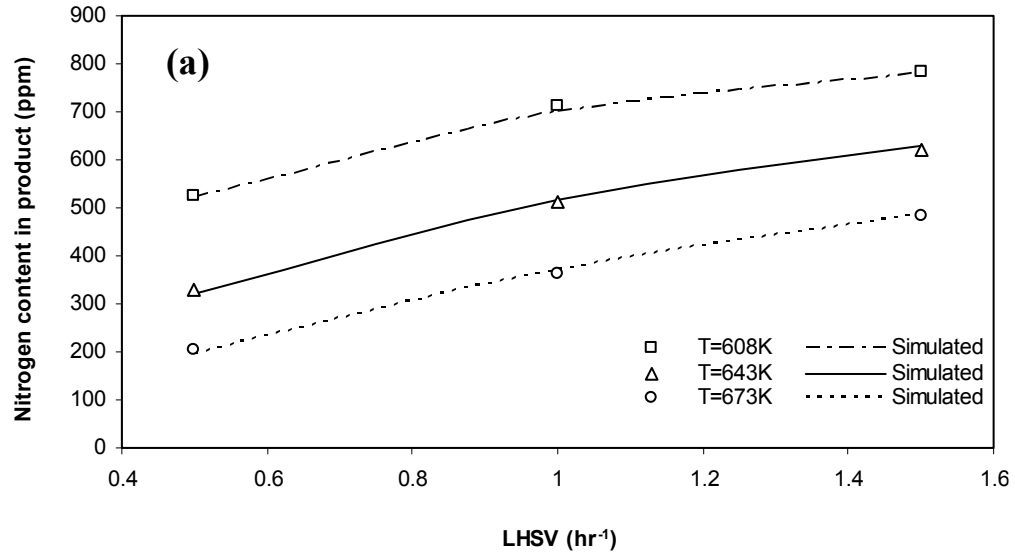

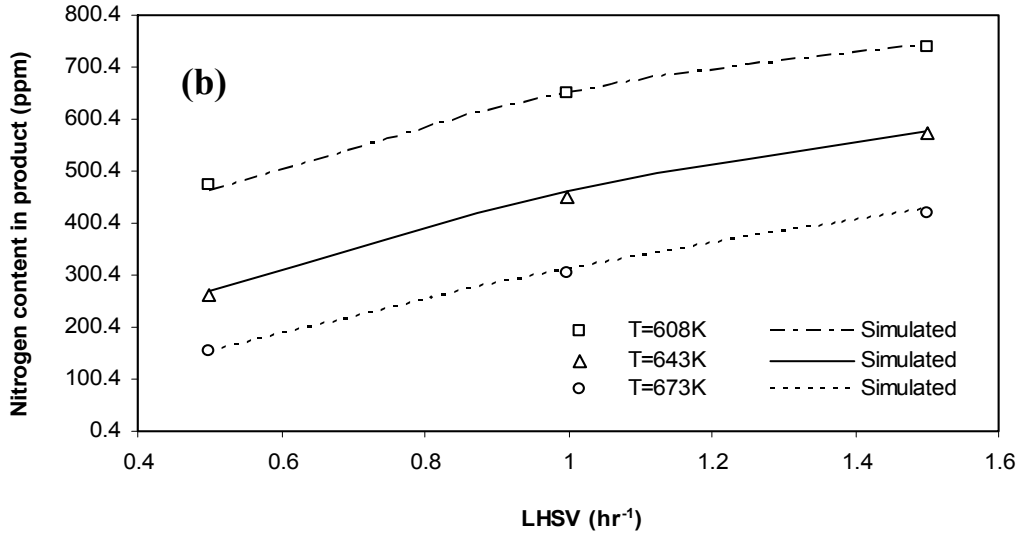

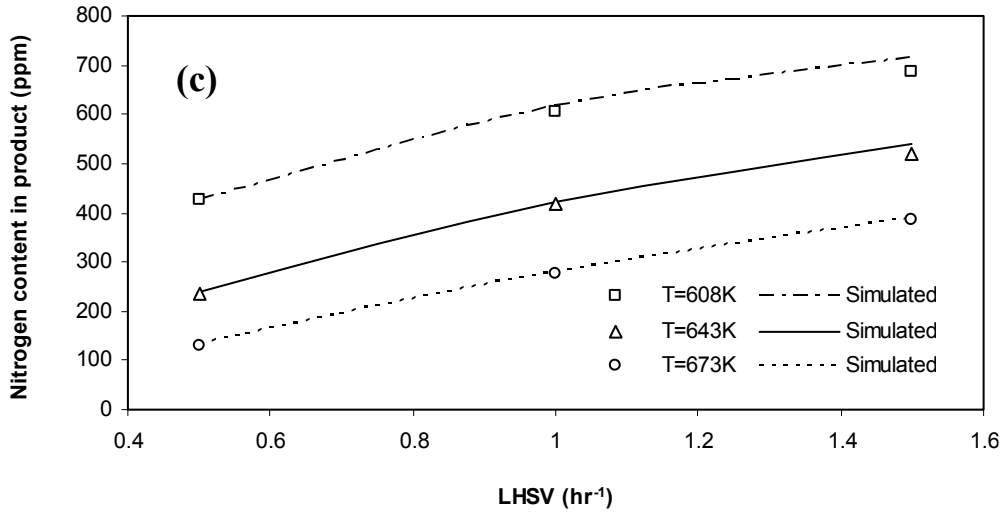

Figure 5.10: Experimental data (points) and simulated (lines) variation of outlet nitrogen content vs. liquid hourly space velocity at different reactor temperature and at pressure (a) 4 MPa, (b) 7 MPa, (c) 10 MPa.

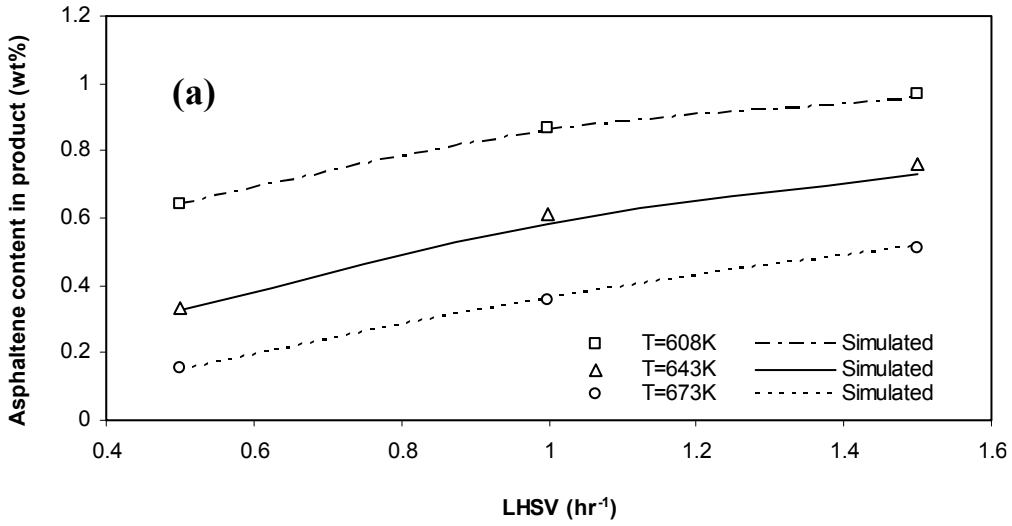

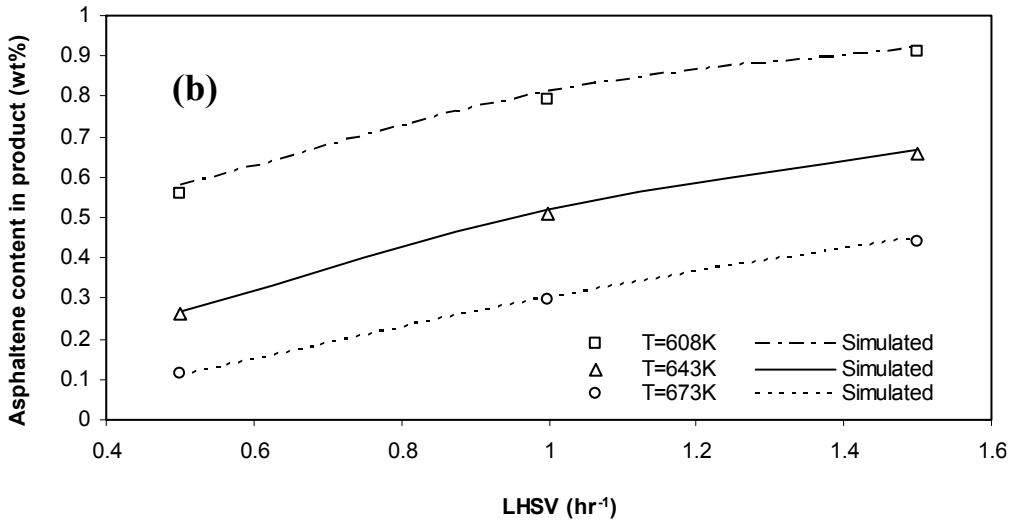

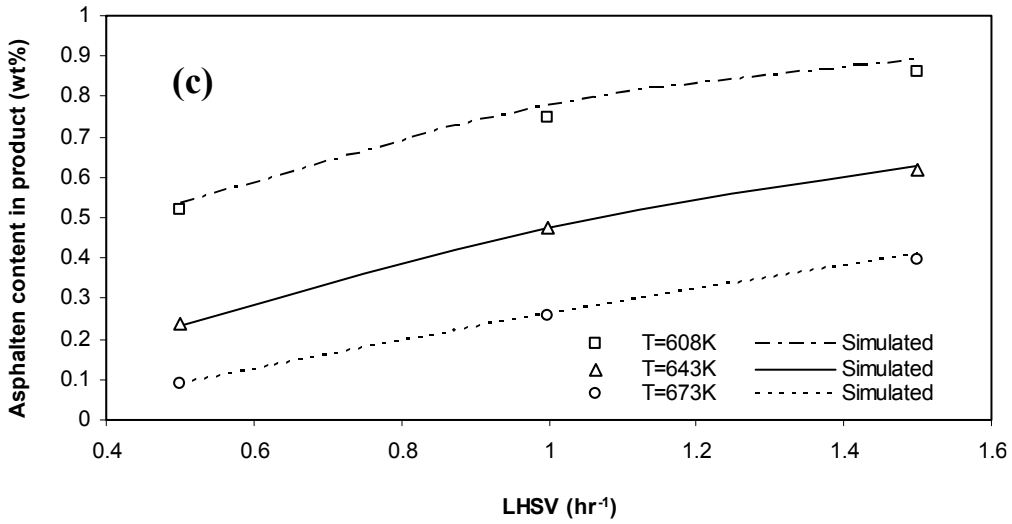

Figure 5.11: Experimental data (points) and simulated (lines) variation of outlet asphaltene content vs. liquid hourly space velocity at different reactor temperature and at pressure (a) 4 MPa, (b) 7 MPa, (c) 10 MPa.

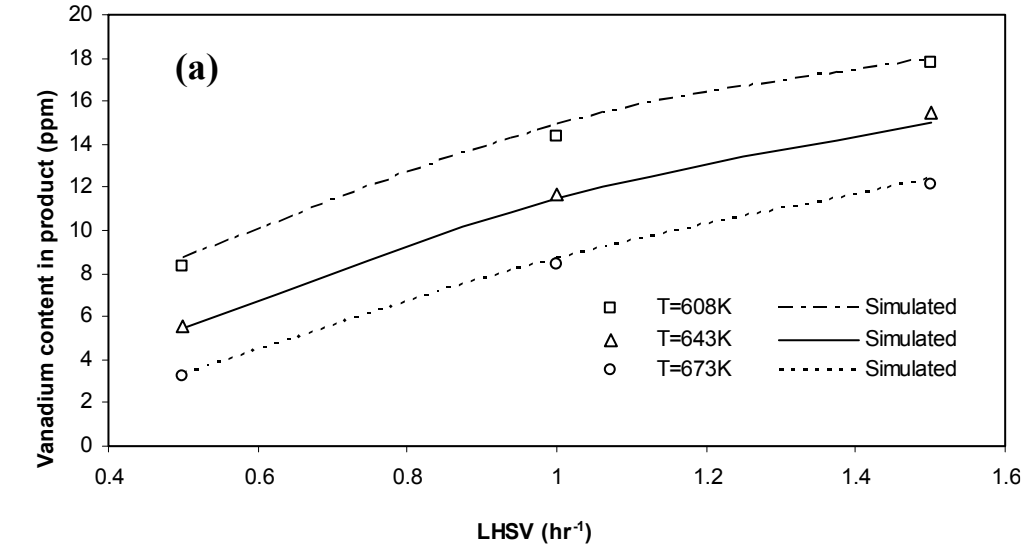

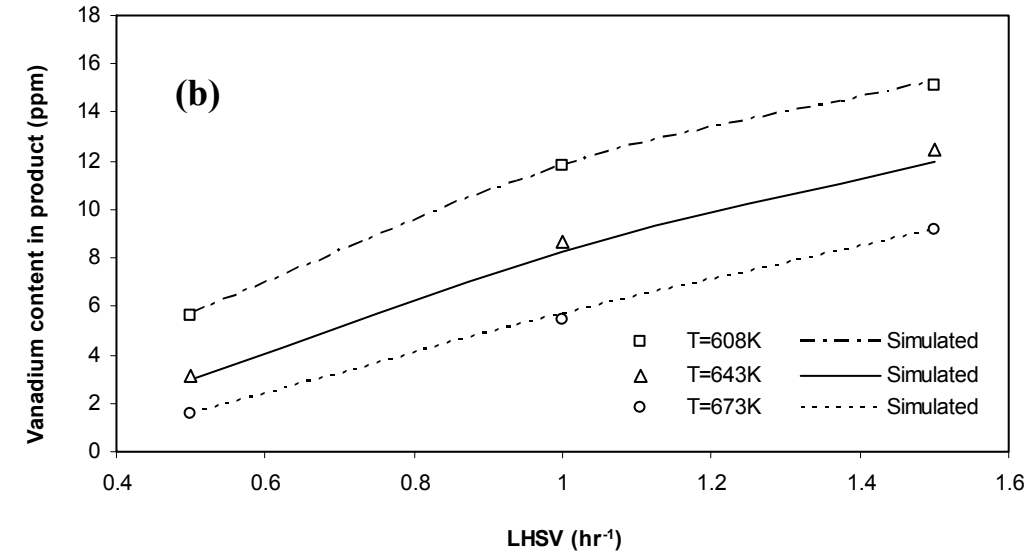

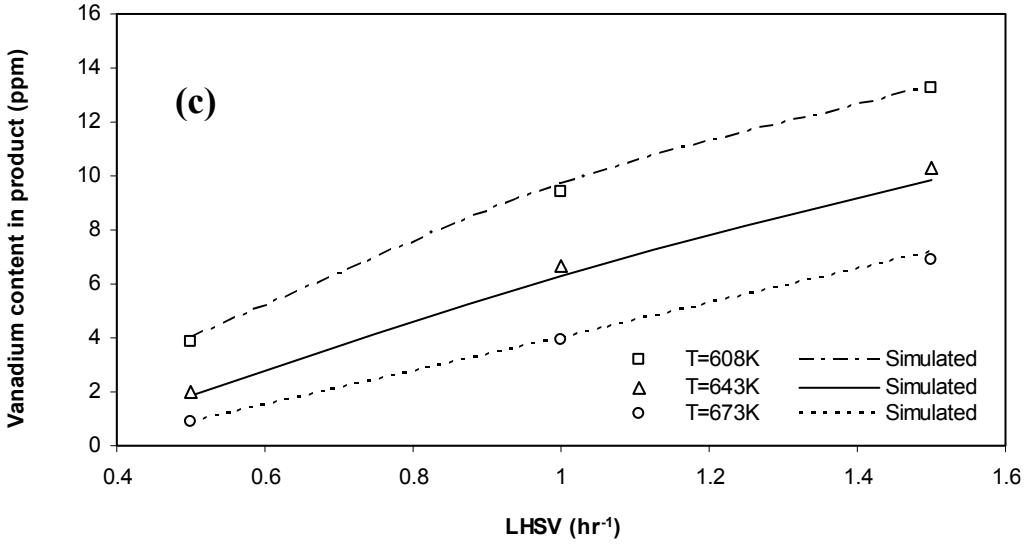

Figure 5.12: Experimental data (points) and simulated (lines) variation of outlet vanadium content vs. liquid hourly space velocity at different reactor temperature and at pressure (a) 4 MPa, (b) 7 MPa, (c) 10 MPa.

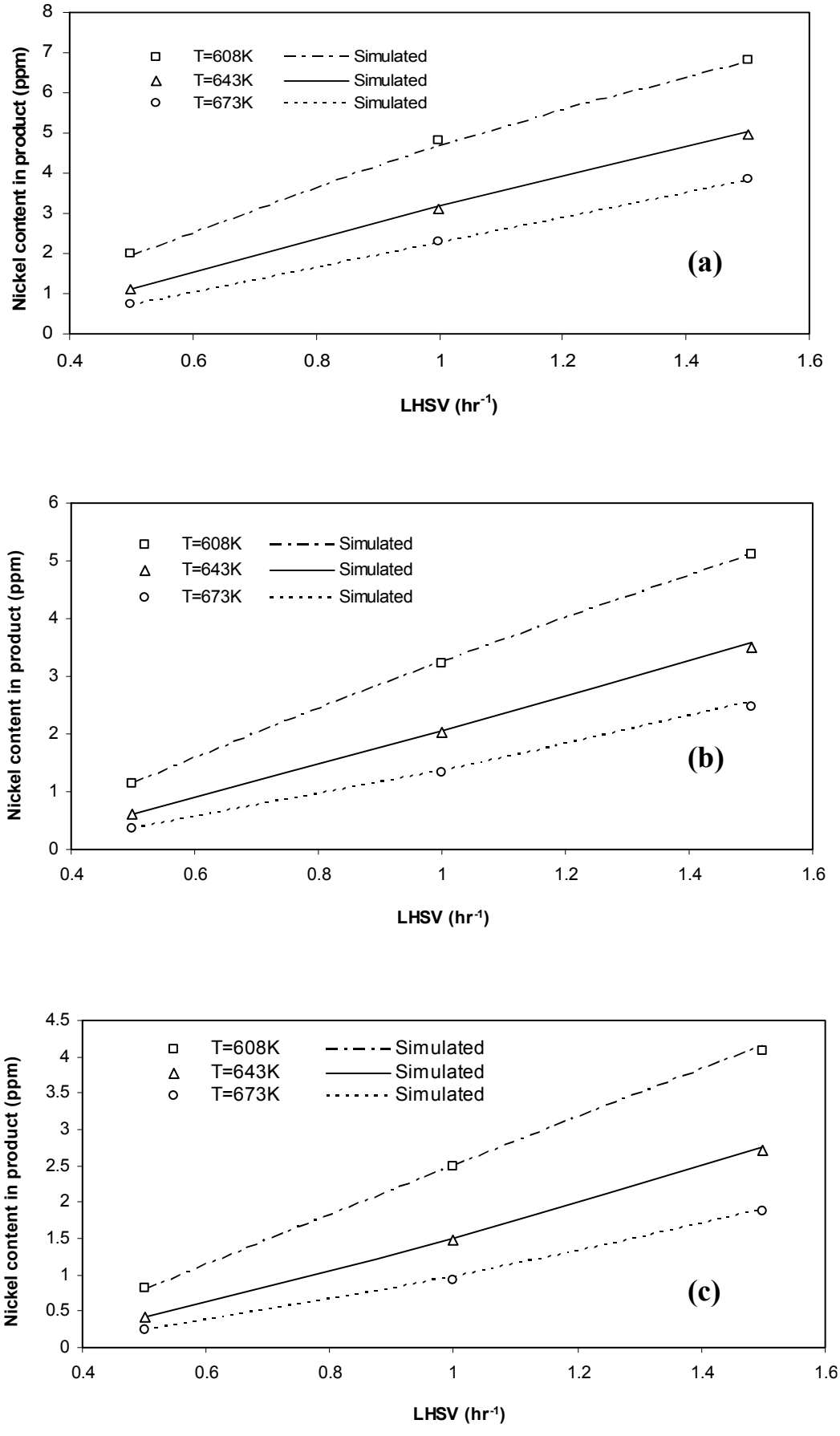

Figure 5.13: Experimental data (points) and simulated (lines) variation of outlet nickel content vs. liquid hourly space velocity at different reactor temperature and at pressure (a) 4 MPa, (b) 7 MPa, (c) 10 MPa.

The operating temperature of the reactor influences the mass velocity of the gases and liquids, the diffusivities of the components, the mass transfer coefficient at the gas–liquid and liquid–solid interfaces, the solubility, and Henry‘s coefficients of hydrogen and hydrogen sulfide in addition to viscosity and density of the compounds.

The temperature also affects the rate constants of HDS, HDN, HDAs, HDV and HDNi processes and the adsorption equilibrium constant of H_2S at the catalyst surface. Increasing the reaction temperature leads to an increase in reaction rate constants defined by the Arrhenius equations. As a result, the reaction rates of these reactions will increase. These results support the fact that the operating temperature is very effective for enhancing the degree of impurities removal.

The liquid hourly space velocity (LHSV) is also a significant operational factor that determines the severity of reaction and the efficiency of hydrotreating. Decreasing liquid hourly space velocity, means increasing the residence time and hence the reaction severity will increase. In other words, as the liquid hourly space velocity is decreased, the quantity of the reaction rates becomes significant (Abbas, 1999; Areff, 2001; Bhaskar et al., 2002; Al-Humaidan, 2004).

In addition, the hydrogen partial pressure has an effect on the reactions used in this study. The mechanisms utilized to describe HDS, HDN, HDAs, HDV and HDNi reactions used a kinetic equation with the order of the hydrogen concentration at the catalyst surface set at a value less than 1. Therefore, conversion of S, N, Asph, V and Ni compounds increases with pressure. The effect of pressures above 100 atm can be neglected due to the fact that the viscosity of the oil feedstock increases with pressure, and the diffusivity and mass transfer coefficient decrease with pressure. Therefore, at high operating pressures, the pressure influence upon S, N, Asph, V and Ni conversions

becomes unimportant (Korsten and Hoffmann, 1996; Bhaskar et al., 2002; Al-Humaidan, 2004).

Figures 5.14 to 5.18 show parity plots of the model for HDS, HDN, HDAs, HDV and HDNi reactions studied in this work (each point represents simulated (Y-axis) and experimental (X-axis) values at the same time with the same operating conditions for each point). The correlation between the experimental results and simulated sulfur, nitrogen, asphaltene vanadium and nickel contents in all products appears to be straight line with a slope close to 1.0, indicating very good agreement between the measured and predicted results. The model can be used to describe the behaviour of the pilot plant trickle bed reactor at different operating conditions for which experimental data are not available.

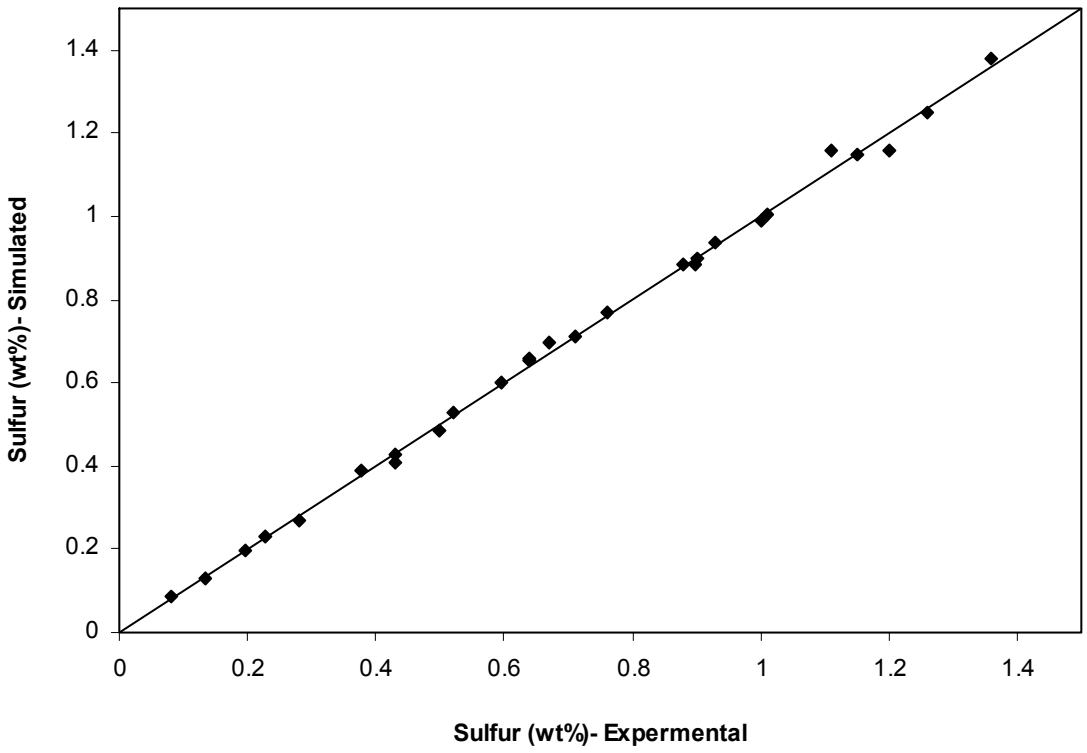

Figure 5.14: Comparison between experimental and calculated concentrations of sulfur

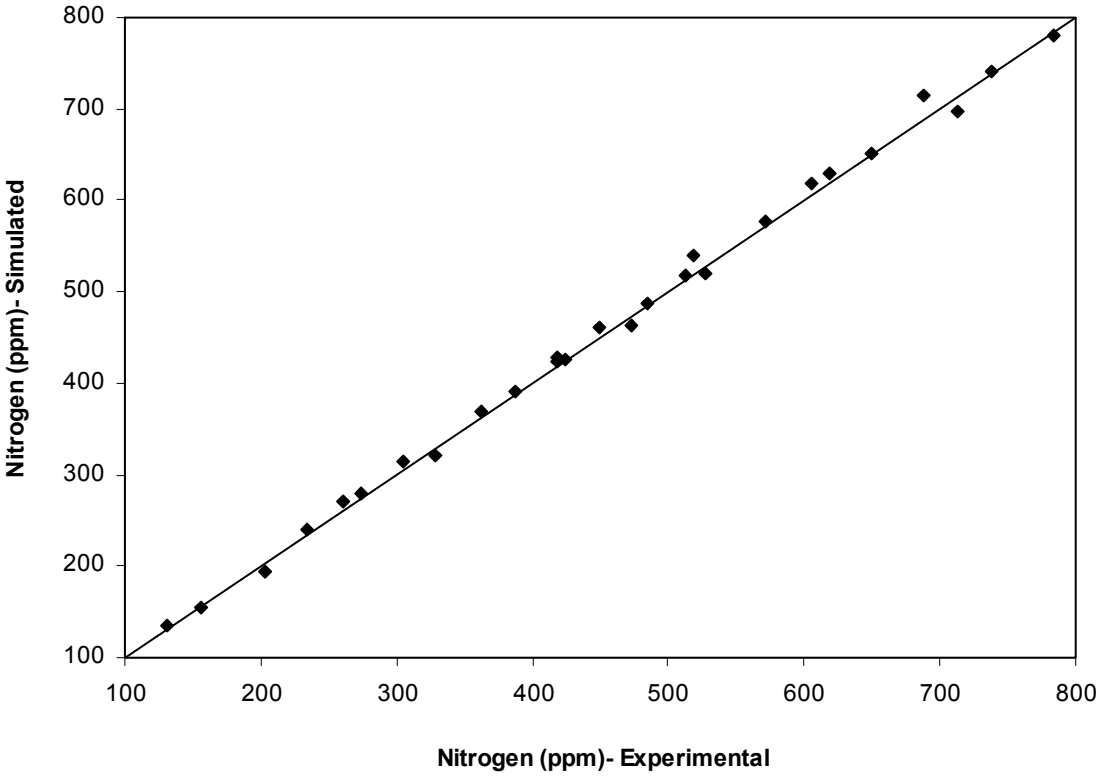

Figure 5.15: Comparison between experimental and calculated concentrations of nitrogen

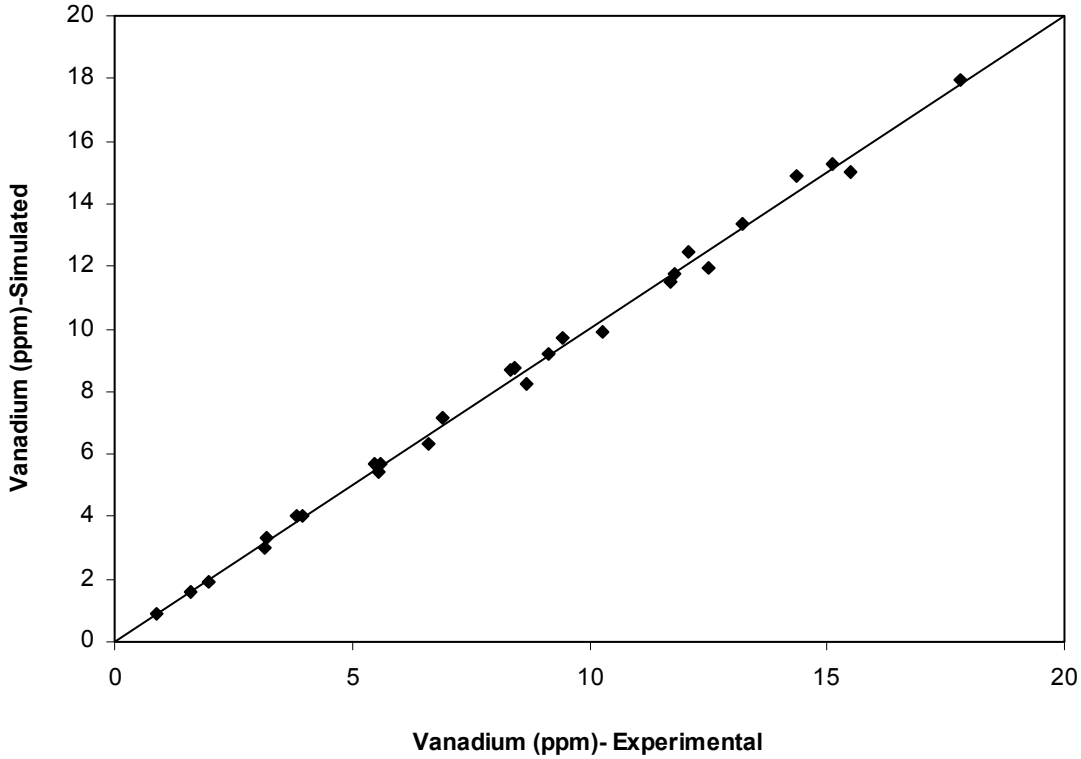

Figure 5.16: Comparison between experimental and calculated concentrations of asphaltene

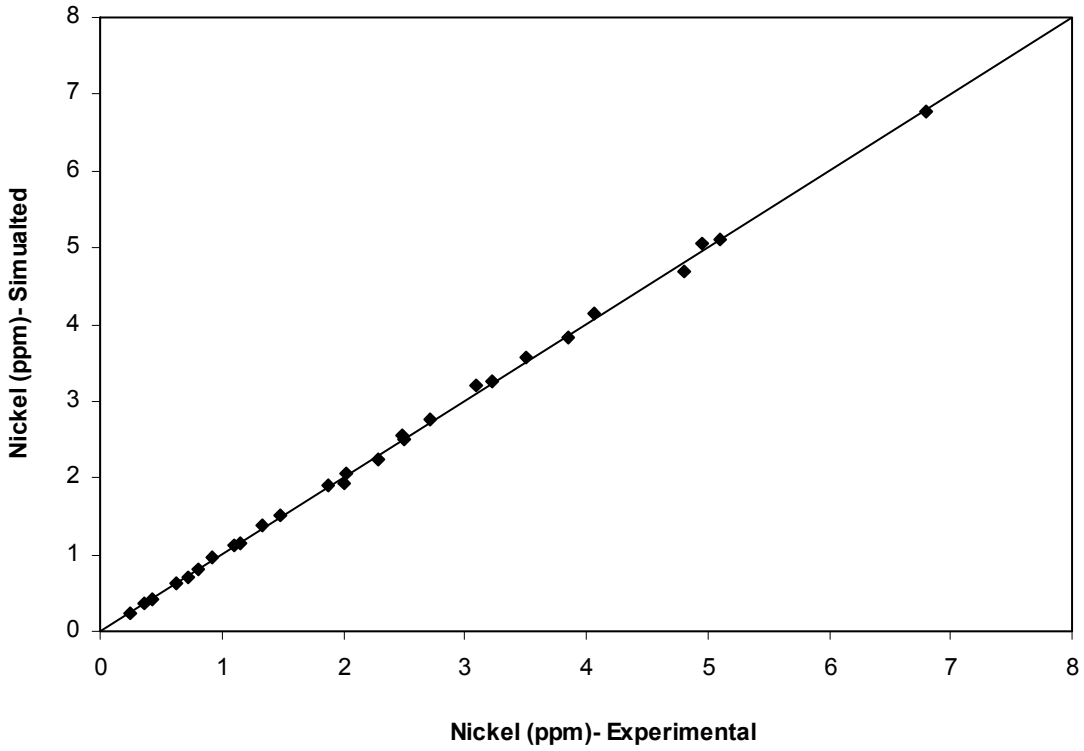

Figure 5.17: Comparison between experimental and calculated concentrations of vanadium

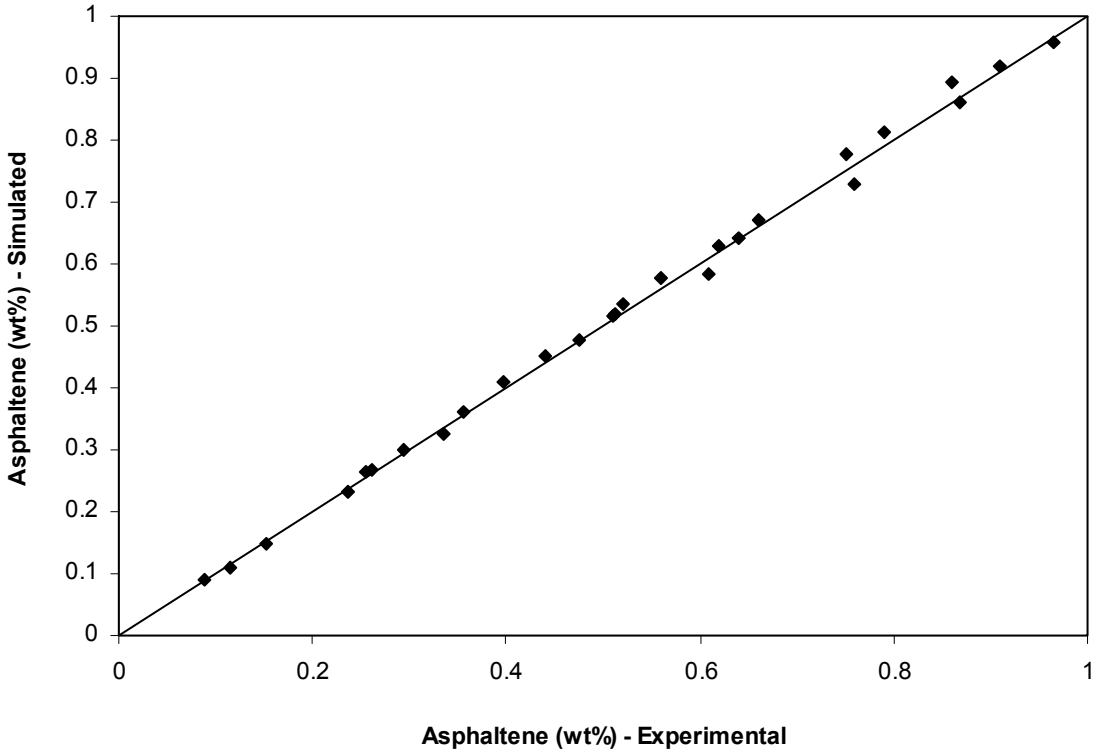

Figure 5.18: Comparison between experimental and calculated concentrations of nickel

5.2.3.2 Simulation of Simultaneous HDT Pilot Plant Reactor System

The model developed can now be used to simulate the performance of the pilot plant trickle bed reactor at different operating conditions for which experimental data are not available. Tables 5.3 to 5.7 show model predictions in terms of sulfur conversion, nitrogen conversion, asphaltene conversion, vanadium conversion and nickel conversion at operating conditions other than experimental conditions. Using the model (with second approach), the concentration profiles of hydrogen and hydrogen sulfide in the gas phase under maximum process condition (T = 400°C, P = 10MPa and LHSV=0.5hr^{-1}) are presented in Figure 5.19. As observed, the hydrogen partial pressure decreases along the catalyst bed length as a result of hydrogen consumption. On the other hand, hydrogen sulfide gas generated from the reaction leads to an increase in the partial pressure of H_2S along the reactor–bed length.

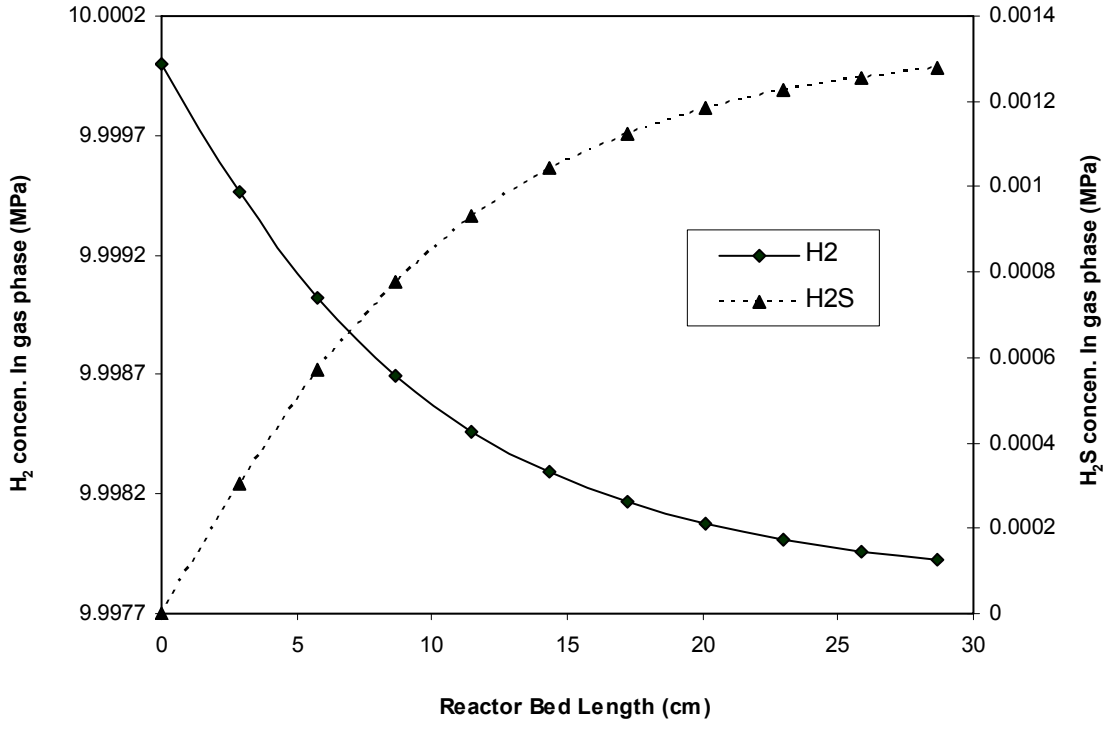

Figure 5.19: Concentration profiles of H_2 and H_2S in gas phase down through the reactor

Figures 5.20 and 5.21 show the molar concentration profiles of hydrogen sulfide and hydrogen in the liquid and solid phases generated at maximum conditions. As is well-known, their forms are calculated from a balance between chemical reaction and gas–liquid mass transfer. The liquid phase and solid phase concentration of H_2S increases initially due to a high reaction rate in this section of the reactor and then decrease substantially along the reactor bed length. This behaviour can be observed owing to the difference in mass transfer rate at gas–liquid and liquid–solid, and reaction kinetics. The concentration of H_2S (given by equation (5.4)) representing the mass transfer at liquid–solid interface becomes predominant, thus the H_2S concentration falls up in both the solid and liquid phases. When the mass transfer from liquid to gas becomes important, the liquid phase concentration as well as solid phase concentration decreases. The concentration of H_2 in the liquid and solid phases along the catalyst length has the opposite behaviour, where the H_2 concentration falls down initially and then falls up along the reactor bed length as shown in Figure 5.21 (Van Hasselt et al., 1999; Bhaskar et al., 2002; Chowdhury et al., 2002).

The concentration profile of S, N, Asph, V and Ni along the catalyst bed length in the liquid phase and on the surface of the catalyst at maximum conditions is shown in Figure 5.22. As can be seen from this figure, the concentration profile of these compounds is reduced in both liquid phase and solid surface along the reactor bed length. Also, there is a concentration gradient between both phases, which is governed by liquid–solid mass transfer rate estimated from the correlations used in the models that depends basically on the physical properties of the liquid, such as density and viscosity, and also liquid mass velocity. Thus, the feedstock becomes lighter and hence the physical properties are improved and mass transfer of liquid–solid will be enhanced, so reducing this concentration gradient (Bhaskar et al., 2002; Alvarez and Ancheyta, 2008a).

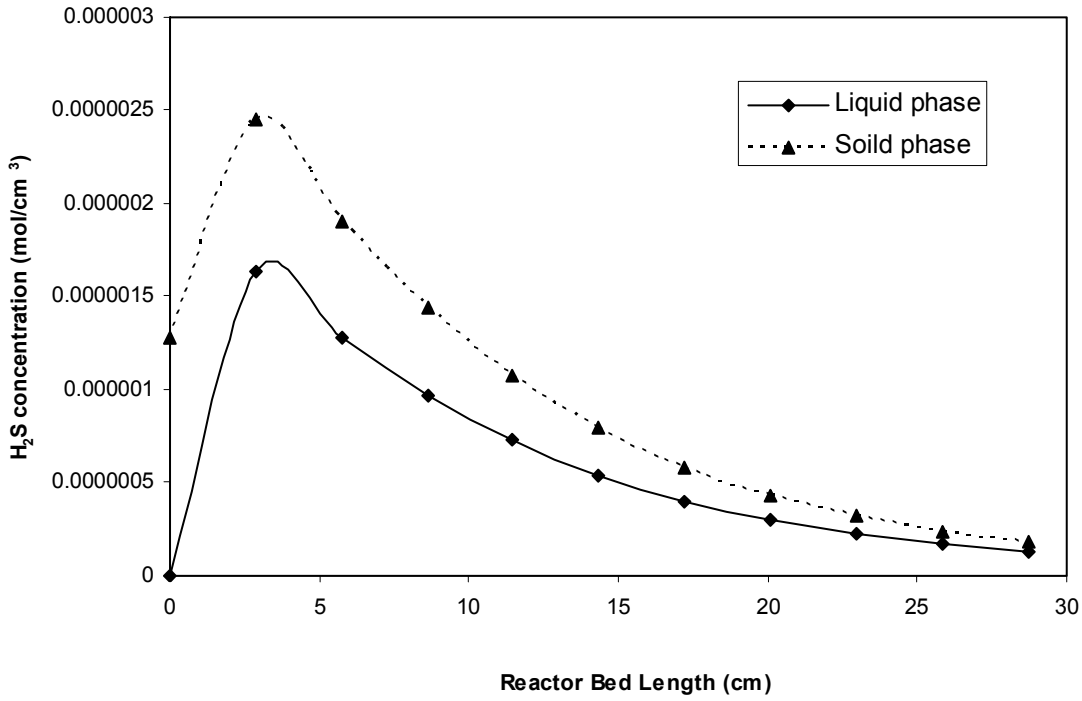

Figure 5.20: Concentration profiles of H_2S in liquid and solid phase down through the reactor

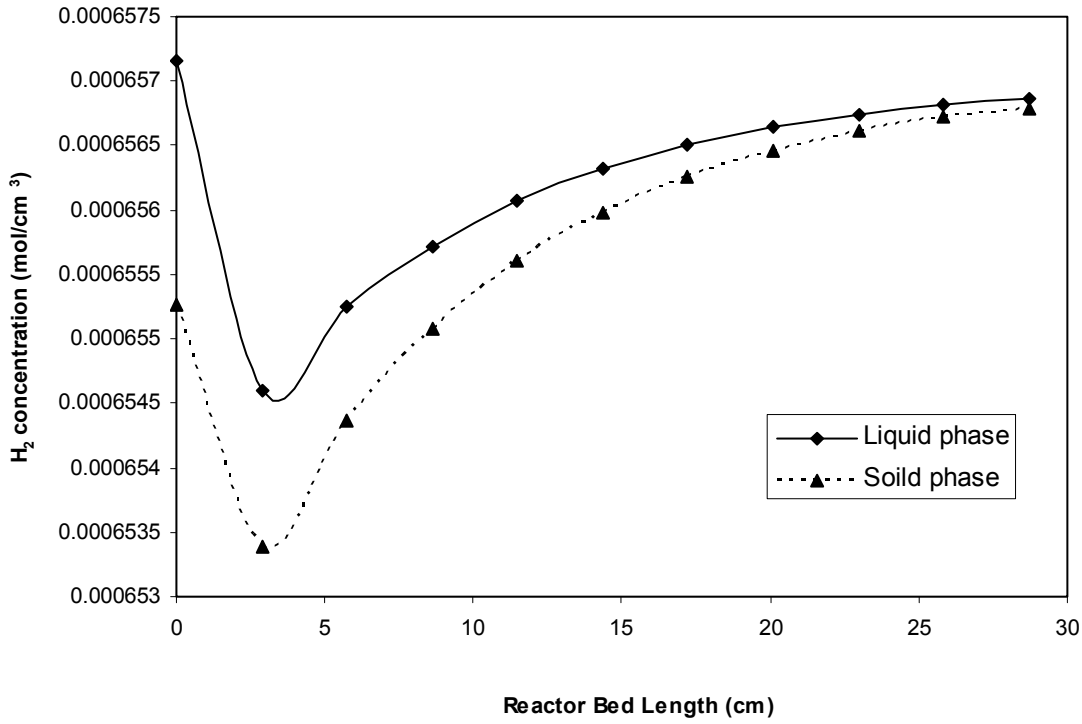

Figure 5.21: Concentration profiles of H_2 in liquid and solid phase down through the reactor

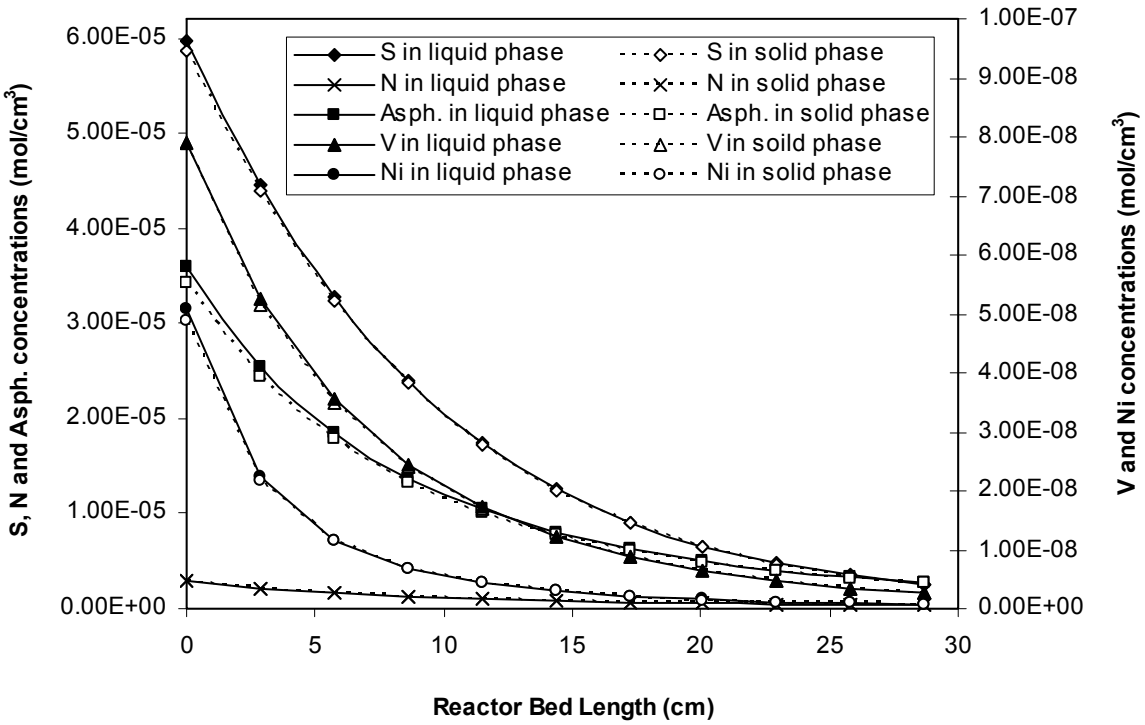

Figure 5.22: Concentration profiles of S, N, Asph, V and Ni in liquid and solid phase down through the reactor

5.3 Mathematical Models for Increasing of Middle Distillates Yield

Process development and optimization is usually achieved by developing reliable models, which can accurately predict the behaviour and product yields of certain operations. As mentioned previously, the worldwide demand for transportation fuels with a quality that satisfies environmental regulations has increased. At the same time, the availability of light crude oil has undergone a decline, which has gradually been offset by heavy crudes (Alvarez and Ancheyta, 2009). Catalytic hydroprocessing has the ability to increase the productivity of distillate cuts (Ancheyta et al., 2002c), which is a hydrogen addition process. This permits us to obtain middle distillates and in general low boiling point products from high boiling point fractions at high operating conditions in addition to reducing the amount of impurities (Ancheyta et al., 2005). For preliminary design and optimization of hydroprocessing reactors, knowledge of the effect of operation parameters, type of feed, type of catalyst, etc. upon the reaction conversion and selectivity, needs to be developed via a suitable reactor model

(Ancheyta, 2007). In parallel with the hydroprocesses development of upgrading heavy oils, different kinetic models have also been reported. Catalytic hydroprocessing kinetics of heavy feedstocks has been namely modeled by discrete lumping although other models have also been utilized (Ancheyta et al., 2005).

The model parameters are highly dependent on feedstock type, thus the experimental data and kinetic parameter estimations must be done. The kinetic model for a hydrotreating process which enhances oil distillates productivity is proposed here based on the experimental data obtained in a pilot plant TBR at different operating conditions using the discrete kinetic lumping approach. The kinetic model of middle distillate yields during crude oil hydrotreating is assumed to include five lumps: gases (G), naphtha (N), heavy kerosene (H.K), light gas oil (L.G.O) and reduced crude residue (R.C.R). Here, the modeling, simulation and optimization are carried out by using gPROMS software.

5.3.1 Model Equations

Catalytic upgrading is achieved by the break up of long carbon chains and the extraction of contaminants from their host molecules. Specifying the chemical reactions included in residual hydrotreating and the actual composition of the products is a complicated task. Thus, the liquid product of oil upgrading is usually divided into several product lumps that are based on the true boiling point temperature. In this study, the feed and products composition are defined as follows: gases, naphtha (IBP-150^{o}C), heavy kerosene (150-230^{o}C), light gas oil (230-350^{o}C) and reduced crude residue (350^{o}C+). The accuracy and the predictive power of discrete lumping models depends mainly on the number of lumps. However, increasing the number of lumps will complicate the model by increasing the number of kinetic parameters (Laxminarasimhan et al., 1996). The proposed kinetic model is shown in Figure 5.23, which consists of 5 lumps (R.C.R,

L.G.O, H.K, naphtha (N) and gases (G)) and 14 kinetic parameters ($k_1, \ldots, k_{10}, n_1, \ldots, n_4$). For each reaction, a kinetic rate expression (r_i) is formulated as a function of the product composition (weight fractions) (y_i), reaction order (n_i) and kinetic constants (k_i).

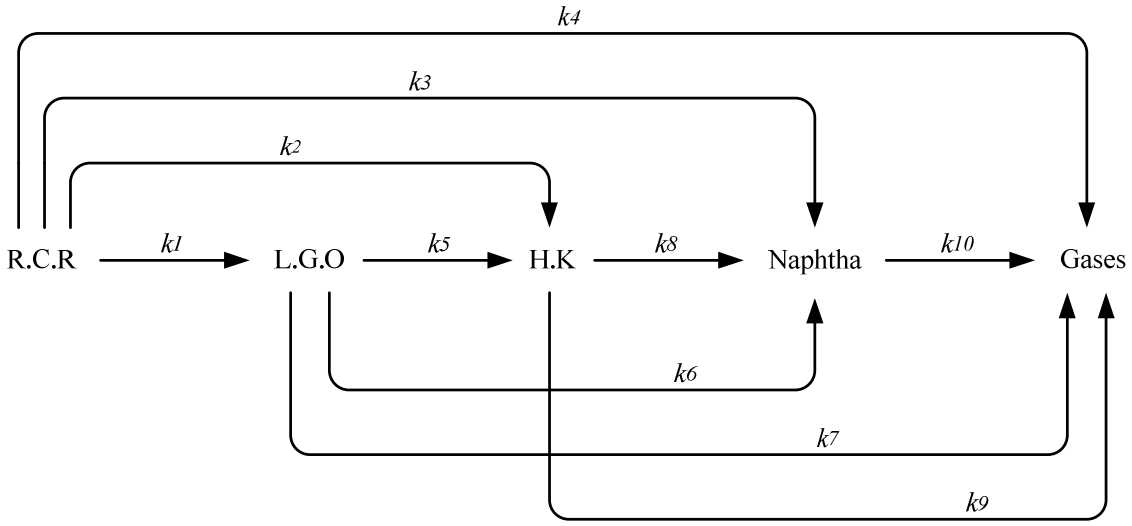

Figure 5.23: Proposed kinetic model for increasing of middle distillates yields

The kinetic model was incorporated into an isothermal reactor model. The following mass balance is used to evaluate the weight fractions from a set of kinetic parameters:

$$\frac{dy_i}{d\tau} = \frac{dy_i}{d(1/LHSV)} = r_i \tag{5.96}$$

τ is the residence time. Product compositions are estimated with pilot plant mass balances. The reaction rates expressions of the proposed mode are:

R.C.R: $$r_R = -(k_1 + k_2 + k_3 + k_4) y_R^{n_1} \tag{5.97}$$

L.G.O: $$r_{LGO} = k_1 y_R^{n_1} - (k_5 + k_6 + k_7) y_{LGO}^{n_2} \tag{5.98}$$

H.K: $$r_{HK} = k_2 y_R^{n_1} + k_5 y_{LGO}^{n_2} - (k_8 + k_9) y_{HK}^{n_3} \tag{5.99}$$

Naphtha: $$r_N = k_3 y_R^{n1} + k_6 y_{LGO}^{n2} + k_8 y_{HK}^{n3} - k_{10} y_N^{n4} \tag{5.100}$$

Gases: $$r_G = k_4 y_R^{n1} + k_7 y_{LGO}^{n2} + k_9 y_{HK}^{n3} + k_{10} y_N^{n4} \tag{5.101}$$

For instance, estimated residue yields are calculated by integration of equation (5.96) with reaction rate expression (described by equation (5.97)), where y_{R0} is the weight percent of R.C.R in the feed:

$$y_R^{cal} = \left[y_{R0}^{1-n_1} + \frac{(k_1 + k_2 + k_3 + k_4)(n_1 - 1)}{LHSV} \right]^{1/(1-n_1)} \tag{5.102}$$

To estimate the best values of kinetic parameters for all experiments, the sum of the squared errors (*SSE)* between the experimental product compositions (y_i^{exp}) and predicted values of compositions (y_i^{cal}) is minimized using optimization technique, as follows:

$$SSE = \sum_{i=1}^{N_{Data}} \left[y_i^{\exp} - y_i^{cal} \right]^2 \tag{5.103}$$

5.3.2 Optimization Problem Formulation

The optimization problem can be stated as follows:

Given	crude oil compositions, reaction temperature, liquid hourly space velocity.
Optimize	reaction orders (n_i) and reaction rate constants (k_i) for each reaction at different temperatures (335°C, 370°C, 400°C, respectively).
So as to minimize	the sum of square errors (SSE).
Subject to	process constraints and linear bounds on all optimization variables.

Mathematically, the optimization problem can be presented as:

Min *SSE*

n_i, k_j *(i= 1-4, j=1-10)*

s.t $f(z, x(z), \acute{x}(z), u(z), \underline{y}) = 0$ (model, equality constraints)

$n_i^{\,L} \le n_i \le n_i^{\,U}$ (inequality constraints)

$k_j^{i\,L} \le k_j^i \le k_j^{i\,U}$ (inequality constraints)

5.3.3 Results and Discussion

Kinetic models are highly desired in conversion processes as they contribute significantly to controlling product distribution. The purpose of this section is to present

kinetic models for describing the increase in oil distillates productivity during crude oil hydrotreating by using a discrete lumping kinetic approach. After calculating the kinetic parameters, the yield of the lumps can be evaluated. In a discrete lumping model, both feed and products are divided into several lumps based on their boiling ranges. Each of these lumps is considered to be a single chemical species with a single rate constant.

As discussed earlier in Chapter Three, the conversion of high boiling point molecules into lighter molecules increased when the LHSV decreased and the reaction temperature is increased due to the severity of the reaction. Large molecules will be decomposed into smaller molecules at high temperature. Also, there was no change in product compositions (they remain almost unchanged at low process conditions) and the main conversion reaction is usually oriented from R.C.R toward the production of L.G.O, H.K, naphtha and gases, especially at maximum process conditions. The estimated kinetic parameters together with activation energies for each reaction can be summarized in Table 5.8.

Table 5.8 Kinetic parameters of the proposed model

Reaction order (n_j)	**Kinetic constant $(wt\%)^{1-n}\ hr^{-1}$**	**Temperature**			**Activation energy Ea (kJ/mole)**
		335 °C	**370 °C**	**400 °C**	
$n_1 = 1.994$			**R.C.R**		
	k_1	0.00822	0.03724	0.12000	140.38
	k_2	0.00034	0.00253	0.01185	185.14
	k_3	0.0	0.01883	0.03754	82.77
	k_4	0.00261	0.00895	0.02327	114.54
$n_2 = 1.300$			**L.G.O**		
	k_5	0.0	0.02161	0.10319	187.55
	k_6	0.0	0.00162	0.00595	155.55
	k_7	0.0	0.00010	0.00044	171.65
$n_3 = 1.114$			**H.K**		
	k_8	0.0	0.01344	0.03268	106.52
	k_9	0.0	0.0	0.0	
$n_4 = 1.000$			**Naphtha**		
	k_{10}	0.0	0.0	0.0	

The kinetic parameters listed in Table 5.8 illustrate that naphtha cracking is insignificant in the range of operating conditions studied in this work because the values of k_{10} are equal to zero. Gas production is formed exclusively from the conversion of R.C.R and L.G.O according to the values of k_9 and k_{10}, which equal to zero. The kinetic parameters observation of R.C.R conversion indicates high selectivity toward L.G.O, followed by naphtha, gases, and H.K. Conversion selectivity changes at various temperatures. For example, at 335°C there is no formation of naphtha from L.G.O and H.K because the values of k_6 and k_8 are zero. On the other hand, at 370°C and 400°C the values of these parameters are different from zero. Another observation is that the rate constants rise in value as temperature increases. This increase in the rate constant with temperature indicates the increase in reactivity with increasing reaction severity.

The next step is to derive the temperature dependent kinetic model for the n^{th} order for a 5 lump system. The Arrhenius equation is employed for this purpose. For each lump, the Arrhenius-based dependence of the kinetic model with respect to temperature is demonstrated in Figure 5.24.

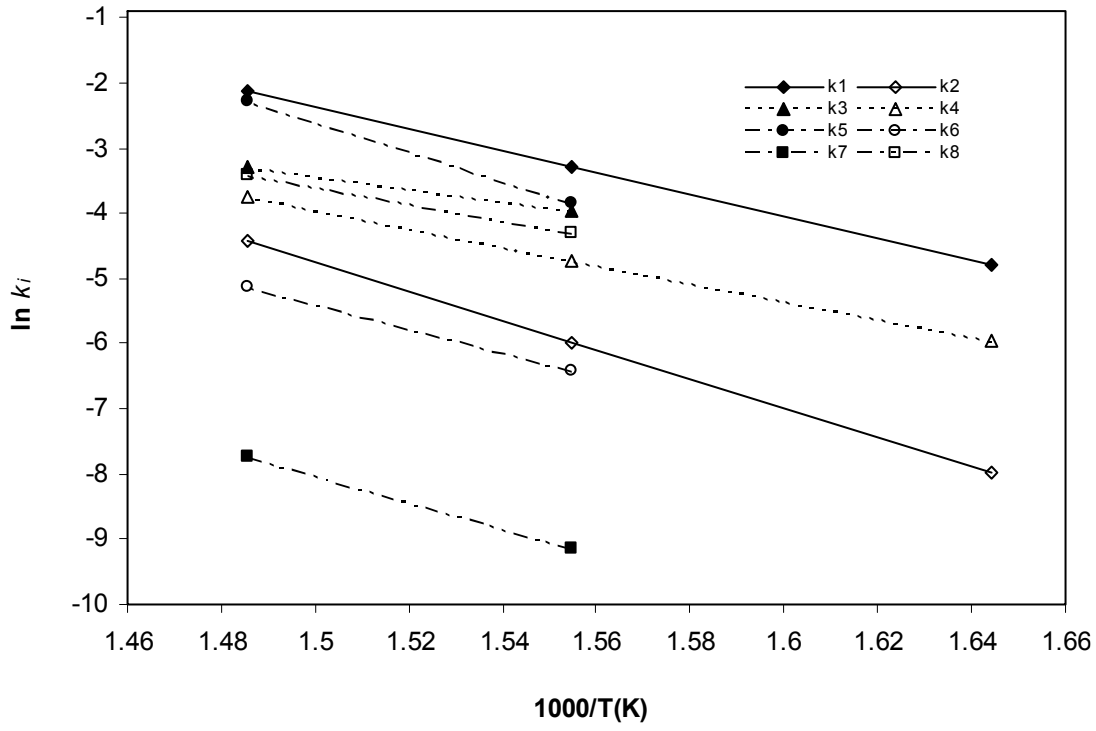

Figure 5.24: Arrhenius plot for the different kinetic parameters

Because some values of the kinetic parameters were found to be zero, not all of the activation energies could be estimated. The values of the activation energies are presented in Table 5.8 above.

Table 5.9 and Figure 5.25 compare the experimental and predicted product compositions at different operating conditions. It is noted that product compositions are quite well predicted and showed excellent fit to the experimental data with an average absolute error of less than 5%, which means that the proposed kinetic model is adequate to represent increasing oil distillates productivity.

Table 5.9 Experimental and predicted product compositions for 5 lumps discrete model

LHSV, hr^{-1}		**0**	**0.5**			**1.0**			**1.5**		
T	**Lumps**	**Feed wt%**	**Exp. wt%**	**Pred. wt%**	**Error %**	**Exp. wt%**	**Pred. wt%**	**Error %**	**Exp. wt%**	**Pred. wt%**	**Error %**
335 °C	**R.C.R**	49.93	49.4	49.38	0.04	49.85	49.65	0.40	49.88	49.74	0.28
	L.G.O	19.0	19.2	19.41	1.09	19.02	19.20	0.94	19.01	19.14	0.68
	H.K	12.8	12.9	12.82	0.62	12.82	12.81	0.07	12.81	12.80	0.07
	Naphtha	14.8	14.9	14.80	0.67	14.83	14.80	0.20	14.82	14.80	0.13
	Gases	3.47	3.6	3.59	0.27	3.48	3.53	1.43	3.48	3.51	0.86
370 °C	**R.C.R**	49.93	45.5	46.76	2.76	47.30	48.29	2.09	48.60	48.83	0.47
	L.G.O	19.0	20.0	20.18	0.90	19.50	19.62	0.61	19.20	19.42	1.14
	H.K	12.8	13.8	13.16	4.63	13.50	12.98	3.85	13.30	12.92	2.85
	Naphtha	14.8	16.7	15.99	4.25	15.90	15.41	3.08	15.20	15.21	0.06
	Gases	3.47	4.0	3.89	2.75	3.80	3.69	2.89	3.70	3.62	2.16
400 °C	**R.C.R**	49.93	42.3	41.85	1.06	45.00	45.54	1.20	47.10	46.92	0.38
	L.G.O	19.0	21.1	21.27	0.80	20.50	20.40	0.48	19.90	20.00	0.50
	H.K	12.8	14.8	15.17	2.50	14.00	13.97	0.21	13.60	13.58	0.14
	Naphtha	14.8	17.5	17.25	1.42	16.50	16.08	2.54	15.60	15.66	0.38
	Gases	3.47	4.3	4.46	3.72	4.00	4.01	0.25	3.80	3.84	1.05

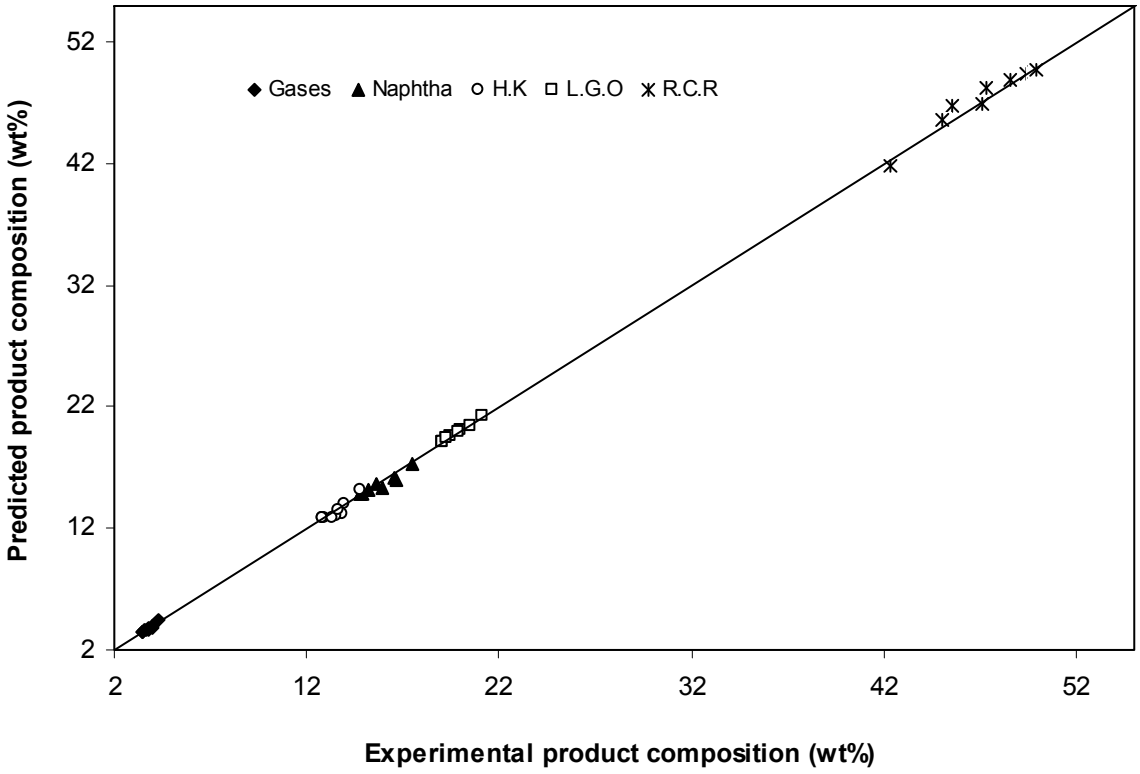

Figure 5.25: Comparison between the experiment and predicted product compositions

5.4 Conclusions

The hydrotreating of crude oil has not been widely reported in the literature, and an accurate process model for HDT of crude oil has not been found in the public domain. Estimation of the kinetic parameters in a trickle bed reactor applied to HDS, HDN, HDAs, HDV and HDNi of crude oil is very important to accurately model the process, so that the model can be effectively used for simulation, optimization and control.

An optimization technique, based upon the minimization of the sum of square errors (*SSE*) between the experimental and model predicted concentrations of sulfur, nitrogen, asphaltene, vanadium and nickel compounds, was developed to estimate the kinetic parameters based on experimental data. Steady state process models of a trickle bed reactor have been developed as a system of differential–algebraic equations (DAEs) to aid the parameters estimation process. Two approaches, linear (LN) and non-linear

(NLN) regression have been used to estimate the best kinetic parameters of trickle bed reactor process for HDS, HDN, HDAs, HDV and HDNi of crude oil. In the first approach, the reaction rate orders of sulfur, nitrogen, asphaltene, vanadium and nickel (n_j), hydrogen (m_j) and reaction rate constants (K_j) were determined simultaneously for each reaction separately. Then, a linearization process is applied to estimate the activation energies (EA_j) and pre-exponential factors (A^0_j) using Arrhenius equation. In the second approach, the activation energies (EA_j), pre-exponential factors (A^0_j), impurities orders (n_j) and hydrogen orders (m_j) were calculated simultaneously for each reaction separately. Based on the objective function (*SSE)*, the parameters estimated with the second approach are found to be more accurate and the simulation results showed very good correspondence with the experimental data with an average absolute error of less than 5%.

Using the models, the effects of reactor temperature (T), partial pressure of hydrogen (P) and liquid hourly space velocity (LHSV) on the S, N, Asph, V and Ni conversion and on the concentration profiles along the reactor bed length were studied. The effects of these operating conditions in crude oil hydrotreating process confirm that high temperature and pressure, and low liquid hourly space velocity improve the impurities conversion. The models can now be confidently applied to reactor design, operation and control, as well as predicting the concentration profiles of any compound at any conditions.

A homogeneous flow model does not describe the inhibiting influence of H_2S upon sulfur conversion, and therefore this impact has been incorporated in the heterogeneous model using a Langmuir–Hinshelwood formulation for the chemical reaction rate in terms of catalyst surface concentrations. The concentration profiles of hydrogen sulfide along the catalyst bed length in the solid and liquid phases increased initially and then decreased owing to the dissimilarity in the mass transfer between gas–liquid and liquid–

solid inter phases, while the concentration of H_2S in the gas phase increased along the catalyst bed length. Opposite phenomena have been observed for hydrogen concentrations. The concentrations of S, N, Asph, V and Ni in the liquid and solid phases decreased along the catalyst bed length.

A 5 lump kinetic model for a trickle bed reactor enhancing oil distillates productivity during crude oil hydrotreatment has been developed. From the results presented, the following observations can be made: **a)** Gases cannot be produced from naphtha and heavy kerosene. **b)** In the range of operating conditions in this study, cracking of naphtha was not observed. **c)** There is no increase in product yield at low operating conditions because some values of the kinetic parameters were found to be zero. **d)** The kinetic parameters of R.C.R conversion indicate high selectivity toward light gas oil (L.G.O), naphtha, gases and heavy kerosene (H.K) **e)** It should be highlighted that an increase of oil distillated can be achieved at moderate operating conditions in order to avoid sludge and sediment formation. **f)** The proposed kinetic model is capable of predicting the weight fraction of R.C.R, L.G.O, H.K, naphtha and gases with average absolute error less than 5%.

Chapter Six

Design of Industrial Trickle Bed Reactor: Optimal Operation of Commercial Hydrotreating Unit

6.1 Introduction

In recent years, chemical reactors have been elevated to the position of being arguably the most significant units for optimization within a chemical processing plant. Until the early 1970s, downstream separation operations were considered to be the key to the profitability of a chemical unit. Little effort was made to obtain both high conversion and selectivity to the desired product within the reactor, and the purity of the desired product was accomplished largely via well designed downstream separation processes. Recently, increased costs and less certain availability of feedstocks, combined with environmental protection regulation, has led the trend towards clean technology with more efficient processing and waste minimization, which can be better achieved by improvements in reactor technology (Winterbottom and King, 1999; Missen et al., 1999).

The new goals are focused around clean technology synthesis, and are mainly (a) to give the desired product as far as possible, (b) to reduce side reactions and pollution to very small proportions, (c) to intensify processing for the purpose of giving improved economics, and (d) to ensure that the operation products are utilized in an environmentally friendly way with emphasis on recycling and re-use. One of the most important factors that led to this was the development in reactor design along with the availability of precise kinetic data and powerful modelling and computational techniques (Winterbottom and King, 1999).

In this chapter, the scale-up of a trickle bed reactor used for crude oil hydrotreating with the optimal operation of industrial hydrotreating unit is investigated in order to evaluate the viability of a large-scale of crude oil hydrotreating process.

For the commercial hydrotreating unit, the heat balance equations along the catalyst bed length are necessary due to the nature of these reactors, which are usually exothermic after calculating the optimal distribution of the catalyst bed. Thus, the dimensions of an industrial trickle bed reactor are taken into considerations (in terms of optimal length to diameter of the reactor).

Due to the exothermic behaviour of an industrial trickle bed reactor, the control of the reaction temperature (regarded as an important factor in hydrotreating units having a large impact on the conversion of process reactions) is the main issue in such operations. Therefore, hydrogen quenching is used to control the temperature, which is achieved by introducing a part of the cold hydrogen stream into the catalyst beds. Many simulations in terms of quench positions and quench rate fractions are investigated here based upon the total annual cost.

The heat integration process with energy consumption is also reported, which was ignored in the pilot plant system for maximizing profitability of process and thus reducing environmental impact in addition to maximum heat recovery.

An economic analysis of the continuous whole process of industrial refining units with the other refinery units up to middle distillate fraction production units is also discussed here in order to compare the economic results of the fractions obtained by this study and those produced by the conventional methods.

6.2 Design of Industrial TBR

Mathematical models are usually used to simulate the performance of the pilot-plant reactor, scaled-up to the industrial scale, and to predict the behaviour of the industrial-scale reactor from the pilot-plant experiments. Therefore, the design of commercial trickle-bed reactors is based on the experimental results obtained from pilot plant experiments in Chapter Three and all the kinetic models of a trickle bed reactor for crude oil hydrotreating presented in Chapter Five to large-scale units (i.e., scale-up). In other circumstances, when the industrial operation is well established, pilot plant investigations are aimed at providing information concerning the behaviour of the scale-up operation (Al-Dahhan and Dudukovic, 1996; Bhaskar et al., 2004). Current economic considerations require that the smallest possible laboratory units be utilized for scale up (Sie, 1991).

A pilot plant reactor is operated isothermally, but this ideal behaviour is very different from industrial units, which are operated in a non-isothermal way, which means an equation transposing the heat balance should be included. But, to describe the performance of an industrial trickle bed reactor for crude oil hydrotreating based on all the mathematical models obtained in Chapter Five, the dimensions of the commercial trickle bed reactor should be known in addition to the energy balance.

The industrial trickle bed reactor in this work has a processing capacity of 10000 bbl/day. The reactor is assumed to operate for 340 days/yr. The hydrotreated crude oil at the best operating conditions selected from experimental results (that showed maximum conversion of sulfur, nitrogen, vanadium, nickel and asphaltene, which are: reaction temperature 400ºC, LHSV 0.5hr^{-1} and hydrogen pressure 10MPa) are used as typical operating conditions for a commercial trickle bed reactor.

The reactor volume can be calculated from the liquid hourly space velocity (LHSV), as follows (Ancheyta and Speight, 2007):

$$LHSV\,(hr^{-1}) = \frac{Total\ volumetric\ feed\ flow\ rate\ to\ the\ reactor\ (\frac{m^3}{hr})}{Total\ catalyst\ volume\ (m^3)} \tag{6.1}$$

$LHSV = 0.5\ hr^{-1}$,

Total volumetric flow rate = 10000 bbl/day (66.243 m^3/hr)

Therefore, total catalyst volume (Vc) = 132. 486 m^3

$$V_C = Area \cdot L_R \tag{6.2}$$

$$Area = \frac{\pi}{4}(D_R)^2 \tag{6.3}$$

Knowledge of the catalyst bed dimensions is an important issue for an industrial reactor, since laboratory scale reactors need to match the space velocity of commercial processes. Generally, the aspect ratio L_R/D_R (L_R is the length of the bed and D_R is the diameter of the reactor) of a commercial reactor is quite different from that of pilot plant reactors as shown in Table 6.1. The gas–liquid velocities in pilot plant reactors are much lower than those in industrial reactors and lower liquid velocity significantly influences the overall performance, heat and mass rates owing to reduced contact efficiencies and increased dispersion (Gunjal and Ranade, 2007; Al-Dahhan and Dudukovic, 1996).

Table 6.1: Differences in length and diameter between pilot plant and industrial TBR (Bhaskar et al., 2004)

	Pilot plant reactor	**Industrial reactor**
Length	0.5 – 2.0 m	10 – 25 m
Diameter	0.5 – 4.0 cm	1 – 4 m

An economic study should be made of the cost of the reactor at different length to diameter ratios. At large diameters and high pressures, the reactor wall must be thicker and hence more expensive. On the contrary, reducing the diameter of the reactor is possible and it will improve the isothermal behaviour, but at the same time, side effects can be noticed with hydrodynamics, such as radial concentration gradient effects. Consequently, an intermediate value for the diameter should be considered (Lamine et al., 1992; Mary et al., 2009).

The radial concentration gradient appears to be responsible for adverse mass velocity effects or low conversion. It represents the degree of flow mixing occurring during the residence time in the reactor. This deviation behaviour affects the performance of such adiabatic reactors. Since radial dispersion impacts tend to reduce conversion, it is necessary to design such reactors with conditions where this effect is minimal (Bischoff and Levenspiel, 1962; Shah and Parakos, 1975; Akosman and Walters, 2004; Mary et al., 2009).

Although the most common ratio of L_R/D_R ranges lies approximately between 2 to 3 (Ancheyta et al., 2002b; Bhaskar et al., 2004; Rodriguez and Ancheyta, 2004; Mederos et al., 2006; Mederos and Ancheyta, 2007), for different oil feedstocks (not full crude oil), it is necessary to find the optimal ratio of L_R/D_R while ensuring the radial concentration gradient is as low as possible in addition to the economic considerations.

6.2.1 Optimal Ratio of L_R/D_R

Bischoff and Levenspiel (1962) as published in Mederos et al. (2009) have presented an important criterion to neglect radial dispersion effect in packed beds based on the ratio of the bed length (L_R) to reactor diameter (D_R) as follows:

$$\frac{L_R}{D_R} > 0.04 \frac{u_l \, D_R}{\varepsilon_l \, D_r^L} \tag{6.4}$$

ε_l is the liquid phase fraction and D_r^L is the radial mass dispersion coefficient.

The liquid phase fraction can be calculated from the following equation (Tarhan, 1983; Cotta et al., 2000):

$$\varepsilon_l = 9.9 \left(\frac{G_L \, d_S}{\mu_L} \right)^{1/3} \left(\frac{d_S^3 \, g \, \rho_L^2}{\mu_L^2} \right)^{-1/3} \tag{6.5}$$

The radial mass dispersion coefficient in equation (6.4) is needed, which can be estimated from the Peclet number (P_e) (Gunn, 1987; Mederos and Ancheyta, 2007):

$$D_r^L = \frac{d_S \, u_l}{P_e \, \varepsilon_l} \tag{6.6}$$

The Peclet number can be determined from correlation presented in the literature depending upon the mode of operation and the type of reactor (pilot plant or commercial reactor). For cocurrent operation with a commercial unit, the Peclet number is calculated from the Sater-Levenspiel correlation as reported in Mederos and Ancheyta (2007) as follows:

$$P_e = 7.58 \times 10^{-3} \, \mathrm{Re}_L^{0.703} \tag{6.7}$$

Re_L is the Reynolds number.

$$\mathrm{Re}_L = \frac{d_S \, G_L}{\mu_L} \tag{6.8}$$

As mentioned earlier, by increasing the diameter and decreasing the length of the reactor, the capital cost of the reactor will increase. Thus, the capital cost of the reactor

as a function of diameter and length is needed. The capital cost of the reactor (C_R, \$) is calculated using the following equation (assuming that the reactor is filled with the catalyst) (Douglas, 1988):

$$C_R(\$) = \left(\frac{M\ \&\ S}{280}\right) 101.9 D_R^{1.066} L_R^{0.802} (2.18 + F_C) \tag{6.9}$$

$$F_C = F_m F_p \tag{6.10}$$

C_R is the capital cost of the reactor (\$), *M&S* is the Marshall and Swift index for cost escalation (*M&S* = 1468.6 (Chemical Engineering, 2010)), F_C, F_m, and F_p are dimensionless factors that are function of the construction material and operating pressure, F_m = 3.67 and F_p = 3.93 (Douglas, 1988).

6.2.1.1 Optimization Problem Formulation

With due attention to equation (6.4),

$$A = \frac{L_R}{D_R} \tag{6.11}$$

$$B = 0.04 \frac{u_l D_R}{\varepsilon_l D_r^L} \tag{6.12}$$

$$C = A - B \tag{6.13}$$

C must be > 0. To know the critical point where $A = B$, the lower limit of C is assumed to be zero.

The optimization problem can be stated as:

Given	feedstock, the catalyst, reaction temperature, hydrogen pressure and liquid hourly space velocity.
Determine	length of the reactor (L_R) and the diameter of the reactor (D_R).
So as to minimize	reactor capital cost (C_R).

Subject to process constraints and linear bounds on all decision variables (mentioned above).

Mathematically the optimization problem can be written as:

$$\begin{aligned} &\textit{Min} && C_R && \\ &L_R,\ D_R && && \\ &s.t && f(x(z),\ u(z),\ \underline{y}) = 0 && \text{(model equation, equality constraint)} \\ & && C \geq 0 && \text{(inequality constraints)} \\ & && L_R^L \leq L_R \leq L_R^U && \text{(inequality constraints)} \\ & && D_R^L \leq D_R \leq D_R^U && \text{(inequality constraints)} \end{aligned}$$

6.2.1.2 Results and Discussions

Table 6.2 shows the simulation results between L_R/D_R ratio in terms of A and radial dispersion in terms of B with the capital cost of the reactor. As can be seen from this Table, the simulation results indicate that an increase in L_R/D_R ratio (in term A) leads to an increase in the cost of the reactor. The difference between A and B (in term C) showed negative results up to 2.5 and less in L_R/D_R ratio, which means that the radial concentration gradient has an impact on the process. This influence disappears or decreases with increasing in L_R/D_R ratio as shown in this Table with A > 2.5 and C > 0, which means that there is no radial dispersion effect. Therefore, to find the critical point where C = 0 and to reduce the capital cost of the reactor, the optimization process is required.

Table 6.2: Simulation results between *A* and B with the cost

A	B	C	COST ($)
1.5	2.3605328	-0.86053276	2140188.5
2.0	2.4542477	-0.45424777	2253500.8
2.5	2.5294936	-0.02949347	2345508.0
3.0	2.5926830	0.40731698	2423465.0
3.5	2.6473390	0.85266100	2491394.8

The optimization results of the decision variables for L_R/D_R ratio in terms of A and radial dispersion in terms of B with the capital cost of the reactor are listed in Table 6.3. From this Table, it is observed that the critical point where A = B can be achieved, occurs at L_R/D_R of 2.53. On the other hand, below this ratio the effect of radial dispersion will appear and above this ratio there will be no impact of radial dispersion upon the process.

Table 6.3: Summary of optimization results between *A* and B with the cost

Decision variable type	**Optimized value**
A	2.53
B	2.53
C	0.0
L_R/D_R	2.53
L_R *(cm)*	1027.19
D_R *(cm)*	405.34
C_R *($)*	2351220

Therefore, to ensure safe operation and in order to avoid any side effect of radial dispersion, 5 % is added on L_R/D_R ratio. The simulation results with the final dimensions of the reactor are shown in Table 6.4 as follows:

Table 6.4: Simulation results with addition 5 % on L_R/D_R ratio

Decision variable type	**Simulation results**
L_R/D_R	2.661
L_R (cm)	**1061.16**
D_R (cm)	**398.80**
C_R *($)*	2371882.8

6.2.2 Mathematical Model of Industrial TBR with Energy Balance

A reliable mathematical model of industrial hydrotreating reactors is essential as fuel quality control is becoming stricter. A common route for simulating the behaviour of a commercial hydrotreating reactor is to conduct kinetic experiments in a pilot-plant scale reactor using the same catalyst, same operating conditions, and same feedstock. The experimental information is then treated with an appropriate model in order to calculate the kinetic parameter, which is necessary for the simulation of industrial reactors. An unavoidable difference in process between the commercial reactors and the small-scale reactors is the catalyst bed temperature profile (Stefanidis et al., 2005).

Industrial hydrotreating reactors operate under non-isothermal adiabatic conditions, and since reactions are usually exothermic, average reactor temperature would always increase along the catalyst bed. In other words, experiments for catalyst screening and process studies are usually carried out in pilot-plant scales. This system commonly operates under the same conditions reported in industrial units but keeping the process in isothermal mode (reaction temperature more or less constant), and thus the heat balance can be omitted for small-scale reactor modelling. However, due to non-isothermal operation modes of commercial hydrotreating reactors, experimental data obtained from small reactors does not represent the industrial process exactly. Therefore, for predicting the real performance of industrial trickle bed reactors using experimental information from small reactors, it is essential to add the heat balance equation in a commercial hydrotreating reactor model (Mederos et al., 2009).

A famous differential heat balance equation used for the industrial trickle bed reactor that takes into account the non-isothermal behaviour along the catalyst bed length can be written as follows (Tarhan, 1983; Rodriguez and Ancheyta, 2004; Mederos and Ancheyta, 2007; Alvarez and Ancheyta, 2008a; Alvarez et al., 2009):

$$\frac{dT}{dz} = \sum\left[\left(-\Delta H_R\right)\left(r_j\right)\rho_B\eta_j\right]\frac{\varepsilon_l}{u_g\rho_G c_p^G\varepsilon_g + u_L\rho_L c_p^L\varepsilon_l} \tag{6.14}$$

ΔH_R is the overall heat of reactions, ε_g is the gas phase fraction, ρ_G is the gas density (includes all reacting gases), c_p^G is the specific heat capacity of gas (includes all gases), c_p^L is the specific heat capacity of liquid, *j* is HDS, HDN, HDAs, HDV, HDNi.

The gas phase fraction (ε_g) can be estimated based on bed void fraction and liquid phase fraction as follows (Tarhan, 1983; Mederos et al., 2009):

$$\varepsilon_g = \varepsilon - \varepsilon_l \tag{6.15}$$

The heat capacity of the liquid oil mixture is determined from the following equation (Perry and Green, 1999; Stefanidis et al., 2005; Alvarez and Ancheyta, 2008b):

$$c_p^L = 4.1868\left(\frac{0.415}{\sqrt{\rho_L^{15.6}}} + 0.0009\left(T - 288.15\right)\right) \tag{6.16}$$

The main gas products that have been taken into account during the hydrotreating process are CH_4, H_2S and NH_3. Therefore, the specific heat capacity of the gas mixture (involves mainly reactants (H_2) and products) can be evaluated using the following expression (Alvarez and Ancheyta, 2008b):

$$c_p^G = c_p^{H_2}x_1 + c_p^{H_2S}x_2 + c_p^{CH_4}x_3 + c_p^{NH_3}x_4 \tag{6.17}$$

The heat capacities of CH_4, H_2S, NH_3 and H_2 in addition to the mass fraction (x_1, x_2, x_3, x_4) for these component can be written as follows (Smith et al., 1996):

$$c_p^{H_2} = 4.124\left(3.249 + 0.000422T + 8300T^{-2}\right) \tag{6.18}$$

$$c_p^{H_2S} = 0.244\left(3.931 + 0.00149T - 23200T^{-2}\right) \tag{6.19}$$

$$c_p^{CH_4} = 0.5182\left(1.702 + 0.009081T - 0.000002164T^2\right) \tag{6.20}$$

$$c_p^{NH_3} = 0.4882\left(3.578 + 0.00302T - 18600T^{-2}\right) \tag{6.21}$$

$$x_1 = \frac{c_p^{H_2}}{cp_T} \tag{6.22}$$

$$x_2 = \frac{c_p^{H_2S}}{cp_T} \tag{6.23}$$

$$x_3 = \frac{c_p^{CH_4}}{cp_T} \tag{6.24}$$

$$x_4 = \frac{c_p^{NH_3}}{cp_T} \tag{6.25}$$

$$cp_T = c_p^{H_2} + c_p^{H_2S} + c_p^{CH_4} + c_p^{NH_3} \tag{6.26}$$

The density of reacting gases (which is hydrogen) as a function of reaction pressure and temperature is calculated using the following equation (Wauquier, 1995):

$$\rho_G = 12.03 \frac{P\, Mw_{H_2}}{Z_c\, T} \tag{6.27}$$

Mw_{H_2} is the molecular weight of H_2 and Zc is the compressibility factor of H_2.

The compressibility factor of hydrogen as a function of process condition can be estimated from the following correlation (Chen et al., 2010):

$$Z_c = 1 + \left(\frac{1.9155P}{T} \right) \tag{6.28}$$

The major problem in industrial trickle bed reactors is the temperature rise inside the reactor due to the exothermal hydrotreating reactions, which can lead to many problems. A common method to solve this type of problem is called a quench system (Ancheyta and Speight, 2007; Alvarez and Ancheyta, 2008b).

6.2.2.1 Quench Process

The process of an industrial hydrotreating reactor is considered to be very close to adiabatic behaviour as heat losses from the reactor are generally negligible in

comparison to the heat generated by the hydrotreating reactions (Shah and Paraskos, 1975). The reaction temperature is an important operating condition that has an enormous influence on the degree of conversion of the reactants and on the catalyst cycle life, particularly when hydrotreating heavy oil feedstock, and hence upon the overall economics of the process (Alvarez et al., 2007).

Due to the exothermic nature of the hydrotreating reactions, the average reactor temperature increases, which subsequently enhances the hydrotreating reaction rates (Song, 2003; Bharvani and Henderson, 2002). However, the reactor temperature has a limit dictated by mechanical constraints or by hydrocracking of the feed that decreases the yield of the desired product. In other words, in hydrocracking operations, excessively increasing the temperature can cause an adverse influence upon the product distribution owing to its strong impact upon hydrocracking selectivity. Also, at high temperatures, hot spots can be formed that result in enhanced coke formation and catalyst deactivation (Hanika et al., 1977; Furimsky and Massoth, 1999). Such an impact decreases the catalyst cycle life, and hence, more frequent shut downs of the units are required that affect the global profitability of the operation. Thus, temperature control in TBRs is one of the most significant issues relating to extended catalyst cycle life and keeping the product quality at desired levels (Mun˜oz et al., 2005).

Commonly, quenching has been the conventional route to control the temperature in most of industrial reactor operations. In hydrotreating, this is achieved by introducing a part of the hydrogen stream among the catalytic beds (at a certain length of the reactor), so-called “quenching” or “cold shot cooling” (Satterfield, 1975; Furimsky, 1998). Since, a lot of equipment for hydrogen and large quantity of quench gas are required, the same composition of the feed gas (which is hydrogen) as that of the base case is employed for the quench gas (Alvarez and Ancheyta, 2008b).

Quenching with H_2 takes place at some point along the reactor length and has several functions (Bharvani and Henderson, 2002; Hsu and Robinson, 2006; Ancheyta and Speight, 2007; Alvarez and Ancheyta, 2008b; Alvarez and Ancheyta, 2009), mainly:

(1) Control of reaction temperature,

(2) Flow distribution enhancement in the bed and deliver the reactants to the next bed,

(3) Reduce radial maldistribution with radial mixing,

(4) Replenishing hydrogen, which has been consumed,

(5) Decreasing H_2S and NH_3 in the reactor that reduces the inhibition influence upon hydrotreating reactions, which always improves product quality.

Figure 6.1 (Alvarez et al., 2007) shows an example of the largely utilized TBR with three catalytic beds and hydrogen quenches, in which feed distributor, quench zones, catalytic beds, and catalyst support are clearly indicated.

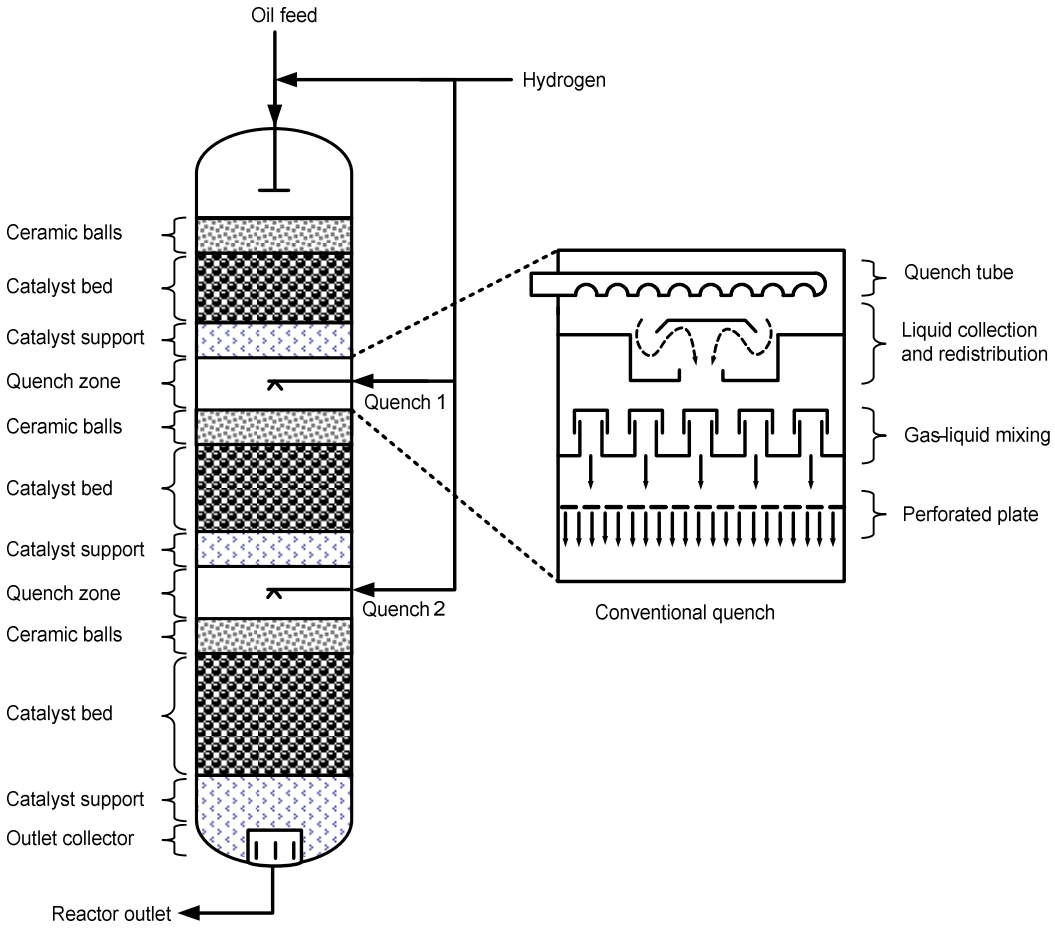

Figure 6.1: Trickle bed reactor with multicatalytic bed and quench technologies

In a quench section (Figure 6.2), hot feedstock fluids from the previous bed are combined with relatively cold hydrogen-rich quench gas before the mixture passes into the next bed. The quench deck consists of the following major parts: quench tube, liquid collector and redistributor, a gas-liquid mixing zone, and the final distributor. Quench tubes bring cold hydrogen quench gas inside the reactor (some are very simple, just a tube with many holes in series). In the liquid collector and redistributor, liquids are forced to flow down two angled slides into a canal. The benefit of using these slides is to give the liquids some angular momentum, while the canal gives them time to mix. In the gas-liquid mixing zone, a tray (usually a bubble-cap tray) provides good contact between gases and liquids from the redistribution zone. Finally, a fine spray of fluids are sent down to the catalyst bed below via the final distributor (Ancheyta and Speight, 2007).

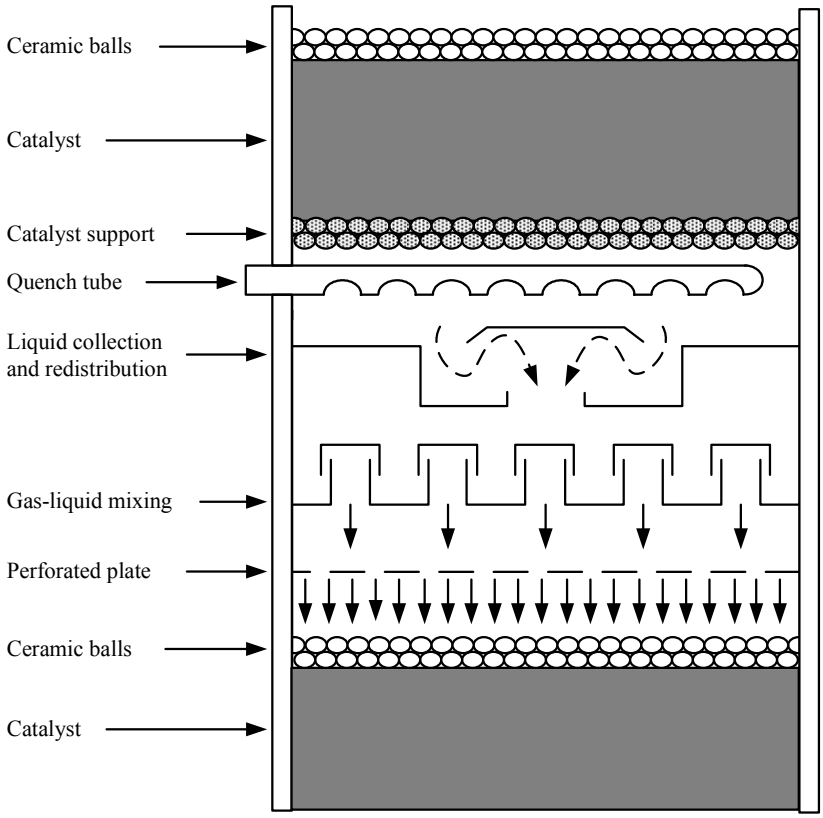

Figure 6.2: Hydrotreating reactor: quench zone

Relating to hydrotreating reactor modelling, simulation and optimization process, basic information about gas quenching can be found in the public domain.

Shah et al. (1976) studied the optimal hydrogen quench position in a trickle-bed reactor used for residual oil hydrodesulfurization in order to achieve a maximum catalyst cycle life. The reactor model took into consideration the activity of the catalyst as a function of time that decreased owing to metals deposition. This work was extended by Mhaskar et al. (1978) into a system with multiple gas quenching. The researchers showed that the catalyst cycle life is increased by using two quench streams in comparison to a single quench system for the same total quantity of quench gas. Also, they observed that the catalyst cycle life increases considerably when increasing the quantity of the first quench and its position near the entrance of the reactor.

Yan (1980) presented a mathematical model for simulating the dynamic behaviour of a trickle-bed hydrocracker reactor with and without a quench system. The model was employed to study the effects of parameters on temperature and product distribution profiles for estimating the best quench position, starting time, and quantity of quench fluid to avoid temperature rise, especially during unit start-up with fresh catalyst.

Lababidi et al. (1998) presented a simulation of a commercial hydrodesulfurization of atmospheric residue unit with four catalyst beds in series and three streams of hydrogen quench. The mathematical model presented took into account HDS, HDM, and coke formation reactions for evaluating the impact of catalyst deactivation. The authors noticed that the temperature rise along the catalyst bed length drops as the operation time increases owing to catalyst deactivation. Catalyst deactivation by coke and metal deposition on catalyst profiles decreased according to the gas quenching between reactor beds, which means that the rate of such reactions has a strong dependence on temperature.

Van Hasselt et al. (1999) investigated the behaviour of a conventional cocurrent trickle-bed reactor with a countercurrent reactor configuration for hydrodesulfurization of vacuum gas oil. The reaction system involved many catalyst bed reactors and the number of quench points was adjusted according to the configuration type. Four beds with three quench points were used for the conventional bed reactor. The quench zone balances equations were extended to take into account the mass transfer between the gas and liquid phases. They reported that controlling the reactor temperature beside the amount of hydrogen quench can reduce the partial pressure H_2S. Therefore, the mass transfer to the gas phase increased due to a decrease in the H_2S concentration in the liquid phase.

Evaluation and analysis of the requirements for revamping a diesel hydrotreating for obtaining ultra low sulfur diesel were reported by Palmer and Torrisi (2003). They recommended that one of the revamp strategies for modifying the single-bed reactor is to divide the total catalyst volume into multi-beds and adding a quench zone. Also, they found that a quench zone could enhance the product quality owing to a reduction of the partial pressure of H_2S. Another observation of adding gas quench was that the overall heating duty decreased due to the quench stream.

Bhaskar et al. (2004) presented a simulation process for a commercial unit used for hydrotreating of diesel oil with two reactors in series and three quenches. The data obtained by simulation bed temperatures were in very good agreement with the experimental results.

Stefanidis et al. (2005) presented a methodology to simulate a representative operating temperature for simulating a commercial hydrodesulfurization reactor with quench zones. The quench zone model included an energy balance with a specific heat capacity

as a function of reaction temperature to simulate the average bed temperature of the fluid after quench or the quench rate at a fixed exit temperature.

Mun˜oz et al. (2005) investigated various alternatives for obtaining the optimal quench position and flow rate during upgrading of heavy oils via hydrotreating under different operating conditions. The process was designed with two reactors in series, each one having three catalytic beds. Scale up was carried out based on the reactor model developed from experimental information at the pilot plant scale. The procedure involved the availability of recycled hydrogen for quenching the reaction mixture in addition to calculating the number and position of hydrogen quenches from the recycle stream.

Murali et al. (2007) developed a two-phase mathematical model for simulating the behaviour of industrial hydrotreating reactors employed for hydrodesulfurization, hydrodearomatization and olefins saturation of diesel oil. The model used predicted the product quality and temperature profiles along the catalyst bed length. The kinetic parameters calculated based on bench scale experiments were used to simulate the industrial hydrotreating reactor. Three catalyst beds with two hydrogen gas quenches were applied to reduce the heat of HDT reactions in order to avoid temperature excesses in the unit and to make the unit flexible enough to handle feed quality variations.

Alvarez and Ancheyta (2008b) presented a heterogeneous reactor model for simulating and analyzing a commercial HDT reactor with different quenching schemes considering the HDS, HDN and HDA of vacuum gas oil reactions. The model was applied to predict the behaviour of the reaction system with and without the injection of different quench fluids. Temperature profiles along the catalyst bed, changes in partial pressure and molar concentration were estimated for each alternative and compared with those

obtained for the system without quenching. They have recognized the removal of impurities affected largely by resulting reactor temperature.

Alvarez and Ancheyta (2009) compared several aspects of using liquid quenching during hydrotreating of heavy oils with hydrogen gas quenching. It has been noted that the conventional hydrogen quenching scheme produced better quality of the main hydrotreating reactions due to the low the catalytic activities in comparison with liquid quench.

Alvarez et al. (2009) presented the modelling and analysis of residue hydrotreating in fixed bed reactor to simulate the performance of industrial hydrotreating reactor. Also, the model was used to analyze different quenching schemes from an economical point of view with inter-bed injection of quench gas or liquid based on the pilot plant results.

6.2.2.2 Model Equations for Quench Zone

The quench zone is represented as a mixer of the quench stream and the effluent from the first catalytic bed as shown in Figure 6.3. The following expressions describe the quench zone mass balances:

$$\text{Global: } q + l_{out} + g_{out} = l_{in} + g_{in} \tag{6.29}$$

$$\text{Gas: } q + g_{out} = g_{in} \tag{6.30}$$

$$\text{Liquid: } l_{out} = l_{in} \tag{6.31}$$

l_i, g_i are liquid and gas mass flow rates of stream *i*, respectively, and q is the quench fluid mass flow rate.

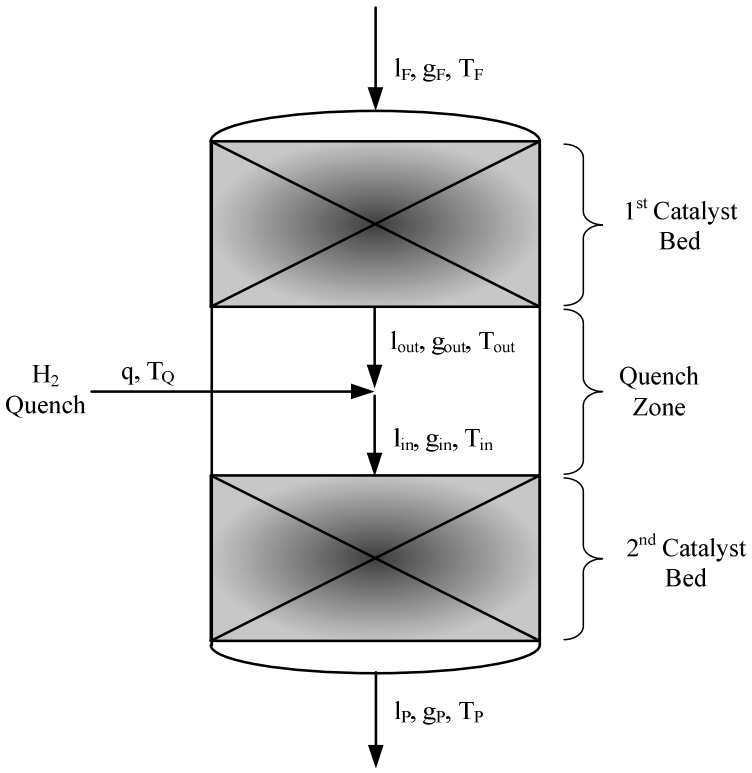

Figure 6.3: Model representation of quench zone

Equation (6.29) describes the global mass balance between the liquid and gas streams leaving the first catalyst bed ($l_{out} + g_{out}$) and the resulting liquid and gas streams entering the next catalyst bed ($l_{in} + g_{in}$), after mixing with the quench fluid (q). Equations (6.30) and (6.31) represent the gas and liquid mass balances, respectively.

In order to determine the necessary quench fluid rate to cool the effluent to a certain temperature, the following energy balance equation with temperature dependent heat capacities is used to simulate the cooled mixture temperature (T_{in}) at a constant quench rate or at the quench rate for a fixed mixture temperature:

$$\int_{T_{out}}^{T_{in}} l_{out}\, c_p^L dT + \int_{T_{out}}^{T_{in}} g_{out}\, c_p^G dT + \int_{T_Q}^{T_{in}} q\, c_p^Q dT = 0 \tag{6.32}$$

$$q = y \quad g_F \tag{6.33}$$

c_p^Q is the specific heat capacity of quench feed (which is hydrogen), T_i is the temperature of stream *i*, and *y* is the mass flow rate fraction of the quench fluid.

To solve the energy balance, it is required to know the liquid and gas mass flow rates at the exit of the first catalyst bed, which can be assumed to be equal to the feed flow rates (l_F and g_F) (Murali et al., 2007; Alvarez and Ancheyta, 2008b; Alvarez et al., 2009).

6.2.2.3 Case Study

The kinetic data generated with all the model equations presented in the previous chapter that include all reactions in addition to model equations in this chapter with the total catalyst volume and dimensions of the industrial trickle bed reactor are used for the quenching process. At a temperature above 410°C thermal cracking of hydrocarbons becomes more significant, leading to catalyst deactivation, and so the maximum allowed temperature limit at the end of each bed (T_{out}) is set to 6°C above the inlet temperature (400°C). Once such a limit is reached, an appropriate quantity of hydrogen quench is injected in order to reduce the temperature to the inlet value (Ancheyta and Speight, 2007). Also, the temperature of the hydrogen quench fluid is kept fixed at 70°C (Alvarez and Ancheyta, 2008b). The heat released by the HDV, HDNi and HDAs is negligible in comparison with that of HDS and HDN (Kam et al., 2005; Juraidan et al., 2006; Marafi et al., 2008) and the values of heat of reactions are (Tarhan, 1983): 251 kJ/kmol and 64.85 kJ/kmol for HDS and HDN, respectively. The following cases are considered:

Case A: Base hydrotreater. As mentioned earlier, hydrotreating processes generate copious amounts of heat during industrial HDT, which is reflected in a sharp temperature rise along the catalyst bed length. Thus, this case is identical to the crude

oil hydrotreater with the absence of a quench stream. This case is studied as a reference to analyse the influence of quenching process on the reactor behaviour.

Case B: Hydrogen quenching. Part of the hydrogen stream is used for quenching the hydrotreating reactions in addition to enhancing the composition of the gas phase. Since this technique is usually utilized for the hydrotreating operations, the present analysis will provide a better understanding of these systems. For the hydrogen quenching system, the best quench position and quench flow rate (described by the mass flow rate fraction of hydrogen quench of the main hydrogen feed) using many simulations on the reaction system is investigated with constraints on temperature. The target of this case is to keep the temperature between 400°C (the base reactor temperature) and 406°C (the maximum allowed temperature at the end of each bed (T_{out})) with minimum total annual cost.

Increasing the number of quenches leads to an increase in the capital cost of the reactor as well as the compressor. Also, increasing the quench flow rate increases the compressor capacity and as a result the compression cost will increase. The total annual cost (*TAC*) can be described as follows:

$$TAC\ (\$/yr) = Annualized\ Capital\ Cost\ (\$/yr) + Operating\ Cost\ (\$/yr) \tag{6.34}$$

$$Capital\ Cost\ (\$) = Reactor\ Cost\ (\$) + Compressor\ Cost\ (\$) \tag{6.35}$$

To calculate the annualized capital cost (ACC) from capital cost (CC), the following equation is used (Smith, 2005):

$$ACC = CC \times \frac{i(1+i)^n}{(1+i)^n - 1} \tag{6.36}$$

n is number of years, and i is the fractional interest per year; n = 10 years, i = 5% (Smith, 2005).

Reactor cost is determined by equations (6.9) and (6.10). The compressor cost (C_{comp}) is estimated from the following correlations (Douglas, 1988):

$$C_{Comp}(\$) = \left(\frac{M\ \&\ S}{280}\right)(517.5)(bhp)^{0.82}(2.11 + F_d) \tag{6.37}$$

$$bhp = \frac{hp}{\eta_{ise}} \tag{6.38}$$

$$hp = \left(\frac{3.03\times10^{-5}}{\gamma}\right)P_{in}Q_{in}\left[\left(\frac{P_{out}}{P_{in}}\right)^{\gamma} - 1\right] \tag{6.39}$$

$$\gamma = \frac{\left(\frac{cp^G}{cv^G} - 1\right)}{\left(\frac{cp^G}{cv^G}\right)} \tag{6.40}$$

$$cv^G = cp^G - R \tag{6.41}$$

bhp is the brake horsepower required in the compressor motor, F_d is a cost correction factor, *hp* is the compressor horsepower, η_{ise} is isentropic efficiency, γ is the specific heat ratio, Q_{in} is the volumetric flow rate at compressor section, cv^G is the specific heat capacity at constant volume, and P_{in} and P_{out} are the pressure in the compressor inlet and outlet, respectively.

η_{ise} ranges between 70-90% (here assumed to be 80%) and F_D = 1 for a centrifugal motor compressor, (Douglas, 1988; Bouton and Luyben, 2008).

The operating cost (*OP*) that includes the compression cost is estimated by using the following equation, which is based upon a motor efficiency of 90% (Bouton and Luyben, 2008) and an average power price of 0.062$/kWh (Alvarez et al., 2009):

$$Compression\ Cost(\$/yr) = \left(\frac{bhp(hp)}{0.9}\right)\left(\frac{1kW}{1.341hp}\right)\left(\frac{0.062\$}{kWh}\right)\left(\frac{24h}{1day}\right)\left(\frac{340day}{1yr}\right) \tag{6.42}$$

6.2.2.4 Results and Discussion

The trickle-bed reactor model described previously is used to simulate the performance of an industrial crude oil hydrotreater with the proposed quenching schemes. Figure 6.4 shows the reactor temperature profiles for case A (without quench). As can be seen from this Figure, the base case presents a reactor temperature increase as high as 16°C, reaching almost 416°C along the catalyst bed length. Operating at such high temperatures will increase the thermal cracking of hydrocarbons and consequently more deposits of carbon on the catalyst that will close the active sites of the utilized catalyst, leading to rapid deactivation and reduction of the cycle life of the catalyst. Therefore, it is necessary to control the reactor temperature with certain temperature range in the beds, which is discussed with case B.

For case B, the simulation results at different quench positions (as a relative reactor length, z/L), quench rate fraction, temperature profiles using one quench-two beds and total annualized cost are listed in Table 6.5.

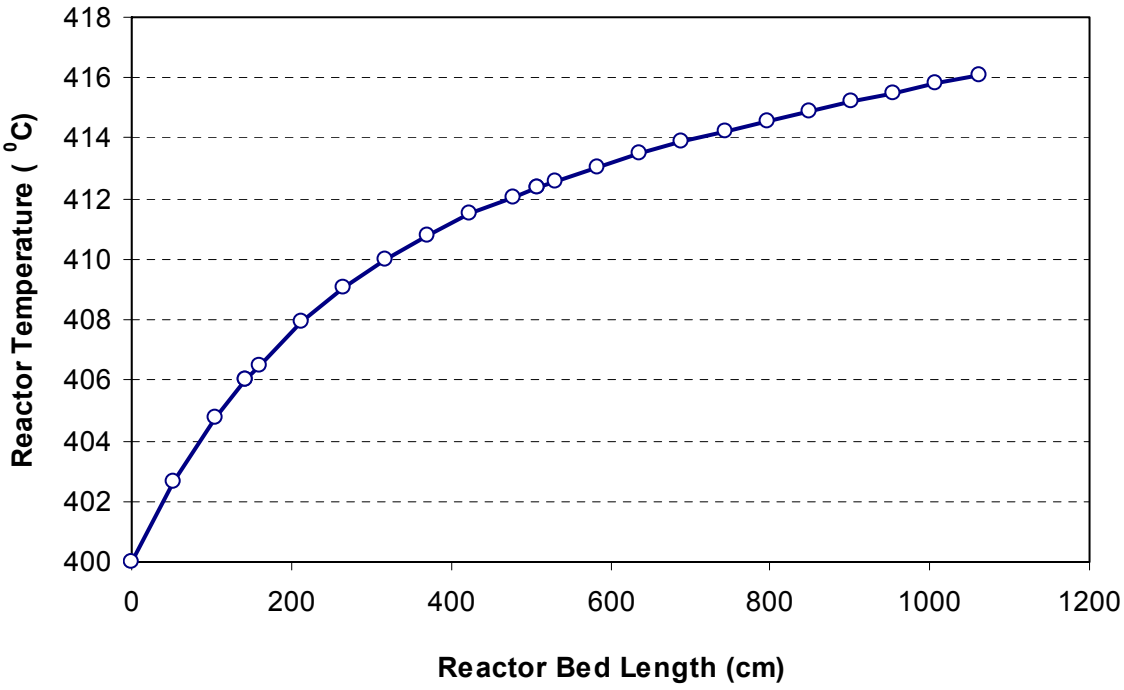

Figure 6.4: Reactor temperature profiles for base hydrotreater along bed length

Table 6.5: Quench positions and rate fractions for two beds with cost results

Case	Reactor	Quench Position (z/L)	Quench Rate fraction (%)	Temperature (°C)		TAC ($/yr)
1	1st Bed			T_F	400.00	760741.60
				T_{out}	404.79	
	Quench Zone 1	0.1	y_1 = 11.10 (%)	T_{in}	400.00	
	2nd Bed	---	---	T_F	400.00	
				T_P	411.35	
2	1st Bed			T_F	400.00	783393.90
				T_{out}	407.93	
	Quench Zone 1	0.2	y_1 = 18.45 (%)	T_{in}	400.00	
	2nd Bed	---	---	T_F	400.00	
				T_P	408.20	
3	1st Bed			T_F	400.00	798624.50
				T_{out}	410.03	
	Quench Zone 1	0.3	y_1 = 23.40 (%)	T_{in}	400.00	
	2nd Bed	---	---	T_F	400.00	
				T_P	406.08	

As can be seen from Table 6.5, with the first simulation (case 1) at a quench position of 0.1 of the total bed length (which means that the hydrogen quench should be injected at this position), the best quench rate fraction to return the temperature to the base hydrotreater temperature (i.e. 400°C) is 11.10% of the main hydrogen feed at this position and the temperature at the end of the 1st bed is 404.79°C (i.e. below the maximum allowed temperature). After quench zone1, the temperature of the mixture was returned to the base hydrotreater temperature, which is then the flow inlet temperature to the next bed. For the 2nd bed, it is clearly observed that the temperature at the end of the 2nd bed is around 411.35°C (i.e. above the maximum allowed temperature), which means that the temperature of the 2nd bed needs to be controlled. For a quench position at 0.2 (case 2) of the total bed length, the temperature at the end of the 1st and 2nd beds is higher than 406°C. While a quench position at 0.3 (case 3) of

the total bed length showed that the temperature at the end of the 1st bed is higher than 406°C inspite of the temperature at the end of the 2nd bed being almost 406°C.

From the results presented in Table 6.5, it is clearly seen that extra quench needs to be injected. On the other hand, the catalyst bed length should be divided into more than two beds. Thus, re-simulation of processes with three beds and two quenches are studied. The reactor configuration with three catalyst beds and two quenches is illustrated in Figure 6.5.

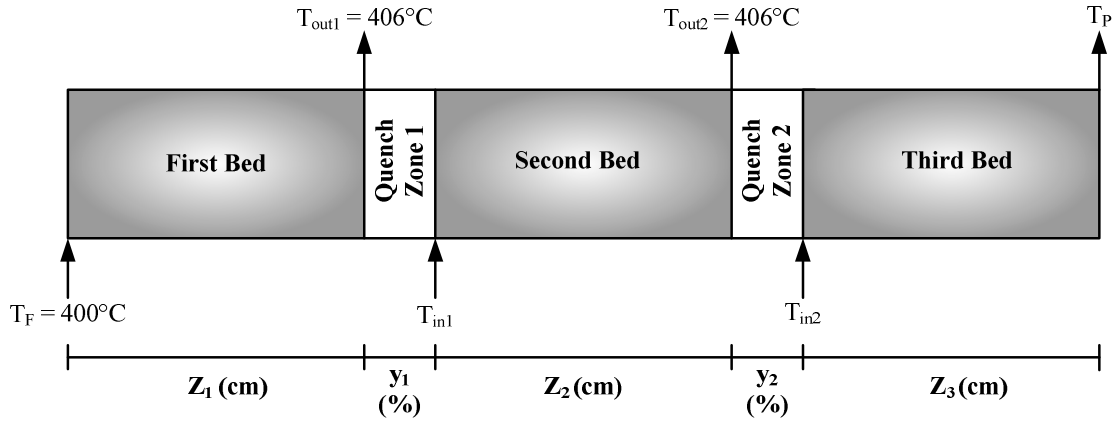

Figure 6.5: Reactor configuration with catalyst beds and quench

The aim of this process is to obtain the best annual cost at the best length of each bed while keeping the temperature between 400°C and 406°C along each bed length. The simulation results with many cases for two quench-three beds are shown in Table 6.6. In each case, the first step is to calculate the first bed length (Z_1) that gives 406°C at the end of the bed. Secondly, the first quench rate fraction (y_1) is estimated to reduce the temperature in quench zone 1 to Tin_1 (which are 404°C, 402°C and 400°C). Each temperature (regarded as the initial temperature to the next bed) is used to determine the length of the second bed (Z_2) that gives 406°C at the end of the bed. Then, the second quench rate fraction (y_2) is calculated in quench zone 2 to reduce the temperature to Tin_2 (which are 404°C, 402°C and 400°C). Finally, the product temperature at the end

of the third bed (T_P) for each case is evaluated after estimating the remaining part of the bed length (which is Z_3). At each case the total annual cost is determined.

Table 6.6: Different simulation results for three beds with cost results

Cases	Z_1 (cm)	y_1 (%)	Tin_1 (°C)	Z_2 (cm)	y_1 (%)	Tin_2 (°C)	Z_3 (cm)	T_P (°C)	TAC ($/yr)
Case 1	141.96	4.59	404	74.67	4.64	404	844.52	412.15	787568.9
Case 2	141.96	4.59	404	74.67	9.29	402	844.52	410.13	801919.3
Case 3	141.96	4.59	404	74.67	13.97	400	844.52	408.12	816360.7
Case 4	141.96	9.24	402	180.39	4.65	404	738.80	410.13	801919.4
Case 5	141.96	9.24	402	180.39	9.29	402	738.80	408.13	816226.6
Case 6	**141.96**	**9.24**	**402**	**180.39**	**13.97**	**400**	**738.80**	**406.02**	**830626.3**
Case 7	141.96	13.93	400	338.18	4.59	404	581.01	408.13	816214.1
Case 8	**141.96**	**13.93**	**400**	**338.18**	**9.24**	**402**	**581.01**	**406.02**	**830478.8**
Case 9	**141.96**	**13.93**	**400**	**338.18**	**13.93**	**400**	**581.01**	**404.18**	**844837.6**

It is noted from Table 6.6 that the constraint on temperature can be achieved by using case 6, 8 and 9 with temperature between 400°C and 406°C in each bed, which are shown in Figure 6.6 along the bed length for each case. The total annual cost (TAC) for case 9 is higher than those of case 6 and 8, thus case 9 is not taken into account. Although the TAC of case 8 is slightly lower than case 6, the comparison of results of impurities removal is necessary (shown in Figure 6.7). As can be seen from this Figure, the conversion of the impurities utilizing case 8 is the better when compared to the conversions obtained via case 6. In other words, the quench rate fraction (y_1 and y_2) of the main hydrogen feed should be injected at position Z_1 and Z_2 respectively using case 8 in order to keep the allowed temperature limit under control. Therefore, case 8 is selected to describe the behaviour of industrial trickle bed reactor for crude oil hydrotreating.

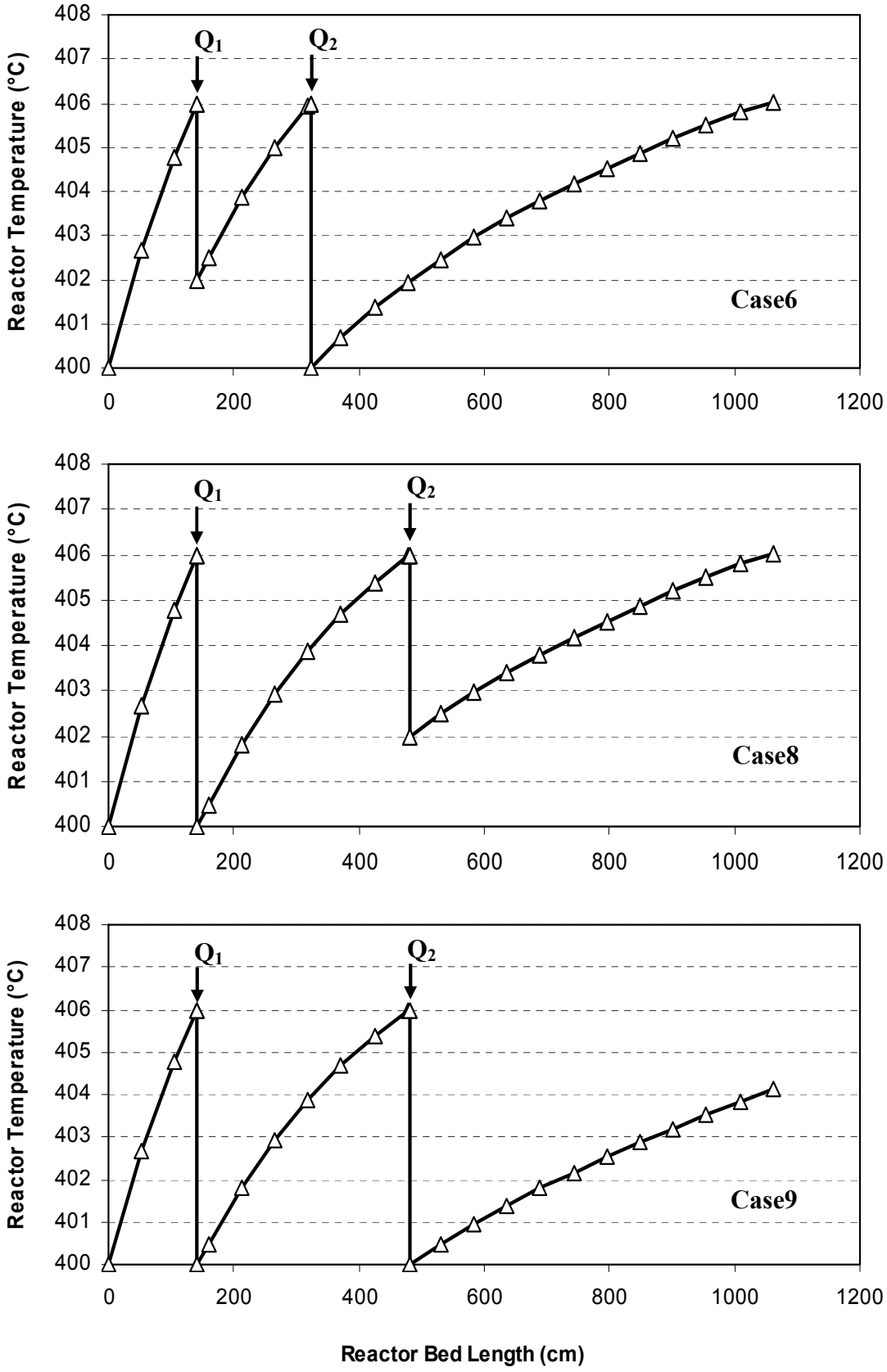

Figure 6.6: Temperature profiles for case 6, 8 and 9 with two quenches-three beds

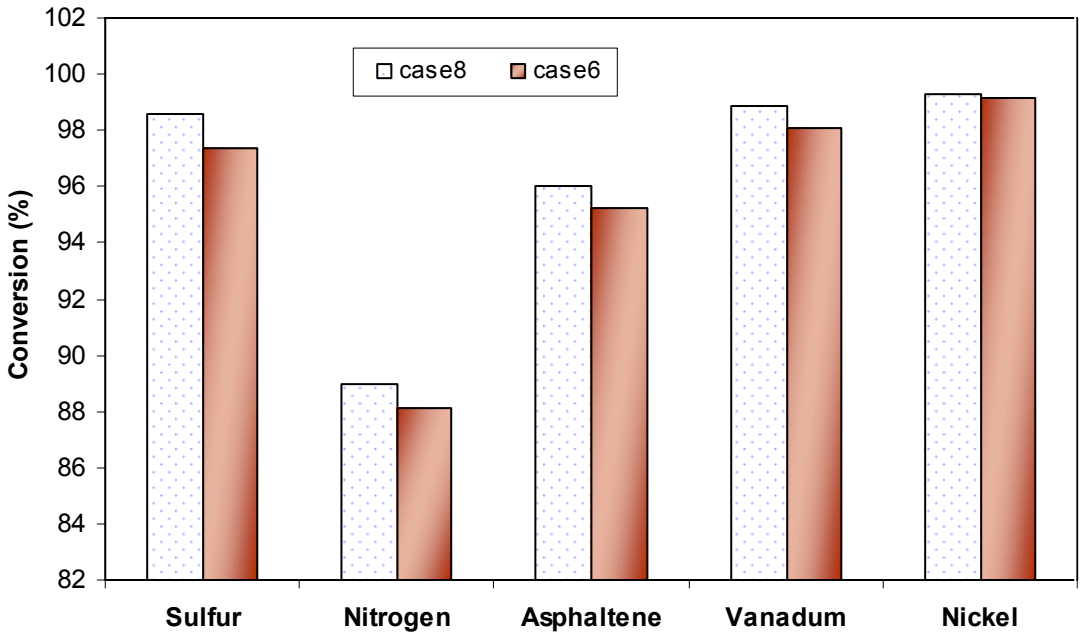

Figure 6.7: Conversion results for case 6 and 8

6.2.2.5 Simulation of an Industrial HDT Reactor

Once the reactor model was validated to reproduce the experimental results obtained in the isothermal reactor at the pilot-plant scale, it is applied to the industrial trickle bed reactor used for crude oil hydrotreating. Due to non-isothermal operation of industrial TBRs, the energy balance is solved simultaneously with mass-balance equations with whole model equations.

Concentration profiles of hydrogen partial pressure along the industrial bed length are illustrated in Figure 6.8. As observed previously with pilot plant performance, hydrogen partial pressure decreases along the catalyst bed reactor as a result of hydrogen consumption. After the quench zones, H_2 partial pressures increased above the value before or without quenching. This jump in hydrogen partial pressure is produced by hydrogen quenching due to temperature reduction. Solubility of hydrogen is directly proportional to temperature, hence when the temperature decreases, the dissolved hydrogen is transferred to the gas phase and consequently its partial pressure will

increase. The partial pressure of hydrogen sulfide has the opposite response as shown in Figure 6.9. It decreases along the reactor bed due to sulfur removal. At the quenching positions, the values of H_2S partial pressure are reduced below that before quenching (seen in Figure 6.9 inset) because the temperature has the contrary effect on H_2S solubility in comparison to that of hydrogen.

The predicted concentration profiles with the conversions of sulfur, nitrogen, asphaltene, vanadium and nickel along the industrial bed length are presented in Figures 6.10 to 6.14. Since the industrial reactor is operated at non-isothermal mode, the industrial process usually is observed to give smaller impurities contents than the pilot plant results (Rodriguez and Ancheyta, 2004). Thus, it can be noted from these Figures that the industrial reactor achieves a higher conversions of sulfur, nitrogen, asphaltene, vanadium and nickel than those obtained at pilot plant reactor.

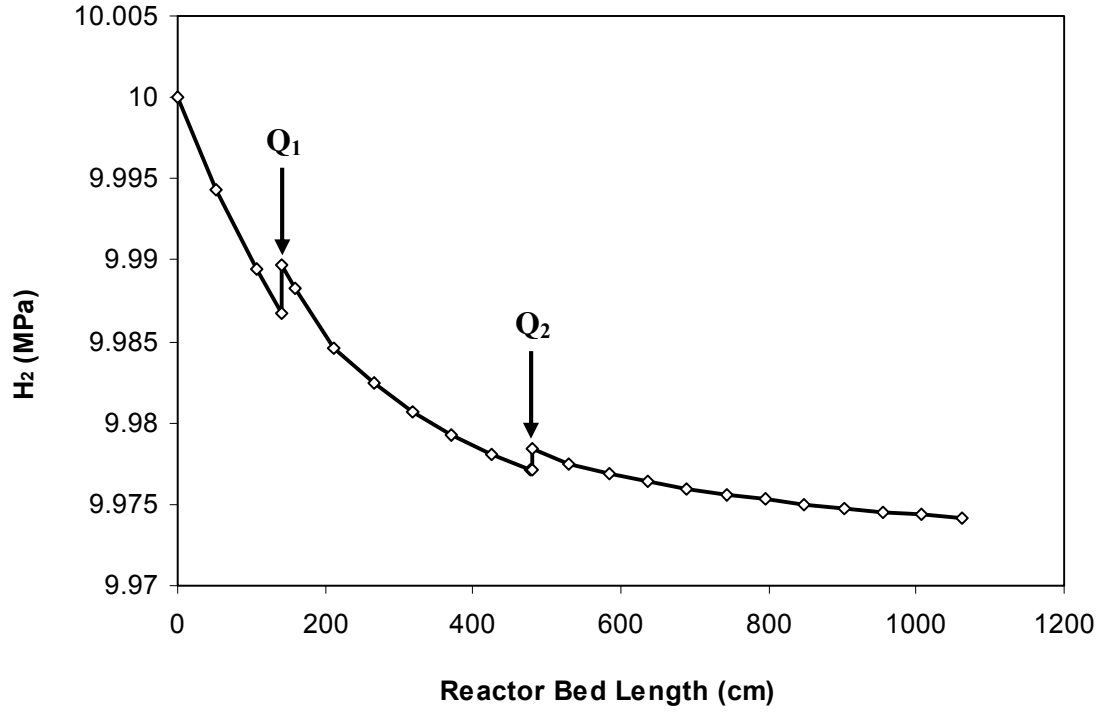

Figure 6.8: Hydrogen profiles with quenching along the industrial bed length

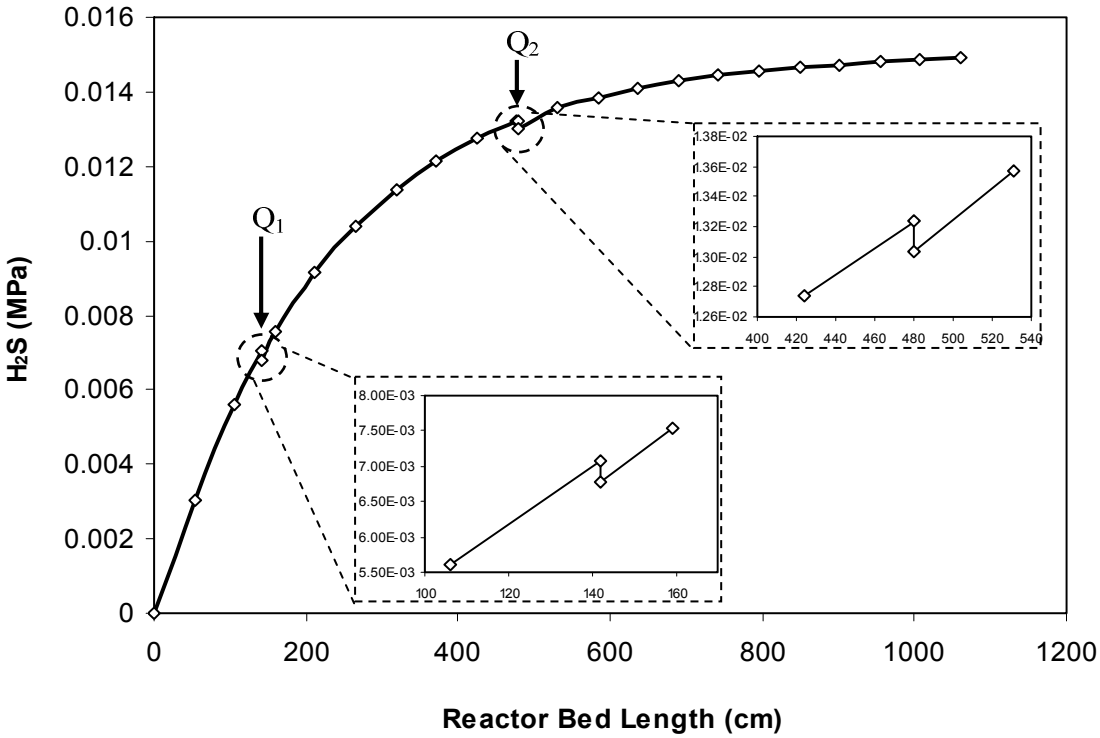

Figure 6.9: Hydrogen sulfide profiles with quenching along the industrial bed length

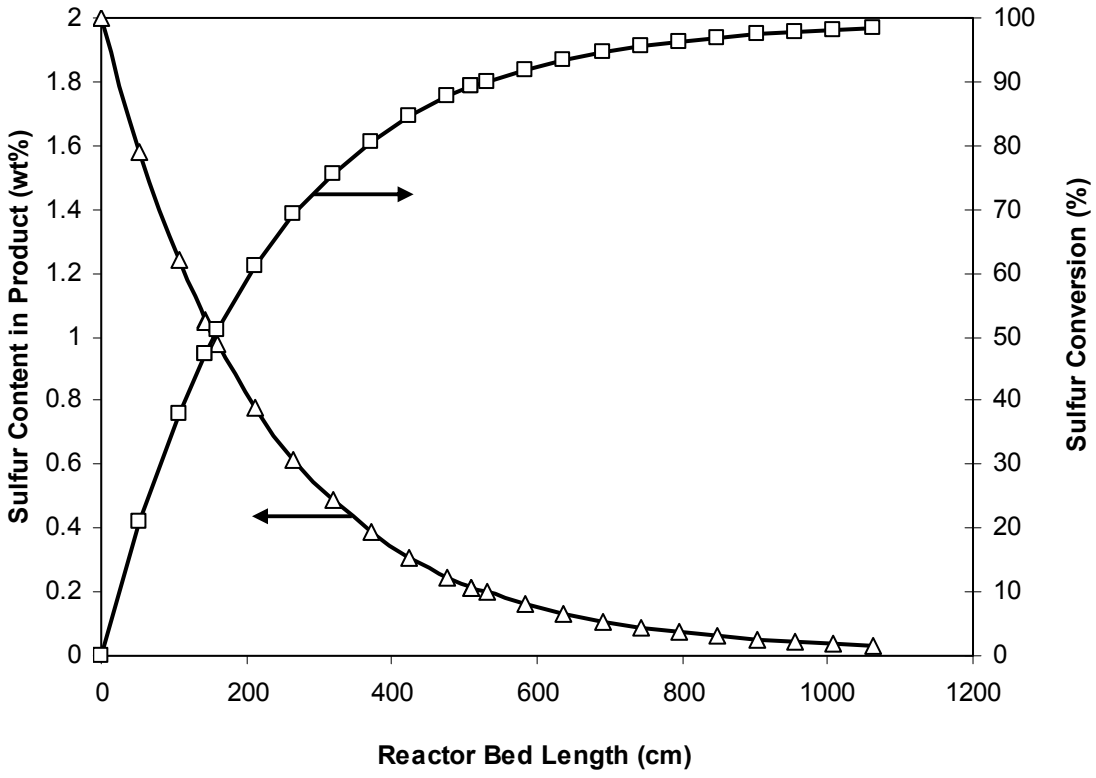

Figure 6.10: Predicted evaluation profiles of sulfur along the industrial bed length

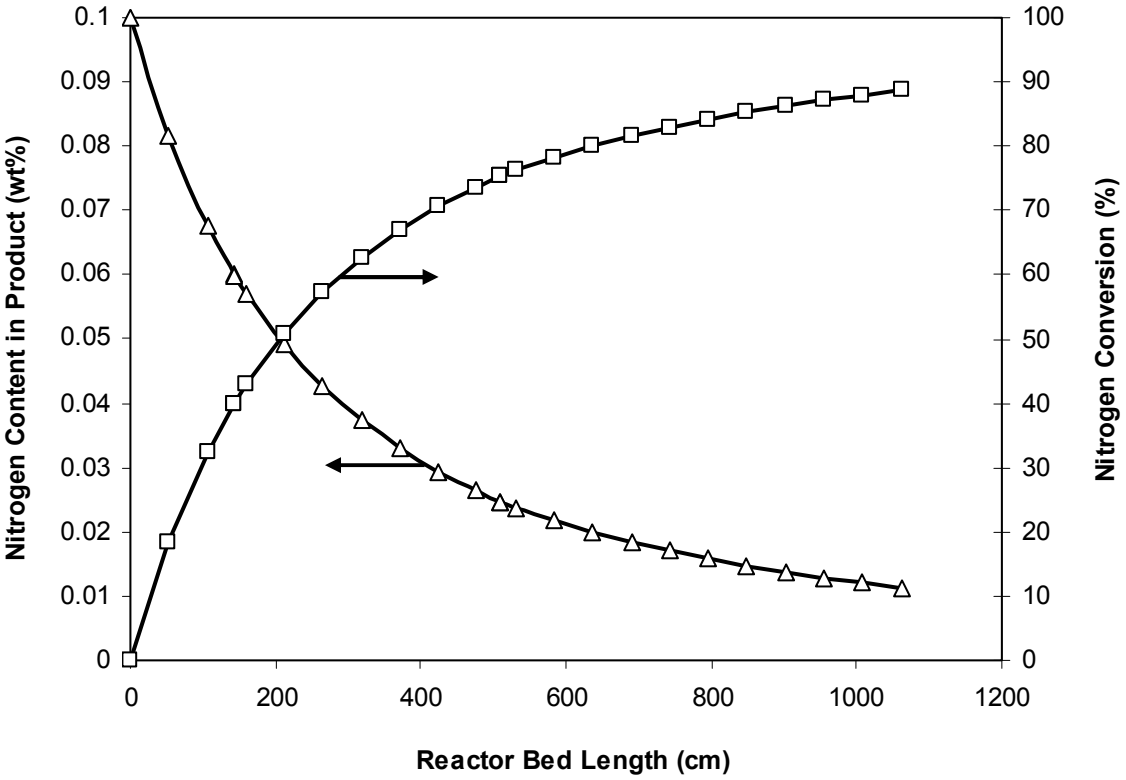

Figure 6.11: Predicted evaluation profiles of nitrogen along the industrial bed length

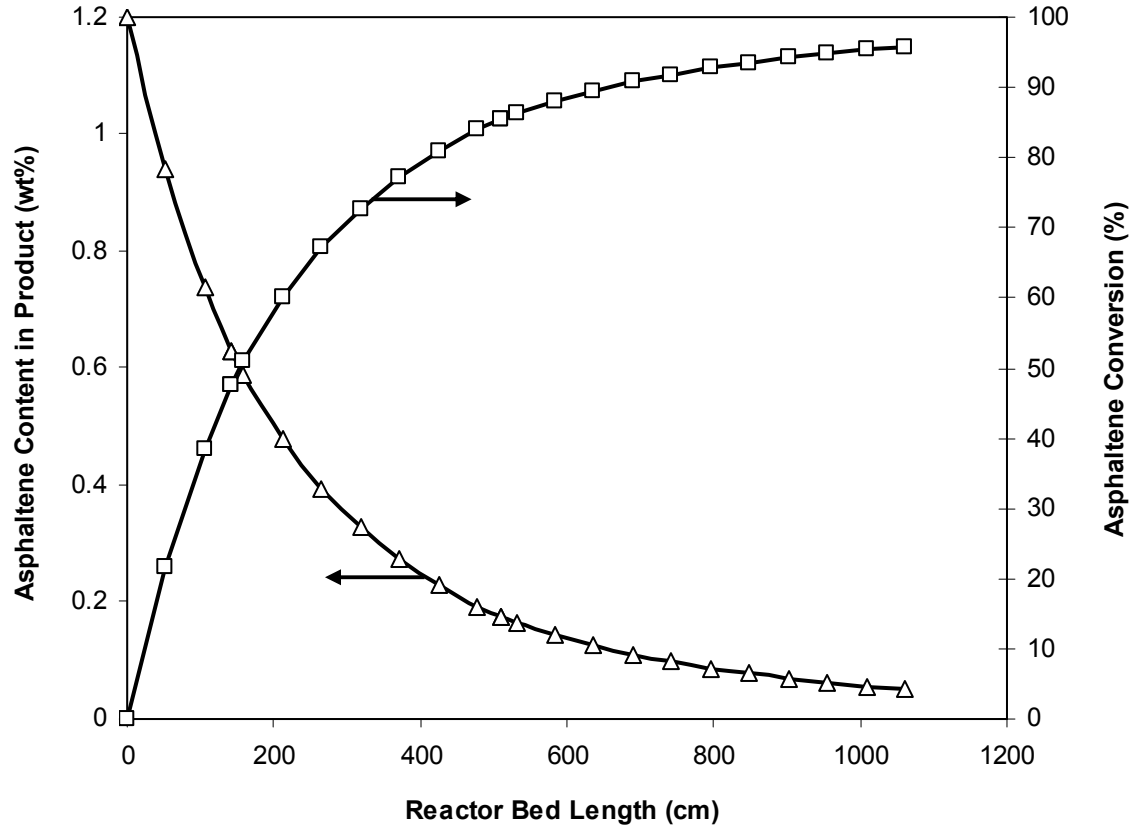

Figure 6.12: Predicted evaluation profiles of asphaltene along the industrial bed length

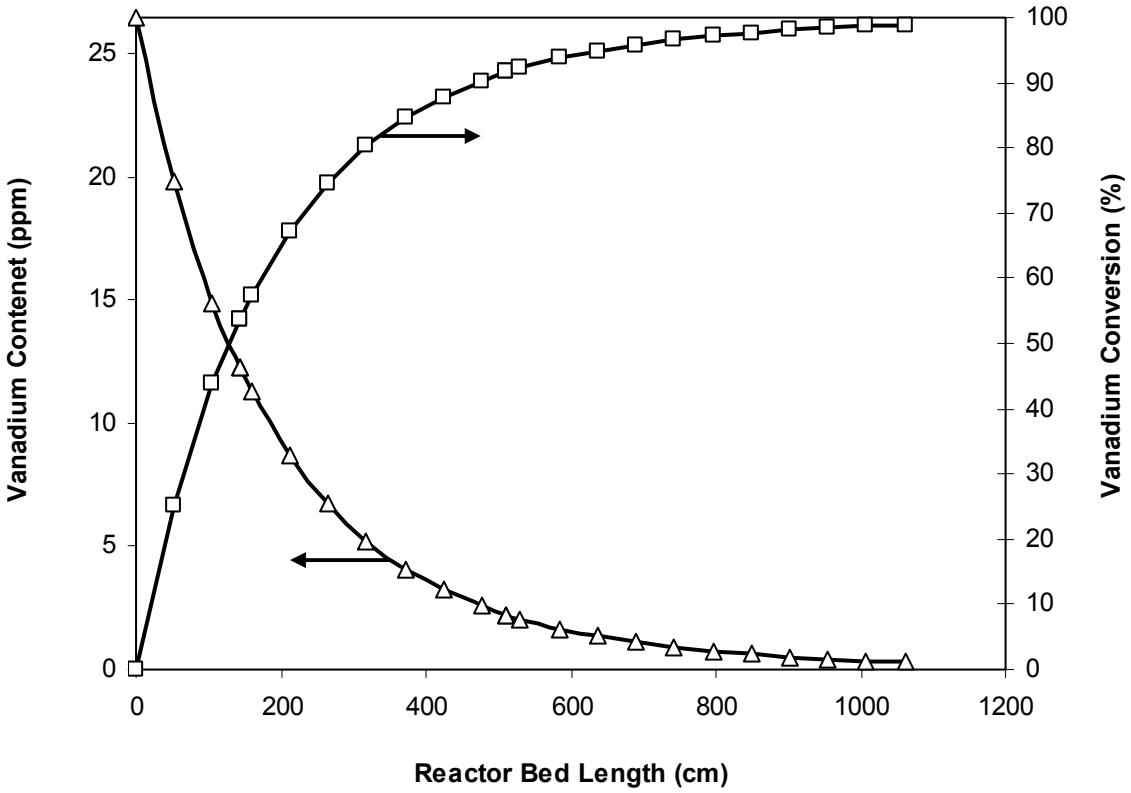

Figure 6.13: Predicted evaluation profiles of vanadium along the industrial bed length

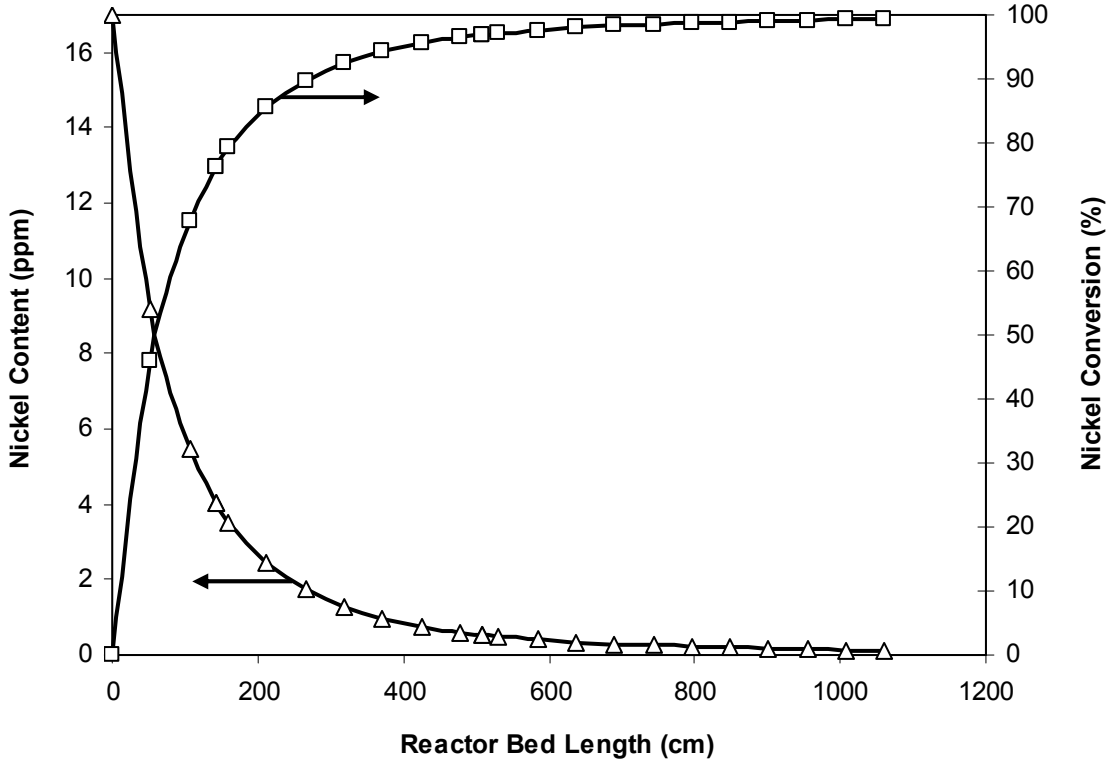

Figure 6.14: Predicted evaluation profiles of nickel along the industrial bed length

This gain in conversion is mainly attributed to a higher reactor temperature that increases the reaction rates of these reactions (all the kinetics parameters used for describing hydrotreating reactions are effected by the reaction temperature).

Also, the bed void fraction of the catalyst, which depends mainly on the reactor diameter, is increased in the industrial trickle bed reactor due to an increase in the reactor diameter. As a result, the surface area of the catalyst particles increases and consequently the compounds transported on the surface of the catalyst where the reactions happen (more diffusion of these compounds) will increase. Therefore, the chemical reaction rates increased that led to higher conversion.

It has also been found that the middle distillate yields increased during the simulation process of the industrial trickle bed reactor employed for crude oil hydrotreating and gave yields slightly higher than those obtained by the pilot plant performance of these fractions (naphtha, heavy kerosene, light gas oil in addition to gases and reduced crude residue). This behaviour is quite clear at high reaction temperature. As discussed previously, the kinetic model used for all hydrotreating reaction including middle distillate yields models (which its reaction rate constants described by the Arrhenius equation) are mainly as a function of reaction temperature.

The industrial TBR configuration that involves all oil feed and products content with quenching is shown in Figure 6.15.

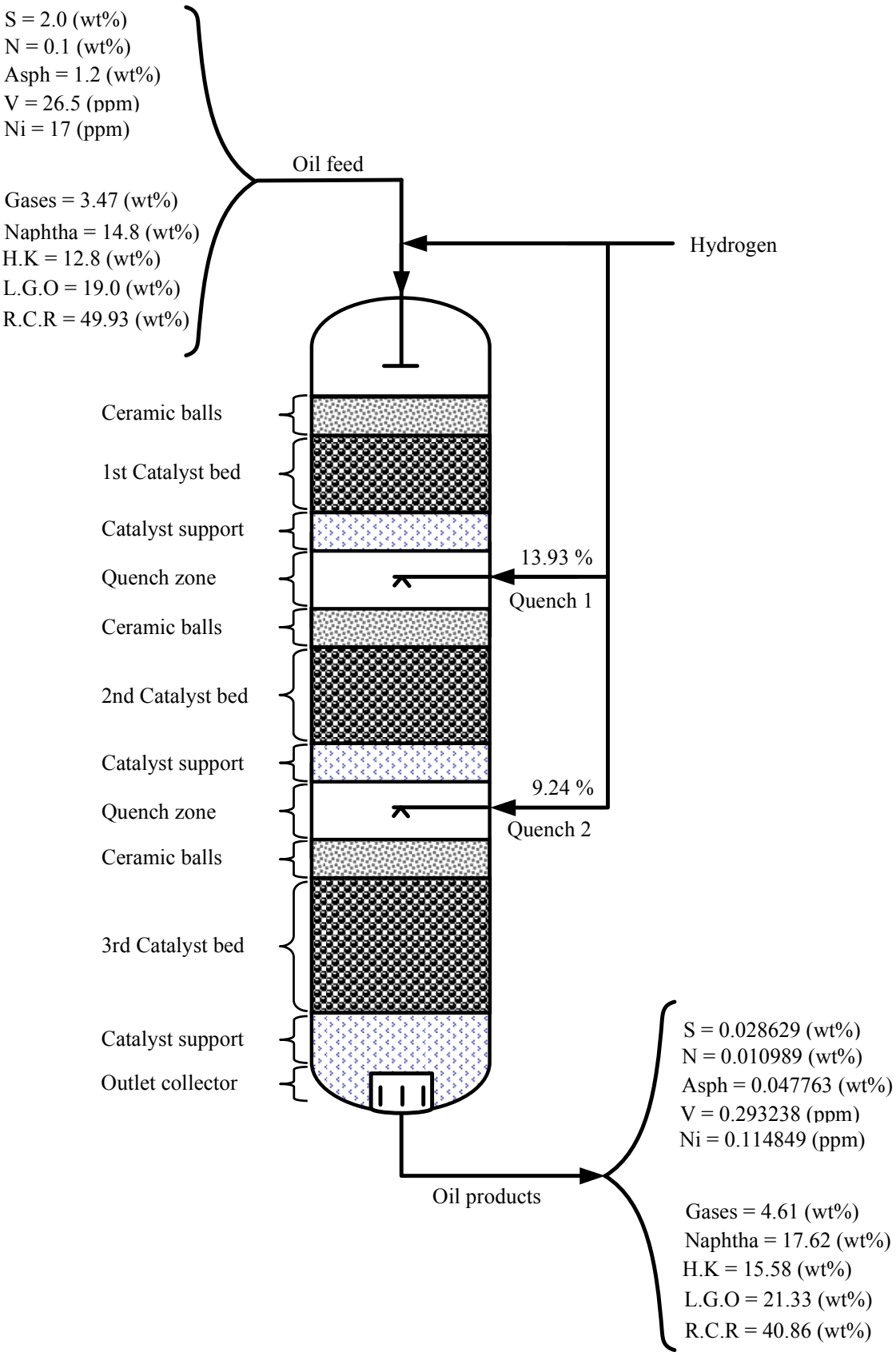

Figure 6.15: Industrial TBR configuration with feedstocks and products properties

6.3 Heat Integration and Energy Consumption in HDT Process

One of the tasks which chemical engineers are continually addressing is the scale up of laboratory experiments to full-scale production. Due to the high cost of a pilot plant study, this step is starting to be surpassed in several instances via designing the full scale unit based on the process of a bench scale plant called a microplant. In order to make this jump successfully, a thorough understanding of the chemical kinetics and transport limitations is required. However, energy conservation is significant in process design. The estimation of the minimum cooling and heating requirements reveal important energy savings. For instance, Union Carbide in the USA and Imperial Chemical Industries in the UK have both reported the results of numerous case investigations that reference 30% to 50% energy savings in comparison to conventional practice (Douglas, 1988).

Concentrations of carbon dioxide (CO_2) in the atmosphere have increased from 270 ppm before the industrial age to 380 ppm by 2006: a 31% increase since 1870 and a 41% increase over pre-industrial values. US EPA (United States Environmental Protection Agency) have recently found that the CO_2 represents the most common greenhouse gas, a danger to human health, clearing the way to greater legislation of carbon dioxide emissions (www.aip.org/history/climate/co2.htm). The primary human source of carbon dioxide in the atmosphere is from the burning of fossil fuels towards energy production and transport. To avoid or reduce global warming, dramatic cuts in all carbon dioxide emissions must be achieved, 25% to 40% below 1990 levels by 2020, and 80% to 95% below 1990 levels by 2050 (www.greenpeace.org).

However, more efficient utilization of energy consumption results in the reduction of the negative effects of carbon dioxide emissions. Thus, process integration is an efficient design methodology, which addresses cases related to energy efficiency, waste minimization and an efficient utilization of raw materials.

Operation units, oil refineries, petrochemical complexes and gas units all generate large amounts of low grade heat. This energy is usually rejected to the atmosphere utilizing either air or cooling water systems. However, there are opportunities for recovering some of this energy, and using it either as part of an operation integration scheme or to heat in domestic and industrial specifications by the installation of a hot water system.

Energy integration is a very beneficial tool and is a significant phase in estimating the cost of preliminary design, where recovery of waste heat provides both financial and environmental benefits to process unit operators. From an energy saving point view a significant energy use improvement relates to heat exchange retrofit projects for maximizing the existing heat recovery (Khalfalla, 2009).

A process unit usually consists of all or some of the following parts:

- A reactor, where the main chemical reactions take place and required product is generated from raw materials.
- A separation system, which divides up the mixture of products, waste and unreacted raw materials emerging from the reactor utilizing separating agent, like heat or solvent.
- A heat exchanger, where recovery of heat from hot product stream takes place in order to heat the cold stream.
- Utility system (cooler and heater).

Traditional design methods begin by designing the reactor, the separation system, the heat exchanger and finally end by utilizing utilities for supplying residual needs (Douglas, 1988).

The utility includes hot and cold utility units. Typically, hot utility units are furnaces, turbines, generators, boilers and motors providing the necessary power, hot water and steam. Cold water from external sources is employed as the cold utility, which provides

the required cooling in the operations. In the recovery system, the process streams exchange heat so as to reduce the cold and hot utility requirements. The heat exchangers are the only units in a heat recovery system (Khalfalla, 2009).

6.3.1 Heat Exchangers

A heat exchanger is a unit in which heat is transferred from a hot stream to a cold stream. A more correct term of reference is a heat exchange match between two streams, as this makes no assumption regarding the type of exchanger or the number of units needed to fulfil a particular duty. The design problem is to devise a network that utilizes as little external energy as possible and as few match as possible. Figure 6.16 displays a simple system, which consists of two streams and a single heat exchanger (Smith, 2005).

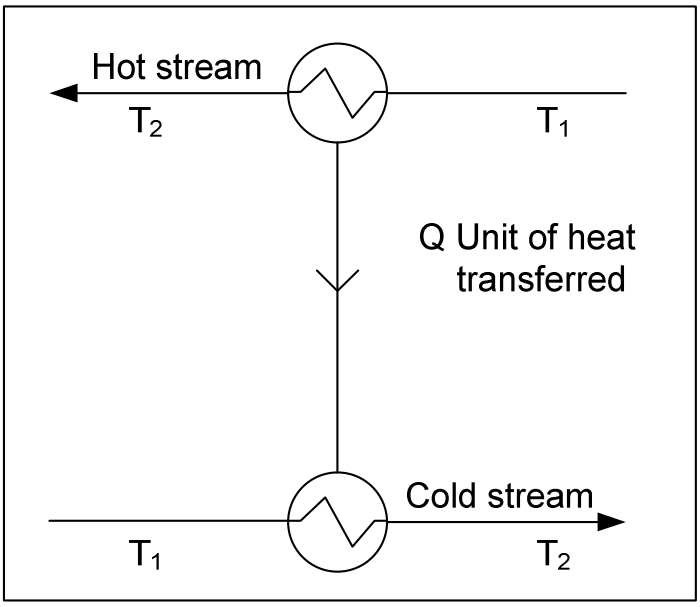

Figure 6.16: Grid notation for heat exchangers

The top line represents the hot stream being cooled from T_1 to T_2, and the bottom line represents the cold stream being heated from T_1 to T_2. The match itself is illustrated as a

dumb-bell shape of two circles joined by a vertical line, with the heat load of the match, *Q*, also marked. This representation is particularly convenient for comparing different arrangements of matches for the same operation.

6.3.2 Energy Consumption and Recovery Issues

Pilot plant trickle bed reactor experiments show that conversion in hydrotreating reactions is better at high reaction temperatures. Energy consumption for the pilot plant scale was negligible and natural cooling after the reaction was sufficient (no additional utility was required as the amounts of reactants and products were small at pilot plant scale), thus heat recovery was not taken into consideration. On the other hand, heat recovery was not an issue in the pilot plant scale process. In industrial processes, energy consumption will be a large issue and heat recovery must be taken into account, especially when the type of reaction is exothermic. Therefore, scaling up a heat integrated hydrotreating process was considered for reducing overall energy consumption (hence reducing environmental effect). However, this leads to the addition of a number of exchangers in the system, requiring capital investment. The objective is to calculate a retrofit design, which can reduce the energy consumption, maximize energy recovery and consequently minimize capital investment.

Generally heat exchangers operate in series with a heater and a cooler. The heater regulates the final temperature of the cold fluid to the required reaction temperature, and the cooler adjusts the final temperature of the hot fluid to requirements of the next step of the process. The exchangers, heaters and coolers used for heat integration and energy consumption in this study are shown in Figure 6.17.

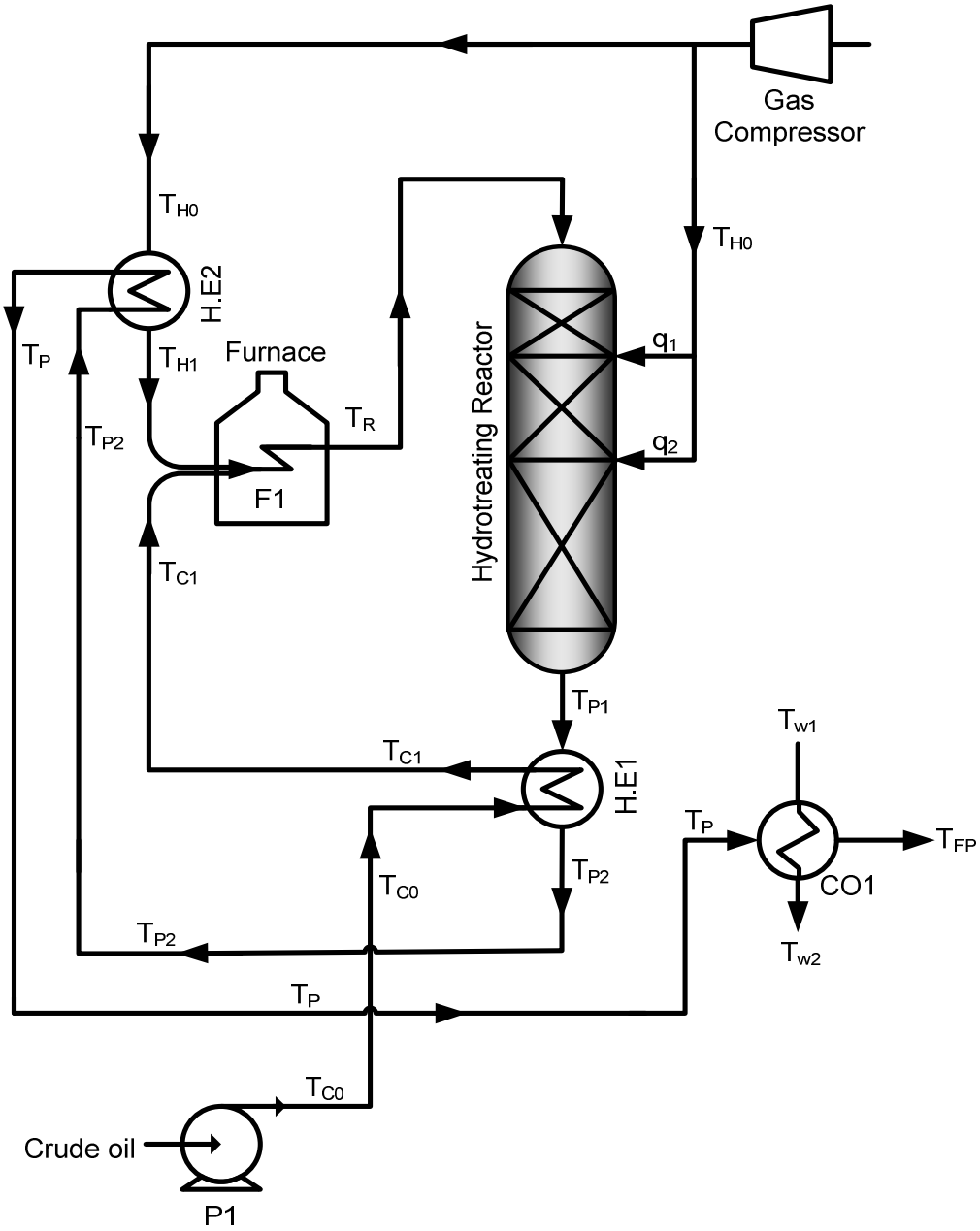

Figure 6.17: Process of heat integrated reaction system

As depicted in Figure 6.17, the crude oil feedstock (cold stream) is pumped by P1 before preheating from T_{C0} to T_{C1} in heat exchanger H.E1. Then, the crude oil is fed into furnace F1 in order to preheat from T_{C1} to the reaction temperature (T_R). The second main feedstock, which is hydrogen (cold stream) is fed into heat exchanger H.E2 to preheat from T_{H0} to T_{H1}. After this, its temperature rises from T_{H1} to the reaction temperature (T_R) by the furnace F1. The product stream leaving the reactor (hot stream) is cooled from T_{P1} to T_{P2} by contacting with the main crude oil feedstock in heat

exchanger H.E1. Due to high reaction products temperature, the products stream is cooled again from T_{P2} to T_P by in contact with hydrogen feed in heat exchanger H.E2, then its temperature is reduced from T_P to the final product temperature (target temperature) T_{FP} in cooler CO1 by using cold water at T_{W1}. The energy balance equations for whole system are given below.

6.3.3 Model Equations

a) Heat Exchanger (H.E1)

The products stream that leaves the reactor is used to preheate the crude oil feedstock from T_{C0} to T_{C1} through H.E1 and at the same time is cooled from T_{P1} to T_{P2}. The heat duties for these streams are described as follows:

$$Q_{1HE1} = (V_L \, c_p^L \, \rho_L)(T_{C1} - T_{C0}) \tag{6.43}$$

$$Q_{2HE1} = (V_L \, c_p^L \, \rho_L + V_G \, c_p^G \, \rho_G)(T_{P2} - T_{P1}) \tag{6.44}$$

$$Q_{2HE1} = Q_{1HE1} \tag{6.45}$$

$$A_{HE1} = \frac{Q_{1HE1}}{U_{HE1} \Delta T_{lm1}} \tag{6.46}$$

$$\Delta T_{lm1} = \frac{\Delta T_1 - \Delta T_2}{\ln\left(\frac{\Delta T_1}{\Delta T_2}\right)} \tag{6.47}$$

$$\Delta T_1 = T_{P1} - T_{C1} \tag{6.48}$$

$$\Delta T_2 = T_{P2} - T_{C0} \tag{6.49}$$

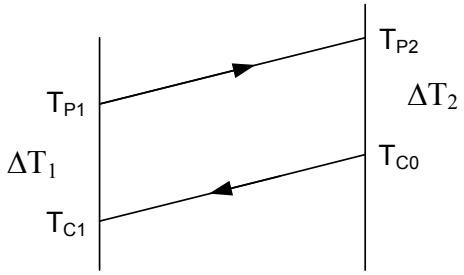

Figure 6.18: Heat exchanger H.E1

Q_{1HE1} and Q_{2HE1} are heat duties of H.E1, T_{C0} is the inlet temperature of the cold fluid, T_{C1} is the outlet temperature of the cold fluid, T_{P1} is the inlet temperature of the hot products mixture, T_{P2} is the outlet temperature of the hot products mixture, V_L is the volumetric flow rate of crude oil, V_G is the volumetric flow rate of hydrogen (includes the main hydrogen feed plus quench feeds), A_{HE1} is the heat transfer area of H.E1, U_{HE1} is the overall heat transfer coefficient for H.E1, and ΔT_{lm1} is the log mean temperature difference for H.E1.

b) Heat Exchanger (H.E2)

The main hydrogen feedstock is heated from T_{H0} to T_{H1} in H.E2 by contact with the products stream that leaves H.E1, which is cooled at the same time from T_{P2} to T_P in H.E2. The model equations for H.E2 are:

$$Q_{1HE2} = (V_{H_2}\, c_p^{H_2}\, \rho_G)\,(T_{H1} - T_{H0}) \tag{6.50}$$

$$Q_{2HE2} = (V_L\, c_p^L\, \rho_L + V_G\, c_p^G\, \rho_G)\,(T_P - T_{P2}) \tag{6.51}$$

$$Q_{2HE2} = Q_{1HE2} \tag{6.52}$$

$$A_{HE2} = \frac{Q_{1HE2}}{U_{HE2}\Delta T_{lm2}} \tag{6.53}$$

$$\Delta T_{lm2} = \frac{\Delta T_3 - \Delta T_4}{\ln\left(\frac{\Delta T_3}{\Delta T_4}\right)} \tag{6.54}$$

$$\Delta T_3 = T_{P2} - T_{H1} \tag{6.55}$$

$$\Delta T_4 = T_P - T_{H0} \tag{6.56}$$

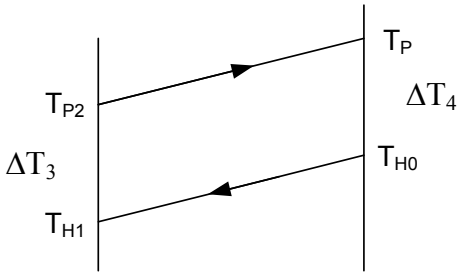

Figure 6.19: Heat exchanger H.E2

Q_{1HE2} and Q_{2HE2} are heat duties of H.E2, T_{H0} is the inlet temperature of the cold fluid, T_{H1} is the outlet temperature of the cold fluid, T_{P2} is the inlet temperature of the hot products mixture, T_P is the outlet temperature of the hot products mixture, V_{H2} is the volumetric flow rate of hydrogen (without quench feeds), A_{HE2} is the heat transfer area of H.E2, U_{HE2} is the overall heat transfer coefficient for H.E2, and ΔT_{lm2} is the log mean temperature difference for H.E2.

c) Cooler (CO1)

The product stream that leaves H.E2 is cooled from T_P to the final product temperature T_{FP} in the cooler by using water at T_{W1}. The model equations for CO1 are shown below:

$$Q_{1CO1} = m_W \; cp_w \, (T_{W2} - T_{W1}) \tag{6.57}$$

$$Q_{2CO1} = (V_L \; c_p^L \; \rho_L + V_G \; c_p^G \; \rho_G)\,(T_{FP} - T_P) \tag{6.58}$$

$$Q_{2CO1} = Q_{1CO1} \tag{6.59}$$

$$A_{CO1} = \frac{Q_{1CO1}}{U_{CO1}\Delta T_{lmc}} \tag{6.60}$$

$$\Delta T_{lmc} = \frac{\Delta T_5 - \Delta T_6}{\ln\left(\frac{\Delta T_5}{\Delta T_6}\right)} \tag{6.61}$$

$$\Delta T_5 = T_P - T_{W2} \tag{6.62}$$

$$\Delta T_6 = T_{FP} - T_{W1} \tag{6.63}$$

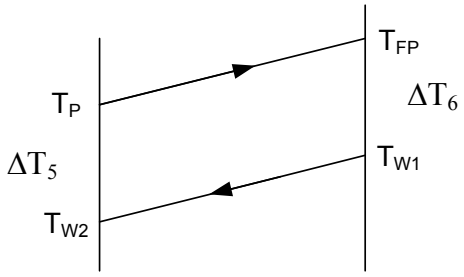

Figure 6.20: Heat exchanger CO1

Q_{1CO1} and $Q_{2\ CO1}$ are heat duties of CO1, T_{W1} and T_{W2} are the inlet and outlet temperature of the cooled water, T_{FP} is the final products temperature, A_{CO1} is the heat transfer area of CO1, U_{CO1} is the overall heat transfer coefficient for CO1, ΔT_{lmc} is the log mean temperature difference for CO1, cp_w is the heat capacity of water and m_w is the mass flow rate of cooling water.

The total heat transfer area (A_t) is given by the following equation:

$$A_t = A_{HE1} + A_{HE2} + A_{CO1} \tag{6.64}$$

d) Furnace (F1)

The main feedstocks, crude oil and hydrogen are fed into furnace F1 separately in order to preheat from T_{C1} to the reaction temperature (T_R) for crude oil and from T_{H1} to T_R for hydrogen. The heat equations for F1 can be written as follows:

$$Q_{H_2} = (V_{H_2}\ c_p^{H_2}\ \rho_G)\,(T_R - T_{H1}) \tag{6.65}$$

$$Q_{Crude} = (V_L\ c_p^{L}\ \rho_L)\,(T_R - T_{C1}) \tag{6.66}$$

$$Q_F = Q_{H_2} + Q_{Crude} \tag{6.67}$$

All of the physical properties of gases and liquids (such as gas and liquid density, heat capacity of gas and liquid, gas compressibility factor) are estimated at an average temperature (T_{av}) for each equipment item using the following equation:

$$T_{av} = \frac{T_{in} + T_{out}}{2} \tag{6.68}$$

T_{in} and T_{out} are the inlet and outlet temperatures for item of each equipment.

.

6.3.4 Optimization Problem Formulation

The optimization problem can be stated as follows:

Given inlet temperature of crude oil (T_{C0}) and hydrogen (T_{H0}), outlet temperature of products mixture (T_{P1}), reaction temperature (T_R), inlet water temperature(T_{W1}), volumetric flow rate of liquid (V_L) and gas (V_{H2} and V_G).

Optimize T_{P2}, T_{H1}, T_{W2}

So as to minimize the total annual cost of the process (C_t).

Subject to process constraints and linear bounds on all decision variables.

Mathematically, the optimization problem can be presented as:

$$\textit{Min} \quad C_t$$

$$T_{P2}, T_{H1}, T_{W2}$$

$$s.t \quad f(x(z), u(z), \underline{y}) = 0 \qquad \text{(model, equality constraints)}$$

$$T_{P2}^{L} \le T_{P2} \le T_{P2}^{U} \qquad \text{(inequality constraints)}$$

$$T_{H1}^{L} \le T_{H1} \le T_{H1}^{U} \qquad \text{(inequality constraints)}$$

$$T_{W2}^{L} \le T_{W2} \le T_{W2}^{U} \qquad \text{(inequality constraints)}$$

$$\Delta T_F^{L} \le \Delta T_F \le \Delta T_F^{U} \qquad \text{(inequality constraints)}$$

$$\Delta T_W^{L} \le \Delta T_W \le \Delta T_W^{U} \qquad \text{(inequality constraints)}$$

$$T_R = T_R^{*} \qquad \text{(equality constraints)}$$

$$T_{FP} = T_{FP}^{*} \qquad \text{(equality constraints)}$$

ΔT_W and ΔT_F are the temperature differences between the inlet and outlet temperatures of water in the cooler and liquid crude oil in the furnace, respectively. T_R^{*} is the required reaction temperature (which is 400°C) and T_{FP}^{*} is the target final temperature of product (which is 26°C). In practice, the best temperature difference between inlet and outlet

water in the cooler is within 5-20°C, and between inlet and outlet crude oil in the furnace within 100-130°C, which are quite practical.

6.3.4.1 Cost Function

The objective function is the overall annual process cost (C_t), which can be calculated using the following expression:

$$C_t\ (\$/yr) = Annualized\ Capital\ Cost\ (\$/yr) + Operating\ Cost\ (\$/yr) \tag{6.69}$$

$$Capital\ Cost\ (\$) = Reactor\ Cost\ (C_R) + Compressor\ Cost\ (C_{Comp}) + Heat\ Exchanger\ Cost\ (C_{HE}) + Pump\ Cost\ (C_P) + Furnace\ Cost\ (C_F) \tag{6.70}$$

To determine the annualized capital cost from capital cost, equation 6.36 is used for this purpose, while, the operating cost is calculated as shown below:

$$Operating\ Cost\ (\$/yr) = Heating\ Cost\ (C_H) + Compression\ Cost\ (C_{Cmpr}) + Pumping\ Cost\ (C_{PU}) + Cooling\ Cost\ (C_{Col}) \tag{6.71}$$

Reactor cost (C_R) is estimated using equations (6.9) and (6.10). Compressor cost (C_{Cmpr}) is determined using equations (6.37) to (6.41). The compression cost (C_{Cmpr}) is calculated using equation 6.42. The other capital costs of equipment can be estimated using the following equations (Douglas, 1988; Smith, 2005; Quintero and Villamil, 2009):

a) Heat Exchanger Cost (C_{HE})

$$C_{HE}(\$) = \left(\frac{M\ \&\ S}{280}\right) 210.78\ A_t^{0.65} (2.29 + F_C) \tag{6.72}$$

$$F_C = (F_d + F_p)\, F_m \tag{6.73}$$

b) Pump Cost *(C_P)*

$$C_P(\$) = \left(\frac{M\ \&\ S}{280}\right) 9.84 \times 10^3 F_C \left(\frac{Q_P}{4}\right)^{0.55} \tag{6.74}$$

$$F_C = F_m F_p F_T \tag{6.75}$$

c) **Furnace Cost *(C_F)***

$$C_F(\$) = \left(\frac{M\ \&\ S}{280}\right) 5.52 \times 10^3\ Q_F^{0.85}\ (1.27 + F_C) \tag{6.76}$$

$$F_C = F_d + F_m + F_p \tag{6.77}$$

A_t is the total heat transfer area, Q_p is the pump power, Q_F is the heat duty of the furnace, and F_C, F_m, F_p, F_T and F_d are the dimensionless factors that are functions of the construction material, operating pressure and temperature, and design type.

The operating cost is calculated using the following expressions:

a) Heating Cost *(C_H)*

$$C_H(\$/yr) = \left(Q_F(kW)\right)\left(\frac{0.062\$}{kWh}\right)\left(\frac{24h}{1day}\right)\left(\frac{340day}{1yr}\right) \tag{6.78}$$

b) Pumping Cost *(C_{PU})*

$$C_{PU}(\$/yr) = \left(Q_P(kW)\right)\left(\frac{0.062\$}{kWh}\right)\left(\frac{24h}{1day}\right)\left(\frac{340day}{1yr}\right) \tag{6.79}$$

b) Cooling Cost *(C_{Col})*

$$C_{Col}(\$/yr) = \left(m_w\left(\frac{kg}{h}\right)\right)\left(\frac{f_w\$}{kg}\right)\left(\frac{24h}{1day}\right)\left(\frac{340day}{1yr}\right) \tag{6.80}$$

f_w is the price of cooling water, which is 0.0305 $ per ton of water (Khalfallah, 2009).

6.3.5 Results and Discussion

The values of constant parameters with factors and coefficients used in this model (Douglas, 1988; Sinnott, 2005; Smith, 2005) are listed in Table 6.7.

Table 6.7: Values of constant parameters, factors and coefficients used in this model

Parameter	**Unit**	**Value**
T_{C0}	°C	28.00
T_{H0}	°C	70.00
T_{P1}	°C	406.02
T_{W1}	°C	20.00
Cp_w	kJ/kg K	4.189
U_{HE1}	W/m^2 K	250
U_{HE2}	W/m^2 K	113
U_{CO1}	W/m^2 K	400
Dimensionless Factors		
	Furnace	**Pump**	**Heat Exchanger**
F_m	0.75	1.0	3.75
F_p	0.15	1.9	0.625
F_d	1.0	0.0	1.0
F_T	0.0	1.0	0.0

The optimization results, which are summarized in Table 6.8 show that the minimum total cost (C_t) and cooling water amounts with heat integration of the hydrotreating process are less than those without the heat integration at specified variables. The cost saving is 55.76% in comparison with the cost obtained without heat integration to achieve the reaction temperature (400°C) and to reduce the final product temperature up to 26°C. Also, the amount of cooling water required for reaching the final product temperature is greater than that with heat integration due to the heat recovery and consequently the cost of the cold utility in addition to capital cost of cooler will decrease.

The results also show that the minimum energy requirement was reduced by 64.2%. Therefore, CO_2 emission will be reduced by 64.2%, which has the added benefit of significantly reducing environmental impact.

Table 6.8: Results of optimization problem for heat integration process

Variables	**Without heat integration**	**With heat integration**	**Decision variable type**	**Optimized value**
A_t (m^2)	475.3148	1033.207	T_{P2} (°C)	202.99
C_t ($/yr)	9744870.8	4310909.8	T_{H1} (°C)	200.57
CS (%)	-------	55.76	T_{W2} (°C)	40.00
m_w (kg/hr)	711873.9	272716.56	T_R (°C)	400.00
Q_t (kJ)	1386189676.8	496317300.5	ΔT_F (°C)	110.25
Q_C (kJ)	1431379037	548357040	ΔT_W (°C)	20.00
Q_{HE1} (kJ)	-------	784918598.4	T_{FP} (°C)	26.00
Q_{HE2} (kJ)	-------	104953777.9	-------	-------
Q_r (kJ)	-------	889872376.3	-------	-------
ES (%)	0.0	64.2	-------	-------

CS = Cost saving, ES = Energy saving, Q_r = Heat recovery, Q_t = Total heating, Q_C = Heat duty of cooler, Q_{HE} = Heat duty of exchanger$_{1,2}$.

6.4 Economic Analysis of Industrial Refining Process

In general, over the past decades it has been noticed a growing dependence on high heavier oils and residua emerge as a result of continuing increases in the prices of the conventional crude oils coupled with the decreasing availability of these crude oils through the depletion of reserves in various parts of the world. The primary objective of developing hydrotreating process is to reduce the content of impurities with high efficiency and high selectivity (Ancheyta and Speight, 2007). The development of a new chemical process, which includes technical and economic effort, should meet a

defined and practical need of an industry. The nature of petroleum refining refers to the use of continuous flow reactor for long production runs of high volume fuel stream.

In this part of this Chapter, the developed hydrotreating unit is joined with the other complementary units up to middle distillates production units in order to compare the results between oil fractions produced by hydrotreating of crude oil directly then distillation process (this study) and produced by the conventional method (hydrotreating process of each fraction separately after distillation process). The difference between this study and conventional method in terms of yields and properties of the middle distillates and R.C.R were discussed in Chapter three. The economic analysis of these methods is studied in this section.

6.4.1 Process Description

The layout of a developed hydrotreating unit with the other refinery units for middle distillates production is shown in Figure 1.

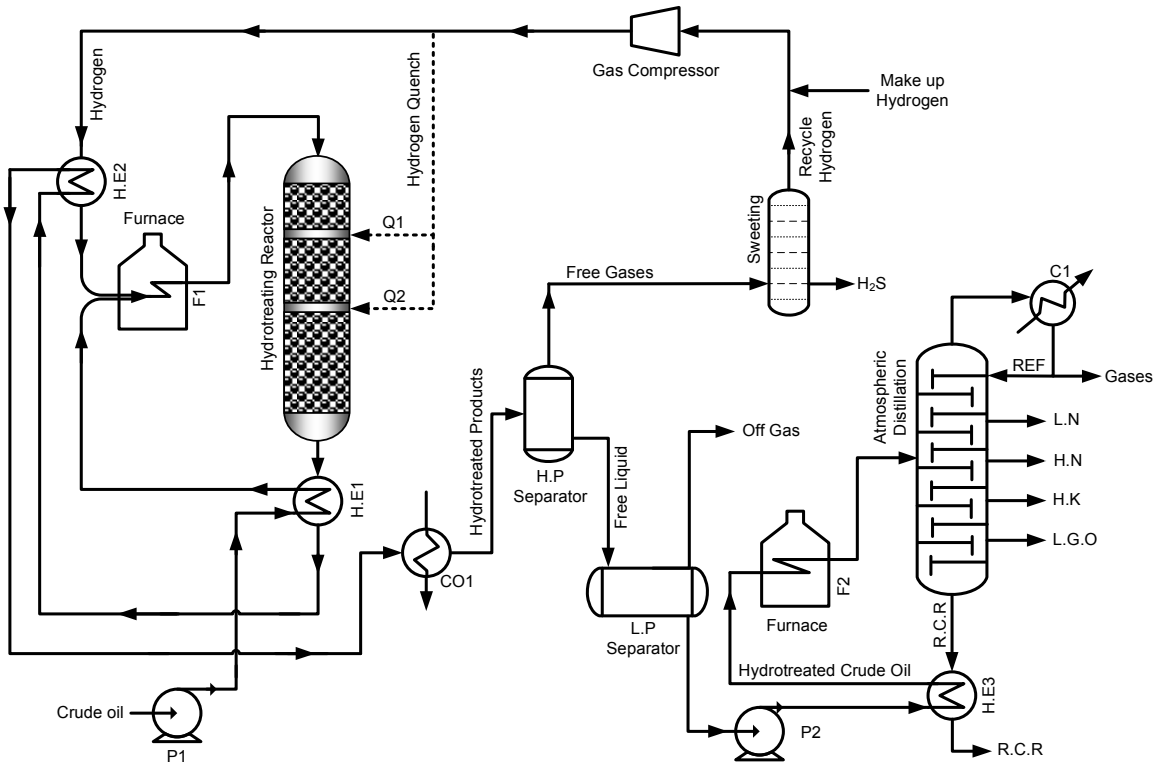

Figure 6.21: Layout of a developed HDT unit with middle distillates production units

As mentioned previously, the crude oil feedstock is pumped by P1 to the heat exchanger (H.E1) and furnace (F1) to raise its temperature to the reaction temperature before entering the reactor. The products mixture that leave the reactor is used to preheat the crude oil inlet by H.E1 and then is utilized to preheat the hydrogen inlet by heat exchanger (H.E2), which is heated again to the reaction temperature by F1. The products mixture is cooled to the final product temperature by cooler (CO1).

The cold hydrotreated product is fed to the high pressure separator (H.P.S) in order to separate the free gases (such as unreacted hydrogen, H_2S) from free liquid hydrocarbons. The unreacted hydrogen is removed from free gases (especially H_2S) in sweeting unit (some time is called amine absorber unit) and is recycled to the system with the make up hydrogen to provide the hydrogen required, which is fed to the reactor by gas compressor. The free liquid products stream that leaves H.P.S is passed to the low pressure separator (L.P.S) where the dissolved gases (which inhibit HDT reactions) are separated from the hydrotreated crude oil. The clean hydrotreated crude oil is pumped by P2 to the atmospheric distillation column. Before entering the column distillation, crude oil is passed through a series of heat exchangers (described by H.E3) to raise its temperature up to 230 °C by in contact with R.C.R drawn from the bottom of the distillation tower, and then to a heating furnace (F2), which brings the temperature up to about 350°C (as usually used in the petroleum refineries (Ashaibani and Mujtaba, 2007)). The hot crude oil enters the distillation column and the principle of the distillation process is based on the boiling point for each fraction, where each cut has a certain boiling point. The vaporized liquid that leaves from the top of the column with the gases is passed through a condenser (C1) to condensate it and then is recycled to the column by refluxing process. The uncondensed gases are drawn as gases products. The R.C.R leaved from the bottom of the distillation column is cooled by in contact with the

inlet crude oil in H.E.3 and then is used as a main feedstock to the vacuum distillation process.

As mentioned previously using the convential method, the basic operation of a refinery in the atmospheric distillation unit is the conversion of crude oil into its derivatives such as LPG (gases), gasoline (Light Naphtha (L.N) and Heavy Naphtha (H.N)), heavy kerosene (H.K) and light gas oil (L.G.O). Then hydrotreating process is carried out on each fraction separately. After that, the hydrotrated products are passed through separation systems where gas-liquid are separated to the amine absorber units to remove the hydrogen unreacted from free gases. A simplified layout of the conventional middle distillates production unit with hydrotreating units is shown in Figure 6.22.

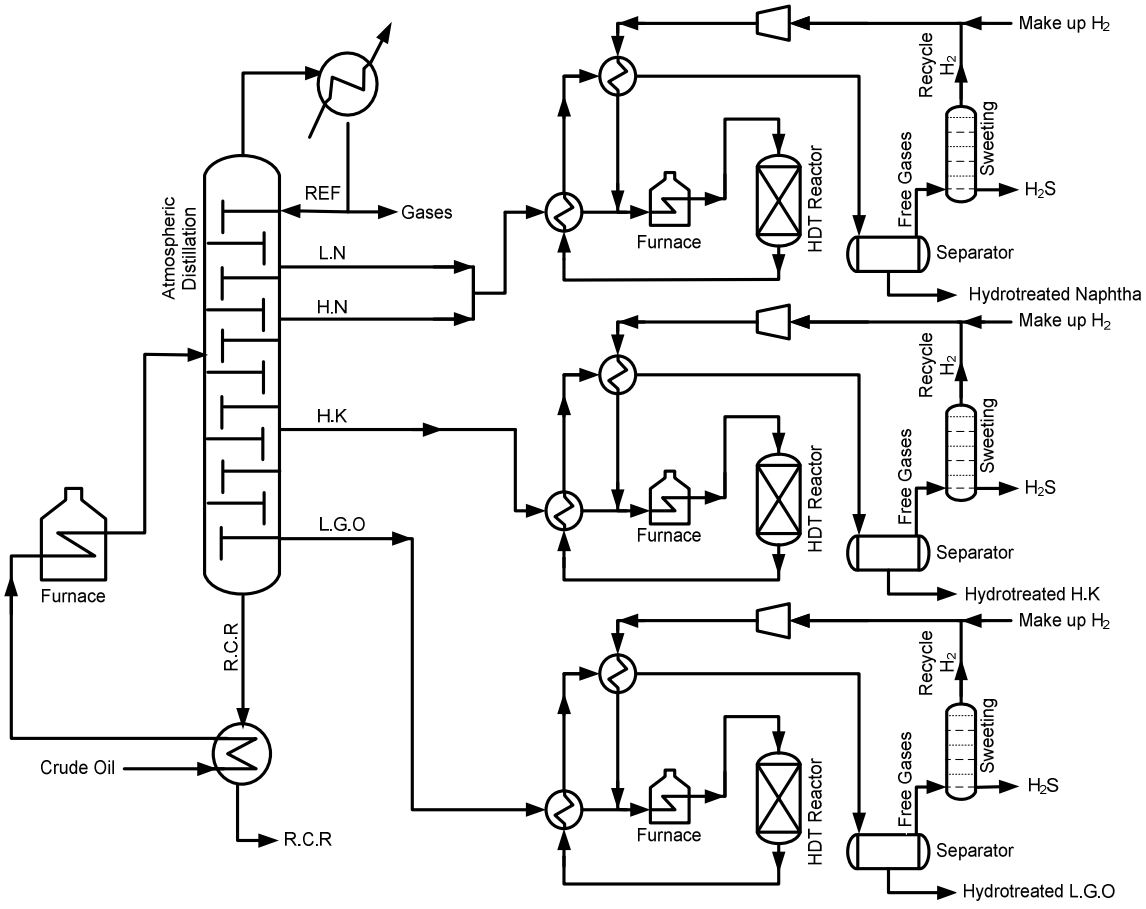

Figure 6.22: Schematic of conventional middle distillates production unit with HDT units

6.4.2 Cost Model Equations

In this section, the design of equipment and cost models for whole the process presented in Figure 6.21 is studied in order to compare the overall annual cost of the developed process with the conventional method used up to middle distillates production unit. Thus, it is important to define the overall annualized cost (OAC) of the process, which can be written as follows:

$$OAC\ (\$/yr) = Total\ Annual\ Capital\ Cost\ (TACC) + Total\ Annual\ Operating\ Cost\ (TAOC) \tag{6.81}$$

$$TACC\ (\$/yr) = Total\ Capital\ Cost\ (TCC) \times \frac{i(1+i)^n}{(1+i)^n - 1} \tag{6.82}$$

The total capital cost is given by following equation (Sinnott, 2005; Smith, 2005):

$$TCC\ (\$) = Total\ Capital\ Cost\ of\ Installed\ Equipment\ (TCI) \times 1.45 \tag{6.83}$$

$$TCI\ (\$) = Reactor + Furnaces\ (1\&2) + Pumps\ (1\&2) + Compressor + Distillation\ Column + Cooler + Heat\ Exchangers\ (1,2\&3) + High\ Pressure\ Separator + Low\ Pressure\ Separator + Condenser + Sweeting\ Column \tag{6.84}$$

The total annual operating cost (TAOC) is estimated by using the following equation (Sinnott, 2005):

$$TAOC\ (\$/yr) = Variable\ Operating\ Cost\ (VOC) + Fixed\ Operating\ Cost\ (FOC) \tag{6.85}$$

$$VOC\ (\$/yr) = Heating\ (with\ F1\&F2) + Pumping\ (with\ P1\&P2) + Compression + Cooling\ Water\ (with\ CO1\&C1) + Catalyst + H_2\ Consumption \tag{6.86}$$

$$FOC\ (\$/yr) = Maintenance\ (f_1) + Operating\ Labour\ (f_2) + Laboratories\ (f_3) + Supervision\ (f_4) + Plant\ Overheads\ (f_5) + Capital\ Charge\ (f_6) + Rates\ (with\ other\ local\ taxes)(f_7) + Insurance\ (f_8) + Licence\ Fees\ (f_9) \tag{6.87}$$

The items defined in fixed operating cost with their values are (Douglas, 1988; Edgar et al., 2001; Sinnott, 2005; Smith, 2005):

a) **Maintenance:** This item involves the cost of maintenance labour and the materials (including equipment spares) needed for the maintenance of the plant. The annual maintenance costs typically 5 to 15 % of the installed capital costs.

b) **Operating labour:** Involves the manpower needed to operate the plant, which directly included with running the process. It represents 15 % of the total annual operating cost.

c) **Laboratory costs:** Includes the laboratory analyses required for process monitoring and quality control. Its value can be taken as 20 to 30 % of the operating labour cost.

d) **Supervision:** This item covers the direct operating supervision, the management directly associated with running the plant. A typical value is 25% of the operating labours cost.

e) **Plant overheads:** Involves all the general costs associated with operating the plant that are not included with other headings (such as, offices, plant security, medical, canteen, warehouses, staff and safety). A typical range would be 50 to 100 % of the operating labours cost.

f) **Capital charges:** Capital is often recovered as a depreciation charge. This would be typically around 10 % of the total capital cost.

g) **Rates:** This term covers local taxes, which would be 1 to 2 % of the total capital cost.

h) **Insurance:** Insurers are usually about 1 to 2 % of the total capital cost.

i) **Licence Fees:** Licence fees are about 1% of the total capital cost. The typical values of fixed operating cost, which can be used to make an approximate estimate of production cost, are summarized in Table 6.9.

Table 6.9: Summary of fixed operating cost

Fixed Operating Cost		Typical Values
f_1	Maintenance	10% of *TCI*
f_2	Operating labour	15% of *TAOC*
f_3	Laboratory costs	25% of f_2
f_4	Supervision	25% of f_2
f_5	Plant overheads	75% of f_2
f_6	Capital charges	10% of *TCC*
f_7	Rates	1.5% of *TCC*
f_8	Insurance	2% of *TCC*
f_9	Licence Fees	1% of *TCC*

The capital cost equations for reactor, furnace1, pump1, compressor, heat exchanger 1&2 and cooler in addition to the operating cost (which are heating for furnace 1, pumping for pump1, compression and cooling water cost for cooler, have been mentioned previously in sections 6.2.1, 6.2.2.3 and 6.3.4.1 of this Chapter. The other capital costs of equipments are calculated using the following equations (Douglas, 1988; Smith, 2005; Quintero and Villamil, 2009):

a) Furnace2 Cost *(C_{F2})*

$$C_{F2}(\$) = \left(\frac{M\ \&\ S}{280}\right) 5.52\times10^{3}\ Q_{F2}^{0.85}\ (1.27 + F_C) \tag{6.88}$$

$$F_C = F_d + F_m + F_p \tag{6.89}$$

$$Q_{F2} = (V_L\ c_p^L\ \rho_L)\,(T_{F\,out} - T_{Cr2}) \tag{6.90}$$

b) Pump Cost *(C_{P2})*

$$C_{P2}(\$) = \left(\frac{M\ \&\ S}{280}\right) 9.84\times10^{3}\ F_C \left(\frac{Q_{P2}}{4}\right)^{0.55} \tag{6.91}$$

$$F_C = F_m F_p F_T \tag{6.92}$$

c) Heat Exchanger (H.E3) Cost *(C_{HE3})*

$$C_{HE3}(\$) = \left(\frac{M\ \&\ S}{280}\right) 210.78\,(A_{HE3})^{0.65}\,(2.29 + F_C) \tag{6.93}$$

$$F_C = (F_d + F_p)\, F_m \tag{6.94}$$

$$Q_{Cr} = V_L\, \rho_L\, cp_L\, (T_{Cr2} - T_{Cr1}) \tag{6.95}$$

$$Q_{RCR} = (V_{RCR}\, c_p^{RCR}\, \rho_{RCR})\, (T_{RCR2} - T_{RCR1}) \tag{6.96}$$

$$Q_{Cr1} = Q_{RCR} \tag{6.97}$$

$$A_{HE3} = \frac{Q_{Cr}}{U_{HE3} \Delta T_{lm3}} \tag{6.98}$$

$$\Delta T_{lm3} = \frac{(T_{RCR1} - T_{Cr2}) - (T_{RCR2} - T_{Cr1})}{\ln\left(\frac{T_{RCR1} - T_{Cr2}}{T_{RCR2} - T_{Cr1}}\right)} \tag{6.99}$$

d) Condenser (C1) Cost *(C_{C1})*

$$C_{C1}(\$) = \left(\frac{M\ \&\ S}{280}\right) 210.78\, (A_{C1})^{0.65} (2.29 + F_C) \tag{6.100}$$

$$F_C = (F_d + F_p)\, F_m \tag{6.101}$$

$$Q_{1C1} = m_{W2}\, cp_w\, (T_{WC2} - T_{WC1}) \tag{6.102}$$

$$Q_{2C1} = V_N\, c_p^N\, \rho_N\, (T_{N2} - T_{N1}) \tag{6.103}$$

$$Q_{2C1} = Q_{1C1} \tag{6.104}$$

$$A_{C1} = \frac{Q_{1C1}}{U_{C1} \Delta T_{lmc1}} \tag{6.105}$$

$$\Delta T_{lmc1} = \frac{(T_{N1} - T_{WC2}) - (T_{N2} - T_{WC1})}{\ln\left(\frac{T_{N1} - T_{WC2}}{T_{N2} - T_{WC1}}\right)} \tag{6.106}$$

e) High Pressure Separator and Low Pressure Separator Cost

$$C_i(\$) = \left(\frac{M\ \&\ S}{280}\right) 937.63\, (D_i)^{1.066}\, (L_i)^{0.802}\, (2.18 + F_C) \tag{6.107}$$

$$F_C = F_m F_p \tag{6.108}$$

f) Distillation Column Cost (C_{Dis})

The total cost of distillation column is given:

$$C_{Dis}\ (\$) = Column\ Cost\ (C_{col}) + Tray\ Cost\ (C_{tray}) \tag{6.109}$$

The column cost is calculated by eq. 6.107 above. The tray cost is estimated as follows:

$$C_{tray}(\$) = \left(\frac{M\ \&\ S}{280}\right) 97.24\, L_{col}\, D_{col}^{1.55}\, F_C \tag{6.110}$$

$$F_C = F_s + F_m + F_t \tag{6.111}$$

g) Sweeting Column Cost (C_{Swe})

$$C_{Swe}\ (\$) = Column\ Cost\ (C_{col}) + Tray\ Cost\ (C_{tray}) \tag{6.109}$$

The column and tray costs of sweeting are calculated using Eq.s 6.107 and 6.110 above.

Q_{F2} is the heat duty of furnace2, Q_p is the power pump of P2, A_{HE3}, A_{C1} are the total heat transfer area of H.E3 and C1, Q_{Cr} and Q_{RCR} are heat duties of H.E3, $T_{Cr1,2}$, $T_{RCR1,2}$ are the inlet and outlet temperature of the hot and cold fluid of H.E3, V_{RCR} is the volumetric flow rate of R.C.R, cp^{RCR} is the heat capacity of R.C.R, ρ^{RCR} is the density of R.C.R, U_{HE3}, ΔT_{lm3} are the overall heat transfer coefficient and the log mean temperature difference for H.E3, Q_{1C1} and Q_{2C1} are heat duties of C1, $T_{N1,2}$, $T_{WC1,2}$ are the inlet and outlet temperature of the hot and cold fluid of C1, V_N is the volumetric flow rate of naphtha, cp^N , ρ^N are the heat capacity and density of naphtha, U_{C1}, ΔT_{lmc1} are the overall heat transfer coefficient and the log mean temperature difference for C1, m_{W2} is the mass flow rate of cooling water, D_i, L_i are the diameter and length of H.P.S, L.P.S and sweeting column, D_{col}, L_{col} are the diameter and length of distillation column, respectively.

The operating cost is calculated using the following equations:

a) Heating Cost of Furnace2 *(C_{H2})*

$$C_{H2}(\$/yr) = \left(Q_{F2}(kW)\right)\left(\frac{0.062\$}{kWh}\right)\left(\frac{24h}{1day}\right)\left(\frac{340day}{1yr}\right) \tag{6.112}$$

b) Pumping Cost of Pump2 *(C_{PU2})*

$$C_{PU2}(\$/yr) = \left(Q_{P2}(kW)\right)\left(\frac{0.062\$}{kWh}\right)\left(\frac{24h}{1day}\right)\left(\frac{340day}{1yr}\right) \tag{6.113}$$

b) Cooling Cost of Condenser *(C_{Col2})*

$$C_{Col2}(\$/yr) = \left(m_{w2}\left(\frac{kg}{h}\right)\right)\left(\frac{0.0305\$}{1000\,kg}\right)\left(\frac{24h}{1day}\right)\left(\frac{340day}{1yr}\right) \tag{6.114}$$

e) Catalyst Cost *(C_{cat})*

$$C_{cat}(\$/yr) = \left(V_C\left(m^3\right)\right)\left(\rho_{cat}\left(\frac{kg}{m^3}\right)\right)\left(\frac{f_{cat}\$}{kg}\right)\left(\frac{1}{t_{cat}(yr)}\right) \tag{6.115}$$

f_{cat} is the price of catalyst, which is 9.92 $/kg (Quintero and Villamil, 2009), t_{cat} is the catalyst life (which is assumed to be 3 years (Edgar et al., 2001)).

f) Hydrogen Consumption Cost *(C_{Hcons})*

$$C_{Hcons}(\$/yr) = \left(J_{H_2}\left(\frac{Nm^3_{H_2}}{m^3_{Oil}}\right)\right)\left(V_L\left(\frac{m^3_{Oil}}{h}\right)\right)\left(\frac{f_{H_2}\$}{Nm^3_{H_2}}\right)\left(\frac{24h}{1day}\right)\left(\frac{340day}{1yr}\right) \tag{6.116}$$

The total H_2 consumption (J_{H2}) is calculated using the following equations (Lee et al., 2008; Stratiev et al., 2009; Mapiour et al., 2010):

$$J_{H2}\ (Nm^3/m^3) = \text{Chemical } H_2 \text{ consumption } (J_C) \times 1.15 \tag{6.117}$$

$$J_C = (J_{HDS} + J_{HDN} + J_{HDAs} + J_{HDV} + J_{HDNi} + J_{H_2S} + J_{NH_3}) + 8.7 \tag{6.118}$$

$$J_{HDS} = J_{H_2S} = \frac{\left[(S)_f - (S)_p\right] \times \rho_f}{Mw_S \times 100} \times 22.414 \tag{6.119}$$

$$J_{HDN} = J_{NH_3} = \frac{\left[(N)_f - (N)_p\right] \times \rho_f}{Mw_N \times 100} \times 22.414 \quad (6.120)$$

$$J_{HDAs} = \frac{\left[(Asph)_f - (Asph)_p\right] \times \rho_f}{Mw_{Asph} \times 100} \times 22.414 \quad (6.121)$$

$$J_{HDV} = \frac{\left[(V)_f - (V)_p\right] \times \rho_f}{Mw_V \times 100} \times 22.414 \quad (6.122)$$

$$J_{HDNi} = \frac{\left[(Ni)_f - (Ni)_p\right] \times \rho_f}{Mw_{Ni} \times 100} \times 22.414 \quad (6.123)$$

Nm^3_{H2} is the hydrogen consumption expressed at normal conditions (0 °C and 1atm), f_{H2} is the price of H_2, which is 0.49 \$/Nm^3_{H2} (Weinert et al., 2007). 1.15 is the mechanical losses and dissolved H_2, J_{HDS}, J_{HDN}, J_{HDAs}, J_{HDV}, J_{HDNi}, are the amount of H_2 necessary to form a hydrocarbon during HDS, HDN, HDAs, HDV and HDNi (Nm^3/m^3), respectively. J_{H2S} and J_{NH3} are the H_2 content of H_2S and NH_3 in the product gas (Nm^3/m^3), respectively, 8.7 is the standard deviation of this process measurement, S, N, Aspha, V and Ni are sulfur, nitrogen, asphaltene, vanadium and nickel contents (wt %), respectively, subscripts *f* and *p* are feed and products, respectively, ρ_f is the feed density. 22.414 is the number of normal cubic meter in a kmol of an ideal gas (Nm^3/kmol), Mw_S, Mw_N, Mw_{Asph}, Mw_V, and Mw_{Ni}, are the molecular weights of S, N, Aspha, V and Ni, respectively. The 100 factor in the denominator is S, N, Aspha, V and Ni in weight percent.

6.4.3 Results and Discussion

The model equations (presented in Chapter Five and this Chapter) for calculating the overall annualized cost of crude oil HDT process for middle distillates production is simulated in gPROMS software.

Note, the conditions and dimensions of column distillation, furnace2, P2, H.E3, condenser and sweeting column were taken from Baiji North Refinery (Al-Sinniyah Refinery), which uses the same capacity (10000 bbl/day) and same crude oil employed in this work. Whereas, the typical dimensions of H.P.S and L.P.S are estimated according to the plant capacity (in term of bbl/day) as presented in Guo et al. (2007). The constant parameters, dimensions, conditions and dimensionless factors are listed in Table 6.10.

Table 6.10: Values of constant parameters, factors and coefficients used in this model

Parameter	**Unit**	**Value**
T_{Cr1}	°C	28.00
T_{Cr2}	°C	230.00
T_{RCR1}, T_{Fout}	°C	350.00
T_{RCR2}	°C	66.60
T_{WC1}	°C	28.00
T_{WC2}	°C	39.00
T_{N1}	°C	100.00
T_{N2}	°C	36.00
m_{W2}	kg/h	14094.00
U_{HE3}	$W/m^2 K$	200
U_{C1}	$W/m^2 K$	850
D_{HPS}	m	1.37
L_{HPS}	m	2.51
D_{LPS}	m	0.915
L_{LPS}	m	3.28
$D_{Sweeting}$	m	1.524
$L_{Sweeting}$	m	15.85
$D_{Distillation}$	m	2.134
$L_{Distillation}$	m	24.69

Dimensionless Factors

	F_m	F_p	F_d	F_T	F_t	F_s
Furnace2	0.75	0.0	1.0	-----	-----	-----
Pump2	1.0	1.5	-----	1.0	-----	-----
Heat Exchanger3	3.75	0.0	1.0	-----	-----	-----
Condenser	3.75	0.0	1.0	-----	-----	-----
H.P.S	3.67	2.5	-----	-----	-----	-----
L.P.S	3.67	1.0	-----	-----	-----	-----
Sweeting Column	2.25	1.19	-----	-----	-----	-----
Distillation Column	3.67	1.0	-----	-----	-----	-----
Tray (distillation)	1.7	-----	-----	-----	0.4	1.0
Tray (sweeting)	1.7	-----	-----	-----	0.0	1.4

The results of economic analysis for crude oil hydrotreating followed by distillation process to produce middle distillates fraction (naphtha, kerosene and light gas oil) and comparative results with conventional method (where distillation process of crude oil then hydrotreating process for each fraction separately) are shown in Table 6.11.

The economic results presented in this Table are based on the total operating and capital annualized cost for the whole process up to the production of middle distillate cuts unit.

Table 6.11: Economic and comparison results of the developed HDT process

Cost Function	**Unit**	**Value**
OAC	($/yr)	32327369.6
TACC	($/yr)	2055359.6
TAOC	($/yr)	30272010.0
	Comparative Results	
	This Study	**Conventional Method**
Plant Capacity (*bbl/day*)	10000	10000
OAC (*$/yr*)	32327369.6	38736200.0
H_2 Consumption (Nm^3/m^3)	40.569	48.70
Cost/barrel (*$/bbl*)	9.508	11.393
Total Cost Saving (*%*)	16.54	0.0
Cost Saving/barrel (*$/bbl*)	1.885	0.0

As can be seen from these results, the biggest impact of the overall annual cost is attributed to the operating cost (particularly, hydrogen consumption) that change throughout the year compared with capital cost. The comparison results indicate that the OAC of this study is less than those obtained by the conventional method (CM) at the same plant capacity. The cost of barrel is 9.508 $/bbl in comparison with the barrel cost produced by conventional method, which is 11.393 $/bbl. On the other hand, the cost

saving is around 16% compared with the CM, which means 1.885 $/bbl cost saving per barrel. This saving in the cost is due to several reasons, mainly: (a) H_2 consumption is 40.569 Nm^3/m^3 compared with CM (48.7 Nm^3/m^3), which gives a clear indications that the HDT of crude oil before distillation is better than HDT of each fraction separately, especially with the heavy fractions that need large quantities of hydrogen. (b) the number of equipments used with CM is more than those used in this study due to the presence of HDT unit for each cut, which leads to increase the operating cost and consequently increase in the overall annual cost.

6.5 Conclusions

Design of industrial trickle bed reactor with the optimal operation of commercial hydrotreating unit is studied for evaluating viability of large-scale operation of crude oil hydrotreating process. Commercial hydrotreating reactors operate under non-isothermal behaviour and such chemical reactions are usually exothermic. Therefore, energy balance equations along the catalyst bed length after estimation the optimal reactor length to reactor diameter have been added to the mathematical models obtained by depending on experimental work. The main problem in such reactor is the control of the reaction temperature inside the reactor, where the reaction temperature increased along the catalyst bed. Thus, quench process has been carried out to control the reaction temperature at maximum allowed temperature limit at each catalyst bed by several simulations of quench position and quench flow rate on the reaction system using one quench-two beds and two quenches-three beds, where the objective function was to minimize the total annual cost.

The concentration profiles of H_2, H_2S, S, N, Asph, V, and Ni along the industrial bed length have also been investigated after validating the industrial reactor model. It has

been found that the hydrogen partial pressure increased after each quench position with opposite phenomena of H_2S. Also, the conversions of sulfur, nitrogen, asphaltene, vanadium and nickel in addition to middle distillate yields at industrial reactor are higher than those obtained at pilot plant reactor.

Heat integration and energy consumption in a HDT process were investigated. It has been observed that the energy consumption and heat recovery is considered a big issue that should be taken into account in industrial operations particularly when the type of reactions are exothermic, the recovery of which is very significant for maximizing profitability of the process. Optimization problem was formulated to optimize some of the design and operating parameters of integrated process while minimizing an objective function, which is a coupled function of capital and operating costs including design parameters. Optimal minimum energy requirements, heat recovery and cost saving were obtained utilizing optimization process. The results show that the cost saving is 55.76% and the energy saving is 64.2% in comparison to the process without heat integration. This saving in the energy consumption provides better minimum energy requirement, hence reducing environmental effect and maximum heat recovery.

The economic analysis of whole industrial refining process, which includes the developed hydrotreating unit with the other complementary units (from crude oil pumping until getting middle distillates fractions) and the comparison results of these fractions produced by conventional method, has also been studied. The economic results indicate that the crude oil hydrotreating directly then separation process by distillation give overall annul cost less than those obtained by the conventional method (separation of crude oil to several cuts then hydrotreating of each cut separately). For example, 16.54% total cost saving and 1.885$ cost saving per barrel has been obtained by the new method compared.

Chapter Seven

Conclusions and Future Work

7.1 Conclusions

Petroleum has become one of the most important energy sources. Oil refining industry is now regarded as a significant part in the field of industries and the worldwide demand for transportation fuels with fuel quality showed an important growth and increasing in recent years. Hydrotreatment of crude oil, which is regarded a new technology that has not been studied and reported in the public domain can upgrade the fuel quality by removing the impurities (mainly sulfur, nitrogen, metals, asphaltene) in addition to enhancement of productivity of distillate fractions. As highlighted in Chapter Two, hydrotreating process has become today nearly half of total refining capacity and can be considered the most common process units in oil refining industries. It has also been observed that the trickle bed reactor can be utilized for large operations in chemical process. Also, development of kinetic model in trickle bed reactor that can be used with high accuracy to describe the behaviour of the HDT process is necessary for developing a reliable kinetic model, which can effectively applied to reactor design and operation.

In order to determine the kinetic parameters and to validate the kinetic models with predicted the expected behaviour for crude oil hydrotreating in addition to middle distillates yields at various operating conditions, detailed experimental data of the relevant reactions are required, which are reported in Chapter Three. It has been found that the hydrotreating of whole crude oil directly can increase the yield of middle distillate fractions (transportation fuels) and simultaneously improve the fuel quality by reducing the contents of contaminants (mainly sulfur (S), nitrogen (N), asphaltene (Asph), vanadium (V) and nickel (Ni)). The effect of different operating conditions such

as reaction temperature, hydrogen pressure and liquid hourly space velocity (LHSV) on crude oil hydrotreating process has also been investigated. The effectiveness of impurities removal is found to be proportional to the reaction temperature, reactor pressure and LHSV. Increasing the reaction temperature and pressure, and decreasing in LHSV leads to the reduction in the contents of S, N, V, Ni and Asph as well as the crude oil becomes more purified by removing these contaminants. The hydrotreated crude oil at the best operating conditions that gave maximum conversion of S, N, V, Ni and Asph has been distilled into light naphtha (L.N), heavy naphtha (H.N), heavy kerosene (H.K), light gas oil (L.G.O) and reduced crude residue (R.C.R) in order to compare the yields of middle distillate produced by this study (distillation process after HDT process) and produced by conventional methods (HDT process of each fraction separately after distillation). It has been observed that the yield of middle distillate fractions produced via HDT of crude oil directly before distillation greater than those obtained by conventional methods. The results also indicated that the properties of R.C.R obtained by crude oil HDT are better compared with the properties of R.C.R produced by conventional methods. The contents of S, N, V, Ni and Asph are found to be much lower than those contents of R.C.R produced by conventional methods that allows producing good fuel oils.

Simulation and optimization help achieving better design and operation of hydrotreating processes. For carrying out meaningful simulation and optimization to create alternative design and operation scenarios cheaply, development of a reliable process model is required by obtaining the best kinetic parameters in trickle bed reactor applied for HDS, HDN, HDAs, HDV and HDNi of crude oil in addition to the kinetic models for increasing of middle distillate yields, which have been done in Chapter Five. For HDS, HDN, HDAs, HDV and HDNi processes, an optimization technique, based on minimization of the sum of square errors (*SSE*) between the experimental and model

predicted concentrations of S, N, V, Ni and Asph with two approaches, linear (LN) and non-linear (NLN) regression have been used to calculate the best kinetic parameters of these reactions. Based on the values of *SSE*, the kinetic parameters calculated using non-linear regression is found to be more accurate and showed very well agreement with the experimental data with an average absolute error of less than 5% among all results at different operating conditions, which give a clear indication that the models can be effectively employed to reactor design in addition to predict the concentration profiles of any compound at any conditions. The inhibiting effect of hydrogen sulfide on the sulfur conversion that has not been described in a homogeneous model, is incorporated in our model (which is a heterogeneous model) using a Langmuir–Hinshelwood formulation. Simulation of simultaneous HDT reactor system along the catalyst bed length in many phases has also been studied. For increasing of middle distillates yield, 5 lumps kinetic models are developed by using discrete lumping kinetic approach. It can be concluded that conversion of heavy or high molecules into light molecules are demonstrated at high operating conditions (high temperature and low LHSV) and there is no significant conversion at low operating conditions the main conversion reactions are achieved from R.C.R toward the production of L.G.O, H.K, naphtha and gases. Also, naphtha and H.K can not produce gases and naphtha cracking has not been noticed. The weight fraction predicted of R.C.R, L.G.O, H.K, naphtha and gases showed very well correspondence with the experimental data with an average absolute error of less than 5%.

In Chapter Six, modelling, design and analysis of an industrial trickle bed reactor with the optimal operation of commercial HDT unit is investigated to evaluate viability of large-scale process for crude oil hydrotreating. The industrial hydrotreating reactors are usually exothermic and the temperature inside the reactor is increasing along the catalyst bed length and the control of the reaction temperature in such reactor is

considered the main issue, which has been processed by using a quench system. The quench numbers, quench positions and quench flow rate are regarded as the main factors of quench process that can be calculated when the reactor length and diameter are given. The optimal reactor length to reactor diameter is found to be 2.66 to ensure safe operation and to avoid any side effects. It has also been observed that the number of quenches during crude oil hydrotreating should be more than one (two quenches with three beds are required) in order to control the temperature inside the reactor and keep it below the maximum allowed temperature. The best values of the first, second and third catalyst bed length, and quench flow rate (of the main hydrogen feed) one and two are 141.96cm, 338.18cm, 581.01cm, 13.93% and 9.24%, respectively. Also, the conversions of S, N, V, Ni and Asph at industrial reactor are greater in comparison with the conversion of these impurities at pilot plant reactor.

In the industrial process, a large amount of energy is required. Therefore, a heat integration and energy consumption in a hydrotreating process are also considered in this Chapter. It is concluded that the heat recovery issues must be taken into considerations in order to minimize the energy consumption and to maximize the profitability of process. Optimization problem has been formulated to minimize the total annual cost while optimize design and operating parameters of integrated process is studied. Optimal minimum energy consumption, heat recovery and cost saving were obtained using optimization process. The cost saving is 55.76% and the energy saving is 64.2% compared with those obtained without heat integration, which provides better minimum energy requirement and as a result reducing environmental influence and maximum heat recovery.

Finally, in Chapter Six an economic analysis of whole commercial refining unit (the developed crude oil hydrotreating unit then distillation process for middle distillates production mainly naphtha, kerosene and light gas oil) and comparative results with

conventional method have also been investigated. It is observed from the economic results that the hydrotreating of whole crude oil before distillation can save 16.54% in the total cost and 1.885$ per barrel compared with those obtained by conventional method at the same capacity, which give clear indication that the presented study can reduce the overall cost.

7.2 Future Work

Some suggestions for future research work are outlined below:

- Application of different catalyst systems (like cobalt-nickel molybdenum) with several catalyst supported (such as zeolites and tungsten) with the objectives to improve reactivity and simplify regeneration of deactivated catalyst during crude oil hydrotreating process, and taking into accounts the effect of surface area and pore size of the catalyst upon the process efficiency.
- Studying the effect of asphaltenes removal by using various solvents (such as Pentane, Hexane and Heptane) under different conditions (mainly temperature, mixing time and solvent to oil ratio) before hydrotreating process and comparing the results obtained by both methods (with and without deasphaltening oil) with taking into considerations the life of the catalyst used in both methods.
- Investigating crude oil feed quenching instead of hydrogen quenching system (as presented in Chapter Six) for an industrial crude oil hydrotreater. This option taking a portion of the main feedstock (crude oil) and injecting it between the catalyst beds. In this case, comparison of the results (impurities removal, energy consumption, total annual cost) between both methods are required.

- Application of dynamic modelling and simulation of catalytic pilot plant and commercial trickle bed reactors for hydrotreating of crude oil. In this case, the experimental data should be collected at dynamic condition of the reactor using many loading of the catalyst and the time on stream must be considered within the calculations in addition to study the effect of operating conditions on the impurities removal as well as kinetic models.
- Possibility of applying a catalytic distillation column (reactive distillation) for crude oil hydrotreating (on the other hand, combination between distillation process and hydrotreating process in one unit). Optimal conditions, total annual cost, impurities concentration and energy consumption must be studied during design, operation and control processes.

References

Abbas, A.S. (1999). *Low Sulfur Feedstock from Basrah Reduced Crude Oil for Coke Production*. MSc Thesis. University of Baghdad.

Abbasi, R. and Fatemi, S. (2009). Mathematical Modeling of Gas Oil HDS and Optimization of Operational Conditions in Trickle Bed Reactor by Genetic Algorithm. *International Journal of Chemical Reactor Engineering*, **7**, pp 1.

Abdelhadi, B., Benoudjit, A. and Nait Said, N. (2004). Identification of Induction Machine Parameters Using an Adaptive Genetic Algorithm. *Electric Power Components and Systems*, **32**, pp 767.

Abdul-Halim, A-K., Abdullah, A., Ayad, B. and Abdul-Salam K. (1987). Catalytic hydrotreatment of petroleum residue. *Petroleum Science and Technology*, **5**, pp 655.

Absi-Halabi, M. and Stanislaus A. (1996). Deactivation and testing of hydrocarbon processing catalysts. *American Chemical Society*, **Ch.17**, pp 229.

Absi-Halabi, M., Stanislaus A., Qamara, A., and Chopra, S. (1996). Effect of presulfiding on the activity and deactivation of hydrotreating catalysts in processing Kuwait vacuum residue. *Studies in Surface Science and catalysis*, **100**, pp 243.

Absi-Halabi, M., Stanislaus A., Qwaysi, F., Khan, Z. H. and Diab, S. (1989). Hydroprocessing of Heavy Residues: Relation Between Operating Temperature, Asphaltene Conversion and Coke FORMATION. *Studies in Surface Science and catalysis*, **53**, pp 201.

Ackerman, S., Chitnis, G.K. and McCaffery, D.S. (2002). Advances in sulfuric acid alkylation process improve gasoline blending economics in world refining. *Am. Chem. Soc*., **46**, pp 241.

Ahmed, T. (1989). *Hydrocarbon Phase Behaviour*. Houston, Gulf Publishing.

Ahn, J., Cho, Ch-Ki. and Kang, S. (2010). An efficient numerical parameter estimation scheme for the space-dependent dispersion coefficient of a solute transport equation in porous media. *Mathematical and Computer Modelling*, **51**, pp 167.

Air Liquid. GasEncyclopaedia. (2008a). URL:http://encyclopedia.airliquid.com/Encycl--opedia.asp?-GasID=36 [Accessed October 14, 2008].

Air Liquid. GasEncyclopaedia. (2008b). URL:http://encyclopedia.airliquid.com/Encycl--opedia.asp?-GasID=59 [Accessed October 14, 2008] .

Akosman, C. and Walters, J.K. (2004). The role of axial dispersion in fixed beds of reacting solid particles. *Chemical Engineering and Processing*, **43**, pp 181.

Alcazar, L.A. and Ancheyta, J. (2007). Sensitivity analysis based methodology to estimate the best set of parameters for heterogeneous kinetic models. *Chemical Engineering Journal*, **128**, pp 85.

Al-Dahhan, M.H. and Dudukovic, M.P. (1996). Catalyst Wetting Bed Dilution for Improving Catalyst in Laboratory Trickle-Bed Reactors. *AIChE J*, **42**, pp 2594.

Al-Dahhan, M.H., Larachi, F., Dudukovic, M.P. and Laurent, A. (1997). High-Pressure Trickle-Bed Reactors: A Review. *Ind. Eng. Chem. Res.*, **36**, pp 3292.

Al-Humaidan, F.S. (2004). *Modelling Hydrocracking of Atmospheric Residue by Discrete and Continuous Lumping.* MSc Thesis. Kuwait University.

Ali, L.H. and Abdul-Karim, E. (1986). *The Oil, Origin, Composition and Technology*. Iraq, AlMosul University.

Alonge, F., Dippolito, F., Ferrante, G. and Raimondi F.M. (1998). Parameter identification of induction motor model using genetic algorithms. *IEE Proceedings on Control Theory and Applications*, **145**, pp 587.

Alvarez, A. and Ancheyta, J. (2008a). Modeling residue hydroprocessing in a multi-fixed-bed reactor system. *Applied Catalysis A: General*, **351**, pp 148.

Alvarez, A. and Ancheyta, J. (2008b). Simulation and analysis of different quenching alternatives for an industrial vacuum gas oil hydrotreater. *Chemical Engineering Science*, **63**, pp 662.

Alvarez, A. and Ancheyta, J. (2009). Effect of Liquid Quenching on Hydroprocessing of Heavy Crude Oils in a Fixed-Bed Reactor System. *Ind. Eng. Chem. Res.*, **48**, pp 1228.

Alvarez, A., Ancheyta, J. and Mun˜oz, J.A.D. (2007). Comparison of Quench Systems in Commercial Fixed-Bed Hydroprocessing Reactors. *Energy & Fuels,* **21**, pp 1133.

Alvarez, A., Ancheyta, J. and Mun˜oz, J.A.D. (2009). Modeling, simulation and analysis of heavy oil hydroprocessing in fixed-bed reactors employing liquid quench streams. *Applied Catalysis A: General*, **361**, pp 1.

Ancheyta, J. (2007). *Reactors for Hydroprocessing. In Hydroprocessing of Heavy Oils and Residua*. Ancheyta, J. Speight J. Eds. New York, Taylor & Francis.

Ancheyta, J., Betancourt, G., Centeno, G., Marroquı´n, G., Alonso, F. and Garciafigueroa, E. (2002a). Catalyst Deactivation during Hydroprocessing of Maya Heavy Crude Oil. 1. Evaluation at Constant Operating Conditions. *Energy & Fuels*, **16**, pp 1438.

Ancheyta, J. Betancourt, G. Marroquı´n, G. Centeno, G. Castan˜eda, L.C. Alonso, F. Mun˜oz, J.A. Go´mez, M.T. and Rayo, P. (2002c). *Appl. Catal*., *A*, **233**, pp 159.

Ancheyta, J., Marroquín, G., Angeles, M.J., Macías, M.J., Pitault, I., Forissier, M. and Morales, R.D. (2002b). Some Experimental Observations of Mass Transfer Limitations in a Trickle-Bed Hydrotreating Pilot Reactor. *Energy and Fuel*, **16**, pp 1059.

Ancheyta, J., Rivera, G. B., Sanchez, G. M., Arellano, A. M. P., Maity, S. K., Cortez, M. T. and Soto, R. R. (2001). An Exploratory Study for Obtaining Synthetic Crudes from Heavy Crude Oils via Hydrotreating. *Energy & Fuels*, **15**, pp 120.

Ancheyta, J., Sa´nchez, S. and Rodrı´guez, M.A. (2005). Kinetic modelling of hydrocracking of heavy oil fractions: A review. *Catalysis Today*, **109**, pp 76.

Ancheyta, J. and Speight, J.G. (2007). *Hydroprocessing of heavy oils and residua*. USA, CRC Press.

Andari, M.K., Behbehani, H. and Stanislaus, A. (1996). Sulfur compound type distribution in Naphtha and gas oil fractions of Kuwaiti crude. *Fuel Science & Technology International*, **14**, pp 939.

Aoyagi, K., McCaffrey, W.C. and Gray, M.R. (2003). Kinetics of Hydrocracking and Hydrotreating of Coker and Oilsands Gas Oils. *Petrol. Sci. Technol*., **21**, pp 997.

Areff, H.A. (2001). *The Effect of Operating Conditions on Vacuum Gas Oil Hydrotreating on Sulfur and Aromatics Content*. MSc Thesis. University of Tikrit.

Aris, R. (1975). *The Mathematical Theory of Diffusion and Reaction in Permeable Catalysts*. Oxford, Clarendon Press.

Armstrong, S.M., Sankey, B.M., and Voordouw, G. (1997). Evaluation of sulfuate reducing bacteria for desulfurizing bitumen or its fractions. *Fuel*, **76**, pp 223.

Ashaibani, A.S. and Mujtaba, I.M. (2007). Minimisation of fuel energy wastage by improved heat exchanger network design-an industrial case study. *Asia-Pacific Journal of Chemical Engineering*, **2**, pp 575.

Avraam, D.G. and Vasalos, I.A. (2003). HdPro: a mathematical model of trickle-bed reactors for the catalytic hydroprocessing of oil feedstocks. *Catal. Today,* **79-80**, pp 275.

Aziz, N. (1998). *Dynamic Modelling and Optimization of Batch Reactor*. MPhil leading to PhD transfer report. University of Bradford.

Bahzad, D. and Kam, E. (2009). Atmospheric Residues of Kuwait Heavy Crude Upgrading: A Pilot Plant and Model Simulation Study. *Energy Fuels*, **23**, pp 1683.

Batholomew, C. H. (1983). *Catalyst Deactivation in Hydrotreating of Residue*. In Applied Industrial Catalysis. Leach, B.E. (Ed.). New York, Academic Press.

Barandiaran, M.J., De Arbina, L.L., De La Cal, J.C., Gugliotta, L.M. and Ausa, J. M. (1995). Parameter estimation in emulsion copolymerization using reaction calorimeter data. *J. Appl. Polym. Sci*., **55**, pp 1231.

Bartholdy, J. and Andersen, S.I. (2000). Changes in Asphaltene Stability during Hydrotreating. *Energy & Fuel*, **14**, pp 52.

Bartholdy, J. and Cooper, B.H. (1993). Metal and coke deactivation of resid hydroprocessing catalysts. USA, ACS Symposium on Resid Upgrading Denver, pp 386.

Bej, S.K., Dalai, A.K. and Adjaye, J. (2001). Effect of Hydrotreating Conditions on the Conversion of Residual Fraction and Microcarbon Residue Present in Oil Sands Derived Heavy Gas Oil. *Energy & Fuels*, **15**, pp 1103.

Benito, A.M., Callejas, M.A. and Martínez, M.T. (1997). Kinetics of asphaltene hydroconversion: 2. Catalytic hydrocracking of a coal residue. *Fuel*, **76**, pp 907.

Bennett, R.N. and Bourne, K.H. (1972). Hydrocracking for middle distillate: A study of process reactions and corresponding product yields and qualities. *In Symposium on Advances in Distillate and Residual Oil Technology*, American Chemical Society, New York Meeting, August 27−September 1, pp G45.

Bharvani, R.R. and Henderson, R.S. (2002). Revamp your hydrotreater for deep desulfurization. *Hydrocarbon Processing,* **81**, pp 61.

Bhaskar, M., Valavarasu, G., Meenakshisundaram, A. and Balaraman, K.S. (2002). Application of a Three Phase Heterogeneous Model to analyse the Performance of a Pilot Plant Trickle Bed Reactor. *Petroleum Science and Technology*, **20**, pp 251.

Bhaskar, M., Valavarasu, G., Sairam, B., Balaraman, K.S. and Balu, K. (2004). Three-Phase Reactor Model to Simulate the Performance of Pilot-Plant and Industrial Trickle-Bed Reactors Sustaining Hydrotreating Reactions. *Ind. Eng. Chem. Res.*, **43**, pp 6654.

Bischoff, K.B. and Levenspiel, O. (1962). Fluid dispersion-generalization and comparison of mathematical models-II comparison of models. *Chemical Engineering Science*, **17,** pp 257.

Boahene, P.E. Soni, K. Dalai, A.K. and Adjaye, J. (2011). Hydrotreating of coker light gas oil on Ti-modified HMS supports using Ni/HPMo Catalysts. *Applied Catalysis B: Environmental*, **101**, pp 294.

Boelhouwer, J.G. (2001). *Nonsteady operation of trickle–bed reactors: hydrodynamics, mass and heat transfer*. PhD Thesis, University of Eindhoven.

Bollas, G.M., Papadokonstantakis, S., Michalopoulos, J., Arampatzis, G., Lappas, A.A., Vasalos, I.A. and Lygeros, A. (2004). A Computer-aided tool for the simulation and optimization of the combined HDS-FCC processes. *Chemical Engineering Research and Design*, **82**, pp 881.

Bondi, A. (1971). Handling Kinetics in Trickle- Phase Reactors. *Chem. Tech.*, **3**, pp 185.

Bonvin, D. (1998). Optimal control of batch reactor- a personal view. *Journal of process control*, **8**, pp 355.

Bouton, G.R. and Luyben, W.L. (2008). Optimum Economic Design and Control of a Gas Permeation Membrane Coupled with the Hydrotreating (HAD) Process. *Ind. Eng. Chem. Res.*, **47**, pp 1221.

Calemma, V., Rausa, R., D'Antona, P. and Montanari, L. (1998). Characterization of Asphaltenes Molecular Structure. *Energy & Fuel*, **12**, pp 422.

Callejas, M.A. and Martínez, M.T. (1999). Hydrocracking of a Maya Residue. Kinetics and Product Yield Distributions. *Ind. Eng. Chem. Res*., **38**, pp 3285.

Callejas, M.A. and Martínez, M.T. (2000). Hydroprocessing of a Maya Residue. 1. Intrinsic Kinetics of Asphaltene Removal Reactions. *Energy & Fuel*, **14**, pp 1304.

Carberry, J.J. (1976). *Chemical and Catalytic Reaction Engineering*. New York, McGraw-Hill.

Carloff, R., Probss, A. and Reichert, K.H. (1994). Temperature oscillation calorimetry in stirred tank reactors with variable heat transfer. *Chem. Eng. & Technol*., **17**, pp 406.

Chang, J., Liu, J. and Li, D. (1998). Kinetics of resid hydrotreating reactions. *Catalysis Today,* **43**, pp 233.

Chaudhuri, U.R., Chaudhuri, U.R., Datta, S., and Sanyal, S.K. (1995). Mild hydrocracking- a state of the art. *Petroleum Science and Technology*, **13**, pp 1199.

Chemical Engineering. (2010). Economic Indicators. www.che.com [Accessed January 16, 2010].

Chen, H., Zheng, J., Xu, P., Li, L., Liu, Y. and Bie, H. (2010). Study on real-gas equations of high pressure hydrogen. *International Journal of Hydrogen Energy*, **35**, pp 3100.

Chen, J. Mulgundmath, V. and Wang, N. (2011). Accounting for Vapor-Liquid Equilibrium in the Modeling and Simulation of a Commercial Hydrotreating Reactor. *Ind. Eng. Chem. Res*., **50**, pp 1571.

Cheng, Z., Fang, X., Zeng, R., Han, B., Huang, L. and Yuan, W. (2004). Deep removal of sulfur and aromatics from diesel through two-stage concurrently and countercurrently operated fixed-bed reactors. *Chem. Eng. Sci.*, **59**, pp 5465.

Choudhary, N. and Saraf, D. N. (1975). Hydrocracking: A Review. *Ind. Eng. Chem. Prod. Res. Dev.*, **14**, pp 74.

Chowdhury, R., Pedernera, E. and Reimert, R. (2002). Trickle-Bed Reactor Model for Desulfurization and Dearomatization of Diesel. *AIChE J.,* **48**, pp 126.

Chung, S.Y.K. (1982). *Thermal Hydroprocessing of Heavy Gas Oils*. MSc Thesis. University of Alberta.

Cotta, R.M., Wolf-Maciel, M.R. and Filho, R.M. (2000). A cape of HDT industrial reactor for middle distillates. *Computers and Chemical Engineering,* **24**, pp 173.

Doraiswamy, L.K. and Sharma, M.M. (1984). *Heterogeneous Reactions: Analysis, Examples and Reactor Design.* Vol.2, NewYork, JohnWiley & Sons.

Douglas, J.M. (1988). *Conceptual Design Chemical Processes*. New York, McGraw-Hill.

Dudukovic, M.P., Larachi, F. and Mills, P.L. (2002). Multiphase catalytic reactors: A perspective on current knowledge and future trends. *Catal. Rev.*, **44**, pp 123.

Edgar, Th.F., Himmelblau, D.M. and Lasdon, L.S. (2001). *Optimization of Chemical Processes*. 2nd ed. New York, McGraw-Hill.

Ekpo, E.E. (2006). *Dynamic Optimization and Control of Batch Polymerization Process*. PhD Thesis. University of Bradford.

Ekpo, E.E. and Mujtaba, I.M. (2007). Performance analysis of three controllers for the polymerisation of styrene in a batch reactor. *Chemical Product and Process Modeling,* **2**, pp 1.

Elizalde I., Rodrı´guez, M.A. and Ancheyta, J. (2009). Application of continuous kinetic lumping modeling to moderate hydrocracking of heavy oil. *Applied Catalysis A: General*, **365**, pp 237.

El Kady, F.Y.A. Abd El Wahed, M.G. Shaban, S. and Abo El Naga, A.O. (2010). Hydrotreating of heavy gas oil using CoMo/γ-Al_2O_3 catalyst prepared by equilibrium deposition filtration. *Fuel*, **89**, pp 3193.

Environmental Chemistry. com. (1995a). Periodic Table of Elements: Sulfur-S.URL: http://environmentalchemistry.com/yogi/periodic/S.html. [Accessed October 9, 2008].

Environmental Chemistry. com. (1995b). Periodic Table of Elements: Nitrogen-N. URL :http://environmentalchemistry.com/yogi/periodic/N.html. [Accessed October 9, 2008].

Environmental Chemistry. com. (1995c). Periodic Table of Elements: Vanadium-V. URL: http://environmentalchemistry.com/yogi/periodic/S.html. [Accessed October 9, 2008].

Environmental Chemistry. com. (1995d). Periodic Table of Elements: Nickel-Ni. URL :http://environmentalchemistry.com/yogi/periodic/N.html. [Accessed October 9, 2008].

Eykhoff, P. (1974). *System Identification*. London, J. Wiley.

Farahani, H.F. and Shahhosseini, Sh. (2011). Simulation of Hydrodesulfurization Trickle Bed Reactor. *Chemical Product and Process Modeling*, **6**, pp 1.

Fletcher, R. (1987). *Practice Methods of Optimization*. 2nd ed. Chichester, John Wiley and Sons.

Flinn, R.A., Larson, O.A. and Beuther, H. (1963). How Easy is Hydrodenitrogenation. *Hydrocarbon Proc. Petr. Refiner,* **42**, pp 129.

Fogler, H. S. (1999). *Elements of Chemical Reaction Engineering*. 2nd ed. New Jersey, Prentice-Hall.

Fowler, R. and Book, L. (2002). *AdVanta FCC catalyst*. Latin American and Caribbean Refining Seminar. Peru, Lima.

Froment, G.F. and Bischoff, K.B. (1990). *Chemical Reactor Analysis and Design*. 2nd ed. New York, Wiley.

Froment, G.F., Depauw, G.A. and Vanrysselberghe, V. (1994). Kinetic Modeling and Reactor Simulation in Hydrodesulfurization of Oil Fractions. *Ind. Eng. Chem. Res.*, **33**, pp 2975.

Furimsky, E. (1998). Selection of catalysts and reactors for hydroprocessing. *Applied Catalysis A: General,* **171**, pp 177.

Furimsky, E. and Massoth, F.E. (1999). Deactivation of hydroprocessing catalysts. *Cataysis. Today*, **52**, pp 381.

Gajardo, P., Pazos, J.M. and Salazar, G.A. (1982). Comments on the HDS, HDM and HDN activities of commercial catalysts in the hydrotreating of heavy crude oils. *Applied Catalysis*, **2**, pp 303.

Gary, J.H. and Handwerk, G.E. (1994). *Petroleum Refining: Technology and Economics*. 3rd edition. New York, Marcel Dekker.

Gasoling, I. (2005). Process simulation and modelling for industrial bioprocessing tools and techniques. *Ind. Biotechnology*, **1**, pp 106.

Gates, B.C., Katzer, J.R. and Schuit, G.C.A. (1979). *Chemistry of Catalytic Processes*. 3rd ed. New York, McGraw-Hill.

Ge, H., Li, X., Qin, Z., Lü, Z. and Wang, J. (2008). Highly active Mo/Al_2O_3 hydrodesulfurization catalyst presulfided with ammonium thiosulfate. *Catalysis Communications,* **9**, pp 2578.

Georgiadis, M.C., Giovanoglou, A., Pistikopoulos, E.N., Palacin-Linan, J. and Pantelides, C.C. (2005). gPROMS: An advanced tool for research and teaching on process modelling, simulation, design, control and optimization. Italy, In Proceedings of PRES05, Giardini Naxos, Sicily, 15-18 May, pp 393.

Gianetto, A. and Specchia, V. (1992). Trickle-bed reactors: state of art and perspectives. *Chem. Eng. Sci.,* **47**, pp 3197.

Giannakopoulos, N. (2002). *Modelling and optimization of semi-batch reactors*. MSc Thesis. University of Bradford.

Gilbert, J.B. and Kartzmark, R. (1965). *Proc. Amer. Inst. Petr.*, **45**, pp 29.

Girgis, M.J. and Gates, B.C. (1991). Reactivities, reaction networks, and kinetics in high-pressure catalytic hydroprocessing. *Ind. Eng. Chem. Res.*, **30**, pp 2021.

Goto, S. and Smith, J.M. (1978). Performance of slurry and trickle -bed reactors: Application to sulfur dioxide removal. *AIChE J.,* **24**, pp 286.

gPROMS, (2005). gPROMS Advanced User Guide. Process Systems Enterprise Ltd. London, Bridge studies.

Gunn, D.J. (1987). Axial and radial dispersion in fixed beds. *Chemical Engineering Science*, **42,** pp 363.

Gunjal, P.R. and Ranade, V.V. (2007). Modeling of laboratory and commercial scale hydro-processing reactors using CFD. *Chemical Engineering Science*, **62,** pp 5512.

Gully, A.L. and Ballard, W.P. (1963). *Advances in Petroleum Chemistry and Refining*. New York, J. Wiley & Sons.

Guo, B., Lyons, W.C. and Ghalambor, A. (2007). *Petroleum production engineering: a computer-assisted approach*. UK, Gulf Professional Publishing.

Haitham, M.S., Chedadeh, D., Riazi, M.R., Al-Qattan, A. and Al-Adwani, H.A. (2011). Prediction of product quality for catalytic hydrocracking of vacuum gas oil. *Fuel*, **90**, pp 719.

Hanika, J., Sporka, K., Ruzicka, V. and Pistek, R. (1977). Dynamic behaviour of an adiabatic trickle bed reactor. *Chem. Eng. Sci.*, **32**, pp 525.

Harding, R.H., Peter, A.W. and Nee, J.R.D. (2001). New development in FCC catalyst technology. *Appl. Catal. A.,* **44**, pp 389.

Henry, H.C. and Gilbert, J.B. (1973). Scale Up of Pilot Plant Data for Catalytic Hydroprocessing. *Ind. Eng. Chem. Process Design Dev.*, **12**, pp 328.

Ho, T.C. (2010). Hydrodenitrogenation property–reactivity correlation. *Applied Catalysis A: General,* **378**, pp 52.

Hobson, G.D. (1984). *Modern Petroleum Technology*. 5th ed. New York, J. Wiley & Sons.

Hofmann, H. (1977). Hydrodynamics, Transport Phenomena, and Mathematical Models in Trickle- Bed Reactors. *Int. Chem. Eng.*, **17**, pp 19.

Holland, J.H. (1975). *Adaptation in Natural and Artificial Systems*. The University of Michigan, Press: Ann Arbor, MI.

Hossain, M.M., Al-Saleh, M.A., Shalabi, M.A., Kimura, T. and Inui, T. (2004). Pd–Rh promoted Co/HPS catalysts for heavy oil upgrading. *Applied Catalysis A: General*, **278**, pp 65.

Hsu, Ch.S. and Robinson, P.R. (2006). *Practical Advances in Petroleum Processing.* New York, Springer.

Huang, J.J. and McBean, E.A. (2007). Using Bayesian statistics to estimate the coefficients of a two-component second-order chlorine bulk decay model for a water distribution system. *Water Research*, **41**, pp 287.

Iliuta, I. Ring, Z. and Larachi, F. (2006). Simulating simultaneous fines deposition under catalytic hydrodesulfurization in hydrotreating trickle beds-does bed plugging affect HDS performance. *Chemical Engineering Science*, **61**, pp 1321.

Ingham, J., Dunn, I.J., Heinzle, E. and Prenosil, I.E. (1994). *Chemical Engineering Dynamics.* Weinheim, VCH.

Isoda, T., Kusakabe, K., Morooka, Sh. and Mochida, I. (1998). Reactivity and Selectivity for the Hydrocracking of Vacuum Gas Oil over Metal-Loaded and Dealuminated Y-Zeolites. *Energy & Fuels*, **12**, 493.

Jimenez, F., Nunez, M. and Kafarov, V. (2005). Study and modelling of simultaneous hydrodesulfurization, hydrodenitrogenation and hydrodearomitization on vacuum gas oil hydrotreatment. *Computer Aided Chemical Engineering*, **20**, pp 619.

Jimenez, F., Nunez, M. and Kafarov, V. (2007a). Modeling of industrial reactor for hydrotreating of vacuum gas oils Simultaneous hydrodesulfurization, hydrodenitrogenation and hydrodearomatization reactions. *Chemical Engineering Journal*, **134**, pp 200.

Jimenez, F., Ojeda, K., Sanchez, E., Kafarov, V. and Filho, R.M. (2007b). Modeling of trickle bed reactor for hydrotreating of vacuum gas oils: effect of kinetic type on reactor modelling. *Computer Aided Chemical Engineering*, **24**, pp 515.

Juraidan, M., Al-Shamali, M., Qabazard, H. and Kam, E.K.Y. (2006). A Refined Hydroprocessing Multicatalyst Deactivation and Reactor Performance Model-Pilot-Plant Accelerated Test Applications. *Energy & Fuels*, **20**, pp 1354.

Kaernbach, W., Kisielow, W., Warzecha, L., Miga, K. and Klecan, R. (1990). Influence of petroleum nitrogen compounds on hydrodesulphurization. *Fuel*, **69**, pp 221.

Kallinikos, L.E., Bellos, G.D. and Papayannakos, N.G. (2008). Study of the catalyst deactivation in an industrial gas oil HDS reactor using a mini-scale laboratory reactor. *Fuel*, **87**, pp 2444.

Kam, E.K.Y., Al-Shamali, M., Juraidan, M. and Qabazard, H. (2005). A Hydroprocessing Multicatalyst Deactivation and Reactor Performance Model-Pilot-Plant Life Test Applications. *Energy & Fuels*, **19**, pp 753.

Khalfhallah, H.A. (2009). *Modelling and optimization of Oxidative Desulfurization Process for Model Sulfur Compounds and Heavy Gas Oil.* PhD Thesis. University of Bradford.

Kim, L.K. and Choi, K.S. (1987). Hydrodesulfurization over hydrotreating catalysts. *International chemical engineering*, **27**, pp 340.

Kiparissides, C. (1996). Polymerization reactor modelling: A review of recent developments and future directions. *Chem. Eng. Sci.*, **51**, pp 1637.

Korsten, H. and Hoffmann, U. (1996). Three-Phase Reactor Model Pilot Trickle-Bed for Hydrotreating in Reactors. *AIChE J.*, **42**, pp 1350.

Kosanovich, K.A., Piovoso, M.J., Rokhlenko, V. and Guez, A. (1995). Nonlinear adaptive control with parameter estimation of a CSTR. *J. Proc. Control*, **5**, pp 137.

Krishna, R. and Saxena, A.K. (1989). Use of an axial-dispersion model for kinetic description of hydrocracking. *Chem Eng. Sci*., **44**, pp 703.

Kumar, V.R., Balaraman, K.S., Rao, V.S.R. and Ananth, M.S. (2001). Performance study of certain commercial catalysts in Hydrodesulfurization of Diesel Oils. *Petroleum Science and Technology,* **19**, pp 1029.

Kuzmic, P. (1996). Program DYNAFIT for the analysis of enzyme kinetic data: application to HIV proteinase. *Anal. Biochem*., **237**, pp 260.

Lababidi, H.M.S., Shaban, H.I., Al-Radwan, S. and Alper, E. (1998). Simulation of an Atmospheric Residue Desulfurization Unit by Quasi-Steady State Modeling. *Chem. Eng. Technol*., 21, pp 193.

Lamine, A.S., Colli, M.T. and Wild, G. (1992). Hydrodynamics and heat transfer in packed bed with cocurrent upflow. *Chemical Engineering Science*, **47,** pp 3493.

Latz, J., Peters, R., Pasela, J., Datsevichb, L. and Jess, A. (2009). Hydrodesulfurization of jet fuel by pre-saturated one-liquid-flow technology for mobile fuel cell applications. *Chemical Engineering Science,* **64**, pp 288.

Laxminarasimhan, C.S., Verma, R.P. and Ramachandran, P.A. (1996). Continuous lumping model for simulation of hydrocracking. *AICHE Journal*, **42**, pp 2645.

Lee C.K., Magalhaes, C. L.E. and Osowski C.A. (2008). Study compares methods that measure hydrogen use in diesel hydrotreaters. *Oil & Gas J*, **13**, pp 58.

LeNobel, J.W. and Choufoer, J.H. (1959). Development in Treating Process for the Petroleum Industry. New York, 5th World Petroleum Congress, May 30-June 5.

Leprince, P. (2001). *Conversion processes*. Paris, Institute Francais du Petrole.

Levenberg, K. (1944). A method for the solution of certain nonlinear problems in least squares. *Q. Appl*. *Math*., **2**, pp 164.

Leyva, C., Rana, M.S., Trejo, F. and Ancheyta, J. (2007). On the Use of Acid-Base-Supported Catalysts for Hydroprocessing of Heavy Petroleum. *Ind. Eng. Chem. Res.*, **46**, pp 7448.

Li, C., Chen, W. and Tsai, C. (1995). Highly Restrictive Diffusion under Hydrotreating Reactions of Heavy Residue Oils. *Ind. Eng. Chem. Res.*, **34**, pp 898.

Liebermeister, W. and Klipp, E. (2006). Bringing metabolic networks to life: integration of kinetic, metabolic, and proteomic data. *Theoretical Biology and Medical Modelling*, **3**, 42.

Lister, A. (1964). Engineering Design and Development of Desulfurizer Reactors. *3rd Eur. Symp. Chem. Reaction Eng*., pp 225.

Lopez, R. Dassori, and C.G. (2001). Mathematical Modeling of a VGO Hydrotreating Reactor. *SPE Int.*, 69499, pp 1.

Ma**,** C.G. and Weng, H.X. (2009). Application of Artificial Neural Network in the Residual Oil Hydrotreatment Process. *Petroleum Science and Technology*, **27**, pp 2075.

Ma, X., Sakanishi, K., Isoda, T. and Mochida, I. (1995). Hydrodesulfurization Reactivities of Narrow-Cut Fractions in a Gas Oil. *Ind. Eng. Chem. Res.*, **34**, pp 748.

Macı´as, M.J. and Ancheyta, J. (2004). Simulation of an isothermal hydrodesulfurization small reactor with different catalyst particle shapes. *Catal. Today,* **98**, pp 243.

Magee, J. and Dolbear, G.E. (1998). *Petroleum Catalysis in Nontechnical Language*. Tulsa, PennWell Books.

Maity, S.K., Ancheyta, J., Soberanis, S. and Alonso, F. (2003). Catalysts for Hydroprocessing of Maya heavy crude. *Applied Catalysis A: General,* **253**, pp 125.

Mahmood, Sh., Abdul-Karim, R. and Hussein, E.M. (1990). *Technology of oil and gas*. Baghdad, Oil Training Institute.

Mapiour, M., Sundaramurthy, V., Dalai, A.K. and Adjaye, J. (2009). Effect of Hydrogen Purity on Hydroprocessing of Heavy Gas Oil Derived from Oil-Sands Bitumen. *Energy Fuels*, **23**, pp 2129.

Mapiour, M., Sundaramurthy, V., Dalai, A.K. and Adjaye, J. (2010). Effects of Hydrogen Partial Pressure on Hydrotreating of Heavy Gas Oil Derived from Oil-Sands Bitumen: Experimental and Kinetics. *Energy Fuels*, **24**, pp 772.

Marafi, A., Maruyama, F., Stanislaus, A. and Kam, E. (2008). Multicatalyst System Testing for Upgrading Residual Oils. *Ind. Eng. Chem. Res.*, **47**, pp 724.

Marafi, M. and Stanislaus, A. (2008). Preparation of heavy oil hydrotreating catalyst from spent residue hydroprocessing catalysts. *Catalysis Today,* **130**, pp 421.

Marafi, A., Fukase, S., Al-Marri, M. and Stanislaus, A. (2003). A Comparative Study of the Effect of Catalyst Type on Hydrotreating Kinetics of Kuwaiti Atmospheric Residue. *Energy and Fuels*, **17**, pp 661.

Marafi, A., Hauser, A. and Stanislaus, A. (2006). Atmospheric Residue Desulfurization Process for Residual Oil Upgrading: An Investigation of the Effect of Catalyst Type and Operating Severity on Product. *Energy & Fuels*, **20**, pp 1145.

Maria, A.C. and Martinez, M.T. (1999). Hydroprocessing of a Maya Residue. Intrinsic Kinetics of Sulfur-, Nitrogen-, Nickel-, and Vanadium-Removal Reactions. *Energy and Fuels*, **13**, pp 629.

Marquardt, D.W. (1963). An Algorithm for least-squares estimation of non-linear parameters. *SIAM J*, **11**, pp 431.

Marroquin, G., Ancheyta, J. and Esteban, C. (2005). A batch reactor study to determine effectiveness factors of commercial HDS catalyst. *Catalysis Today*, **104**,: pp 70.

Matos, E.M. and Guirardello, R. (2000a). Modelling and simulation of the hydrocracking of heavy oil fractions. *Braz. J. Chem. Eng.*, **17**, pp 79.

Matos, E.M. and Guirardello, R. (2000b). Modelling and simulation of hydrodemetallation and hydrodesulfurization processes with transient catalytic efficiency. *Braz. J. Chem. Eng.*, **17**, pp 171.

Mary, G., Chaouki, J. and Luck, F. (2009). Trickle-Bed Laboratory Reactors for Kinetic Studies. *International Journal of Chemical Reactor Engineering*, **7**, pp 1.

Mears, D.E. (1971). The role of axial dispersion in trickle-flow laboratory reactors. *Chemical Engineering Science*, **26**, pp 1361.

McCulloch, D.C. (1983). *Catalytic Hydrotreating in Petroleum Refining*. In Applied Industrial Catalysis. Leach, B.E. (Ed.). New York, Academic Press.

Mederos, F.S. and Ancheyta, J. (2007). Mathematical modeling and simulation of hydrotreating reactors: Cocurrent versus countercurrent operations. *Applied Catalysis A: General*, **332**, pp 8.

Mederos, F.S., Ancheyta, J. and Chen, J. (2009). Review on criteria to ensure ideal behaviors in trickle-bed reactors. *Applied Catalysis A: General*, **355**, pp 1.

Mederos, F.S., Rodrı´guez, M.A. Ancheyta, J. and Arce, E. (2006). Dynamic Modelling and Simulation of Catalytic Hydrotreating Reactors. *Energy & Fuels*, **20**, pp 936.

Mendes, P. and Kell, D. (1998). Non-linear optimization of biochemical pathways: applications to metabolic engineering and parameter estimation. *Bioinformatics*, **14**, pp 869.

Metaxas, K.C. and Papayannakos, N.G. (2006). Kinetics and Mass Transfer of Benzene Hydrogenation in a Trickle-Bed Reactor. *Ind. Eng. Chem. Res.*, **45**, pp 7110.

Meyers, R.A. (1997). *Handbook of petroleum refining processes*. 2nd ed. New York, McGraw-Hill.

Mhaskar, R.D., Shah, Y.T. and Paraskos, J.A. (1978). Optimum Quench Location for a Hydrodesulfurization Reactor with Time Varying Catalyst Activity. 2. Cases of Multiple Gas Quenches and a Liquid Quench. *Ind. Eng. Chem. Proc. Des. Dev.*, **17**, pp 27.

Mohammed, A-H., Hussain, H., Karim, H.N. and Najeeb, I. (1987). Hydrotreating of Qaiyarah deasphalted residue. *Fuel*, **67**, pp 36.

Mohanty, S., Kunzru, D. and Saraf, D.N. (1990). Hydrocracking: a review. *Fuel*, **69**, pp 1467.

Mohanty, S., Kunzru, D. and Saraf, D.N. (1991). Modeling of a hydrocracking reactor. *Fuel Processing Technology*, 29, pp 1.

Mosby, J.F. Buttke, R.D. Cox, J.A. and Nikolaides, C. (1986). Process characterization of expanded-bed reactors in series. *Chem. Eng. Sci*., **41**, pp 989.

Morrison, K.R. (1984). *Optimal control of processes described by systems of differential-algebraic equations*. PhD Thesis. University of London.

Mujtaba, I.M. (2004). *Batch distillation: Design and operation. Series on Chemical Engineering*, vol. 3. London: Imperial College Press.

Mun˜oz, J.A.D., Alvarez, A., Ancheyta, J., Rodrı´guez, M.A. and Marroquı´n, G. (2005). Process heat integration of a heavy crude hydrotreatment plant. *Catalysis Today*, **109**, pp 214.

Murali, C., Voolapalli, R.K., Ravichander, N., Gokak, D.T. and Choudary, N.V. (2007). Trickle bed reactor model to simulate the performance of commercial diesel hydrotreating unit. *Fuel*, **86**, pp 1176.

Muske, K. R. and Rawlings, J.B. (1995). *Nonlinear moving horizon state estimation*. In: Berber R, editor. Methods of model based process control, Netherlands, Kluwer Academic Publisher.

Myszka, E., Grzechowiak, J.R. and Smith, G.V. (1989). Influence of porous structure on HDS [hydrodesulfurization] activity of cobalt-molybdenum-nickel catalysts. *Energy Fuels*, **3**, pp 541.

Nangsue, P., Pillay, P. and Conry, S. (1999). Evolutionary algorithms for induction motor parameter determination. *IEEE Transactionson Energy Conversion*, **14**, pp 447.

Nickos, P. and Marangozis, J. (1984). Kinetics of Catalytic Hydrodesulphurisation of a Petroleum Residue in a Batch-Recycle Trickle Bed Reactor. *Chem. Eng. Sci.*, **39**, pp 1051.

Oh, M. and Pantelides, C.C. (1996). A Modelling and Simulation Language for Combined Lumped and Distributed parameter Systems, *Comp. Chem. Eng*., 20, pp 611.

Orlowska, K.T., Lis, J. and Szabat, K. (2006). Identification of the induction motor parameters at standstill using soft computing methods. *Computation and Mathematics in Electrical and Electronics Engineering*, **25**, pp 181.

Palmer, R.E. and Torrisi, S. (2003). Hydrotreater revamps for ULSD fuel. *Pet. Technol. Q.*, Revamps, pp 15.

Papayannakos, N. and Marangozis, J. (1984). Kinetics of catalytic hydrodesulfurization of a petroleum residue in a batch-recycle trickle bed reactor. *Chem. Eng. Sci.*, **39**, pp 1051.

Pedernera, E., Reimert, R., Nguyen, N.L. and van Buren, V. (2003). Deep desulfurization of middle distillates: process adaptation to oil fractions compositions. *Catal. Today*, **79-80**, 371.

Pereira, C.J., Cheng, J.W. and Suarez, W.C. (1990). Metal deposition in hydrotreating catalyst. *Industrial Engineering Chemistry Process Design and Development*, **29**, pp 520.

Perry, R.H. and Green, D.W. (1999). *Perry's Chemical Engineers' Handbook*. New York, McGraw-Hill.

Poyton, A.A., Varziri, M.S., McAuley, K.B., McLellan, P.J. and Ramsay, J.O. (2006). Parameter estimation in continuous-time dynamic models using principal differential analysis. *Computers and Chemical Engineering*, **30**, pp 698.

PSE (2004). gPROMS introductory user guide. Process System Enterprise. London, Bridge studies.

Qader, S. A. and Hill, G. R. (1969). Hydrocracking of Gas Oil. *Ind. Eng. Chem. Proc. Des. Dev*., **8**, pp 98.

Quintero, A.R. and Villamil, V.F.D. (2009). On the Multiplicities of a Catalytic Distillation Column for the Deep Hydrodesulfurization of Light Gas Oil. *Ind. Eng. Chem. Res.*, **48**, pp 1259.

Reid, R.C., Prausnitz, J.M. and Poling, B.E. (1987). *The Properties of Gases & Liquids*. 4th ed. New York, McGraw-Hill.

Ramachandran, P.A. and Chaudhari, R.V. (1980). Predicting the Performance of Three Phase Catalytic Reactors. *Chem. Eng.*, **87**, pp 74.

Rana, M.S., Ancheyta, J., Maity, S.K. and Rayo, P. (2005). Maya crude hydrodemetallization and hydrodesulfurization catalysts: An effect of TiO_2 incorporation in Al_2O_3. *Catalysis Today*, **109**, pp 61.

Rao, S.K. Imam, R. Ramanathan, K., and Pushpavanam, S. (2009). Sensitivity Analysis and Kinetic Parameter Estimation in a Three Way Catalytic Converter. *Ind. Eng. Chem. Res.*, **48**, pp 3779.

Raol, J.R., Girija, G., and Singh, J. (2004). *Modelling and Parameter Estimation of Dynamic System*. London, The Institution of Engineering and Technology.

Ray, Ch.U., Chaudhuri, U.R., Datts, S. and Sanyal, S.K. (1995). Mild Hydrocracking–A State of Art. *Fuel Science and Technology Int*., **13**, pp 1199.

Regnier, N., Defaye, G., Caralp, L. and Vidal, C. (1996). Software sensor based control of exothermic batch reactors. *Chem. Eng. Sci*., **51**, pp 5125.

Resendiz, E., Ancheyta, J., Rosales-Quintero, A. and Marroquin, G. (2007). Estimation of activation energies during hydrodesulfurization of middle distillates. *Fuel*, **86**, pp 1247.

Rinnooy Kan, A.H.G. and Timmer, G.T. (1989). Global optimization: a survey. *Int. Ser. Numer. Math*., **87**, pp 133.

Robertson, D.G., Lee, J.H., and Rawlings, J.B. (1996). A moving horizon based approach for least squares estimation. *AIChE J*, **42**, pp 2209.

Rodriguez, M.A. and Ancheyta, J. (2004). Modeling of Hydrodesulfurization (HDS), Hydrodenitrogenation (HDN), and the Hydrogenation of Aromatics (HDA) in a Vacuum Gas Oil Hydrotreater. *Energy Fuels*, **18**, pp 789.

Ryan, J.F. (1998). Biotech Blooms in Bavaria. *Today's Chemist at Work*, **7**, pp 84.

Sadighi, S., Ahmad, A. and Irandoukht, A. (2010). Kinetic Study on a Commercial Amorphous Hydrocracking Catalyst by Weighted Lumping Strategy. *International Journal of Chemical Reactor Engineering*, **8**, pp 1 (A60).

Sanchez, S. and Ancheyta, J. (2007). Effect of Pressure on the Kinetics of Moderate Hydrocracking of Maya Crude Oil. *Energy & Fuels*, **21**, pp 653.

Sa´nchez, S., Rodrıguez, M.A. and Ancheyta, J. (2005). Kinetic Model for Moderate Hydrocracking of Heavy Oils. *Ind. Eng. Chem. Res.*, **44**, pp 9409.

Satterfield, C.N. (1975). Trickle-Bed Reactors. *AIChE J*, **21**, pp 209.

Scamangas, A. and Marangozis, N. (1982). Catalytic Hydrodesulfurization of a Petroleum Residue. *Chem. Eng. Sci.*, **37**, pp 812.

Scherzer, J. and Gruia, A.J. (1996). *Hydrocracking Science and Technology*. New York, Marcel Dekker.

Sebos, I., Matsoukas, A., Apostolopoulos, V. and Papayannakos, N. (2009). Catalytic hydroprocessing of cottonseed oil in petroleum diesel mixtures for production of renewable diesel. *Fuel*, **88**, pp 145.

Sertic-Bionda, K., Gomzi, Z. and Saric, T. (2005). Testing of hydrodesulfurization process in small trickle-bed reactor. *Chem. Eng. J.*, **106**, pp 105.

Shah, Y.T. (1979). *Gas – Liquid – Solid Reactors Design*. USA, McGraw-Hill Inc.

Shah, Y.T., Mhaskar, R.D. and Paraskos, J.A. (1976). Optimum Quench Location for a Hydrodesulfurization Reactor with Time Varying Catalyst Activity. *Ind. Eng. Chem. Process Des. DeV.*, **15**, pp 400.

Shah, Y.T. and Paraskos, J.A. (1975). Criteria for axial dispersion effects in adiabatic trickle bed hydroprocessing reactors. *Chemical Engineering Science*, **30**, pp 1169.

Shimura, M., Shiroto, Y. and Takeuchi, Ch. (1986). Effect of Catalyst Pore Structure on Hydrotreating of Heavy Oil. *Ind. Eng. Chem. Fundamen.*, **25**, pp 330.

Shokri, S., Marvast, M.A. and Tajerian, M. (2007). Production of Ultra low Sulfur Diesel: Simulation and Software Development. *Petroleum & Coal*, **49**, pp 48.

Shokri, S. and Zarrinpashne, S. (2006). A Mathematical model for calculation of effectiveness factor in catalyst pellets of hydrotreating process. *Petroleum & Coal*, **48**, pp 27.

Sie, S.T. (1991). Scale Effects in Laboratory and Pilot-Plant Reactors for Trickle-Flow Processes. *Rev. Inst. Fr. Pet*., **46**, pp 501.

Sinnott, R.K. (2005). *Chemical Engineering, Volume 6: Chemical Engineering Design*. 4th ed. UK, Elsevier Butterworth-Heinemann.

Smith, R. (2005). *Chemical Process Design and Integration*. UK, John Wiley & Sons.

Smith, J.M., Van Ness, H.C. and Abbott, M.M. (1996). *Introduction to Chemical Engineering Thermodynamics*. 5th ed. New York, McGraw-Hill.

Song, Ch., (2003). An overview of new approaches to deep desulfurization for ultra-clean gasoline, diesel fuel and jet fuel. *Catalysis Today*, **86**, pp 211.

Soroush M. Nonlinear state-observer design with application to reactors. (1997). *Chem. Eng. Sci*., **52**, pp 387.

Speight, J.G. (2000). *The Desulfurization of Heavy Oils and Residua*. 2nd edition. New York, Marcel Dekker.

Speight, J.G. (2006). *The Chemistry and Technology of Petroleum*. 4th edition. CRC Press/Taylor & Francis, Boca Raton, FL.

Stacy, C.D., Susan, W.D. and Report, G.B. (2008). *Transportation energy data book*. Prepared for the office of energy efficiency and renewable energy U.S. Department of energy.

Stell, J. (2003). Worldwide refineries, capacities as of January 1, 2004. *Oil & Gas J*, **101**(49), December 22.

Stefanidis, G.D., Bellos, G.D. and Papayannakos, N.G. (2005). An improved weighted average reactor temperature estimation for simulation of adiabatic industrial hydrotreaters. *Fuel Processing Technology*, **86**, pp 1761.

Stephanopoulos, G., and San, K.Y. (1984). Studies on on-line bioreactor identification. I. Theory. *Biotechnol*. *Bioengng*., **26**, pp 1176.

Stratiev, D., Tzingov, T., Shishkova, I. and Dermatova, P. (2009). Hydrotreating Units Chemical Hydrogen Consumption Analysis a Tool for Improving Refinery Hydrogen Management. *In: 44th International petroleum conference*, September 21-22, Bratislava, Slovak Republic.

Suo, Z., Lv, A., Lv, H., Jin, M. and He, T. (2009). Influence of Au promoter on hydrodesulfurization activity of thiophene over sulfided Au–Ni/SiO2 bimetallic catalysts. *Catalysis Communications*, **10**, pp 1174.

Sutikno, T. (1999). Optimal HDS for lower-sulfur gasoline depends on several factors. *Oil & Gas Journal*, **97**, pp 55.

Swain, E.J. (1998). U.S. refining crude slates continue towards heavier feeds, higher sulfur contents. *Oil & Gas Journal*, **96**, pp 43.

Tamburrano, F. (1994). Disposal of heavy oil residues. *Hydrocarbon Process*ing, **73**, pp 77.

Tarhan, O.M. (1983). *Catalytic Reactor Design*. New York, McGraw-Hill.

Tatiraju, S, and Soroush, M. Parameter Estimator Design with Application to a Chemical Reactor. *Ind. Eng. Chem. Res*., **37**, pp 455.

Teresa, M., Mata, and Costa, A.V. (2003). Computer modelling and simulation chemical process pollution prevention. *In Modelling and Simulation in Chemical Engineering*, Coimbra-Portugal, June 30-July 4.

Tijl, P. (2005). *Capabilities of gPROMS and Aspen Custom Modeler, Using the Sec-Butyl-Alcohol Stripper Kinetics Case Study*. Geaduation report, Eindhoven Technical University.

Ting, P.D., Hirasaki, G.J. and Chapman, W.G. (2003). Modeling of Asphaltene Phase Behavior with the SAFT Equation of State. *Petroleum Science and Technology*, **21**, pp 647.

Tjoa, J. and Biegler, L.T. (1991). Simultaneous solution and optimization strategies for parameter estimation of differential-algebraic equation systems. *Ind. Eng. Chem. Res.*, **30**, pp 376.

Tjoa, T.B. and Biegler, L.T. (1992). Reduced successive quadratic programming strategy for errors-in-variables estimation. *Comp. Chem. Eng.*, **16**, pp 523.

Topsoe, H., Clausen, B.S. and Massoth, F.E. (1996). *Hydrotreating Catalysis, Science and Technology*. Germany, Springer-Verlag Berlin Heidelberg.

Trambouze, P. (1993). Engineering of hydrotreating processes, in Chemical Reactor Technology for Environmentally Safe Reactors and Products. Lasa, D. Dogu, H.I. and Ravella, G.A. New York, NATO Advanced Study Institute Series E, Plenium.

Trejo, F. and Ancheyta, J. (2005). Kinetics of asphaltenes conversion during hydrotreating of Maya crude. *Catalysis Today*, **109**, pp 99.

Tsamatsoulis, D. and Papayannakos, N. (1998). Investigation of intrinsic hydrodesulphurization kinetics of a VGO in a trickle bed reactor with backmixing effects. *Chemical Engineering Science*, **53**, pp 3449.

Turaga, U.T. (2000). *MCM-41-supported cobalt-molybdenum catalysts for deep hydrodesulfurization of diesel and jet fuel feedstocks*. PhD Thesis. Pennsylvania State University.

Ursem, R.K. and Vadstrup, P. (2003). Parameter Identification of Induction Motors Using Differential Evolution. *The 2003 Congress on Evolutionary Computation CEC03*, **2**, pp 790.

Van Deemter, J.J. (1964). Trickle Hydrodesulfurization-A Case History. *3rd Eur. Symp. Chem. Reaction Eng.*, pp 215.

Valavarasu, G., Bhaskar, M. and Balaraman, K.S. (2003). Mild Hydrocracking-A Review of the Process, Catalysts, Reactions, Kinetics, and Advantages. *Petrol. Sci. Technol*., **21**, pp 1185.

Van Hasselt, B.W., Lebens, P.J.M., Calis, H.P.A., Kapteijn, F., Sie, S.T., Moulijn, J.A. and vanden Bleek, C.M. (1999). A numerical comparison of alternative three-phase reactors with a conventional trickle-bed reactor. The advantages of countercurrent flow for hydrodesulfurization. *Chem. Eng. Sci.*, **54**, pp 4791.

Vanrysselberghe V. and Froment G.F. (1996). Hydrodesulfurization of Dibenzothiophene on a $CoMo/Al_2O_3$ Catalyst: Reaction Network and Kinetics. *Ind. Eng. Chem. Res.*, **3**, pp 3311.

Vrinat, M.L. (1983). The Kinetics of Hydrodesulfurization Processes-A Review. *Applied Catalysis*, **6**, pp 137.

Waguespack, K.G. and Healey, J.F. (1998). Manage crude oil quality for refining profitability. *Hydrocarbon Processing*, **77**, pp 133.

Wauquier, J.P. (1995). *Crude Oil: Petroleum Products; Process Flowsheets*. Paris, Editions Technip.

Weinert, J.X., Shaojun, L., Ogden, J.M. and Jianxin, M. (2007). Hydrogen refueling station costs in Shanghai. *International Journal of Hydrogen Energy*, **32**, pp 4089.

Winkel, M.L., Zullo, L.C., Verheijen, P.J.T. and Pantelides, C.C. (1995). Modelling and simulation of the operation of an industrial batch plant using gPROMS. *Computers and Chemical Engineering*, **19**, pp 571.
Winterbottom, J.M. and King, M.B. (1999). *Reactor Design for Chemical Engineers*. UK, Stanley Thornes.

Wua, D., Zhoua, J. and Li,Y. (2009). Effect of the sulfidation process on the mechanical properties of a $CoMoP/Al_2O_3$ hydrotreating catalyst. *Chemical Engineering Science*, **64**, pp 198.

Yamada, H. and Goto, S. (2004). Advantages of counter-current operation for hydrodesulfurization in trickle bed reactors. *Korean J. Chem. Eng.*, **21**, pp 773.

Yan, T.Y. (1980). Dynamics of a trickle-bed hydrocracker with a quenching system. *Can. J. Chem. Eng*., **58**, pp 259.

Yui, S.M. and Sanford, E.C. (1989). Mild hydrocracking of bitumen-derived coker and hydrocracker heavy gas oils: kinetics, product yields, and product properties. *Ind. Eng. Chem. Res.*, **28**, pp 1278.

Zhukova, T.B., Pisarenko, V.N. and Kafarov, V.V. (1990). Modeling and design of industrial reactors with a stationary bed of catalyst and two-phase gas-liquid flow-a review. *Int. Chem. Eng.*, **30**, pp 57.

Appendix A

Derivation of Mass Balance Equations

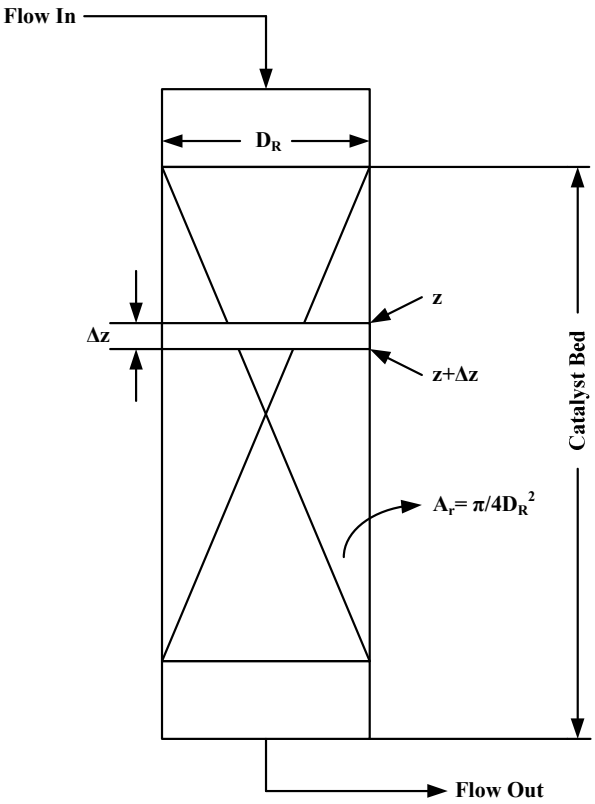

Figure A.1: Schematic representation of a typical TBR

A.1 Mass Balance in Gas Phase

(Flow in) - (Flow out) - (Amount of disappearance (gas_liquid)) = 0 (A.1)

Flow in = $A_r u_g C_i^G \Big|_z$

Flow out = $A_r u_g C_i^G \Big|_{z+\Delta z}$

Amount of disappearance = $A_r \Re \Delta z$

$\Re$ is the rate of mass transferred.

Dividing both sides of the resulting equation by $A_r \Delta z$, gives:

$$\frac{u_g\left(C_i^G\big|_z - C_i^G\big|_{z+\Delta z}\right)}{\Delta z} - \Re = 0 \tag{A.2}$$

When $\Delta z \rightarrow 0$, the left-hand side of equation (A.2) tends toward $u_g(dC_i^G/dz)$ and the equation can be rearranged to

$$u_g \frac{dC_i^G}{dz} + \Re = 0 \tag{A.3}$$

$$C_i^G = \frac{P_i^G}{RT} \tag{A.4}$$

Substituting equation (A.4) in equation (A.3), we get

$$\frac{u_g}{RT}\frac{dP_i^G}{dz} + \Re = 0 \tag{A.5}$$

The rate of mass transferred is calculated as follows:

$$\Re = k \text{ (interfacial area) (concentration difference)} \tag{A.6}$$

or

$$\Re = k_i^L a_L (C_i^* - C_i^L) \tag{A.7}$$

C_i^* is the concentration of compound *i* at the gas-liquid interface. At the gas-liquid interface, the concentration of compound *i* in the liquid phase will be in equilibrium with the partial pressure of this compound, which is represented by the term (P_i^G / h_i).

Therefore the final mass balance equation in gas phase can be written as:

$$\frac{dP_i^G}{dz} = -\frac{RT}{u_g} k_i^L a_L \left(\frac{P_i^G}{h_i} - C_i^L \right) \tag{A.8}$$

$i = H_2, H_2S$

A.2 Mass Balance in Liquid Phase

For gases compounds in liquid phase (H_2 and H_2S)

(Flow in) - (Flow out) - (Amount of disappearance (liquid_solid)-(gas_liquid))= 0 (A.9)

Flow in = $A_r u_l C_i^L \Big|_z$

Flow out = $A_r u_l C_i^L \Big|_{z+\Delta z}$

Amount of disappearance = $A_r (\Re_1 - \Re) \Delta z$

Dividing both sides of the resulting equation by $A_r \Delta z$, gives:

$$\frac{u_l \left(C_i^L \Big|_z - C_i^L \Big|_{z+\Delta z} \right)}{\Delta z} - (\Re_1 - \Re) = 0 \tag{A.10}$$

When $\Delta z \rightarrow 0$, the left-hand side of equation (A.10) tends toward $u_l(dC_i^L/dz)$ and the equation can be rearranged to

$$u_l \frac{dC_i^L}{dz} + (\Re_1 - \Re) = 0 \tag{A.11}$$

$$\Re_1 = k_i^S a_S (C_i^L - C_i^S) \tag{A.12}$$

Substituting equations (A.7) and (A.12) into equation (A.11), we get

$$\frac{dC_i^L}{dz} = \frac{1}{u_l} \left[k_i^L a_L \left(\frac{P_i^G}{h_i} - C_i^L \right) - k_i^S a_S \left(C_i^L - C_i^S \right) \right] \tag{A.13}$$

For liquid compounds in liquid phase (sulfur, nitrogen, asphaltene, vanadium and nickel)

(Flow in) - (Flow out) - (Amount of disappearance (liquid_solid)) = 0 (A.14)

Flow in = $A_r u_l C_i^L \big|_z$

Flow out = $A_r u_l C_i^L \big|_{z+\Delta z}$

Amount of disappearance = $A_r \Re_1 \Delta z$

Dividing both sides of the resulting equation by $A_r \Delta z$, gives:

$$\frac{u_l \left(C_i^L \big|_z - C_i^L \big|_{z+\Delta z} \right)}{\Delta z} - \Re_1 = 0 \qquad \text{(A.15)}$$

When $\Delta z \rightarrow 0$, the left-hand side of equation (A.15) tends toward $u_l(dC_i^L/dz)$ and the equation can be rearranged to

$$u_l \frac{dC_i^L}{dz} + \Re_1 = 0 \qquad \text{(A.16)}$$

Substituting equation (A.12) into equation (A.16), we get

$$\frac{dC_i^L}{dz} = -\frac{1}{u_l} k_i^S a_S \left(C_i^L - C_i^S \right) \qquad \text{(A.17)}$$